Peptidylglutamyl-Peptide Hydrolase Activity of the Multicalytic Proteinase Complex.

By

Hakim Djaballah, BSc. (B'ham).

*Thesis submitted in fulfillment
of the requirement for the
degree of Doctor of
Philosophy in Biochemistry in
the Department of
Biochemistry of the
University of Leicester.*

UMI Number: U539221

UMI

Dissertation Publishing

ProQuest

"In memory of Dr E. A. Wren, BSc, PhD, who was a lecturer, a senior tutor, and a friend; who first introduced the author to the world of proteins, and installed within him the quest for understanding their kinetics, without which this work would have never been made possible. To whom this thesis is dedicated."

Acknowledgements

Abstract

Peptidylglutamyl-Peptide Hydrolase Activity of the Multicatalytic Proteinase Complex.

by
Hakim Djaballah.

The multicatalytic proteinase complex (MCP) or proteasome is a high molecular mass (650 kDa) proteinase found in all eukaryotes and a similar particle has been purified from the archaebacteria *Thermoplasma acidophilum*. MCP can cleave peptide bonds on the carboxyl side of basic, hydrophobic, or acidic amino acid residues, and these activities have been referred to as "trypsin-like", "chymotrypsin-like", and "peptidylglutamyl-peptide hydrolase (Glu-X)" activities, respectively.

In this study, the Glu-X activity, assayed with the substrate Z-Leu-Leu-Glu-β-naphthylamide was investigated. Kinetic studies have shown that it is composed of two distinct components: (a) a noncooperative component (LLE1) obeying Michaelis-Menten kinetics, and (b) a cooperative component (LLE2) exhibiting sigmoidal behaviour. The LLE2 component can easily be distinguished from that of the LLE1 component by the effect of inhibitors, divalent metal ions, KCl, and heat treatment. The addition of 1 mM $MnCl_2$ stimulates both components and permits saturation of MCP with substrate at concentrations below the solubility limits of the substrate, under these conditions, a Hill coefficient of 5.2 was calculated for the LLE2 component.

Using serine protease inhibitors, peptides as model substrates, and other effectors as probes for the different activities, it was found that (a) the proteinase is in fact a novel type of serine protease, (b) there seems to be at least seven distinct proteolytic activities associated with the complex, and (c) the specificity of the various activities is more complex than first proposed, where the "trypsin-like" activity can cleave after tyrosine residues.

Possibility of conformational changes associated with the activation by $MnCl_2$, and with the action of different effectors of the Glu-X were investigated by sedimentation velocity analysis, dynamic light scattering measurements, and electron microscopy of negatively stained preparations. The results provide a direct evidence for conformational changes associated with the activation by $MnCl_2$. Electron microscopic observations indicate a transition from a compact to an extended conformation of the complex in the presence of $MnCl_2$. The hydrodynamic results also provide a structural evidence for the observed positive cooperativity exhibited by the LLE2 component. A correlation between activity and shape of the conformational state of MCP was obtained.

Table of Contents

Title page.
Dedication.
Acknowledgments.
Abstract.
Table of Contents.
List of abbreviations.

List of abbreviations

AAF-AMC	Ala-Ala-Phe-7-amido-4-methylcoumarin.
ACT	antichymotrypsin.
AMPS	ammonium persulfate.
APMSF	(p-amidinophenyl)-methanesulphonyl fluoride.
LSTR-AMC	Boc-Leu-Ser-Thr-Arg-7-amido-4-methylcoumarin.
Boc	*tert*-butoxycarbonyl.
BSA	bovine serum albumin.
Cbz, Z	benzyloxycarbonyl.
DCI	3,4 dichloroisocumarin.
DFP	diisopropylfluorophosphate.
DMSO	dimethylsulfoxide.
DTNB	5,5'-dithiobis-(2-nitrobenzoic acid).
DTT	dithiothreitol.
EDTA	ethylenediaminetetraacetic acid.
FPLC	fast protein liquid chromatography.
Hepes	4-(2-hydroxyethyl)-1-piperazineethanesulfonic acid.
HPLC	High pressure liquid chromatography.
LLE1	high affinity site assayed at 0.1 mM LLE-NA.
LLE2	low affinity site(s) assayed at 0.4 mM LLE-NA.
LLE-NA	Cbz-Leu-Leu-Glu-β-naphthylamide.
MCP	multicatalytic proteinase complex.
NCDC	2-nitro-4-carboxylphenyl-N-N'-diphenylcarbamate.
PAGE	polyacrylamide gel electrophoresis.
Pefabloc	4-(2-aminoethyl)benzenesulphonyl fluoride.
PGO	phenylglyoxal.
PMSF	phenylmethanesulphonyl fluoride.
LLVY-AMC	N-succinyl-Leu-Leu-Val-Tyr-7-amido-4-methyl-coumarin.
SBzl	thiobenzyl.
SDS	sodium dodecyl sulfate.
TEMED	N,N,N',N'-tetra-methylethylene diamine.
TFA	trifluoroacetic acid.
Tris	tris(hydroxymethyl)aminomethane.
Ub	ubiquitin.

CHAPTER 1

Introduction.

"It is difficult to establish the precise function of a protease from its specificity since, with a few exceptions, proteases are generally not specific for particular peptide or protein substrates. Nonetheless, the catalytic properties as well as the structure and localization of proteolytic enzymes can give some indication of possible function. Proteinases which catalyse the extensive degradation of protein substrates may play an important role in protein turnover, whereas proteinases catalysing only limited cleavage of proteins possibly play a role in protein modification events".

Rivett (1989)

1.1 Introduction.

The past several years have witnessed a growing interest by biologists in understanding the process or processes by which cells degrade proteins in general, and the enzymes involved in such processes in particular.

Our current understanding, however, of intracellular protein degradation has been made possible due to the recent advents of isotope labelling techniques and microinjection procedures, which has led to a general recognition that intracellular protein degradation is a fundamental process, and is as important as the whole concept of protein synthesis, with some implications for biochemical regulation (Schimke, 1973; Goldberg and St John, 1976; Hershko and Ciechanover, 1982).

1.2 Intracellular protein degradation

In order to survive, all cells must be able to adapt to a changing extracellular environment. The concentration of specific cellular proteins is a key element in such an adaptive process, since the concentration of a protein is determined by the balance between its rate of synthesis and its rate of degradation, and the cell can alter either or both parameters. Olson and Dice (1989) have pointed out the importance of both alteration processes, with the degradative one being as equally regulated as the biosynthetic one.

Intracellular protein is the major source of amino acids for metabolic needs when intestinal absorption slows down or ceases.

Cellular proteins are divided into two categories according to readily discernible differences in average rates of turnover, based on general isotopic labelling. A short-lived category of proteins, having a half-life of the order of minutes, comprises about 0.6 % of total protein. Its degradation is not physiologically controlled, and the mechanism is probably nonlysosomal (Mortimore et al., 1989). Examples in such a category are ornithine decarboxylase with a half-life of 11 min (Schimke, 1973), δ-aminolevulinate synthetase with a life-life of 70 min (Schimke, 1973), and some oncogene products (E1A, myc, fos) with half-lives less than 30 min (Rivett, 1990a).

A long-lived category of proteins having an average half-life of 250 times greater than the short-lived ones, constitutes more than 99 % of the cell's protein. By contrast, its breakdown is strongly regulated and the site of catabolism is believed to be the vacuolar-lysosomal system (Mortimore et al., 1989). Examples of long-lived proteins include arginase with a half-life of 5 days (Schimke, 1973), lactate dehydrogenase isoenzyme-5 with a half-life of 16 days (Fritz et al., 1969), and histones with an average half-life of 117 days (Rivett, 1990a,b).

It has been reported that the half-life of a protein can alter in response to changes in extracellular stimuli or to changes in levels of individual metabolites. In skeletal muscle, it was shown that insulin, IGF-I and II, long-term fasting, protein deficiency, and hypophysectomy have a down regulatory effect on protein degradation, whereas thyroid hormones, glucocorticoids, short-term fasting, and endotoxin treatment stimulate protein degradation (Kettelhut et al., 1988). In the case of rat liver, it was reported that

glucagon, cyclic AMP, and epinephrine stimulate protein degradation but it is not clear as yet whether the stimulation is through the α-adrenergic pathways or not. Insulin and amino acids suppress the spontaneous degradation of intracellular proteins (Mortimore et al., 1989).

With reference to changes in levels of individual metabolites affecting half-lives of proteins, Hershko and Ciechanover (1982) have reported that depletion of the cellular metabolite ATP caused a cease in intracellular protein degradation, an observation that led to the discovery of the ATP-dependent proteolytic pathways. ATP levels can also affect other kinds of covalent modification reactions, especially phosphorylation, which mark some proteins for degradation (Rivett, 1986; Stadtman, 1990), and ATP can have a destabilizing effect on some enzymes (Rivett, 1990a).

The wide range of half-lives of proteins in eukaryotic cells suggests that there is a high degree of selectivity in the degradation process. An approach in understanding the relationship between intracellular stability and other properties of proteins was to attempt to correlate various physicochemical properties to the half-lives of different proteins.

Cellular proteins, however, vary rather a lot in their biochemical characteristics and subcellular localization, and such correlations have proved unsuccessful (Rivett, 1990a). Part of the complexity of such analyses can be attributed to the evolution of several pathways for intracellular protein degradation.

1.3 Pathways of intracellular protein degradation.

1.3.1 Lysosomal degradation pathways.

The potential role of lysosomes, well characterized organelles containing a number of highly active proteases, in intracellular protein degradation was recognized many years ago (Dean and Barrett, 1974; Goldberg and St John, 1976; Hershko and Ciechanover, 1982; Bond and Butler, 1987).

The extent to which lysosomes are involved in the degradation of intracellular proteins has been estimated using inhibitors of lysosomal function or of lysosomal proteases (Seglen, 1983). It is worth mentioning here the classical study of Poole and coworkers, who first showed that weak bases such as chloroquine partially inhibited protein catabolism in cultured embryo fibroblasts in the absence of serum (Wibo and Poole, 1974).

As weak bases, chloroquines accumulate within lysosomes where they get protonated, which prevent them from diffusing out of the lysosomes. Their high concentration in lysosomes thereby increase the intralysosomal pH to about pH 6.5 (Ohkuma and Poole, 1978), at which the lysosomal proteases are inactive. Other examples of the so-called lysosomotropic agents include ammonia, methylamine, and ionophores (Rivett, 1990a).

Pepstatin, a specific inhibitor of the lysosomal protease cathepsin D (Aoyagi and Umezawa, 1975) was first used to study the involvement of lysosomes. Its addition, via liposomes which get

endocytosed and thus enter lysosomes, was found to cause 50 % drop in protein degradation in perfused rat liver. Other inhibitors have been subsequently tested (Seglen, 1983).

Macroautophagy is the most widely studied pathway by which cytosolic proteins are internalised by lysosomes (Dice, 1990). In this pathway, membranes derived from the smooth endoplasmic reticulum surround areas of cytoplasm to form autophagic vacuoles, which then fuse with lysosomes to form autophagosomes, which digest the content (Olson and Dice, 1989; Dice, 1990). The process is rather non-selective in that any cytosolic molecule can be internalized at equivalent rates. However, cytoskeleton-associated proteins and other organelles may avoid degradation via this pathway (Rogers and Rechsteiner, 1988). Macroautophagy is greatly enhanced during starvation.

Lysosomes are also able to take up and degrade proteins by another pathway called microautophagy. It is a vesicular internalization at the lysosome surface, accounts for a non-selective process of degradation, and may be the primary mode of lysosomal proteolysis in well-nourished cells (Dice, 1990). Microautophagy, on the other hand, is suppressed during acute starvation suggesting some link between itself and macroautophagy (Olson and Dice, 1989).

There also appear to be an additional process by which a class of long-lived cytoplasmic proteins can be taken selectively into the lysosomes for degradation. This process was first identified by Dice (1987), while studying the degradation of RNAase A in cultured cells in response to serum withdrawal, and later led to the characterization

6

of a sequence motif within proteins that can be degraded via this process. The sequence motif is exemplified by KFERQ, and recent studies have identified a peptide recognition protein (prp) 73 that binds to the KFERQ sequence (Dice, 1990).

The prp 73 protein is a constituvely expressed member of the heat-shock protein 70 family. It is thought to function in membrane translocation, possibly by aiding the protein to be translocated in attaining a translocation-competent conformation (Chiang et al., 1989). This process is enhanced in cultured cells during serum deprivation, largely due to a marked increase in the cytosolic concentration of prp 73. It should also be added that the accessibility of the KFERQ-like peptide region may be a regulatory point in the degradation of those specific proteins (Dice, 1990).

The general conclusions from the above and other studies are that lysosomes play an important role in the degradation of endocytosed proteins and of "long-lived" intracellular proteins. They are also responsible for the enhanced degradation observed under conditions of nutrient deprivation (Dice, 1990).

1.3.2 Ubiquitin-dependent degradation pathways.

Observations from several laboratories that degradation of most short-lived or abnormal proteins is not influenced by nutritional deprivation, hormones treatment, inhibitors of protein synthesis, or most importantly inhibitors of lysosomal proteases, have led to the widely accepted view that there are multiple pathways of protein

degradation other than the lysosomal ones (Hershko and Ciechanover, 1982; Varshavsky, 1992; Goldberg, 1992; Goldberg and Rock, 1992).

The first major nonlysosomal pathway of intracellular protein degradation to be described was the ubiquitin-dependent pathway. In this pathway, the highly conserved and abundant 76-residue protein called ubiquitin (Ub) (Hershko and Ciechanover, 1982; 1992), functions as a signal for protein degradation by conjugation to proteins, step referred to as conjugation. The degradation step, on the other hand, involves a high molecular mass protease complex, called the 26S protease. ATP is required in both steps (Hershko and Ciechanover, 1982; 1992; Hershko, 1991; Jentsch, 1992; Goldberg, 1992).

The conjugation step is itself a multi-step process. In an initial ATP-dependent step, Ub is activated by a thioester formation between its C-terminus and an internal cysteine residue of a Ub activating enzyme (E1). The activated Ub is then transferred to a Ub-conjugating enzyme (E2). Several E2s have been identified (Hershko and Ciechanover, 1992). Finally, Ub is donated to protein substrates. The participation of Ub-protein ligases (E3) in the final step is generally, although not always, requires as it has been reported that Ub conjugation to histone 2A takes place in the absence of E3 (Hershko and Ciechanover, 1992).

A simple conjugation to Ub does not always signal degradation, as there have been reports describing stable conjugates (Finley and Chau, 1991; Hingamp et al., 1992). Recent studies have shown that linear multi-ubiquitination chain (when a single lysine residue of Ub is used) or multi-ubiquitination "trees" (when more than one lysine

residue is used) appear to be required for at least rapid degradation, although the attachment of a single Ub to a substrate protein can also be sufficient as a degradation signal (Jentsch, 1992; Johnson et al., 1992).

Little is known about the degradation step. Rechsteiner and coworkers and later Hershko and coworkers have identified and purified the 26S protease. It is composed of three distinct components, called conjugate-degrading factors (CF1 (500 kDa), CF2 (250 kDa), and CF3 (600 kDa)) (Hough et al., 1987; Ganoth et al., 1988). Recently, there have been reports describing the CF3 factor as the multicatalytic proteinase complex (MCP), which will be discussed in Section 1.5 (Eytan et al., 1989; Driscoll and Goldberg, 1990; Hershko and Ciechanover, 1992).

Two recent studies (Seelig et al., 1991; Kuehn et al., 1992) have questioned the incorporation of MCP into the 26S protease, while several other groups have observed the presence of MCP in the 26S protease. The best evidence so far supporting the latter observations comes from studies by Wolf and coworkers on yeast MCP, where they have showed that mutations in MCP subunits caused Ub-protein conjugates to accumulate, while deletion of the genes of yeast MCP subunits was lethal (Heinemeyer et al., 1991).

Another line of evidence comes from studies by Seufert and Jentsch (1992), where they showed that a yeast mutant with a defective MCP fails to degrade proteins which are subject to Ub-dependent degradation in wild type cells.

Although the CF3 component has been identified as MCP, recently Goldberg and coworkers have managed to identify the CF2 component as being an ATP-stabilised inhibitor of MCP's peptidase activities (Driscoll et al., 1992), and the CF1 component as an ATP-binding activator of MCP's peptidase activities (Goldberg, 1992), it is however unclear as yet on how CF1, CF2, and CF3 function and what role plays ATP in the active 26S protease, although it is thought that ATP has two distinct sites of action in the Ub pathway: 1) The activation reaction catalysed by E1 is accompanied by ATP hydrolysis to yield AMP and PPi, and 2) The 26S protease hydrolyses ATP to Pi during degradation of conjugated proteins (Johnston and Cohen, 1991; Hershko and Ciechanover, 1992).

More recently another 26S protease has been described by Goldberg (1992), which is composed of two proteases: MCP and an ATP-dependent thiol protease. This 26S protease is being called multipain (Goldberg, 1992).

The mechanism and substrate selection of the Ub pathway are still poorly understood (Hershko and Ciechanover, 1992). Ub production has been shown to be enhanced by heat, which links the Ub pathway to the heat/stress response, and to be repressed by cyclic AMP, which can make Ub a limiting factor in the conjugation step. The E2 and E3 enzymes have been shown to have more than one isoform with different substrate specificities, which could be one form of selectivity for conjugation (Varshavsky, 1992).

Furthermore, the degradation of N-α-acetylated proteins by the Ub pathway has been shown to be possible only in the presence of a

protein specifier, referred to as protein factor H (factor Hedva) (Gonen et al., 1991). Recently, Kong and Chock (1992) have demonstrated the *in vitro* phosphorylation of the E1 and one isoform of the E2s, which led to a two-fold stimulation in the ubiquitination of histone H2A, suggestive of an in vivo situation where protein ubiquitination may well be regulated by phosphorylation.

A striking example of highly selective and regulated protein degradation by the Ub pathway is that of cyclins (Hershko et al., 1991; Glotzer et al., 1991). Cyclins are proteins that are synthesized and then degraded at different phases of the cell cycle, thus serving as oscillators that determine cell cycle progression (Glotzer et al., 1991).

The simplest model for protein recognition and marking for degradation is that discovered by Varshavsky and coworkers, while studying the degradation of β-galactosidase and derivatives as test proteins (Varshavsky, 1992). Such proteins were found to be degraded by the "N-end rule" pathway, which degrades proteins depending on the identity of their N-terminal residues via the Ub pathway (Varshavsky, 1992). The half-lives of these substrates are apparently dictated by the affinity of an E3 to their N-terminal residues (Varshavsky, 1992).

Three distinct types of E3 have been detected in the reticulocyte-derived *in vitro* system (Varshavsky, 1992). The E3 type I is specific for the positively charged destabilizing N-terminal residues Arg, Lys, & His. The type II is specific for bulky hydrophobic destabilizing N-terminal residues Phe, Trp, Tyr, and Leu (and Ile in yeast). The type III is specific for the N-terminal residues Ala, Ser, and

Thr, which share the properties of small size and lack of charge. They were found to be destabilizing in reticulocytes but stabilizing in yeast, thus implying that *Saccharomyces   cerevisiae* lacks type III (Varshavsky, 1992).

Cyclins (eg sea urchin cyclin B, human cyclin B1, yeast CLB1, and CLB2) have been found to bear a conserved sequence motif of 9 amino acids, the "destruction-box" (RXALGXIXN consensus sequence, where X can be any amino acid), which is required for their degradation by the Ub pathway (Jentsch, 1992). All mitotic cyclins characterized so far have lysine-rich sequences C-terminal of the "destruction-box", suggesting that some of these lysine residues must function as ubiquitination sites (Glotzer et al., 1991; Varshavsky, 1992).

The existence of metabolically stable Ub conjugates and the identification of isopeptidases that remove Ub from conjugates suggest that protein degradation is not the sole function of the Ub system (Finley and Chau, 1991; Hingamp et al., 1992; Hadari et al., 1992; Hershko and Ciechanover, 1992).

1.3.3   Ubiquitin-independent   degradation   pathways.

Another nonlysosomal and cytoplasmic pathway of protein degradation involves the Ca(II)-dependent calpains, which may be particularly important in the turnover of cytoskeleton and plasma membrane proteins (Pontremoli and Melloni, 1986). In addition, there are speculations that short-lived proteins containing proline, glutamic acid, serine, and threonine (PEST sequence) can be phosphorylated in

the PEST region, and subsequently bind Ca(II) and this trigger their degradation by calpains (Rogers et al., 1986). Many Ca(II)-binding proteins (calmodulins) are found to be good substrates for calpains (Wang et al., 1989). The exposure of calpains, however, to high local substrate proteins would be through interactions between calpain substrates and other Ca(II)-binding proteins (Olson and Dice, 1989).

Recent studies have revealed yet another degradative pathway that occurs within the vacuolar membrane system of the endoplasmic reticulum (Klausner and Sitia, 1990). This pathway, which is distinct from the lysosomal pathway, appears to be responsible for the degradation of newly synthesized abnormal or unassembled proteins, and of certain proteins that are retained within the endoplasmic reticulum (Klausner and Sitia, 1990; Bonifacino and Lippincott-Schwartz, 1991).

More recently, Mukarami et al. (1992) have shown the degradation of ornithine decarboxylase (ODC) by the 26S protease, without ubiquitination of the former. ODC degradation was stimulated by ODC antizyme and found to be ATP-dependent. They also shown that ODC antizyme has no sequence homology to ubiquitin, which is an interesting observation, in that the 26S protease can degrade non ubiquitinated proteins. However, it has been suggested that ODC contains structural domains responsible for its rapid degradation (Mukarami et al., 1992), which could well have been a recognition requirements for degradation by the 26S protease.

Their findings suggest that the 26S protease may have a selective role in removing short-lived proteins by recognizing specific degradation signals other than ubiquitin.

1.4 Cellular proteinases.

The terms proteases, peptidases, or peptide hydrolases are all interchangeable terms used to describe enzymes that cleave peptide bonds (Barrett, 1986). Proteases can be divided into two categories: the exopeptidases which group the aminopeptidases and the carboxypeptidases, where proteolytic action is directed by the amino- or carboxy-terminus of the peptide, and the endopeptidases, where the peptide cleavage occur internally in the peptide sequence (Barrett, 1986; Bond and Butler, 1987).

Cellular proteases range in size from 20 to 1,500 kDa. some of the well characterized ones fit the traditional concept of the small monomeric proteases. In general, the lysosomal proteinases are small (20-40 kDa) and they are maximally active under acidic conditions. However, it is now known that many extra-lysosomal proteases are oligomeric, and optimally active at a neutral or mildly alkaline pH (Bond and Butler, 1987; Rivett, 1989a).

1.4.1 Classification of proteases.

Many different proteases have been described from a wide variety of sources, and their classification is based on their respective catalytic mechanism. There are four major classes of proteases: serine, cysteine, aspartic proteases, and metalloproteases, with some

14

proteases not belonging to any of the four above classes (Barrett, 1986).

Serine proteases.

They are a class of proteolytic enzymes characterized by the presence of a unique reactive serine side chain, together with a histidine and an aspartic acid residues at the active site (Kraut, 1977). Work on the inactivation of chymotrypsin by diisopropylfluoro-phosphate (DFP) led to the discovery that DFP covalently and specifically modified the serine residue, that was essential for activity (Barrett, 1986). Subsequently, the importance of histidine was shown by their uniquely alkylation by peptidylchloromethylketones (Shaw, 1990). Since the aspartic acid residue is buried in the structure of the enzyme, it was not possible to label it (Shaw, 1990).

The serine proteases are of extremely widespread occurrence and diverse function, and they fall into two superfamily classes: the "chymotrypsin" superfamily and the "subtilisin" superfamily, although is is likely that other distinct superfamilies do exist (Kraut, 1977; Barrett, 1986). The subtilisin-related enzymes have been found only in bacteria, whereas the chymotrypsin-related ones are found in both prokaryotes and eukaryotes (Barrett, 1986).

An important feature common to both superfamilies is that they both have their catalytically functional groups arranged in the same geometrical relationship, nevertheless, they have entirely different

overall three-dimensional structures, and are therefore very probably descended from unrelated ancestral enzymes (Kraut, 1977).

Cysteine   proteases.

They are another class of proteolytic enzymes characterized by the presence of a unique reactive side chain, together with a histidine residue forming the active site (Barrett, 1986; Shaw, 1990). The importance of the thiol group in papain was realized because of the inhibitory action of mild oxidizing reagents, which could be reversed by thiols, apparently cleaving a disulfide bond that had been formed (Barrett, 1986). This deduction was later reinforced by studying the action of mercurials and iodoacetic acid that was shown to inactivate papain in a stoichiometric fashion at a site identified as cysteine-25 (Shaw, 1990).

Cysteine proteases are found in prokaryotes and eukaryotes, and there seem to be at least three or more distinct superfamilies of cysteine proteases (Barrett, 1986), as three cysteine proteases gene families are known (Shaw, 1990). The largest and mostly studied is the papain superfamily. Recently, mammalian lysosomal cysteinyl proteases (cathepsins B, L, H, and S) were found to be homologous with papain (Barrett, 1986).

They also share with papain a specificity largely dominated by an affinity for hydrophobic side chains, but differ in that some have endopeptidase and exopeptidase activities (Shaw, 1990). The largest subunit of the calpains, on the other hand, has a domain near to the N-terminal homologous with papain (Shaw, 1990).

Clostripain, a cysteine protease from *Clostridium histolyticum*, is highly specific for substrates with an arginyl residues at the P1 position. In this respect, it is quite different from the papain superfamily, and furthermore, its sequence around the catalytic cysteine, indicates that it is the product of distinct gene family (Barrett, 1986; Shaw, 1990).

Viral encoded proteases, such as 2A and 3C of picorna viruses, and type 2 of human rhinovirus, have been proposed to be cysteine proteases (Barrett, 1986; Shaw, 1990). However, sequence comparison has led to the conclusion that they represent homologs of serine proteases in which the active centre serine is replaced by a cysteine residue (Barrett, 1986; Shaw, 1990).

Aspartic proteases

Harltey (1960) termed the enzymes that are now known as aspartic proteases "acid proteases" because it was not possible to identify, at that time, the catalytic residues. It was not until the amino acid sequence of pepsin was reported, where the aspartic acid residues were identified as the catalytic ones. It is now clear that both aspartic acid residues form the catalytic site (Barrett, 1986).

The aspartic proteases seem to be confined to the eukaryotes, and may be one of the younger classes of proteases (Barrett, 1986). Pepsin is the mostly studied aspartic protease. The mammalian gastric proteinases and cathepsin D have been shown to be evolutionary relatives of pepsin. With amino acid sequence and X-ray structure

availability for several aspartic proteases, it has become evident that the enzymes have evolved by gene duplication (Barrett, 1986).

Metalloproteases.

They are a class of probably the oldest proteolytic enzymes around, characterized by the absolute requirement of zinc for activity, although some of the metalloproteases retain activity when zinc is replaced by another divalent metal ion such as cobalt (Barrett, 1986).

Thermolysin, from *Bacillus thermoproteolyticus*, has been thoroughly characterized. The active site cleft contains a zinc atom bound by two histidine side chains and one glutamic acid. The molecule also has four binding sites for Ca(II), but the metal ion has a structural role rather than a catalytic one (Barrett, 1986).

1.4.2 Regulation of cellular proteases.

Proteolytic activity in cells must be highly and tightly regulated, to prevent inappropriate and uncontrolled protein degradation, and to fulfil their requirement with respect to many specialized processes in which they are involved. The action of cathepsins is controlled by compartmentalization on the one hand, and by protein uptake by the lysosomes on the other. Cathepsins are highly active in an acidic environment, and this limits their activity at neutral or alkaline pHs.

The role of endogenous inhibitors or activators of proteases has also been studied as a way of regulating proteolytic activity. Calpains

are regulated by Ca(II) concentration as well as the interaction with a specific endogenous inhibitor protein, referred to as calpastatin (Murachi, 1983; Suzuki et al., 1987).

Similarly, Barrett (1987) has reported an 11 kDa protein inhibitor of cathepsins B, H, and L. the inhibitor was found to belong to the cystatin family of cysteine protease inhibitors (Barrett, 1987), but its cytosolic localization is probably to protect against any leakage of these lysosomal enzymes (Rivett, 1989a).

There have been several reports in the literature on the existence of calpain activator proteins (Pontremoli et al., 1988; 1990; Shiba et al., 1992). Shiba et al. (1992) have described a 47 kDa heat stable protein activator, which caused a two-fold activation without any effects on the Ca(II) requirement of calpains.

Several proteases have now been suggested to be present in the cell in a latent form, as a way of physiologically regulating them (Bond and Butler, 1987). However, Rivett (1989a) argues that there is very little solid evidence available for this occuring.

Recognition of substrates may play an important role in the regulation of protease activity has been suggested (Bond and Butler, 1987). Substrates protein structure has been shown to have an influence on the susceptibility to proteolytic attack both for specific cleavage events, and for extensive proteolysis (Bond and Butler, 1987). Moreover, the proteolytic susceptibility of proteins can be dramatically affected by specific covalent modification reactions (Rivett, 1986; Stadtman, 1990).

1.5 The system of study: the multicatalytic proteinase complex.

The multicatalytic proteinase complex (MCP), first described in the pituitary by Wilk and Orlowski (1980), is a very unusual protease in that it is of a nonlysosomal nature, has a high molecular mass of 600 - 700 kDa, and is composed of a series of low molecular mass nonidentical subunits. Since then, similar or even identical MCPs have been isolated, under a variety of different names, from a variety of eukaryotic tissues and cells.

The basic properties of this widely distributed protease appear to be similar regardless of the source; however, studies with monoclonal and polyclonal antibodies show interspecies cross-reactivity but also suggest some differences in immunological properties of the MCPs isolated from different sources (Rivett and Sweeney, 1991; Tanaka et al., 1992).

There is, however, a general agreement now to refer to these novel proteases as either proteasomes (Arrigo et al., 1988) or multicatalytic proteinase complexes (Dahlmann et al., 1988). A related protease with a simpler subunit composition has been isolated from the archaebacterium Thermoplasma acidophilum (Dahlmann et al., 1989), and will be referred to as the archaebacterial MCP. Two recent studies have questioned the presence of MCPs in the prokaryotic *Escherichia* coli K12 and *Frankia* actimycetes strain BR (Benoist et al., 1992; Vaithilingam and Cook, 1989).

It is now widely accepted that MCP is present in all eukaryotic cells and tissues tested, it has a half life of 12-15 days in rat liver (Tanaka and Ichihara, 1989) and a half life of 5.5 days in HeLa cells (Hendil, 1988), and MCP constitutes up to 1.5 % of the soluble protein in cell extracts (Hendil, 1988; Tanaka et al., 1992).

One dimensional SDS polyacrylamide gel electrophoresis of highly purified MCPs reveals a characteristic pattern of 8 to 12 protein bands within the molecular masses range of 22 to 34 kDa, but a more complex pattern was observed on two-dimensional gels, where up to 25 different protein spots (pI values in the range of pH 4 to 10) were noted in the case the rat liver MCP (Rivett and Sweeney, 1991). Yeast MCP has 14 different subunits (Heinemeyer et al., 1992), Plant MCP has 12-15 different subunits (Schliephacke et al., 1991), whereas the archaebacterial MCP is composed of only two types of subunit (Zwickl et al., 1992), suggesting that the number of subunits is species dependent.

However, it is possible that some of the observed protein spots on two-dimensional gels may be related to each other by proteolysis (Lee et al., 1990; Rivett and Sweeney, 1991), phosphorylation (Haass and Kloetzel, 1989), or glycosylation (Tomek et al., 1988; Schliephacke et al., 1991), many are antigenically distinct (Rivett and Sweeney, 1991). It has also been shown that protein patterns vary during development (Haass and Kloetzel, 1989; Ahn et al., 1991).

Proteolysis of some of the subunits of eukaryotic MCPs may occur during purification, storage, activation of the enzyme, or during the isofocusing step of the two-dimensional gels where MCP gets

21

exposed to high concentrations of urea (Tanaka and Ichihara, 1989; Lee et al., 1990; Rivett and Sweeney, 1991; Weitman and Etlinger, 1992). There is also evidence suggesting that some specific proteolytic events may take place *in vivo*.

Weitman and Etlinger (1992) have detected cross-reactivity between a 41 kDa protein and a monoclonal antibody raised against the 32 kDa subunit of the human erythrocyte enzyme. Furthermore, Kreutzer-Schmid and Schmid (1990) have also detected cross-reactivity with a monoclonal antibody raised against the 27 kDa subunit of prosomes. The archaebacterial MCP β subunit has been shown to be post-translationally processed (Zwickl et al., 1992).

There have been reports in the literature regarding the association of RNA (repressed RNA as well as integral RNA species of 80-100 nucleotides in length) with prosome preparations (Schmidt et al., 1984; Martins de Sa et al., 1986; Arrigo et al., 1987). Falkenburg et al. (1988) have described RNA association with immunoprecipitated MCP from rat liver. These observations have led to the suggestions that MCP/prosomes represents a new type of ribonucleoproteins, and have led other investigators to question the presence of RNA with rigorous purification of MCP preparations (Arrigo et al., 1988; Kleinschmidt et al., 1988).

Recent studies, however, have confirmed the presence of at least one small RNA species (about 80 nucleotides) in highly purified MCP and prosome preparations (Coux et al., 1992; Northwang et al., 1992), suggesting that some of the discrepancies in the literature may be due to differences in methodology as discussed by Skilton et al. (1989).

The non-stoichiometric amounts of RNA led to the suggestion of possible MCP subpopulations containing RNA (Rivett, 1993). Recently, Northwang et al. (1992) have sequenced and identified a major proteasomal RNA from HeLa cells and from duck erythroblasts as $tRNA^{Lys3}$. The functional property of the RNA remains unclear (Coux et al., 1992; Northwang et al., 1992).

The description of MCP as being multicatalytic was made by Wilk and Orlowski (1983), after they found that it can cleave on the carboxyl side of basic, hydrophobic, and acidic amino acid residues. These activities have been referred to as trypsin-like, chymotrypsin-like, and peptidylglutamyl-peptide hydrolase activities, respectively (Wilk and Orlowski, 1983).

From their different sensitivities to various inhibitors, activators, and covalent modifiers, it is widely accepted now that these activities are distinct from each other, and are being catalysed at independent sites within the enzyme complex (Dahlmann et al., 1985; Rivett, 1985; Tanaka et al., 1986a; Orlowski and Michaud, 1989; Rivett et al., 1990; Dick et al., 1991; Yu et al., 1991; Pereira et al., 1992).

Recently, genetic studies on the yeast MCP have provided further evidence reinforcing the above view. Wolf and coworkers have isolated mutant cells (PRE 1-1 and PRE 2-1) lacking the chymotrypsin-like activity but with higher levels of the two other activities (Heinemeyer et al., 1991). They have also isolated mutants cells (PRE 4-1) deficient in only the peptidylglutamyl-peptide hydrolase activity (Enenkel et al., 1990). Thus, the three activities appear to be present

in distinct subunits encoded by distinct genes, reflecting the multicatalytic property of MCP.

The proteinase can degrade a variety of protein and peptide substrates and activity at all sites is optimal at neutral to weakly alkaline pH values (Orlowski, 1990). The multiple proteolytic activities should be advantageous for rapid degradation of proteins. Dick et al. (1991) have shown such an advantage via a possible channelling pathway for the degradation of oxidized insulin B chain. Although it seems likely that the various peptidase activities contribute towards protein degradation (Orlowski, 1990; Rivett, 1993), there have been, however, reports on a protein degrading activity within the complex (Mykles and Haire, 1991; Pereira et al., 1992).

So far, there have been several reports in the literature describing the activation of the different proteolytic activities of MCPs from various sources. Examples of such non-physiological treatments included dialysis against deionised water (McGuire et al., 1989), exposure to either polycations, heat, fatty acids, or SDS (Dahlmann et al., 1985; Mykles and Haire, 1991; Mellgren, 1990). These observations have led to the introduction of the term "latent form" for the non-activated MCPs (Tanaka et al., 1992; Rivett, 1993), especially for human erythrocyte MCPs (Lee et al., 1990; Weitman and Etlinger, 1992).

In view of the *in vivo* regulation of the different activities of MCPs, there have been several reports describing endogenous protein inhibitors or activators of MCPs. Etlinger and coworkers, working on

human erythrocytes have described two protein inhibitors of MCP with molecular masses of 240 kDa (Murakami and Etlinger, 1986) and 200 kDa (Li et al., 1991), each composed of identical subunits of 40 and 50 kDa, respectively. These two inhibitors differ in structure and in immunological properties but, unexpectedly and curiously, both inhibited calpain and Ca(II)-dependent neutral proteases (Murakami and Etlinger, 1986; Li et al., 1991).

DeMartino and coworkers, working on bovine erythrocytes, have characterized a protein inhibitor with a molecular mass of 60 kDa composed of identical 30 kDa subunits (Chu-Ping et al., 1992a). Furthermore, Goldberg and coworkers, working on reticulocytes, have identified a protein inhibitor with a molecular mass of 250 kDa composed of identical 40 kDa subunits (Driscoll et al., 1992).

In addition, several groups have reported the identification of protein activators of the complex (Yukawa et al., 1991; Goldberg and Rock, 1992; Chu-Ping et al., 1992b; Dubiel et al., 1992). It seems likely the the activator proteins reported independently by DeMartino's and Rechsteiner's groups are similar. At present, not a lot can be added about the described activators and inhibitors until their physiological function and mechanistic action, if any, has been fully understood.

Electron microscopic studies have shown that MCP has a hollow cylindrical structure arranged in a stack of four rings (Kopp et al., 1986; Baumeister et al., 1988) but there is disagreement about the exact arrangement of the subunits (Kopp et al., 1986; Tanaka et al., 1988c; Rivett et al., 1991). Recent detailed structural investigations of the archaebacterial MCP by image analysis of negatively stained

25

particles (Dahlmann et al., 1989; Hergel et al., 1991) and of small three-dimensional crystals (Puhler et al., 1992) show that the MCP is composed of four stacked rings, each consisting of seven subunits.

The structure shows a clear seven-fold symmetry, but subunits making the outer and inner rings are not in register along the axis of the barrel, rather the outer rings are rotated with respect to the inner ones by approximately 25°. The stoichiometry of the molecule is $\alpha_{14}\beta_{14}$. An immunoelectron microscopic investigation has demonstrated that the α subunits form the outer while the β subunits form the inner ones (Grziwa et al., 1991). The observed seven fold symmetry is similar to the molecular chaperones of the GroEL family (Zwickl et al., 1990).

The multicatalytic proteinase complex is similar to other cylindrical structures, which are widely distributed 19S ribonucleoprotein particles thought to be involved in the control of translation (Schmid et al., 1984; Martins de Sa et al., 1986), erythrocyte cylindrin (Harris, 1988), and a number of other partially characterized 16-22S cylindrical particles (Rivett, 1989a). However, prosomes and certain related particles have been shown to have proteolytic activity and to share antigenic cross-activity with MCP, and are therefore believed to be the same(Falkenburg et al., 1988; Arrigo et al., 1988; Northwang et al., 1992).

During the past few years, well over 29 cDNAs or genes for subunits of MCPs from various sources have been isolated and sequenced (Tanaka et al., 1992; Tamura et al., 1992). In the case of the rat liver MCP, ten of its subunits have been, so far, cloned and

sequenced, these are RC1, RC2, RC3, RC5, RC8, RC9, rIOTA, rZETA, rDelta, and rRING12, and have also been shown to have a high inter-subunit homology (Tamura et al., 1992). Because of the significant homology (often 20 to 40 % identity) among themselves and not with other known proteins, suggesting an evolutionary relatedness, Tanaka and coworkers have named this novel gene family as the "proteasome gene family" (Tanaka et al., 1992).

The striking similarity of the α subunit of the archaebacterial MCP (Zwickl et al., 1991) to the various subunits of the eukaryotic MCPs suggests that these MCP subunits are encoded by a gene family of ancient origin (Rivett, 1993).

The possibility of at least two groups of closely-related MCP subunits has been recently proposed (Tanaka et al., 1992; Rivett, 1993). Close examination of sequences of MCP subunits obtained from different species shows that they can be divided into two major groups (A and B), and one minor group. Group A comprises those sequences that are closely related to the archaebacterial α subunit, where many of the cloned subunits fall into this group.

The α subunit of the archaebacterial MCP is very similar to the eukaryotic C3 which in turn is very highly conserved between rat, human, and Xenopus (Rivett, 1993). On-all, most of the subunits in group A are also very highly conserved between different animal species (Tamura et al., 1991). Sequences of N-terminal regions of different MCP subunits, in group A, are highly conserved while the C-terminal regions are often not (Rivett, 1993).

27

Group B comprises those which are closely related to the β subunit of the archaebacterial MCP. The β subunit has an unblocked N-terminus (Zwickl et al., 1992) so do seven of the related rat liver MCP subunits (Lilley et al., 1990), while the group A subunits RC2, RC3, and RC8 have been shown to be N-acetylated (Tokunaga et al., 1990). Sequences of MCP subunits, in group B, share some highly conserved regions but have variable lengths at the N-terminal (Rivett, 1993), which suggests somekind of post-translational modification for these subunits. The minor group comprises those which do not fit in either A nor B, and that includes the sequence deduced for C5 (Tamura et al., 1992; Lee et al., 1992).

Members of the proteasome gene family are not found in a single gene cluster in yeast (Lee et al., 1992) or in *Drosophila* (Frentzel et al., 1992). In general, there are no sequence motifs which are characteristic of other discovered proteases in MCP subunits (Tanaka et al., 1992).

Computer analysis has revealed that certain subunits of various MCPs contain three types of segments showing partial identity with amino acid sequences of known functional domains: 1) Nuclear translocation signal (NLS) X-X-K-K(R)-X-K(R) (where X any amino acid residue) was found in some subunits (eg XC3, RC3, HC3, Taα), and its location is different in different subunits (eg PROS-29, RC9, HC9, PRS2, hIOTA, PROS-28.1, PRE1). 2) Another unique sequence appearing at the C-terminus region of different MCP subunits is a cluster of acidic amino acids that is rich in Glu and Asp residues (eg PROS-35, RC2, HC2, PRS1, RC8, HC8, Y13, RC9, HC9, PROS-28.1, Taα), the function of such a cluster is in complementing NLS. and 3) A conserved tyrosine

phosphorylation site located in the middle region of certain subunits of various MCPs (eg XC3, RC3, HC3, Y13, PROS-29, RC9, HC9, PRS2, hIOTA, Taα), suggesting that the function(s) of MCPs may be regulated by a phosphorylation/dephosphorylation system. It is interesting to note that all the three segments were found in the α subunit of the archaebacterial MCP (Tanaka et al., 1992).

Immunocytochemical studies have shown the MCPs to be present in both the nucleus and cytoplasm of a variety of cells and tissues (Haass et al., 1989; Klein et al., 1990). Recently, studies by Rivett et al. (1992) have shown that a proportion of MCPs are also close to or actually on the rough endoplasmic reticulum and in polysomes in rat hepatocytes and cultured human L-132 cells. The distribution of MCPs between different cell compartments seems to vary with cell type (Haass et al., 1989) and changes in localization of MCP have been found to occur during oogenesis, embryogenesis, and development in lower eukaryotic organisms (Rivett, 1993).

Studies with mutant cells that cannot express some of the MCP subunits were found to be incapable of proliferating, which has led to the implication of MCP in cell proliferation. Deletion of some of the genes which code for MCP subunits in yeast MCP (YC1, YC7a or YC8, Y7, PRE1, PRS3; PUP2) resulted in cells which cannot proliferate (Fujiwara et al., 1990; Heinemeyer et al., 1991; Emori et al., 1990; Georgatsou et al., 1992). However, not all yeast MCP genes are essential for proliferation, as studies by Emori et al. (1990) have found that deletion of the YC13 gene resulted in cells which could proliferate but at half the rate of wild type cells.

MCP is also located predominantly in the nucleus of transforming and proliferating cells, suggesting a role in nuclear functions such as transcription and DNA processing (Grossi de Sa et al., 1988, Kumatori et al., 1990; Kanayama et al., 1991). The expression of the gene for one subunit of the rat liver MCP (RC2) has been found to be upregulated in transforming cells (Kumatori et al., 1990), and the expression of RC2 has been shown to be high in the presence of phytohemagglutinin and interleukin-2 which cause blastogenic transformation (Shimbara et al., 1992). Because of no detectable differences in the level of MCP in these transforming cells, Tanaka and coworkers have suggested an accelerated turnover of MCPs in these rapidly proliferating cells (Shimbara et al., 1992).

Recent studies by Kahawara and Yokosawa (1992) have shown a cell cycle-dependent change of MCP distribution during embryonic development of the Ascidian Halocynthia roretzi. They found that during interphase, MCP was localized in the nucleus. In prophase and prometaphase, MCP disappeared from the nucleoplasm and the nuclear envelope, respectively. during metaphase, MCP was detected in the chromosomes, whereas no detection was noted in the mitotic apparatus in anaphase. In telophase, MCP was localized in the newly formed nucleus. Their observations are suggestive of an involvement of MCP in the progression of cell division cycle.

More recently, Tanaka and coworkers have reported similar observations, and more interestingly they reported that inhibition of MCP expression by antisense oligodeoxynucleotide for the RC2 subunit was found to cause partial arrest of cell cycle progression in T-lymphocytes (Shimbara et al., 1992). Their finding is in support of

Kahawara and Yokosawa's (1992) suggestion for the involvement of MCP in cell cycle progression and proliferation. The ubiquitin-dependent degradation of cyclins (Hershko and Ciechanover, 1992) is also in support of the involvement of MCP in the control of cell cycle

The role of MCP in protein turnover is poorly understood, probably due to our little understanding of the system or the lack of potent inhibitors of the different activities of the complex. Removal of MCP from reticulocyte lysates has been reported to cause a deficiency in degradation of ubiquitin-protein conjugates, thus substantially reducing the breakdown of proteins. Thus, MCP must play an important role in at least the ubiquitin-dependent pathway of protein degradation (Hershko and Ciechanover, 1992).

More recently, studies by Tanaka and coworkers have shown the involvement of MCP as part of the 26S protease in the degradation of the short-lived protein ornithine decarboxylase without the latter being ubiquitinated (Mukarami et al., 1992), thus identifying a novel nonlysosomal pathway of protein degradation, and invoking the involvement of MCP in the ubiquitin independent pathway of protein degradation .

Studies have identified mutant MCPs in cultured yeast cells, making them deficient in one or more of their proteolytic activities. These cells were found to be sensitive to elevated temperatures and to amino acid analogues. Close examination of these cells, however, revealed an accumulation of ubiquitin-protein conjugates, thus providing a genetic evidence for the involvement of MCP in the

ubiquitin pathway of protein degradation (Heinemeyer et al., 1991; Seufert and Jentsch, 1992; Richter-Ruoff et al., 1992).

Recently, recognition of the possible involvement of MCP in antigen processing has been a very exciting development from the earlier observations of Monaco and McDevitt (1982), who are the co-discoverers of the MHC-linked low molecular mass proteins (LMP) and who suggested their involvement in the generation of peptides for presentation by the MHC class I molecules (Monaco and McDevitt, 1986). In 1990 Parham reported the resemblance in size and in peptide composition between LMPs and MCPs.

Since then, there have been several reports in the literature providing some evidence for LMPs as being a special type of MCP: 1) Similar subunits were precipitated by anti-LMP and anti-MCP antibodies (Brown et al., 1991), 2) Two subunits of the immunoprecipitated MCP show an allelic polymorphism in the class II region of the MHC locus (Brown et al., 1991; Oritz-Navarette et al., 1991), 3) Two distinct cDNAs (LMP 2 and LMP 7 or RING 10 and RING12) encoded in the MHC region are homologous to known MCP subunits (Glynne et al., 1991; Martinez and Monaco, 1991; Kelly et al., 1991), 4) Only a small proportion of MCP was precipitated by antisera against.LMP 2 and LMP 7 (Brown et al., 1991), and finally, LMP particles have proteolytic activity (Goldberg and Rock, 1992).

However, two recent studies have found that the two MHC-encoded subunits were not essential for the processing of peptides bound by the MHC class I molecules (Momburg et al., 1992; Arnold et al., 1992), which disputes the hypothetical involvement of MCPs in

antigen processing, although such observations do not preclude a role for MCPs lacking the two subunits in antigen processing. To add complications to the matter, Goldberg and Rock (1992) on the one hand, and Hershko and Ciechanover (1992) on the other, have suggested a possible involvement for the 26S protease in antigen processing.

Aims of the present investigation.

Not a great deal of work has been carried out on the kinetics, structural, and mechanistic properties of the multicatalytic proteinase complex. Attention, however, has focused, over the past four years, on the molecular biology aspects of the proteinase.

At the start of this project, little information was available regarding the peptidylglutamyl-peptide hydrolase activity, in contrast to the well defined trypsin-like and chymotrypsin-like activities. The latter activities were found to obey Michaelis-Menten kinetics, and there have been several lines of evidence supporting their distinction.

The aim of this study was an attempt to fully characterize the peptidylglutamyl-peptide hydrolase activity, and to try to understand some of its kinetic behaviours with the synthetic substrate Z-Leu-Leu-Glu-NA, as Wilk and Orlowski (1983) reported that the activity of the pituitary enzyme did not obey Michaelis-Menten kinetics.

The observation that manganese activated the peptidylglutamyl-peptide bond hydrolase activity, extended my kinetic aim to a structural one. This time investigating the structure of the complex

33

using biophysical methods. In view of the size and shape of the complex, conformational changes were investigated as a possible explanation for the observed activation by manganese. Other effectors of the peptidylglutamyl-peptide hydrolase activity were also investigated with respect to possible conformational changes upon their action.

I have attempted to learn more about the different proteolytic activities, by means of looking at the degradation of peptide substrates by the complex using MCP as well as partially inhibited versions of MCP. The exercise also focused on the identification of peptides with specific cleavage sequences to respective activity.

CHAPTER 2

Materials and Methods

" *A higher level of organization is reached if the catalysts which are part of a given unit are themselves associated structurally in a manner which either increases their efficiency as a system or provides the system with special properties. That such organized chains of enzymes may be present in the insoluble framework of the cell now appears fairly probable and it has even been maintained that soluble catalysts may be grouped in labile polyenzymic functional units in the intact cell.*"

de Duve (1959).

2.1 Materials.

Frozen rat livers were obtained from North East Biomedical (Denham, Middlessex). Wistar rats were obtained from the University of Leicester Biomedical Services Unit (Leicester).

N-tBoc-Ala-Ala-Asp-SBzl and H-Glu-β-naphthylamide were a kind gift from Dr Martin Poe (Merck, Sharp and Dohme Research Lab., New Jersey, USA). Chymostatin analogues were a kind gift from Dr Robert J. Beynon (University of Liverpool, England).

The affinity label Cbz-Tyr-Ala-Glu-CH$_2$Cl, the peptidyl-chloromethylketones and the peptidyldiazomethanes were a kind gift from Dr Elliot Shaw (Friedrich Miescher-Institute, Basel, Switzerland). 4-(2-Aminoethyl)-benzenesulfonyl fluoride (Pefabloc) was obtained from Dr John Harrison (GIBCO BRL, UK). Antichymotrypsin and its mutant were a kind gift from Dr Harvy Rubin (University of Pennsylvania, Philadelphia, USA).

The Oxford peptides were obtained from Dr A. Townsend (Institute of Molecular Medicine, John Radcliffe Hospital, Oxford, England). The Carlsberg peptides were obtained from Dr K. Breddam (Carlsberg Laboratory, Department of Chemistry, Gamble Carlsberg Vej 10, Denmark). Other chemicals and materials were purchased from the following companies:

Aldrich Chemical Co. Ltd.
Phenylglyoxal and diisopropylfluorophosphate.

Amersham UK.

Amplify reagent.

Amicon Ltd.

Diaflo ultrafiltration membranes: PM10 (25 mm) and XM50 (76 mm).
Centricon 30 microconcentrators.

Anderman & Co. Ltd.

Collodion bags (10,000 and 75,000 molecular cutoff).

Bio-Rad Laboratories Ltd.

SDS-PAGE standard markers and protein assay dye reagent
concentrate.

Du Pont (UK) Ltd.

[1,3-^{3}H]-Diisopropylfluorophosphate (318.2 GBq/mmol).

Fisons Scientific Equipments.

Acetonitrile (HPLC grade), ethanol, methanol (HPLC grade), 1-
propanol (HPLC grade), diaminoethanetetra-acetic acid disodium salt,
ammonium sulphate, magnesium chloride, potassium chloride,
potassium hydroxide, potassium dihydrogen orthophosphate,
dipotassium hydrogen orthophosphate, hydrochloric acid, and
trichloroacetic acid.

May & Baker Ltd.

Cadmium chloride.

Millipore Products Division.

Ultrafree-MC filters (10,000 NMWL filter unit, polysulfone membrane, 10,000 molecular cutoff).

Pall Process Filtration Ltd.

Polyvinylidene difluoride (PVDF) membranes.

Peptide Institute Inc. (Osaka, Japan).

Boc-Leu-Ser-Thr-Arg-7-amido-4-methylcoumarin.

Pharmacia LKB Biotechnology Ltd.

Sephadex G50 (fine).

Rathburn Chemical Ltd.

Methanol and acetonitrile.

Romil Chemicals.

Acetonitrile 190 (far UV).

Sigma Chemical Co. Ltd (UK).

Z-Leu-Leu-Glu-β-naphthylamide, bovine serum albumin, Ala-Ala-Phe-7-amido-4-methylcoumarin, methylmethanethiosulfonate, chelex-100, N-ethylmaleimide, antipain, leupeptin, chymostatin, elastatinal, 3,4 dichloroisocoumarin, calcium chloride, diethyl p-nitrophenyl phosphate, trifluoroacetic acid, 2-nitro-4-carboxylphenyl N,N-diphenylcarbamate, 2-mercaptoethanol, bis tris propane, bradykinin, luteinizing hormone releasing hormone, neurotensin, splenopentin, oxidized insulin B chain, N-succinyl-Leu-Leu-Val-Tyr-7-amido-4-methylcoumarin, N,N,N',N'-tertra-methylethylene diamine (TEMED), bromophenol blue, ammonium persulphate, coommassie brilliant blue

R-250, 4-(2-hydroxyethyl)-1-piperazineethanesulfonic acid (Hepes), 5,5'-dithiobis-(2-nitrobenzoic acid), *Staphylococcus aureus* V8 proteinase, (p-amidinophenyl)-methanesulfonyl fluoride (APMSF), N-acetylimidazole, methylmethanethiosulfonate, manganese chloride, hydroxylamine, α-casein, and dimethyl sulfoxide.

Whatman Ltd.

Diethylaminoethyl cellulose (DE52) and nitrocellulose membranes (0.25 μm, 47 mm in diameter).

2.2 Purification of the multicatalytic proteinase complex.

The purification of the multicatalytic proteinase complex from fresh or frozen rat livers was carried out by a modification of the method of Rivett (1989b) and Rivett and Sweeney (1991).

The preparation was kept on ice or at 4°C during all steps of the purification except those involving use of the FPLC, which were performed at room temperature. EDTA (0.1 mM) and 2-mercaptoethanol (1mM) were added after each purification step.

Step 1: Homogenisation.

About 200 g of either fresh or frozen rat livers were used. The livers were homogenised in a Waring blender with 5 volumes of homogenisation buffer (20 mM Hepes/KOH buffer, pH 8.0, containing 1.0 mM EDTA and 1 mM 2-mercaptoethanol). After 3 bursts of 30 seconds each with 15 seconds in between, the homogenate was centrifuged for two hours at 12,500 rpm (26,000 x g) on the Sorvall RC5B GSA rotor. The supernatant was kept and the pellet discarded.

Step 2 : Ammonium sulphate fractionation.

Solid ammonium sulphate (194 g/l) was added to the supernatant from above to a 35 % saturation. After being left stirring on ice for 30 minutes, the preparation was centrifuged for 30 minutes at 12,500 rpm (26,000 x g) on the Sorvall RC5B GSA rotor. The pellet was discarded. Solid ammonium sulphate was again added to the supernatant to give a 60 % saturation (151 g/l). Once the ammonium sulphate had dissolved, the preparation was stirred for 45 minutes on ice and centrifuged as before.

The supernatant was discarded and the pellet was dissolved in 200 ml of 10 mM Tris/HCl buffer, pH 7.2. The preparation was then dialysed overnight against 10 mM Tris/HCl buffer, pH 7.2 containing 0.05 M KCl, 0.1 mM EDTA and 1 mM 2-mercaptoethanol with one buffer change.

Step 3 : Ion exchange chromatography.

The dialysed ammonium sulphate fraction was centrifuged at 18,000 rpm (39,000 x g) in the Sorvall SS-34 rotor for 20 minutes, after which it was applied to a C24/40 column of DEAE-cellulose which had been equilibrated in 10 mM Tris/HCl buffer, pH 7.2 containing 0.05 M KCl. The column was washed with the same buffer, and the proteinase was eluted by applying a linear gradient (2 x 1.5 l) of 0.05-0.350 M KCl in 10 mM Tris/HCl buffer, pH 7.2.

Fractions containing proteinase activity were pooled, diluted two fold with 10 mM Tris/HCl buffer, pH 7.2 and then concentrated

approximately 4-fold by ultrafiltration in an Amicon 400 concentrator using an XM 50 membrane.

Step 4 : Mono Q chromatography.

The preparation was centrifuged for 20 minutes at 20,000 rpm (49,000 x g) on the Sorvall SS-34 rotor. The filtered supernatant was then loaded, at room temperature, on to a Mono Q 10/10 FPLC column (Pharmacia) which was equilibrated in 20 mM Tris/HCl buffer, pH 7.2 containing 0.1 M KCl. The proteinase was eluted by applying a linear gradient of 0.1-0.5 M KCl in 20 mM Tris/HCl buffer, pH 7.2. The pooled active fractions were concentrated by ultrafiltration to a volume of 2 ml, using the Amicon 400 (XM 50 membrane) at first then the Amicon 10 (PM10 membrane).

Step 5 : Gel filtration chromatography.

The sample from step 5 was centrifuged for 5 minutes at high speed in a bench centrifuge, and filtered using a 0.2 μm acrodisc filter. The filtered sample was then loaded on to a Superose 6 FPLC column (preparative size, Pharmacia) which was equilibrated in 50 mM potassium phosphate buffer, pH 7.0, containing 0.1 M KCl. Peak fractions were collected, pooled, and dialysed against two changes of 20 mM Tris/HCl buffer, pH 7.2 containing 0.01 M KCl, 1 mM 2-mercaptoethanol and 0.1 mM EDTA.

Step 6 : Mono Q chromatography.

The dialysed preparation was loaded on to a Mono Q 5/5 FPLC column (Pharmacia) which was equilibrated in 20 mM Tris/HCl buffer,

pH 7.2 containing 0.01 M KCl. The proteinase was eluted from the column with a linear gradient of 0.1-0.5 M KCl in 20 mM Tris/HCl buffer, pH 7.2. Peak fractions were pooled for final dialysis.

Step 7 : Final dialysis.

The purified proteinase was dialysed, overnight, against 50 mM potassium phosphate buffer, pH 7.0 containing 0.1 mM EDTA, 1 mM 2-mercaptoethanol and 10 % glycerol (v/v). The purity of the proteinase was checked by SDS-polyacrylamide gel electrophoresis and by determining specific activities of each activity. The enzyme was then stored as 1mg/ml solution at -20°C.

2.3 Protein estimation.

Protein concentrations were estimated by the method of Bradford (1976) using the reagent from Bio-Rad with bovine serum albumin (BSA) as standard. Protein standard and unknowns (up to 10 μg protein) were made up to a final volume of 100 μl using either buffer or deionised distilled water.

The blank was set up similarly. Bio-Rad reagent (1 ml of a 1/5 diluted solution) was added to each sample, the solutions were vortexed, and left at room temperature for 10 min. After which the absorbance at 595 nm was recorded. The concentration of protein was determined from a standard curve (Figure 2.1).

2.4 Assays of the different activities of the Proteinase complex.

The different proteolytic activities of the proteinase complex were assayed using a variety of synthetic fluorogenic peptide substrates, using either a stopped assay or a continuous assay as described below.

The fluorescence was measured in a Perkin-Elmer Fluorimeter, model LS-3B, which was equipped with a thermostated cell holder linked to a water bath, temperature of which was set at 37°C. The excitation and emission wavelengths were set depending on the nature of the fluorescent group of the synthetic substrate as described below.

The continuous assay method involved capture of data from the LS-3B RS-232C interface of the Perkin-Elmer Fluorimeter with a Viglen IBM compatible Personal Computer, using the Flusys software package for data storage and analysis (Rawlings and Barrett, 1990).

Assays with synthetic peptidyl 7-amino-4-methylcoumarin substrates.

Assays were carried out as described by Rivett (1989b). Proteinase (0.005-0.01 mg/ml) was incubated in a total volume of 0.2 ml of 50 mM Hepes/KOH buffer, pH 7.5, containing 40 μM of either Ala-Ala-Phe-7-amido-4-methylcoumarin (AAF-AMC), Boc-Leu-Ser-Thr-Arg-7-amido-4-methylcoumarin (LSTR-AMC), or N-succinyl-Leu-Leu-Val-Tyr-7-amido-4-methylcoumarin (LLVY-AMC). The incubation was for 20 or 30 min at 37°C, and the reaction was stopped by addition of 0.1 ml stop mix (an acid solution containing 0.25 g sodium acetate

trihydrate and 4.375 ml of 1 M acetic acid in 25 ml of water); followed by 2 ml of distilled and deionised water.

The fluorescence of the released 7-amino-4-methylcoumarin was read at an excitation of 370 nm and an emission of 430 nm. A calibration curve was prepared using free 7-amino-4-methylcoumarin as standard (Figure 2.2).

Assays with synthetic peptidyl naphthylamide substrates.

Assays were carried out by a modified version of the method of Dahlmann et al. (1985). Proteinase (0.005-0.01 mg/ml) was incubated in a total volume of 0.2 ml of 50 mM Hepes/KOH buffer, pH 7.5, containing 0.1 , 0.4 mM Cbz-Leu-Leu-Glu-β-naphthylamide (LLE-NA) or as indicated. The incubation was for 20 or 30 min at 37°C. The reaction was stopped by addition of 0.3 ml ethanol followed by the addition of 2 ml of distilled and deionised water.

The fluorescence of the released β-naphthylamine was read at an excitation of 333 nm and an emission of 450 nm. The substrate H-Glu-β-naphthylamide was used under similar assay conditions at a concentration of 0.4 mM.

A calibration curve for free β-naphthylamine (NA) estimation was prepared by digesting the substrate LLE-NA with the *Staphylococcus aureus* strain V8 proteinase, in 50 mM ammonium bicarbonate buffer, pH 7.8, under which conditions the protease is specific for glutamyl bonds (Drapeau, 1977). In a typical digestion, 0.1 mg/ml V8 proteinase (4 μl of 5 mg/ml proteinase) were added to

0.1 mM LLE-NA (2 µl of 10 mM LLE-NA) in a total volume of 0.2 ml of 50 mM ammonium bicarbonate buffer, pH 7.8.

The course of reaction was monitored continuously at 37°C until all the substrate was converted to products ie no more change in fluorescence was observed (Figure 2.3). Free β-naphthylamine which was produced was used to construct a calibration curve for both stopped assays (Figure 2.4) and continuous assays (Figure 2.5).

Assays with synthetic peptidyl thioester substrates.

The multicatalytic proteinase activity was also measured with a peptide thioester, Boc-Ala-Ala-Ala-Asp-SBzl (BAAADT), as described by Poe et al. (1988). The reaction mixture (0.2 ml) contained 0.4 mM substrate(8 µl of 10 mM BAAADT) and 0.01 mg/ml proteinase in 50 mM Hepes/KOH buffer, pH 7.5. Incubations were for 30 min at 37°C.

The released 4-nitrobenzenethiol was quenched by the addition of 0.5 mM DTNB (25 µl of 5 mM DTNB), and the increase in absorbance was measured at 412 nm using a Perkin-Elmer Lamda 5 spectrophotometer. Absorbance increase was converted to enzymatic rates using an extinction coefficient of 13600 cm^{-1} M^{-1}.

The same volume of DTNB was also added to the reference cell in order to correct for the background reaction of DTNB with the sulfhydryl groups on the proteinase and the nonenzymatic hydrolysis of the thiobenzyl ester.

Assays with synthetic peptides containing anthraniloyl and 3-
nitrotyrosine groups: The Carlsberg peptides.

The hydrolysis of substrates containing the anthraniloyl and 3-
nitrotyrosine groups, based on intramolecular quenching, was assayed
by monitoring the increase in fluorescence emission at 420 nm upon
excitation at 320 nm (Breddam and Meldam, 1992).

Assay mixtures contained 0.01 mg/ml proteinase and 0.25 μM
substrate (10 μM stock solution in DMSO) in 50 mM Hepes/KOH
buffer, pH 7.5. Reactions were started by the addition of substrate
and the course of the reaction was monitored continuously for a
period of up to 60 min.

A conversion coefficient, to convert values from fluorescence
units to pmoles, was obtained from digesting the substrate DG8
(sequences: ABz-Ala-Phe-Ala-Phe-Glu-Val-Phe-TyrNO$_2$-Asp-OH) with
the *Staphylococcus aureus* strain V8 proteinase. This peptide was
found by Breddam and Meldam (1992) to be a relatively good
substrate for the V8 proteinase. In a typical digestion, 0.025 mg/ml
V8 proteinase (5 μl of 1 mg/ml proteinase) were added to 0.25 μM
DG8 (5 μl of 10 μM DG8) in a total volume of 0.2 ml of 50 mM
ammonium bicarbonate buffer, pH 7.8. The course of reaction was
monitored continuously at 37°C, until all the substrate was converted
to products ie no more change in fluorescence (Figure 2.6).

Assays with peptide substrates.

Solutions (1 mg/ml) of commercial or custom made peptides
were dissolved in 5 mM KOH to give a 1 mg/ml peptide solution with a

pH of 8.5. The use of 5 mM KOH was found helpful to solubilize the peptides in water, where the treatment was milder enough not to cause any deamination of peptides. Dick et al. (1991) have used similar approach to solubilize their peptides, with no report of any deamination occuring.

A typical reaction mixture in 50 mM Hepes/KOH buffer, pH 7.5 (0.2 ml) contained 0.05 mg/ml enzyme (10 µl of a 1 mg/ml solution) and 0.1 mg/ml peptide (20 µl of a 1 mg/ml solution). The incubation was at 37°C for 60, 120 min. The reaction was stopped by the addition of 25 µl of 1% TFA solution, also to reduce the pH to about pH 2. Subsequently, the products were separated by HPLC and analysed by amino acid analysis as described in Section 2.5.

2.5 HPLC separation of peptides.

The sample, from Section 2.4, was centrifuged at high speed on a bench microfuge for five minutes. The sample was then loaded onto a Helwett Packard HP1090 liquid chromatograph using a Vydac C18 (5 µm, 250 x 4.6 mm) reverse phase column. The products were eluted from the column on a linear gradient of 0-100% acetonitrile containing 0.05% TFA in 35 min.

The peak fractions, monitored at 215 nm or 278 nm, were collected manually. The fractions obtained were then lyopholized, and sent for amino acid analysis, kindly performed by John Keyte (Department of Biochemistry, Queen's Medical centre, Nottingham).

2.6 Buffers for the pH study.

The buffer systems, for the effect of pH studies, were made up as described in Data Biochemical Research (3rd Ed.), where the ionic strength was kept constant. The pH of the different buffer solutions was measured at room temperature using a Corning pH meter 140, which was calibrated at room temperature with standard solutions of pH 7 and pH 4 or pH 7 and pH 10.

2.7 Inhibitors and activators studies.

For inhibitor studies, the multicatalytic proteinase complex was preincubated at $25^{\circ}C$ in the presence of inhibitor prior to 20-fold dilution and assay for 20 min at $37^{\circ}C$. MCP was put through a Sephadex G-50 spun column equilibrated with 50 mM Hepes/KOH buffer, pH 7.5, before preincubation with DFP.

Stock solutions of inhibitors were made up in water (Pefabloc, APMSF, protein protease inhibitors), dimethylsulfoxide (peptide aldehydes, peptidylchloromethylketones, peptidyldiazomethanes, 3,4-dichloroisocoumarin), or propanol (DFP, PMSF). These solvents were included in control incubations where appropriate.

For studies with metal ions, the Hepes buffer was pre-treated with chelex-100 (Sigma). Salt solutions of Metal ions were made up in water.

2.8 Labelling of the non-cooperative component of the peptidylglutamyl-peptide hydrolase activity.

The strategy adopted for the labelling was to make a chemically modified proteinase complex where most of the proteolytic sites were chemically blocked, except the LLE1 site which could then be labelled with [^{3}H]-DFP.

The chemical modification involved the inhibition of the so far described proteolytic activities, namely the trypsin-like activity (assayed with LSTR-AMC), the chymotrypsin-like activity (assayed with AAF-AMC and LLVY-AMC), and the cooperative component of the LLE2 activity (assayed with 0.4 mM LLE-NA), using specific irreversible serine protease inhibitors as described below. LLE1.MCP was defined as a modified MCP with the LLE1 component being active (Chapter 4).

The results presented below were from one such experiment, and the adopted methodology could be scaled up for labelling higher amount of the proteinase complex.

<u>The Making of LLE1.MCP.</u>

MCP (1.5 ml, 1 mg/ml) was concentrated in a centricon 30 microconcentrator to a volume of 290 μl, and was dialysed overnight against 50 mM Hepes/KOH buffer, pH 7.5. To the dialysed solution was added 6 μl of 50 mM Pefabloc stock solution (giving a final concentration of 1 mM) and the mixture was incubated for 60 min at 25°C. Then 1.4 μl of 5 mM 3,4 dichloroisocoumarin solution (giving a final concentration of 22 μM) was added to the mixture, which was further incubated for 30 min at 25°C.

The mixture was then dialysed overnight against 50 mM Hepes/KOH buffer, pH 7.5 to remove excess inhibitors. The generated LLE1.MCP (0.83 mg, 2.76 mg/ml) was used in subsequent the labelling step.

Labelling the LLE1 active site.

The LLE1.MCP solution (300 μl, 2.76 mg/ml) was incubated with 60 μl of 0.12 mM [1,3-^{3}H]-DFP (318.2 GBq/mmol in propylene glycol, 20 μM final concentration) for a period of 4 h at 25°C. Then 10 μl of 200 mM DFP (in propanol, giving a final concentration of 5 mM) was added to the mixture. The mixture was further incubated overnight at 4°C for the ageing process to occur (see Figure 4.13).

The labelled solution was then put through a G-50 Sephadex gel filtration column to separate the protein from the propylene glycol and excess DFP, 1 ml fractions were collected (protein eluted at fractions 6 and 7). The yield of the labelled protein was 0.83 mg in 50 mM Hepes/KOH buffer, pH 7.5 (0.4 mg/ml solution).

Fluorography of the labelled LLE1.MCP.

Labelled LLE1.MCP (150 μl, 60 μg, 1,650 cpm) was lyophilized and resuspended in SDS sample buffer for polyacrylamide gel electrophoresis as described under Section 2.10. After destaining the gel, the latter was immersed in the fluorographic reagent Amplify (Amersham) for 30 min. Then the gel was dried in a Bio-Rad dual temperature slab gel drier for 2 hours at 60°C. The dried gel was exposed to a Kodak X-Omat AR film at -70°C for a period of two to four weeks.

Identification of the labelled subunit.

The identification procedure involved first the separation of the proteinase subunits on reverse phase chromatography (HPLC), and second the radioactivity counting of the separated subunits.

The remaining labelled LLE1.MCP solution (1.85 ml, 20,064 cpm) was concentrated in a centricon 30 microconcentrator to a volume of 200 μl. The concentrate was found to contain only 0.4 mg of labelled protein. The concentrate was used for the separation of the subunits as described under Section 2.9.

The collected subunits were counted for radioactivity as described below.

Radioactive isotope counting.

The counting of vials containing tritium was performed in United Technologies Packard, 2000CA TRI-CAMD, liquid scintillation analyzer. The counting was on a 10 min program designed for counting low energy emission spectrum of tritium.

Scintillation fluid (10 ml of Optiphase safe) was added to up to 0.5 ml of solution to be counted, in a 20 ml plastic vial. The vials were then thoroughly mixed and placed in the chamber of the analyzer. They were left in the dark for a period of at least four hours before being counted.

2.9 HPLC separation of the multicatalytic subunits.

Separation of the subunits of the multicatalytic proteinase complex can be achieved after dissociation of the complex under acid conditions, followed by reverse phase chromatography on HPLC (Tanaka et al, 1988).

MCP sample (up to 0.5 mg protein) was treated with TFA (1% stock solution) to give an acidic solution with a pH of approximately pH 2. The mixture was then incubated, at room temperature, for at least three hours in order to achieve dissociation of the complex. The sample was filtered under centrifugation, before being loaded on to an Anagel-TSK phenyl-5PW (10 μm, 75 x 7.5 mm) reverse phase column (HPLC), which had been equilibrated in 0.05% TFA. The subunits were eluted, at a flow rate of 0.2 ml/min, according to the following protocol:

Step 1: Time   0-11   min: loading of sample.

Step 2: Time   11-71   min: 0-30% acetonitrile in 0.05% TFA.

Step 3: Time   71-251 min: 30-50% acetonitrile in 0.05% TFA.

Step 4: Time 251-281 min: 50-80% acetonitrile in 0.05% TFA.

Step 5: Time 281-291 min: 80-100% acetonitrile in 0.05% TFA.

Step 6: Time 291-301 min: 100-0% acetonitrile in 0.05% TFA.

The diode array detector system was set at two wavelengths namely 215 and 280 nm, which were monitored simultaneously. The maximal back pressure on the HPLC was set at 80 bar. The subunits (30-50% acetonitrile in 0.05% TFA) were collected manually as they eluted from the column.

2.10 Polyacrylamide gel electrophoresis.

<u>Solutions for polyacrylamide gel elctrophoresis.</u>

<u>1) Acrylamide/bisacrylamide (30:0.8).</u>

To 30 g acrylamide and 0.8 g N,N' methylenebisacrylamide was added water to 100 ml. The solution was stirred until all the acrylamide had dissolved, then filtered, and stored at 4°C.

<u>2) 3x sample buffer (SDS-PAGE).</u>

2.0 ml of 10 % (w/v) SDS.

2.0 ml of 0.5 M Tris/HCl buffer, pH 6.8.

20 μl of 10 % bromophenol blue solution in ethanol.

2.0 ml of glycerol.

0.5 ml of 2-mercaptoethanol.

3.48 ml of water.

<u>3) 3x sample buffer (non-denaturing-PAGE).</u>

20 μl of 10 % bromophenol blue solution in ethanol.

2.0 ml of glycerol.

7.48 ml of water.

<u>4) 10x running buffer for SDS-PAGE.</u>

10 g of SDS.

30 g of Tris.HCl.

144 g of glycine.

11 of water.

5) 10x running buffer for non-denaturing-PAGE.

30 g of Tris.HCl.

144 g of glycine.

1l of water.

6) Gel stain.

0.25% (w/v) of Coomassie brilliant blue R.

10% (v/v) of acetic acid.

40% (v/v) of methanol.

7) Gel destain.

10% (v/v) of acetic acid.

40% (v/v) of methanol.

SDS polyacrylamide gel electrophoresis.

SDS polyacrylamide gel electrophoresis (SDS-PAGE) was carried out using the discontinuous buffer system described by Laemmli (1970), with 4% polyacrylamide in the stacking gel and 15% polyacrylamide in the separating gel, using the mini-protean II apparatus (Bio-Rad) with 0.75 mm spacers and 10 well combs.

Composition of SDS-PAGE gels

1) Separating gels

    6.3 ml of 30% acrylamide/0.8% bisacrylamide.

    1.55 ml of 3M Tris/HCl buffer, pH 8.9.

    4.53 ml of filtered and deionised water.

    125 μl of 10% SDS.

    6.25 μl of TEMED.

    50 μl of 10% ammonium persulphate.

2) Stacking gels

    0.5 ml of 30% acrylamide/0.8% bisacrylamide.

    1.38 ml of 0.1M Tris/HCl buffer, pH 6.8.

    3 ml of filtered and deionised water.

    50 μl of 10% SDS.

    4 μl of TEMED

    20 μl of 10% ammonium persulphate.

Ethanol washed gel plates were clamped together firmly in the casting stand. The acrylamide/Tris/SDS/water separating gel solution was degased. After addition of ammonium persulphate and TEMED, the solution was carefully poured between the plates to avoid any air bubbles in the gel. The gel was overlayed with butanol-saturated water solution and allowed to set.

Once the gel was set, the stacking gel was prepared as described above, with the solution being degased before the addition of ammonium persulphate and TEMED. The butanol solution was washed

away with water. After removal of excess water, the stacking gel was carefully poured. A 10 well comb was then inserted and the gel allowed to set. The prepared gels were located in a cradle in an electrophoresis tank, with the inner chamber and the bottom of the tank filled with 1x SDS buffer.

Protein samples (up to 50 μg protein) for SDS-PAGE analysis were prepared by adding to the protein solution a 1/3 volume of 3x sample buffer. The samples were then denatured by heating at 95°C for 3 min. After cooling, the samples were applied to wells of the gels with a Hamilton syringe. Gels were then electrophoresed at 100V until the bromophenol blue had reached the end of the separating gel.

Gels were then stained for protein by immersion in gel stain solution for 3 hours followed by destaining for several hours with three changes of solution. The gels were photographed or dried.

Non-denaturing polyacrylamide gel electrophoresis.

Non-denaturing polyacrylamide gel electrophoresis was carried out with 4% polyacrylamide separating gels, using the mini-protean II apparatus (Bio-Rad) with 0.75 mm spacers and 10 well combs.

Composition of Non-denaturing-PAGE gels.

1.65 ml of 30% acrylamide/0.8% bis-acrylamide.

1.24 ml of 3M Tris/HCl buffer, pH 8.9.

9.46 ml of filtered and deionised water.

10 μl of TEMED.

60 μl of 10% ammonium persulphate.

The gel plates were set up as described above. The acrylamide/Tris/water gel solution was degased. After addition of ammonium persulphate and TEMED, the solution was carefully poured. A 10 well comb was then inserted and the gel allowed to set. The prepared gels were located in a cradle in an electrophoresis tank, with the inner chamber and the bottom of the tank filled with a chilled 1x non-denaturing-PAGE running buffer.

Samples were prepared by adding to the protein solution a 1/3 volume of 3x non denaturing sample buffer. The gel was pre-run for 1 hour at 100V at 4°C, before samples were applied. The electrophoresis was at 100 V at 4°C for four hours. Gels were stained and destained as described above.

Gels were also stained for enzyme activity by incubating the gel slice in a petri dish with a substrate solution, either 0.1 mM or 0.4 mM LLE-NA in 50 mM Hepes/KOH buffer, pH 7.5, with continuous shaking at 37°C, for a period of up to two hours. The gel slice was removed, washed with water, and then viewed under UV light to visualise any proteinase activity associated with protein band(s). In the case of the LLE-NA substrate, it was not possible to take pictures of activity stains.

2.11 Electroblotting of proteins from gel to membrane.

The method is based on the wet electrotransfer system described by Matsudaira (1987), from SDS PAGE protein gel to polyvinylidene difluoride (PVDF) membrane, using the Bio-Rad wet blotting system.

<u>Solutions for the electroblotting.</u>

<u>1) Transfer buffer.(1x)</u>

5.8 g of Tris.HCl.

2.9 g of glycine.

0.3 g of SDS.

100 ml of methanol.

900 ml of water.

<u>2) PVDF membrane Stain.</u>

0.1 % (w/v) of Coomassie brilliant blue R.

50 % (v/v) of methanol.

49.9 % dionised distilled water.

<u>3) PVDF membrane destain.</u>

50 % methanol.

10 % acetic acid.

40 % deionised water.

SDS PAGE gels are run as described in Section 2.10. When the bromophenol blue has nearly reached the end of the gel, the Scotch pads and two pieces of 3MM blotting paper are soaked in the transfer buffer, while a gel size piece of membrane is first soaked in methanol then in transfer buffer until needed.

Once the gel has finished running, the blotting cassette was used to construct a gel sandwich, as shown in diagram 1., with care not leave any air bubbles between the layers:
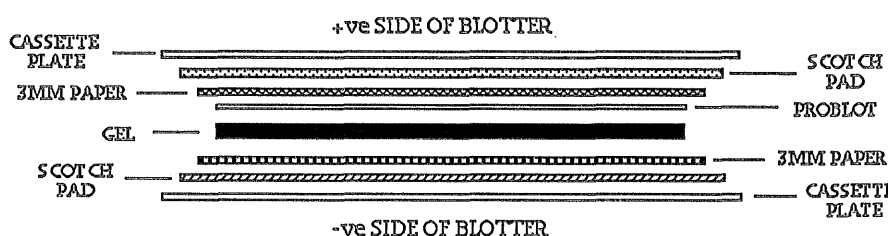

Diagram 1.

The cassette is then placed in the blotter tank full of transfer buffer, and ensuring that the buffer completely covers the gel. The transfer is then run for three hours at 150 mA. When the transfer is complete, the PVDF membrane is then stained for only 5 min (just to be able to see the protein bands), and destained until the protein bands are clearly visible. The blot is then rinsed several times in deionised water and left to dry.

Protein sequencing was kindly performed by Dr Kathryn Lilley and Liz Cavanagh (Department of Biochemistry, University of Leicester).

2.12 Electron microscopy.

Negative staining of MCP samples was carried out on copper grids covered with carbon film, which had been rendered hydrophilic by a 30 seconds exposure to glow discharge in a plasma cleaner (In

house built vacuum coating unit with a Polaron Bio-Rad power supply). MCP preparations (0.01-0.2 mg/ml) were applied to a grid and the molecules were left to adsorb for 5 minutes. After removal of the droplet with a thin strip of filter paper, 10 μl of uranyl acetate (2%, pH 4.2) were applied to the grid. After 1 minute, excess stain was removed with thin strips of filter paper and the grids were dried in air.

The preparations were viewed with a Siemens Elmiskop 102 or a JEOl 100 CX electron microscope at magnifications of 100,000 to 250,000 and an acceleration voltage of 80 kV. Photographs were then taken and film developed later. The electron microscopes were calibrated using a difracting grating replica.

2.13 Sedimentation velocity.

Sedimentation velocity analysis was carried out using scanning absorption optics at a wavelength of either 280 nm or 231 nm, on either the MSE Centriscan-75 analytical ultracentrifuge or the Beckman Optima XL-A analytical ultracentrifuge. For samples containing the substrate LLE-NA scanning absorption optics at a wavelength of 295 nm were employed, thus reducing the background absorption of the naphthylamide group.

Samples for analysis were freshly prepared with a dialysed proteinase solution (1.0 mg/ml) solution dialysed against 50 mM Hepes/KOH buffer, pH 7.5 containing 1mM 2-mercaptoethanol). Volumes of the samples were 400 μl in the case of the Centriscan 75 and 300 μl for the XLA. When metals were added, the buffer system used was treated with chelex-100.

Proteinase samples (0.4-0.8 mg/ml), in 50 mM Hepes/KOH, pH 7.5 containing 2-mercaptoethanol, were loaded into cells avoiding generation of shearing forces. The cells were placed in rotor and taken up to 25,000 rpm at 20°C. The sedimentation boundaries were recorded for each sample at fixed intervals (5-20 min).

Sedimentation coefficients ($s_{20,b}$) were estimated from the rate of migration of the mid-point of the sedimenting boundary for each time point. These positions were digitised directly from the recorder traces using an Apple Graphics Tablet linked to an Apple II+ microcomputer.

The program used permits the full precision of the tablet to be used and calculate the $s_{20,b}$ values corrected for rotor expansion, reference to reference calibration and true rotor speed (Bowen and Rowe, 1970). These values were then corrected to standard solvent conditions (water at 20°C) using the following equation (obtained from Van Holde (1985):

$$s_{20,w} = s_{20,b} \times [((1-\upsilon\rho)_{20,w} \times \eta_{20,b}) / ((1-\upsilon\rho)_{20,b} \times \eta_{20,w}))] \qquad (2.1)$$

Where b = buffer used, υ = partial specific volume, ρ = density of the solution, and η = viscosity of the solvent.

As the solvent used, 50 mM Hepes/KOH buffer, pH 7.5, has similar characteristics in density and viscosity to water, it could then be assumed that $s_{20,b}$ values are equivalent to the standard $s_{20,w}$ values.

2.14 Dynamic light scattering.

Translational diffusion coefficients were measured on a Biotage Model 801 Molecular Size Detector using dynamic light scattering. The technique is based on the measurement of fluctuations in scattered light intensity caused by the relative movements of the proteinase complex in solution. Light from a near infra-red semiconductor laser ($\lambda=$ 780 nm) is passed through a measurement cell and is scattered by molecules moving under "Brownian" motion. Photons which are scattered at 90° to the incident laser beam are collected by a lens and conducted to an Avalanche Photo Diode (APD) via an optical fibre.

The APD produces a single electrical pulse for each photon detected and these pulses are stored by an integral computer. The time scale of these fluctuations depends on the speed of movement of the proteinase complex, hence the translational diffusion coefficient (D_T) can be obtained from these measurements. Photons are counted into windows or channels and the time constant of intensity fluctuation obtained by autocorrelation of this data (Claes et al., 1992).

MCP (1.0 mg/ml) was dialysed overnight against 50 mM Hepes/KOH buffer, pH 7.5 The dialysed preparation was then used for the dynamic light scattering studies, where 0.5 ml of 0.1 mg/ml MCP solution was prepared for each study. For the studies where $MnCl_2$ was used, the dialysis of the proteinase and subsequent sample preparation was performed using a Hepes buffer which was treated with chelex-100. Before before injected, all samples were carefully filtered. All experiments were performed at room temperature, and

the obtained data are the average of at least thirty measurements taken in succession.
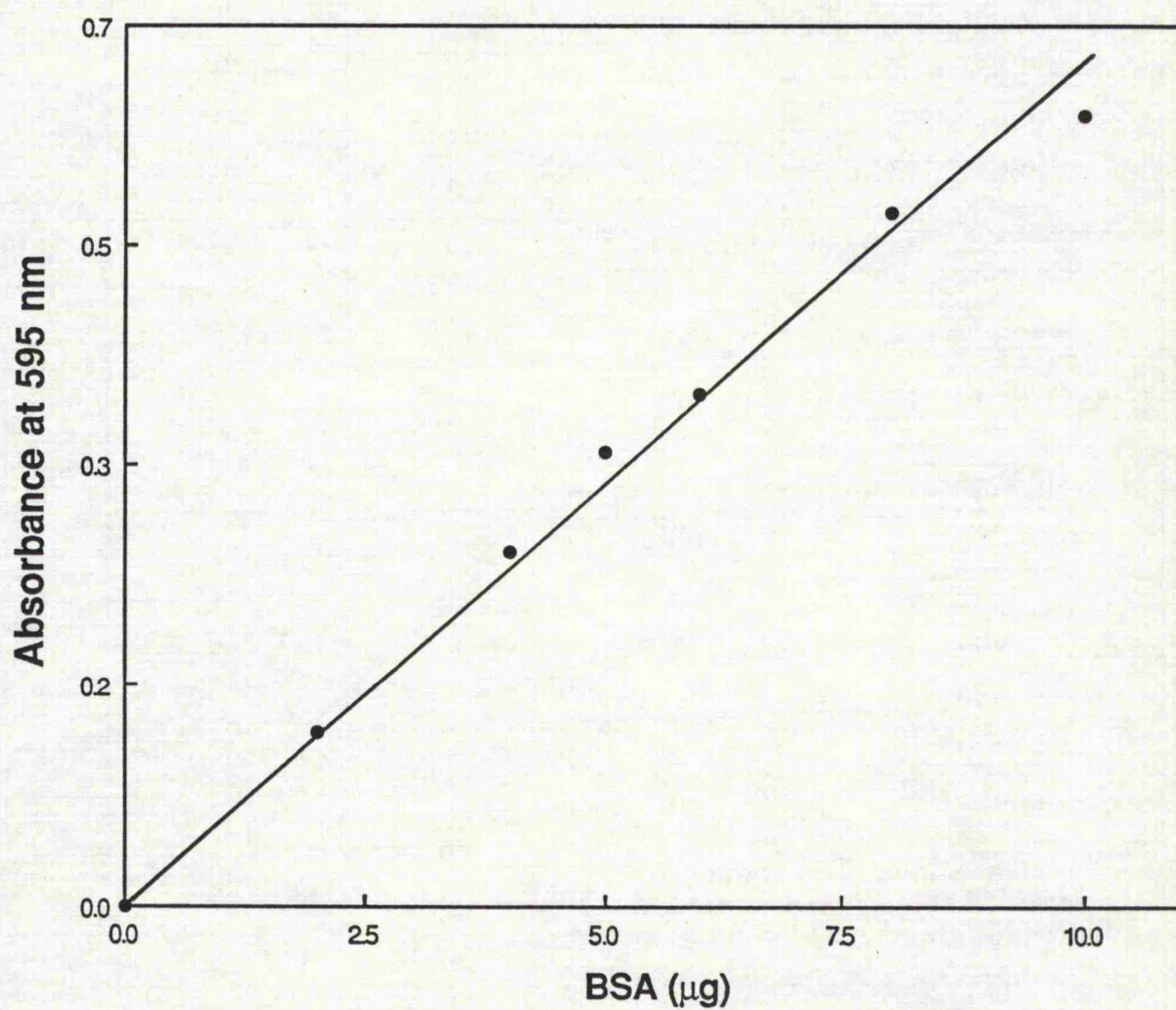
Figure 2.1: Calibration curve for protein estimation.

The curve was prepared as described under Section 2.3, with bovine serum albumin as a standard.
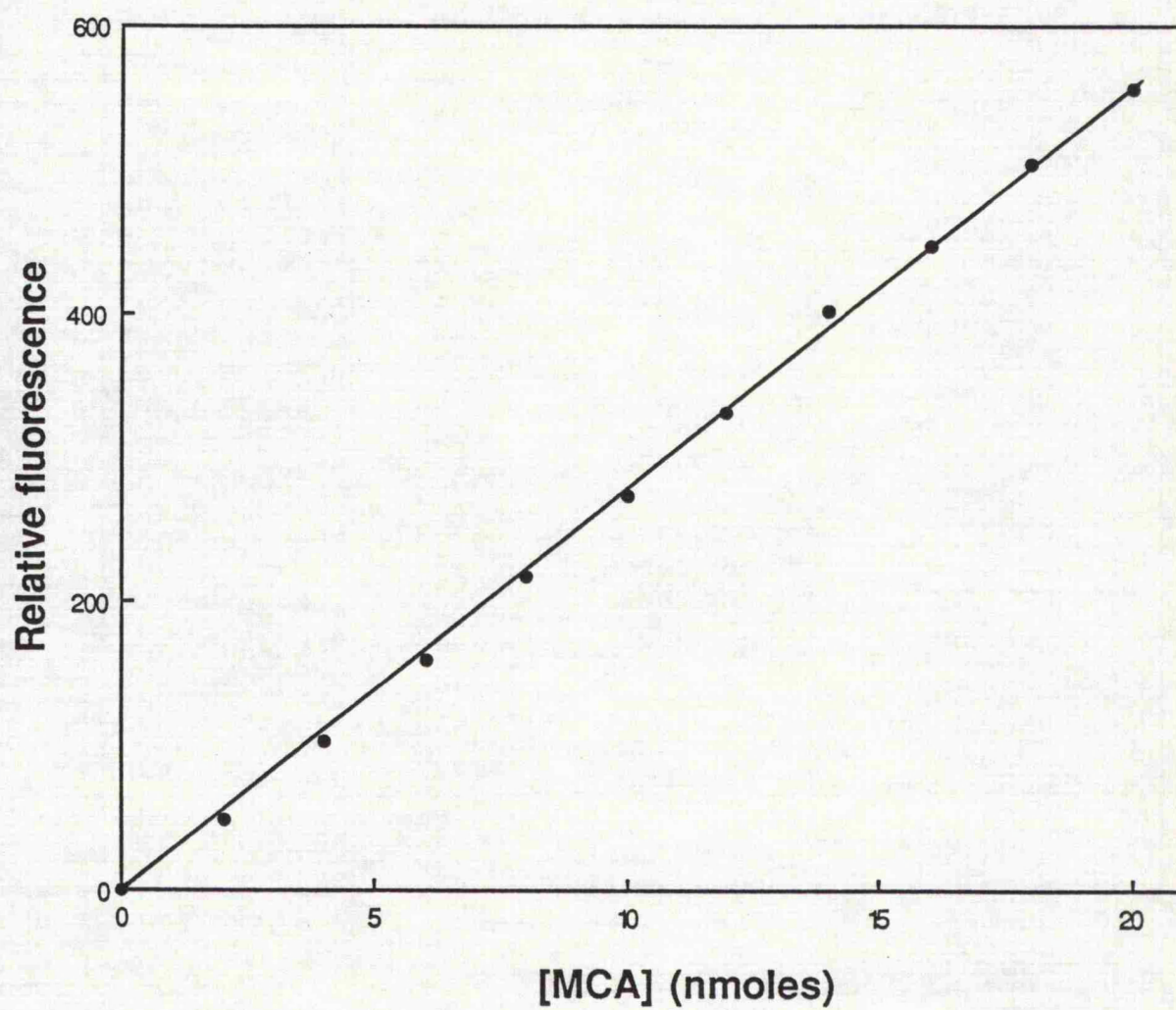
Figure 2.2: Calibration curve for free MCA estimation.

The curve was prepared as described under Section 2.4. MCA = 7-amino-4-methylcoumarin.

Figure 2.3: Time course of digestion of Z-Leu-Leu-Glu-β-
naphthylamide with *Staphylococcus aureus*
strain V8 protease.

The digestion was performed as described under Section 2.4.

Figure 2.4: Calibration curve for free β-naphthylamine estimation for the stopped assay method.

The calibration curve was prepared as described under Section 2.4. The stopped assay method involves the use of 3 ml cuvettes for measuring the fluorescence intensity.
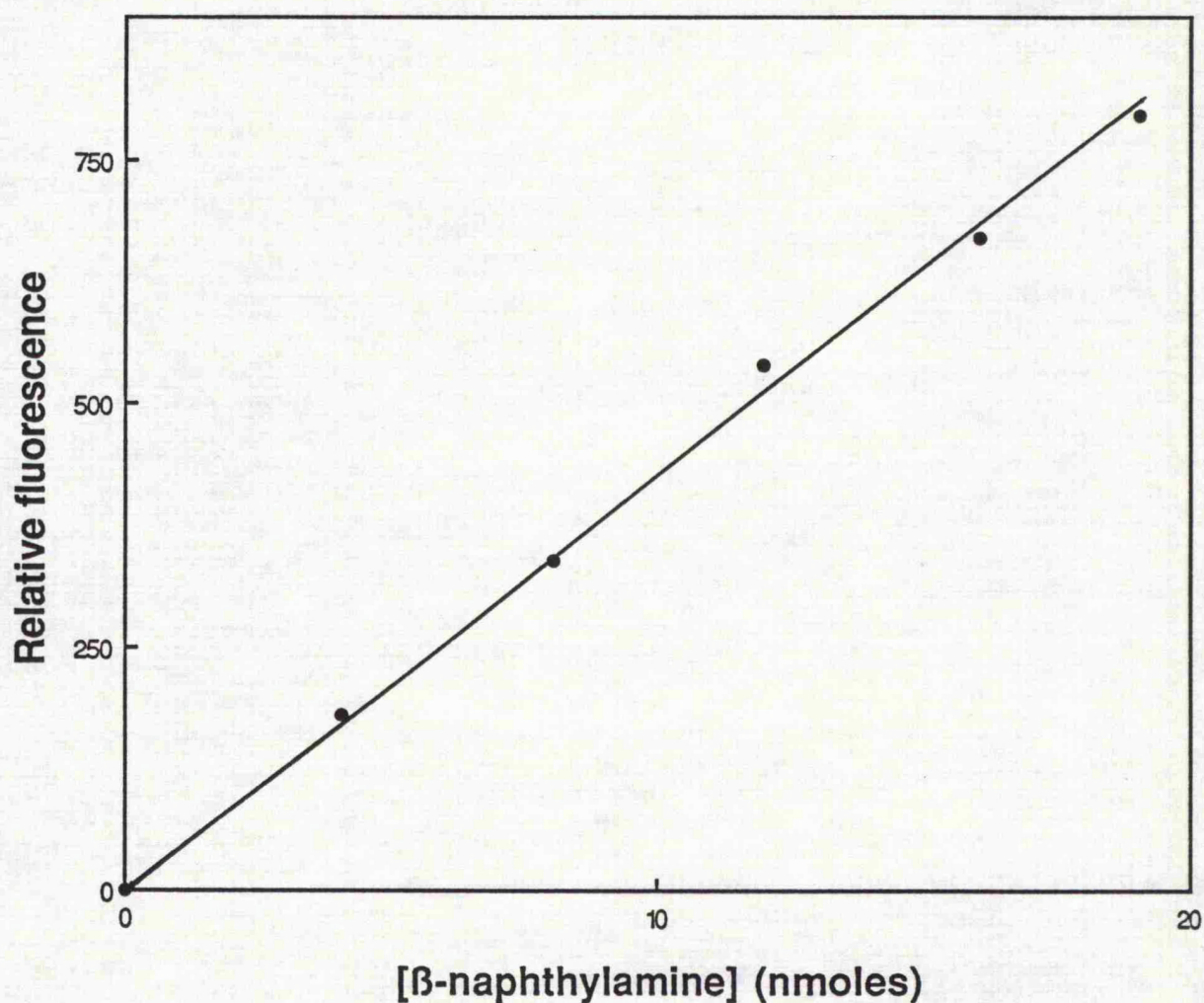
Figure 2.5: Calibration curve for free β-naphthylamine estimation for the continuous assay method.

The calibration curve was prepared as described under Section 2.4. The continous assay method involves the use of microcuvettes for measuring the fluorescence intensity with the Flusys package.
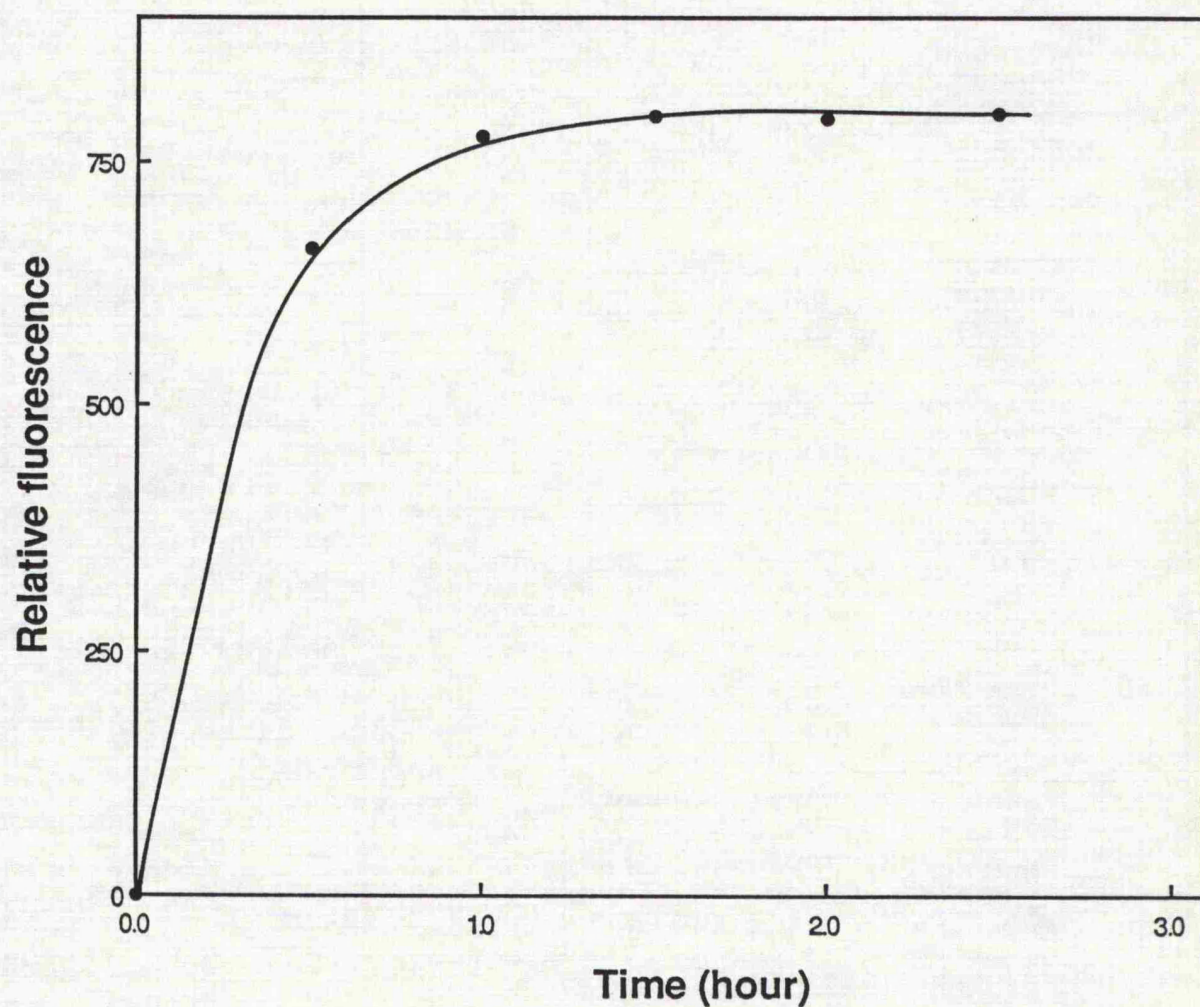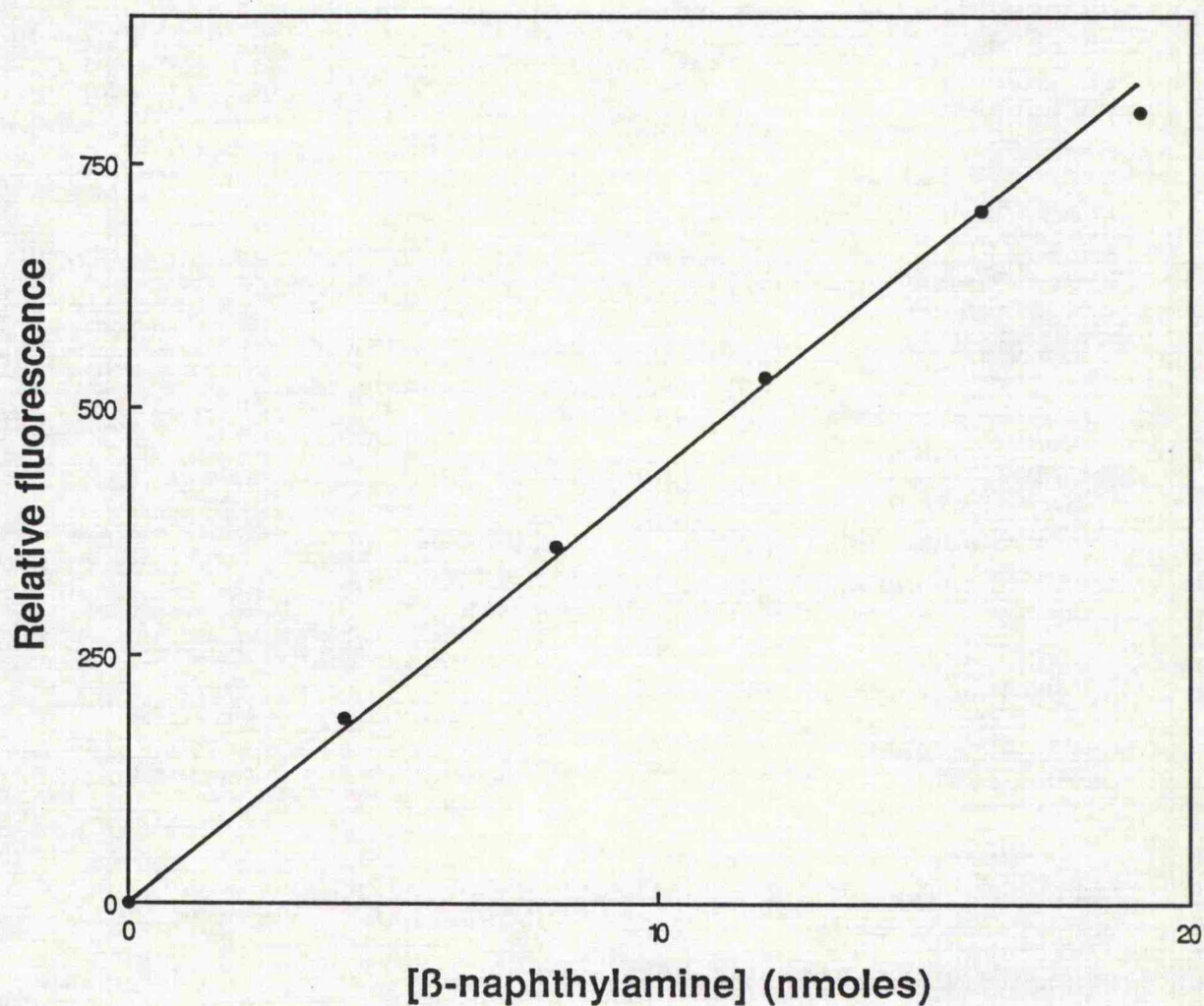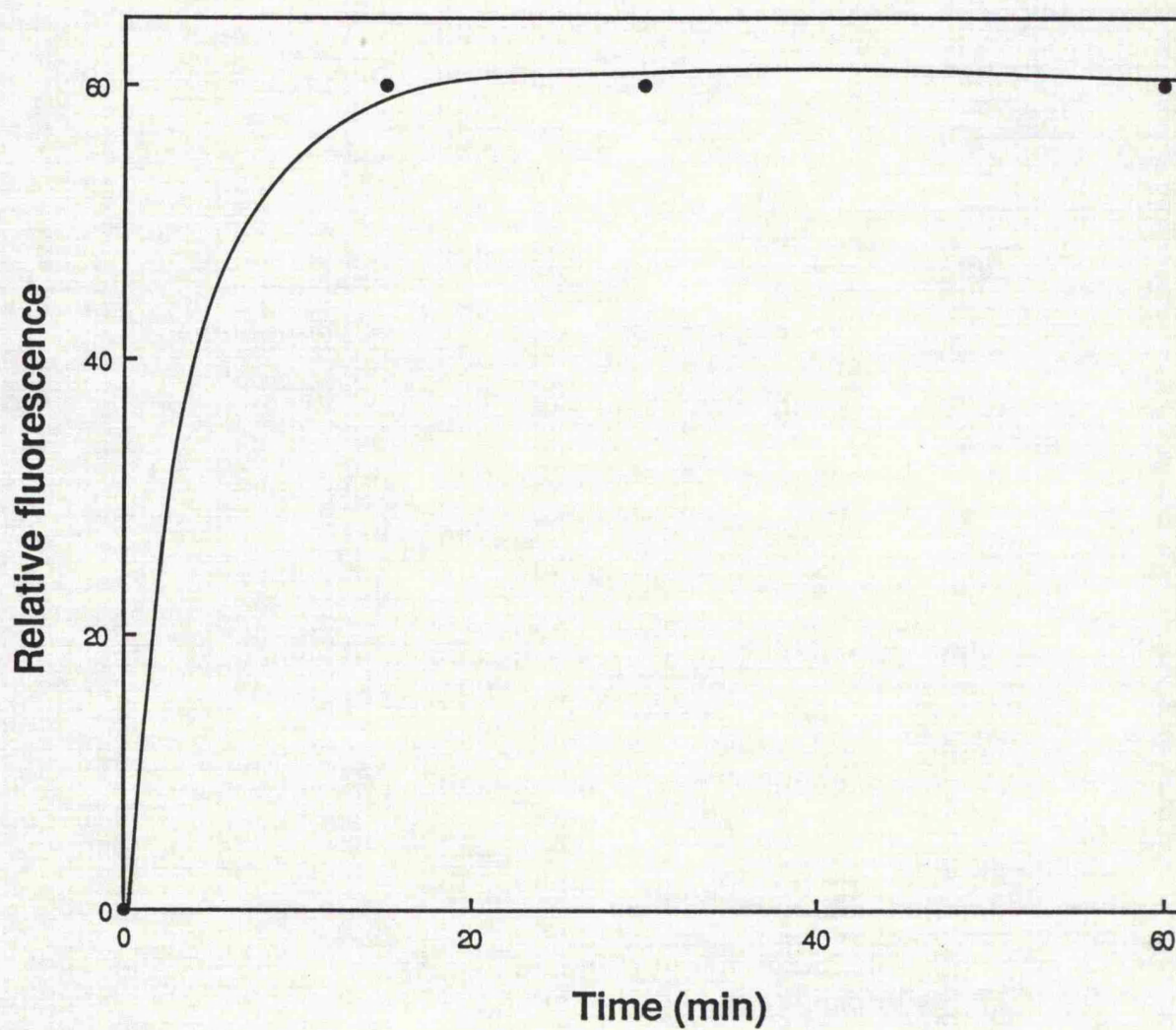
Figure 2.6: Time course of digestion of DG8 with
staphylococcus aureus strain V8 protease.

The digestion was performed as described under Section 2.4. DG8 = ABz-Ala-Phe-Ala-Phe-Glu-Val-Phe-TyrNO$_2$-Asp-OH.

CHAPTER 3

Characterization of the Peptidylglutamyl-Peptide Hydrolase Activity of the Multicatalytic Proteinase Complex.

" Mangania is the Greek word for majic or, in modern parlance, for voodooism. If this is the root of the metal's name, it reflects some reality in the biology of manganese, which is rich in phenomena and lacking in adequate guiding principles."

Cotzias (1958).

3.1 Introduction.

So far, most of the information available on the characterization of the peptidylglutamyl-peptide hydrolase activity comes from studies carried out by Wilk and Orlowski (1983) in the early eighties. They showed that activity was stimulated up to nine-fold by low concentrations of SDS (0.02%) and inhibited by higher concentrations. Bovine serum albumin, at concentrations of 0.1 mg/assay, inhibited this activity, but had no inhibitory effect on the trypsin-like and the chymotrypsin-like activities.

Monovalent and divalent metal ions were found to be inhibitory, hence the name cation-sensitive endopeptidase. Linearity with enzyme concentration was up to 2 μg/assay followed by inhibition. However, linearity over a wider range was observed with the SDS-treated enzyme. No saturation kinetics was observed with respect to substrate concentrations by up to 1.6 mM LLE-NA (the upper limit of substrate solubility in their case). In contrast, the SDS-treated enzyme was found to obey Michaelis-Menten kinetics with a K_m value of 96 μM (Wilk and Orlowski, 1983).

Zolfaghari et al. (1987), while working on MCP from human kidney, have reported that the peptidylglutamyl-peptide hydrolase activity obeyed Michaelis-Menten kinetics in the presence and the absence of SDS, with k_{cat}/K_m values of 7970 and 11570 $M^{-1}s^{-1}$, respectively; in the substrate range 0.05-0.2 mM LLE-NA. The optimum pH for the activity was 7.3, and the activity was inhibited by monovalent cations but a different response to divalent ions was observed with no stimulatory effects.

Although some preliminary characterization work has been carried out on the peptidylglutamyl-peptide hydrolase activity of the proteinase complex (Wilk and Orlowski, 1983; Dahlmann et al., 1985; Zolfaghari et al., 1987), evidence for it being a third distinct proteolytic activity is rather weak and it is still poorly understood. This chapter describes several studies carried out in order to fully characterize the activity as being distinct from the so far characterized ones and to try to understand its kinetics.

3.2 Purification of the proteinase complex.

The purification of the proteinase was performed using the methodology previously adopted in this laboratory (Rivett, 1989b; Rivett and Sweeney, 1991), with modification to the storage conditions of the purified enzyme where 10% glycerol was included in the final dialysis buffer. The purification protocol yielded an apparently homogeneous preparation of the proteinase as ascertained by SDS-PAGE (Figure 3.1).

Results of a typical purification are shown in Table 3.1. Peptidylglutamyl-peptide hydrolase activity was assayed at both 0.1 mM and 0.4 mM LLE-NA. The purification of the activity, assayed at 0.1 and 0.4 mM LLE-NA, was comparable in steps 1-3, but not from step 4 onwards. The overall purification of the activity, assayed at 0.1 mM LLE-NA, was only around 34-fold as compared to 234-fold for the activity assayed at 0.4 mM LLE-NA (Table 3.1). Also an increase in total activity, assayed at 0.4 mM LLE-NA, was observed after step 4, suggesting activation of the enzyme, possibly as a result of removal of inhibitory or competing proteins.

The purified proteinase gave specific activities of 17 and 140 nmol/min/mg for activity assayed at 0.1 and 0.4 mM LLE-NA, respectively. Proteinase preparations gave rise to the usual pattern of 8-12 protein bands on SDS PAGE, with molecular masses in the range from 20 to 35 kDa (Figure 3.1). On non-denaturing gels, activity assayed at both 0.1 and 0.4 mM LLE-NA was both found to be associated with the single protein band (activity stain gels not shown) (Figure 3.2). Proteinase preparations were stored, at a concentration of 1 mg/ml, in 50 mM phosphate buffer, pH 7.0 including 0.1 mM EDTA, 1 mM 2-mercaptoethanol, and 10% glycerol.

3.3 Activity with varying time or enzyme concentration.

Activity assayed at 0.1 mM LLE-NA was linear with enzyme concentration up to 10 μg/assay, but activity assayed at 0.4 mM LLE-NA was linear only up to 4 μg/assay (Figure 3.3), suggesting that the complex readily interacts with itself, at higher concentrations, leading to the inactivation of the activity. The enzyme concentration used in subsequent studies was 2μg/assay or as indicated.

In earlier experiments, where the purified proteinase was not stored in 10% glycerol, product formation with time was linear only for activity assayed at higher LLE-NA concentrations (Figure 3.4). However, activity assayed at lower LLE-NA concentration was found to be non linear with time, starting with a fast rate which reverts back to a much slower rate as illustrated in Figure 3.5. This behaviour is typical of enzymes exhibiting burst-type kinetics (Fersht, 1985).

Product formation, using purified enzyme stored in 10% glycerol, was linear with time even at LLE-NA concentrations as low as

10 μM (Figure 3.6). The final glycerol concentration in assays was 0.1%. Time course with 0.6 mM LLE-NA, however, exhibited an upward curvature as illustrated in Figure 3.7. The upward curvature is indicative of conformational changes taking place within the complex as described by Frieden (1970).

The inclusion of 10% glycerol in the final dialysis buffer of the purification of the proteinase seemed to have eliminated the earlier burst effects (see Figures 3.5 and 3.6). Thus, the effects could have been caused either by a conversion to a less active conformational state of the complex on combination with the first mole of substrate, or by the enzyme dying off. In presence of glycerol, however, the conversion to the less active state is abolished and the enzyme complex is maintained in an active conformational state.

3.4 Solubility of the synthetic peptide LLE-NA.

The solubility limits of the substrate LLE-NA were investigated by means of measuring turbidity due to insoluble peptide at 340 nm, under the assay conditions described under Section 2.4. At pH 7.5, the effects of temperature on the solubility were investigated (Figure 3.8). It was found that solubility profiles were temperature dependent and the limits of which are as follows: 500 μM LLE-NA at 20°C and 600 μM LLE-NA at 37°C.

Similarly, the effects of pH, on the solubility of the peptide, were investigated by keeping the temperature constant at 37°C (Figure 3.9). It was found that solubility profiles were pH dependent with 600 μM LLE-NA as limit for both pHs. The above observations suggest that the solubility of the peptide is both pH and temperature dependent.

The limit of interest is 600 µM LLE-NA at pH 7.5 and at 37°C and was used in subsequent studies.

3.5 Activity with varying substrate concentration.

The range of substrate concentrations used for assays was limited by the solubility of the synthetic peptide (Section 3.4). The kinetics of the peptidylglutamyl-peptide hydrolase activity with LLE-NA as the substrate are very complex as illustrated by the plot of activity as a function of substrate concentration (Figure 3.10). The first part of the curve (substrate range 0-0.1 mM) was less variable with standard deviation less than 5%. It follows normal Michaelis-Menten kinetics at concentrations below the estimated V_{max}, with a K_m value of 114 µM and a V_{max} of 33 nmol/min/mg.

The second part of the curve, however, (substrate range 0.2-0.6 mM) was variable with standard deviations greater than 5% and yielded an apparent sigmoidal curve (Figure 3.10). Because saturation could not be reached at substrate concentrations below the solubility limit of the substrate (Section 3.4), it was not possible to estimate either V_{max} or $K_{0.5}$ from the inflexion point from the curve. Moreover, double reciprocal plots were found to be biphasic with an upward concavity (Figure 3.11), indicating the presence of positive kinetic cooperativity with respect to substrate for allosteric enzymes as described by Kurganov (1982).

The above observations suggest that the peptidylglutamyl-peptide hydrolase activity is composed of two components: one component obeying Michaelis-Menten kinetics and the other component exhibiting cooperativity with respect to substrate

concentration. Therefore, further assays of the activity were carried out at both 0.1 mM and 0.4 mM LLE-NA and the activities are referred to as the LLE1 and the LLE2 activities, respectively.

3.6 The effects of pH on the the peptidylglutamyl-peptide hydrolase activity.

There have been several reports describing the proteinase as either an alkaline or a neutral proteinase because of its pH optimum (Wilk and Orlowski, 1983; Rivett, 1985; Dahlmann et al., 1985; Zolfaghari et al., 1987; Rivett, 1989b). This investigation was undertaken in order to determine a pH profile for the LLE1 and LLE2 activities. The effects of pH were investigated in the range 6.5 - 9.0 in three different buffer systems with 0.1 mM (LLE1 activity) and 0.4 mM (LLE2 activity) LLE-NA (Figure 3.12).

In the 50 mM Hepes/KOH buffer system, the LLE2 activity gave an optimum pH of 7.0 - 7.5 with a decrease in activity after pH 7.5, whereas the LLE1 activity did not show any difference in activity with an optimum pH of 7.0. In the 50 mM Tris/HCl buffer system, the LLE1 activity exhibited a bell shape curve up to pH 8.0 with no further change in activity was observed. The optimum pH for the LLE1 activity is pH 7.0 as for the Hepes/KOH buffer system. The LLE2 activity also showed a bell shaped curve with an optimum pH of 7.0 - 7.5.

In the 50 mM Bis-Tris propane/HCl buffer system, the LLE1 activity exhibited a decay in activity with an optimum pH of 6.5. The LLE2 activity, on the other hand, exhibited a bell shaped curve with an optimum pH of 7.0 (Figure 3.12).

3.7 Substrates for the peptidylglutamyl-peptide hydrolase activity.

The peptidylglutamyl-peptide hydrolase activity, unlike the chymotrypsin-like and the trypsin-like activities (Dahlmann et al, 1985; McGuire and DeMartino, 1986; Rivett, 1989b), can be assayed with a single amino acid derivative such as H-Glu-β-naphthylamide, but has a very low specific activity with this substrate compared to that determined for Z-Leu-Leu-Glu-β-naphthylamide (Table 3.2). This result suggests that the substrate binding pocket P1 is only a partial requirement for specificity.

Z-Ala-Ala-Ala-Asp-SBzl, an example of a new class of protease substrates (Odake et al., 1991) was also found to be a substrate for the proteinase, clearly demonstrating for the first time that the enzyme can catalyze cleavage on the carboxyl side of aspartic acid residues. The site responsible for the cleavage could be one of the other proteolytic sites within the complex as well as the LLE sites. The specific activities using the above synthetic peptide substrates with either Glu or Asp in the P1 position are summarized in Table 3.2.

3.8 Effect of casein on the the peptidylglutamyl-peptide hydrolase activity.

Casein has been shown to be a substrate for the multicatalytic proteinase complex (Rivett, 1989a,c; Orlowski, 1990). Figure 3.13 summarizes the effect of casein on the hydrolysis of the fluorogenic peptide LLE-NA. The LLE1 and LLE2 activities were found to be inactivated, where only 50% of the original activity remained in the presence of less than 2.5 μg casein/assay.

Furthermore, there was 20% residual LLE1 activity observed at concentrations of casein up to 50 μg/assay. At similar casein concentrations, only 7% residual activity was observed in the case of the LLE2 activity (Figure 3.13).

3.9 Effect of KCl on the the peptidylglutamyl-peptide hydrolase activity.

The effect of KCl on the LLE1 and the LLE2 activities as a function of its concentration was investigated. It was found that the LLE2 activity was most affected by KCl (Figure 3.14), where 75% of activity was lost in presence of 25 mM KCl and little inhibition was observed up to 50 mM KCl.

The LLE1 activity, on the other hand, was not as affected by KCl, with 78% activity remaining in the presence of 50 mM KCl; thus providing a clear distinction between the two activities. The remaining 25% activity of the LLE2 are not due to the LLE1 activity as illustrated in Figure 3.14, but probably to a partly inactivated LLE2 activity.

Activity with varying substrate concentration in presence of 50 mM KCl was also investigated (Figure 3.15). It was found that the LLE1 activity still obeys Michaelis-Menten kinetics with a higher K_m value of 132 μM and an estimated V_{max} of 27.48 nmol/min/mg. A linear relationship was observed above 200 μM LLE-NA, with no strong indication of a cooperative effect with respect to substrate concentration (Figure 3.15).

3.10 Thermal stability of the peptidylglutamyl-peptide hydrolase activity.

The thermal stability of both the LLE1 and the LLE2 activities was investigated at 55°C and 60°C. The LLE1 activity was not affected by exposures of up to 10 min at 55°C, where no overall loss of activity was detected (Figure 3.16). However, the LLE2 activity was found to be heat-sensitive with 50% activity lost after 8 min exposure at 55°C. The LLE1 activity became heat-sensitive at 60°C (Figure 3.16) with 50% activity lost after 5 min exposure, whereas the LLE2 activity lost 50% of its activity in approx. 2 min (Figure 3.16). The above results suggest a difference in thermal stability between the two activities, thus confirming above observations that the two activities are distinct from each other.

3.11 Effect of divalent metal ions on the peptidylglutamyl-peptide hydrolase activity.

The effects of selected divalent metal ions, at a concentration of 1 mM, on the LLE1 and the LLE2 activities were investigated and are summarized in Table 3.3. The LLE1 activity was activated by $MnCl_2$ (up to three-fold), $MgCl_2$ (up to two-fold), and $CaCl_2$ (up to two-fold) in the following order $MnCl_2 > MgCl_2 > CaCl_2$. The LLE1 was inactivated by $ZnCl_2$, $CdCl_2$, and $CoCl_2$ in the following order $ZnCl_2 > CdCl_2 > CoCl_2$ (Table 3.3).

The LLE2 activity, on the other hand, was only stimulated by $MnCl_2$ (up to two-fold). $CaCl_2$, and $CoCl_2$ had no stimulatory nor inhibitory effects on the activity. The LLE2 activity was inactivated by

$ZnCl_2$, $CdCl_2$, and $MgCl_2$ in the following order $ZnCl_2$ > $CdCl_2$ > $MgCl_2$ (Table 3.3).

$MnCl_2$ (1.0 mM) activated both the LLE1 and LLE2 activities by up to three and two-fold, respectively; thus, it was worthy of further investigations. The effects of $MnCl_2$ on the LLE1 and the LLE2 activities as a function of $MnCl_2$ concentration are illustrated in Figure 3.17. The optimum activity was at 1.0 mM $MnCl_2$ for both activities, with inhibitory effects above 5.0 mM $MnCl_2$.

Examination of the peptidylglutamyl-peptide hydrolase activity, as a function of substrate concentration, in the presence of 1 mM $MnCl_2$, yielded a curve similar to that obtained in the absence of the metal ion except that saturation was achieved at the higher end of the substrate range (See Figures 3.10 and 3.18). The non-sigmoidal part of the curve obeyed Michaelis-Menten kinetics with a more effective binding of the substrate, giving a K_m value of 67 μM and an estimated V_{max} of 28 nmol/min/mg. Analysis of the sigmoidal part of the curve gave a $K_{0.5}$ of 0.28 mM, a V_{max} of 302 nmol/min/mg. The Hill plot was linear with a slope of 5.1 (Figure 3.19).

3.12 Reversibility between activity at high and low LLE-NA concentration.

By increasing the LLE-NA concentration, activation of the activity occurred by exhibiting a positive cooperative effect with respect to substrate as illustrated by Figures 3.10 and 3.18. In this study, an attempt was made to investigate whether starting with 0.5 mM LLE-NA (where the enzyme exhibits sigmoidal behaviour) and decreasing it by dilution to 0.1 mM LLE-NA (where the complex appears to exhibit

Michaelis-Menten kinetics) will lead to similar activity performed with 0.1 mM LLE-NA as a control, it was found that activity with 0.1 mM LLE-NA was similar to the diluted one (Table 3.4).

This finding suggests that reversibility easily occurs between activity with 0.5 mM LLE-NA and activity with 0.1 mM LLE-NA. However, when 1 mM $MnCl_2$ was present in the assay, the diluted activity was up to two-fold higher than control activity under similar conditions (Table 3.4). In contrast to the above finding, the latter one suggests that $MnCl_2$ is bringing the enzyme complex into a novel conformational state, which is two-fold more active than control.

3.13 Effects of ATP, EDTA, SDS and Nonidet P40 on the peptidylglutamyl-peptide   hydrolase   activity.

In an investigation of whether the proteinase complex is an ATP dependent protease, it was found that Mg-ATP had no stimulatory effects on either the LLE1 or LLE2 activity when included in the assays at concentrations of 0.5 and 1.0 mM, respectively (Table 3.5). A different approach to the investigation was to preincubate the enzyme with ATP then dilute it 20-fold in the assay. This approach, however, gave similar results to the above (Table 3.5), suggesting that the purified enzyme is not stimulated by ATP, but slightly inhibited.

The effects of EDTA on the LLE1 and LLE2 activities were also investigated and are summarized in Table 3.6. EDTA inhibited the LLE1 activity with 60% and 44% activity remaining at 1.0 and 10.0 mM EDTA, respectively. EDTA had little effect on the LLE2 activity (Table 3.6).

The ionic detergent SDS was found to activate the peptidyl-glutamyl-peptide hydrolase activity (Figure 3.20). The extent of activation was dependent upon the substrate concentration, with the fold activation decreasing with increasing in LLE-NA concentration. In presence of 0.03% SDS, the LLE1 activity was stimulated by up to nine-fold, whereas the LLE2 activity was only stimulated by up to three-fold. Activity assayed with 200 μM LLE-NA was also stimulated by up to seven-fold.

In view of this stimulation, similar experiments were performed in presence of 0.03% SDS but also including 1 mM of either of the following divalent metal ions: $MgCl_2$, $CaCl_2$, $MnCl_2$, or $CoCl_2$; in order to see whether having the two activators in the assay will lead to an additive stimulatory effect or not.

The results, however, show that except for the stimulation of the LLE1 activity in presence of 0.03% SDS and 1 mM $MnCl_2$, all the other treatments were found to be inhibitory (Table 3.7). The LLE1 activation by 0.03 % SDS was decreased by nearly two-fold when 1 mM $MnCl_2$ was included in the assay, suggesting that SDS and $MnCl_2$ could be interacting at different sites within the complex, in contrast to the interaction of the other metal ions with SDS.

The effects of Nonidet P40, a non-ionic detergent, on the LLE1 and LLE2 activities were investigated (Table 3.8). It was found that both activities were inhibited by the treatment with 15% and 35% remaining activity for the LLE1 and LLE2 activities, respectively . It is interesting to note that SDS (an ionic detergent) activated the LLE activities but Nonidet P40 (a non-ionic detergent) inhibited the activities.

3.14 Comparing the effects of some of the effectors on the trypsin-like and chymotrypsin-like activities.

Investigation of the effects of the selected divalent metal ions on the other proteolytic activities of the proteinase provided a direct evidence for the LLE1 and LLE2 activities as being distinct from the others, as illustrated in Figure 3.21. The AAF and the LLVY activities differed in their response to divalent metal ions, confirming the suggestion that they are catalyzed by distinct sites within the complex (Djaballah et al., 1992).

The AAF and LSTR activities were not stimulated by the metals, but no or inhibitory effects were observed. Striking stimulation of the LLVY activity by $MgCl_2$, $CaCl_2$, and $CoCl_2$ was observed, but a slight inhibition by $MnCl_2$, which provides an evidence for the LLVY being distinct from the LLE activities as it was not activated by $MnCl_2$ (Figure 3.21).

Casein was also found to inhibit the LLVY activity. There was 50% activity remaining in the presence of less than 2.5 μg/assay (Figure 3.13), and 30% activity remaining in the presence of 50 μg/assay. The AAF and LSTR activities were not affected by casein up to concentrations of 50 μg/assay (figure 3.22). The above observation supports the suggestion of the AAF and LLVY activities being distinct (Djaballah et al., 1992). The detergent Nonidet P40 activated the LSTR activity, with inhibitory effects on the AAF and LLVY activities (Table 3.8). Apart from the activation of the LLE activities by SDS treatment, the other proteolytic activities were inhibited by the treatment (Wilk and Orlowski, 1983; Tanaka et al., 1986a; Arribas and Castano, 1990; Mykles and Haire, 1991).

3.15 Discussion.

Purification of the multicatalytic proteinase complex by the procedure described yields apparently pure preparations which show the characteristic set of polypeptides on SDS-PAGE gels. The difference in relative activity measured at 0.1 mM and 0.4 mM LLE-NA at various stages of the purification probably reflects the problems of accurately assaying the enzyme activity in crude preparations which occur as a result of interference by other proteases as well as other proteins.

The peptidase assay is reliable for the purified proteinase, although LLE-NA hydrolysis is only linear with enzyme concentration over a limited range, in agreement with similar findings reported for the pituitary enzyme (Wilk and Orlowski, 1983) and the rat skeletal muscle enzyme (Dahlmann et al., 1985).

The specific activity of the purified rat liver proteinase complex is similar to values reported for the enzyme from bovine pituitary (Orlowski and Michaud, 1989), bovine lens (Wagner et al., 1985), and human brain (McDermott et al., 1991) in assays under comparable conditions. Apparent discrepancies in the literature values can largely be explained by the differences in substrate (LLE-NA) concentration and buffer composition (see later).

Casein inhibited both the LLE1 and LLE2 activities. The inhibition of the LLE2 activity correlates well with the above observations that the activity was inhibited by higher concentrations of enzyme, and provides a supporting evidence with the inhibitory effects on the LLE1 activity that the two LLE activities are distinct from at least the AAF and LSTR activities. The effects also suggest a difference in behaviour

of the chymotrypsin-like activity assayed with either the AAF-AMC or the LLVY-AMC substrate.

The inhibition by casein is in agreement with published results for human erythrocyte MCP (McGuire and DeMartino, 1986), human kidney MCP (Zolfaghari et al., 1987), bovine pituitary MCP (Wilk and Orlowski, 1983; Orlowski et al., 1991), and human brain MCP (McDermott et al., 1991).

The peptidylglutamyl-peptide hydrolase activity has a pH optimum of 7.0-7.5. The sharp decline in the LLE2 activity above pH 8.0, in the Tris/HCl and in the Bis-Tris propane/HCl buffer systems, is unlikely to be due to instability of the proteinase (Rivett, 1985) but may reflect the loss of sensitivity of the allosteric enzyme towards the effector due to pH changes, which could have caused either a change in the state of the ionogenic groups at the effector binding site (with a consequent loss of the ability of the site to bind the effector), or a change in the conformation of the molecule such that allosteric interaction between the spatially separated active and allosteric sites is no longer possible as described by Kurganov (1982).

The difference in behaviour of the complex in the three buffer systems described is not well understood, but could be explained by an interactive effect between the enzyme and each of the individual buffers. Dahlmann et al. (1985) have reported a pH optimum of 9.0, measured in 0.1 M phosphate/borate/acetate buffer, for the LLE2 activity of rat skeletal muscle MCP. Tanaka et al. (1988) have also reported optimum pHs of 8.0-9.0, measured in 0.1 M Tris/HCl buffer including 0.05% SDS, for the LLE2 activity of MCP from various

sources. Again, the apparent discrepancies in the literature could be due to the different response of MCP in different buffer systems.

The peptidylglutamyl-peptide hydrolase activity was found to differ in its response to a variety of divalent metal ions and to EDTA when assayed at 0.1 mM (LLE1 activity) and 0.4 mM LLE-NA (LLE2 activity). The diversity in response provides a direct evidence for the two LLE activities as being distinct from each other and also as being distinct from the other activities. Of the divalent metal ions tested in this study, manganese was the most effective stimulator of the LLE activities.

Since the metal ion requirement is not absolute for activity, it seems likely that the proteinase complex falls in the category of metal-activated enzymes rather than metalloenzymes. Further evidence supporting the suggestion comes from studies showing the lack of inhibition of the proteinase activities by 1,10-phenanthroline and EDTA (McGuire and DeMartino, 1986; Sacchetta et al., 1990a,b; McDermott et al., 1991; Table 3.6; Djaballah and Rivett, 1992). The observed activation could be a result of $MnCl_2$ playing some structural role, and will be discussed in Chapter 6.

Stimulation of hydrolase activity by calcium and cobalt ions is not unusual for proteases. Degradation of α-crystallin by lens neutral endopeptidase (MCP) has been reported to be stimulated by calcium and magnesium ions, but this effect apparently decreases with purification of the complex (Ray and Harris, 1986). However, divalent metal ions such as calcium, magnesium, and manganese have been reported to have no stimulatory effects on MCP activities but rather inhibitory ones (Wilk and Orlowski, 1980; Dahlmann et al., 1985;

Rivett, 1989b; Kinoshita et al., 1990b). These observations could have been due to the use of higher metal ion concentrations (up to 10 mM), as the latter have been shown in this study to be inhibitory.

At concentrations of LLE-NA below 0.2 mM, the enzyme complex behaved in Michaelis-Menten fashion, suggesting the presence of one type of relatively high-affinity site (Table 3.9). Zolfaghari et al. (1987) have reported similar observations in the case of the human kidney enzyme but with a much higher k_{cat}/K_m value. Wilk and Orlowski (1983) have also reported similar findings with the SDS-treated pituitary enzyme with a K_m value of 96 μM.

In contrast to the above, Arribas and Castano (1990) suggested the presence of a cooperative component with a similar K_m. The above high affinity active site has probably gone unnoticed in other studies because of the high LLE-NA concentrations (up to 0.8 mM) used for assays (Wilk and Orlowski, 1983; Dahlmann et al., 1985; Orlowski et al., 1991). At high LLE-NA concentrations the proteinase complex deviates from Michaelis-Menten kinetics but gives rise to an apparent positive cooperativity effect with respect to substrate concentration.

The activity with high concentrations of LLE-NA was somewhat variable in different experiments. The variation could be reduced considerably by the addition of 1 mM $MnCl_2$, which was found not only to stimulate the activity but also to reduce the concentration at which saturation with substrate was reached. A Hill coefficient of 5.1 is indicative of a positive kinetic cooperativity effect with respect to substrate for allosteric enzymes as described by Kurganov (1982), and can be explained either by the presence of at least five relatively

low-affinity sites acting in a cooperative manner or by an allosteric effect. $MnCl_2$ increased the affinity of substrate binding at the high affinity active site (Table 3.9).

Inhibition by monovalent ions has been reported for the pituitary MCP (Wilk and Orlowski, 1983), the human lung MCP (Zolfaghari et al., 1987), the human brain MCP (McDermott et al., 1991), and the lobster muscle MCP (Mykles and Haire, 1991). Inhibition by KCl of the LLE2 activity support the finding that the activity consists of two components.

The inhibitory effect of KCl could be explained by the loss of allostericity of the cooperative component of the LLE activity, as illustrated in Figure 3.15, where a linear relationship between activity and substrate concentration was observed. The LLE1 activity still obeys Michaelis-Menten kinetics in the presence of 50 mM KCl (Table 3.9).

The SDS activation of the peptidylglutamyl-peptide hydrolase activity was found to be substrate dependent. The extent of activation decreased with increase in substrate concentration, where fold-activation was reduced from nine-fold at 0.1 mM LLE-NA to three-fold at 0.4 mM LLE-NA. Although the activation was substrate dependent, optimal activation for each of the LLE activities were due to different SDS concentrations as demonstrated in Figure 3.20.

However, the activation was abolished in the presence of divalent metal ions with a resulting inhibitory effect on both activities. Moreover, the LLE1 activity was not inhibited by SDS in the presence of manganese, whereas 50% of the LLE2 activity remained under similar condition. Nonidet P40, a non ionic detergent, inhibited both

the LLE activities in contrast to the ionic detergent SDS. Arribas and Castano (1990) have also described the non stimulatory effects of both non ionic and zwitterionic detergents on the different proteolytic activities of the complex.

The ATP dependence of the proteinase is still a very controversial question. Several groups have reported ATP stimulation of hydrolysis of synthetic as well as degradation of protein substrates by the multicatalytic proteinase complex (Tanaka and Ichihara, 1988; Tsukahara et al., 1988; McGuire et al., 1988; Driscoll and Goldberg, 1989; Fagan and Waxman, 1989). Whereas, in this study, there was no stimulation by ATP of the LLE1 and LLE2 activities, in agreement with several reports that the proteinase is ATP independent (Rivett, 1989b; Orlowski, 1990).

The above conclusions concerning the cooperative effect differ from those of two recently published studies, both of which addressed the effects of SDS on the catalytic properties of the complex. Arribas and Castano (1990), on one hand, suggested the presence of two components: a cooperative one in the lower end of substrate concentration in contrast to my findings, and a non-cooperative component at the higher end. Orlowski et al. (1991), On the other hand, have described one cooperative component with an estimated Hill coefficient of 2.2-2.4.

There may be differences in the kinetic properties of MCP isolated from rat liver and bovine pituitary. Another possible explanation of the discrepancies is the dependence of the Hill plot on the accurate determination of V_{max}. The improvement in data obtained by addition of $MnCl_2$, as well as a large number of data

points averaged from six separate experiments, allowed the calculation of a Hill coefficient of 5.1.

Finally, the undertaken studies have led to the characterization of the peptidylglutamyl-peptide hydrolase activity as being distinct from the, so far, described ones. The activity appears to be composed of two distinct component: a high affinity non-cooperative component obeying Michaelis-Menten kinetics and a low affinity cooperative component showing positive cooperativity with respect to substrate concentration. The activity exhibits very unusual and complex kinetics. In addition, the studies have also shown activation by manganese ions, SDS, and substrate via possible involvement of conformational changes within the complex.

Table 3.1:   Summary of the purification of the multicatalytic
             proteinase complex from rat liver.

Purification of the proteinase was from 115g of rat liver. Activities were
determined with either 0.1 mM LLE-NA (LLE1 Activitiy) or 0.4 mM LLE-NA
(LLE2 Activity) as described under Section 2.4. Samples from steps 2-4 and
6 were dialysed against low salt containing buffer prior to the
determination of activities and specific activities. Values in parantheses
indicate fold of purification. The overall yield of puried proteinase was 11
mg.

STEP	Volume (ml)	Protein (mg/ml)	Total protein (mg)	LLE1 Activity		LLE2 Activity	
				Total activity (nmoles/min)	Specific activity (nmoles/min/mg)	Total activity (nmoles/min)	Specific activity (nmoles/min/mg)
1- Supernatant	870	19	16,530	8,265	0.5(1)	10,550	0.6(1)
2- ammonium sulphate fractionation	270	30	8,100	2,430	0.3(1)	4,860	0.6(1)
3- DEAE-cellulose chromatography	110	4.4	484	1,160	2.4(5)	968	2.0(4)
4- Anion exchange FPLC	88	0.4	38	152	4.0(8)	418	11.0(18)
5- Superose 6 gel filtration	8	1.6	13	196	15.0(30)	884	68.0(114)
6- Anion exchange FPLC	3	3.7	11	187	17.0(34)	1,540	140.0(234)

Table 3.2:   MCP substrates for cleavage on the carboxyl side
of acidic amino acid residues.

Substrate	Concentration (mM)	Specific activity[a] (nmoles/min/mg)
Z-Leu-Leu-Glu-β-NA	0.4	165 ± 73
H-Glu-β-NA	0.4	13 ± 3
Boc-Ala-Ala-Asp-SBzl	0.4	41 ± 3

[a]Hydrolysis rates were measured in 50 mM Hepes/KOH buffer, pH 7.5, containing appropriate substrate concentration with 0.01 mg/ml purified proteinase as described under Section 2.4. The mean ± S.D. was calculated from two separate experiments done in duplicate, with at least two different proteinase preparations.

Table 3.3: Effects of divalent metal ions on the peptidyl-glutamyl-peptide hydrolase activity.

Compound	LLE1 activity (% control)	LLE2 activity (% control)
MgCl$_2$	229 ± 55[a]	79 ± 39
CaCl$_2$	188 ± 50	111 ± 65
MnCl$_2$	306 ± 44	192 ± 100
CdCl$_2$	34 ± 9	10 ± 5
ZnCl$_2$	28 ± 11	8 ± 6
CoCl$_2$	88 ± 16	93 ± 55

Prior to activity determination, 50 mM Hepes/KOH buffer was pretreated with chelex-100. 1.0 mM of each divalent metal ion was used. Activities were determined as described under Section 2.4 with 0.1 mM (LLE1 activity) and 0.4 mM LLE-NA (LLE2 activity). Metal ions were not included in controls. [a] Values are given as the mean ± S.D. of at least six separate experiments performed in duplicate.

Table 3.4: Reversibility of activity assayed at high LLE-NA to activity assayed at low LLE-NA.

Treatment	Activity expressed as percentage[$]
A) In absence of 1 mM MnCl$_2$.	
30 min assay under normal assay conditions[a]	100
30 min assay using diluted assay mix[b]	106
B) In presence of 1 mM MnCl$_2$.	
30 min assay under normal assay conditions[a*]	100
30 min assay using diluted assay mix[b*]	234

[a]MCP was preincubated for 10 min at 37°C then the solution was diluted five-fold, and added to a 0.1 mM LLE-NA solution in 50 mM Hepes/KOH buffer, pH 7.5. Activity t_0 was noted as did activity after 30 min incubation at 37°C. [a*]Similar experiment as [a] except that 1 mM MnCl$_2$ was included throughout. [b]MCP was preincubated with 0.5 mM LLE-NA for 10 min at 37°C then the solution was diluted five-fold, activity after dilution was noted (t'_0), and also activity after 30 min incubation at 37°C. [b*]Similar experiment as [b] except that 1 mM MnCl$_2$ was present throughout. Activities were corrected for background and for activity that occured during the 10 min preincubation period. [$]Data is average of at least three separate experiments performed in duplicate.

Table 3.5:   Effects of ATP on the peptidylglutamyl-peptide
              hydrolase activity.

Treatment	LLE1 activity (% control)	LLE2 activity (% control)
0.5 mM ATP + 2 mM MgCl$_2$[a]	83 ± 1[c]	99 ± 13
1.0 mM ATP + 2 mM MgCl$_2$[a]	71 ± 2	91 ± 9
0.5 mM ATP + 2 mM MgCl$_2$[b]	88 ± 2	107 ± 3
1.0 mM ATP + 2 mM MgCl$_2$[b]	82 ± 3	111 ± 4

[a]MCP (0.2 mg/ml) was preincubated with appropriate ATP concentration for 10 min at 25°C. Assays were started by addition of aliquots of treated enzyme to substrate mixes containing either 0.1 mM or 0.4 mM LLE-NA in 50 mM Hepes/KOH buffer, pH 7.5 and incubations at 37°C were for 30 minutes as described under Section 2.4. [b]assays were carried out at 37°C with the addition of appropriate ATP concentration to 50 mM Hepes/KOH buffer, pH 7.5 containing 0.01 mg/ml proteinase and 0.1 mM or 0.4 mM LLE-NA as described under Section 2.4. [c]Values are given as the mean ± S.D. of at least three separate experiments performed in duplicate.

Table 3.6:   Effects of EDTA on the peptidylglutamyl-peptide hydrolase activity.

Compound	LLE1 activity (% control)	LLE2 activity (% control)
1.0 mM EDTA	64 ± 10[a]	106 ± 16
10.0 mM EDTA	44 ± 4	96 ± 3

Prior to activity determination, 50 mM Hepes/KOH buffer was pretreated with chelex-100. Activities were determined as described under Section 2.4 with 0.1 mM (LLE1 activity) and 0.4 mM LLE-NA (LLE2 activity). EDTA was not included in controls. [a] Values are given as the mean $\pm$ S.D. of six separate experiments performed in duplicate.

Table 3.7: Effects of divalent metal ions on the peptidyl-glutamyl-peptide hydrolase activity in the presence of 0.03% SDS.

Treatment	LLE1 activity	LLE2 activity
None	100	100
0.03% SDS	920 ± 13[a]	334 ± 5
0.03% SDS + 1 mM MgCl$_2$	17 ± 5	8 ± 1
0.03% SDS + 1 mM CaCl$_2$	42 ± 16	22 ± 5
0.03% SDS + 1 mM MnCl$_2$	778 ± 2	50 ± 9
0.03% SDS + 1 mM CoCl$_2$	3 ± 1	1 ± 1

Prior to activity determination, 50 mM Hepes/KOH buffer was pretreated with chelex-100. Activities were determined as described under Section 2.4 with 0.1 mM (LLE1 activity) and 0.4 mM (LLE2 activity) in the presence of 0.03% SDS. [a] Values are given as the mean $\pm$ S.D. of at least two separate experiments performed in duplicate.

Table 3.8:   Effect of Nonidet P-40 on the different activities
of the mulicatalytic proteinase complex.

Substrate	Activity (% control)	
	0.5% Nonidet P-40	1.0% Nonidet P-40
AAF-AMC	83 ± 10[a]	67 ± 3
LSTR-AMC	185 ± 24	122 ± 14
LLVY-AMC	31 ± 3	22 ± 2
LLE-NA (0.1 mM)	15 ± 2	10 ± 2
LLE-NA (0.4 mM)	35 ± 5	23 ± 7

Assays were carried out at 37°C with the addition of 0.5 or 1.0% Nonidet P-40 to 50 mM Hepes/KOH buffer, pH 7.5 containing 0.01 mg/ml proteinase and 50 mM AAF-AMC, LSTR-AMC, LLVY-AMC, 0.1 mM LLE-NA or 0.4 mM LLE-NA as described under Section 2.4. [a]Values are given as the mean ± S.D. of at least three separate experiments performed in duplicate.

Table 3.9: Kinetic parameters of the non-cooperative component of the peptidylglutamyl-peptide hydrolase activity.

Treatment	K_m (mM)	V_{max} (nmol/min/mg)	K_{cat} (s^{-1})	K_{cat}/K_m ($M^{-1} s^{-1}$)
normal assay conditions	114	33.00	0.357	3130
including 1 mM MnCl2	67	27.32	0.296	4420
including 50 mM KCl	132	27.48	0.299	2265

Kinetic constants were determined using the method of Eisenthal and Cornish-Bowden (1974).
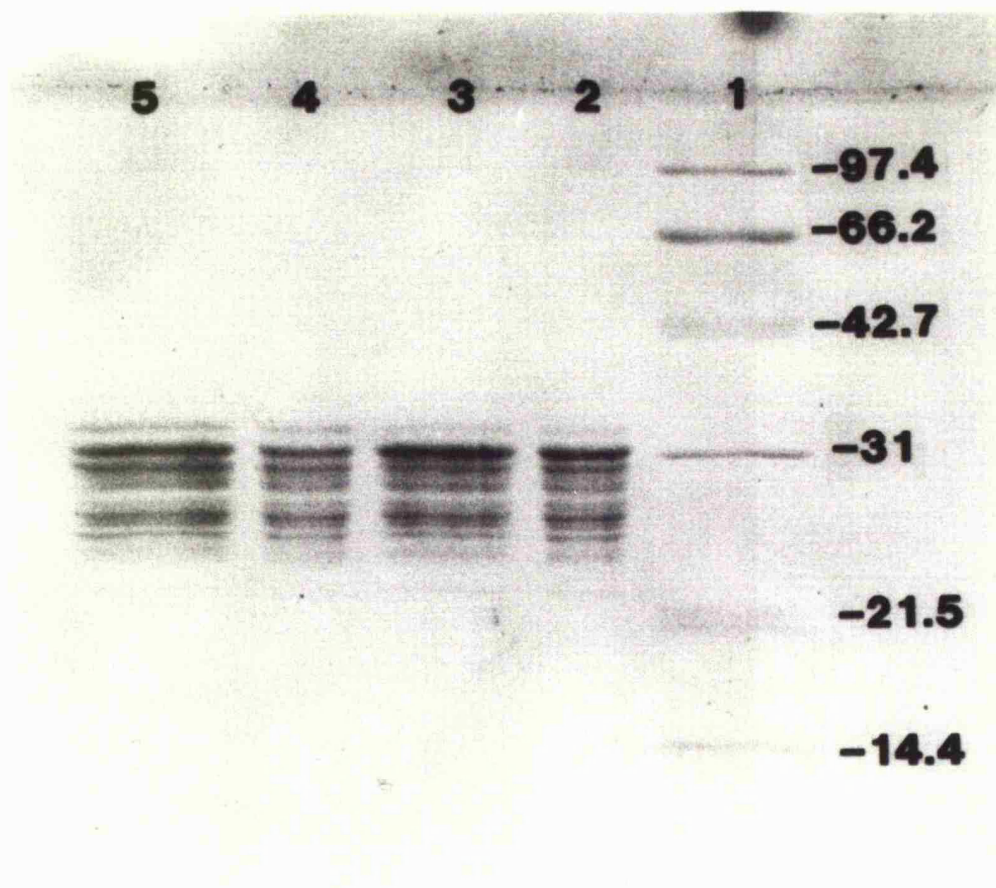
Figure 3.1: SDS polyacrylamide gel electrophoresis of purified proteinase.

Lane **1**: Molecular weight markers. Lanes **2** and **3** : 5 and 10 μg of enzyme preparation of 11.89. Lanes **4** and **5** : 5 and 10 μg of enzyme preparation of 03.90. Gel was run as described under Section 2.7.
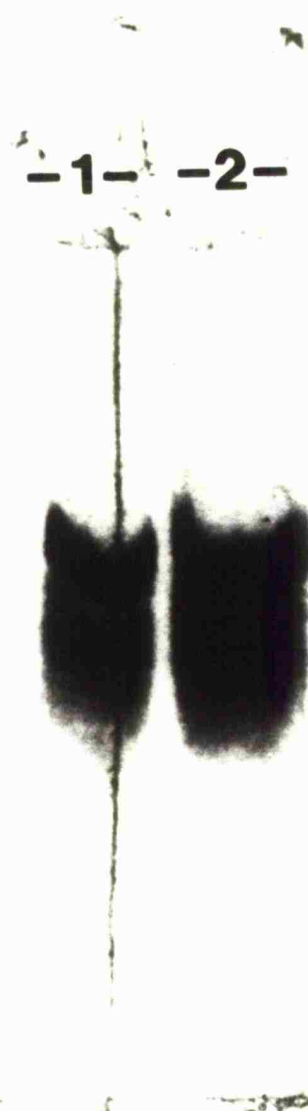
Figure 3.2: Non-denaturing polyacrylamide gel electrophoresis of the purified proteinase.

Lanes **1** and **2** have been loaded with 20 and 40 μg of the purified proteinase, and run as described under section 2.7.
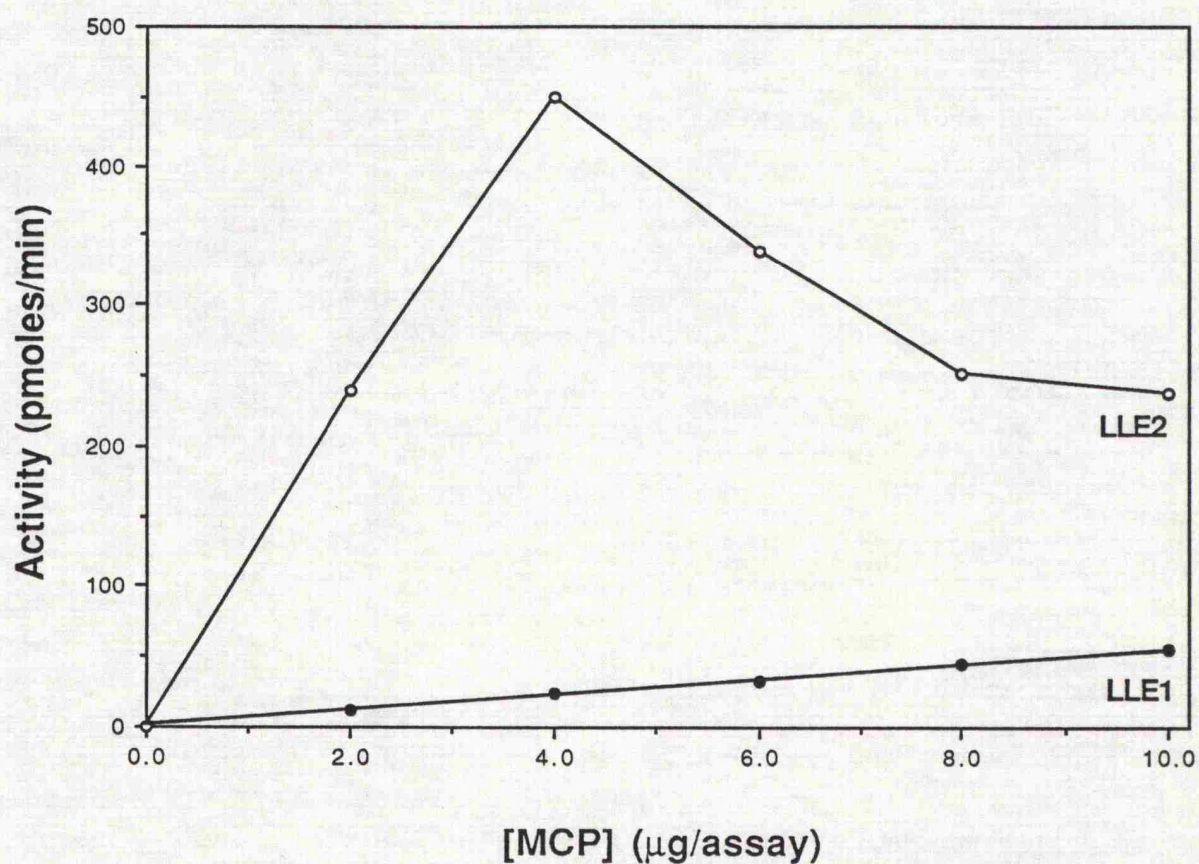
**Figure 3.3:** Dependence of activity on proteinase concentration.

Incubations were performed, using the stopped assay method, for 30 min at 37°C. They contained either 0.1 mM (LLE1) or 0.4 mM (LLE2) LLE-NA and appropriate amounts of the proteinase complex in 50 mM Hepes/KOH buffer, pH 7.5. Data are the average of at least three separate experiments performed in duplicate.
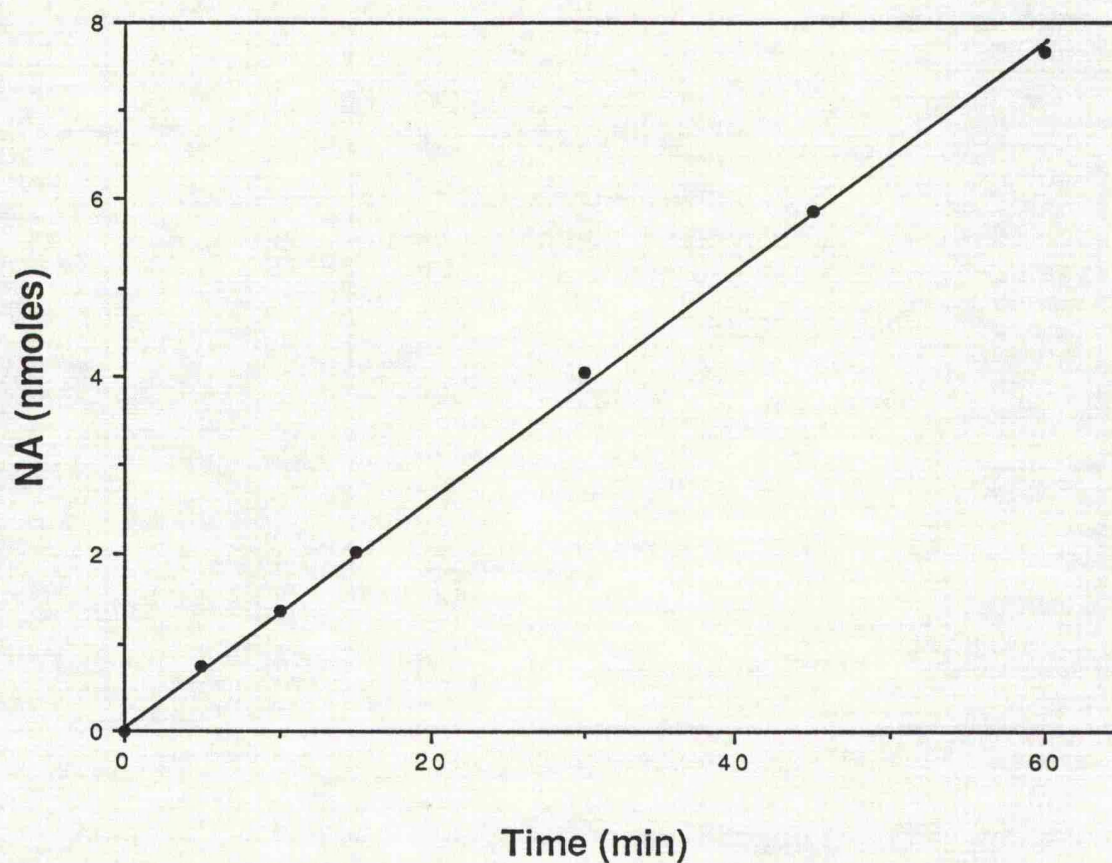
Figure 3.4: Hydrolysis of 400 μM LLE-NA by the proteinase complex as a function of time.
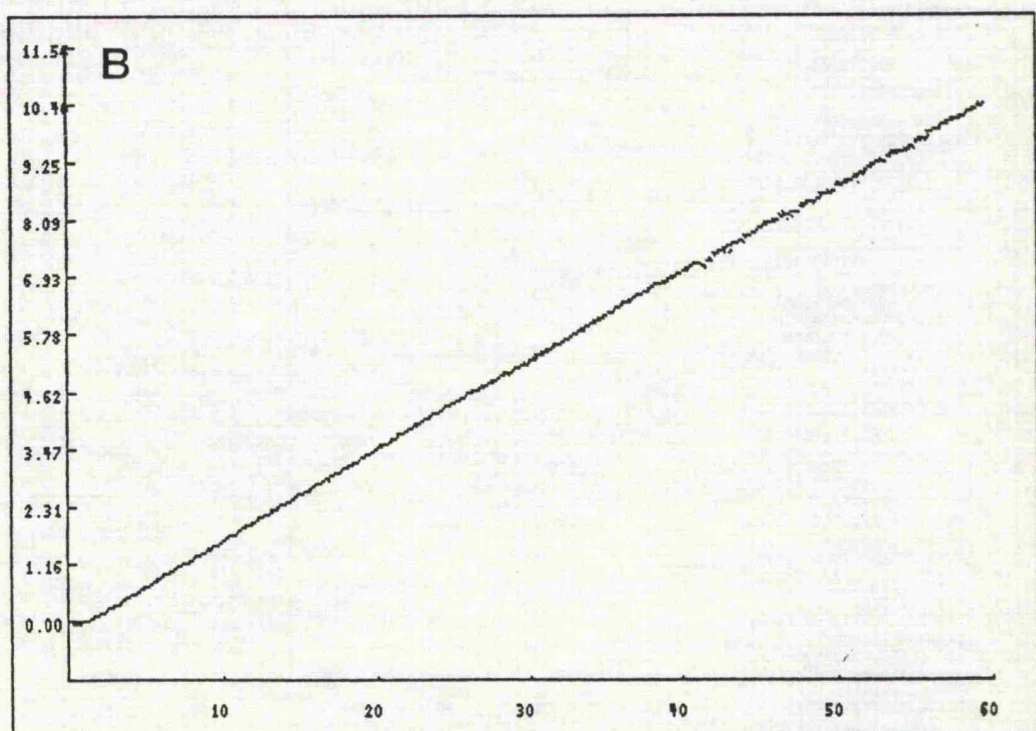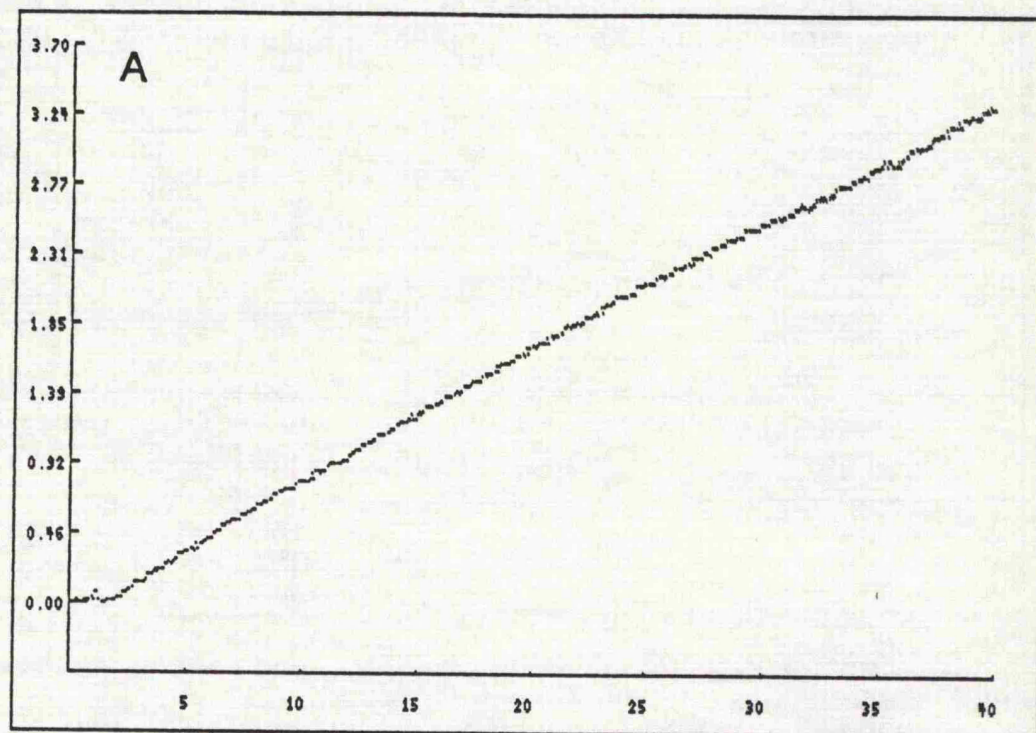
Incubations were performed, using the stopped assay method, at 37°C with 400 μM substrate and 0.01 mg/ml enzyme in 50 mM Hepes/KOH buffer, pH 7.5 as described under Section 2.4.
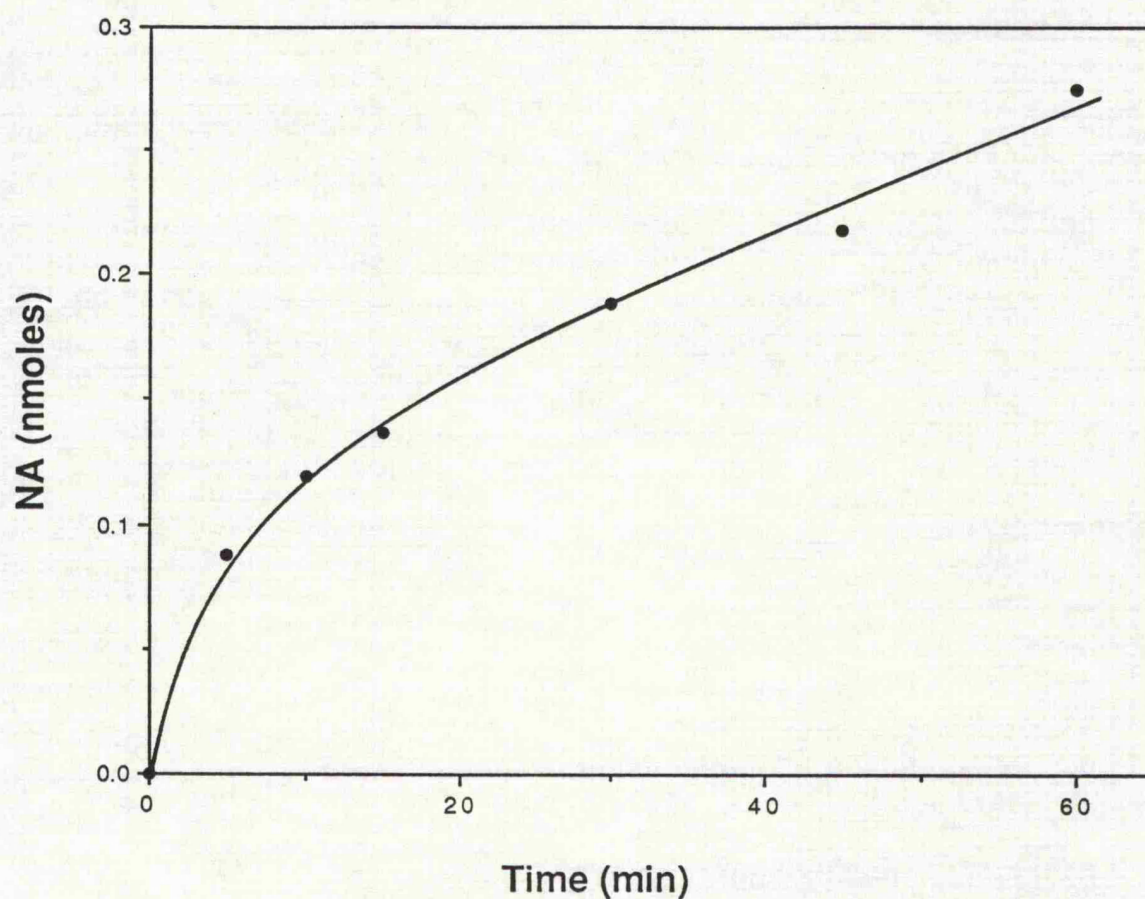
Figure 3.5:   Hydrolysis of 40 μM LLE-NA by the proteinase
                complex as a function of time.

Incubations were performed, using the stopped assay method,   at 37°C
with 40 μM substrate and 0.01 mg/ml enzyme in 50 mM Hepes/KOH
buffer, pH 7.5 as described under Section 2.4.
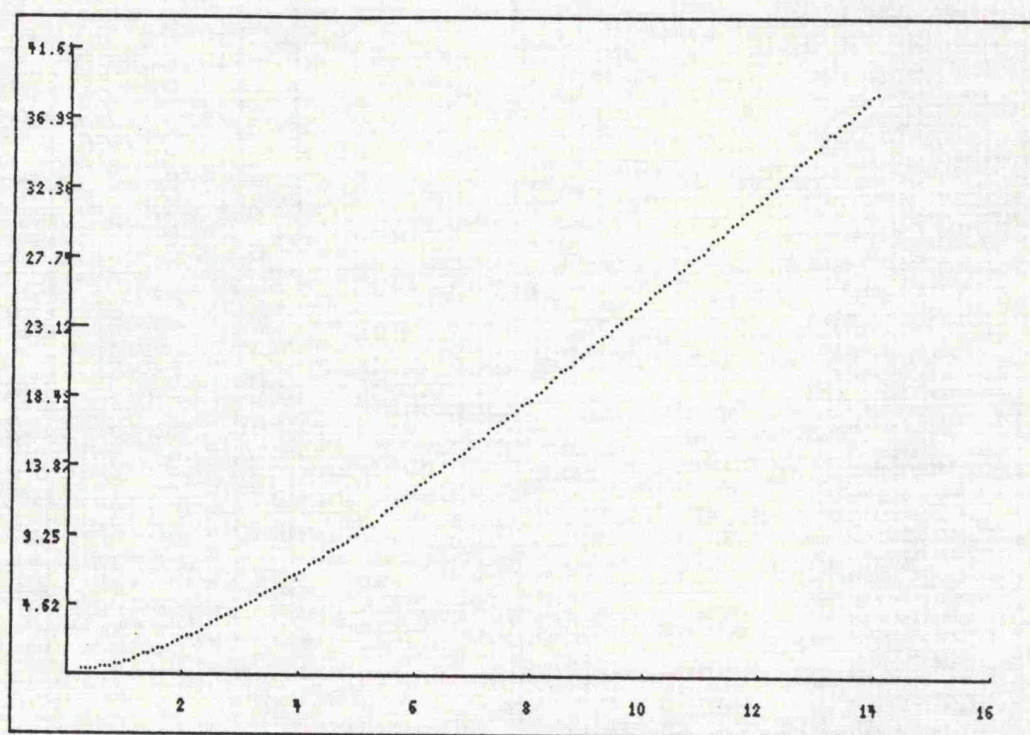
Figure 3.6:   Hydrolysis of 10 μM (A) and 50 μM (B) LLE-NA by
the proteinase complex as a function of time.

Incubations were performed, using the continuous assay method,   at 37°C
with 10 (A) or 50 μM (B) substrate and 0.01 mg/ml enzyme in 50 mM
Hepes/KOH buffer, pH 7.5 as described under Section 2.4.

Figure 3.7:   Hydrolysis of 600 μM LLE-NA by the proteinase complex as a function of time.

Incubations were performed, using the continuous assay method,   at 37°C with 600 μM substrate and 0.01 mg/ml enzyme in 50 mM Hepes/KOH buffer, pH 7.5 as described under Section 2.4.
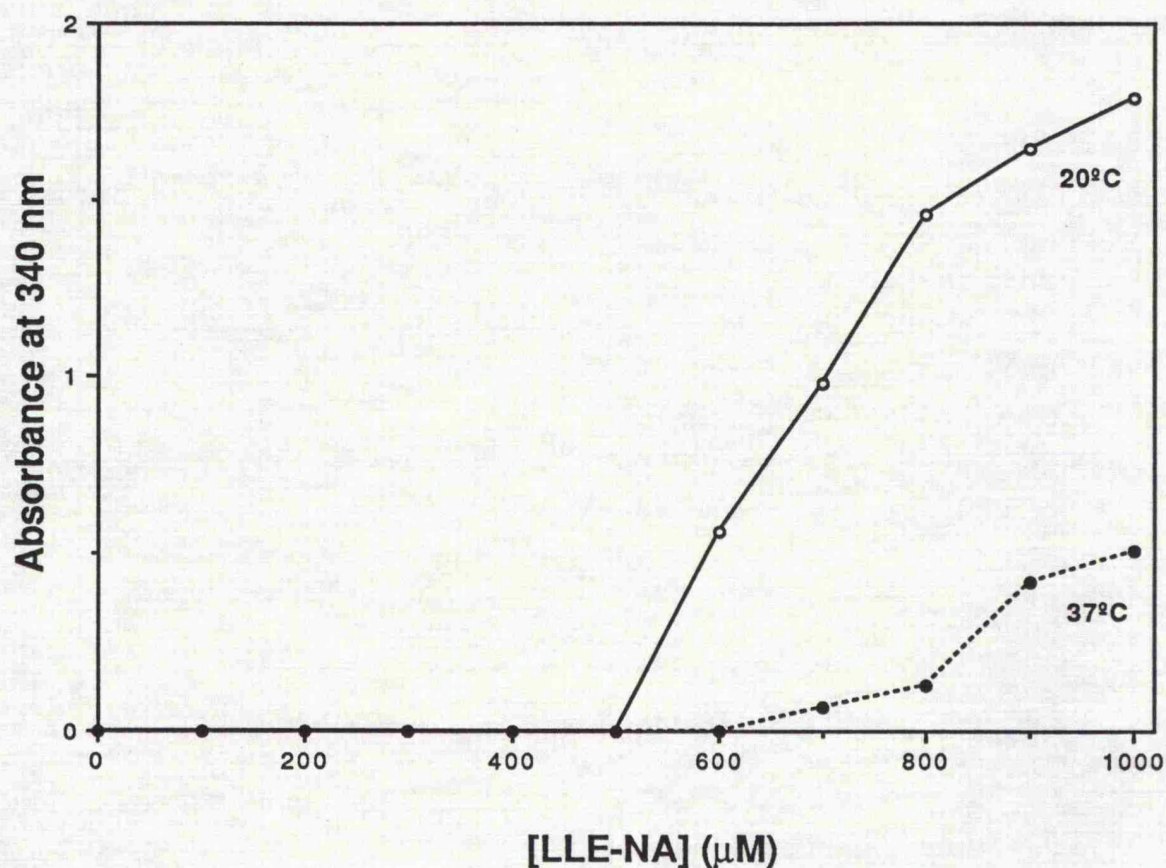
Figure 3.8: Dependence of the solubility of LLE-NA on temperature.

The absorbance at 340 nm was measured in a double beam spectrophotometer with a thermostated cell holder set either at 20°C or 37°C. Samples were set out under assay conditions in 0.2 ml of 50 mM Hepes/KOH buffer, pH 7.5 or 8.0 containing 6% DMSO and appropriate LLE-NA concentration as indicated. Test tubes were first equilibrated at either 20°C or 37°C in a water bath before addition of LLE-NA, vortexing, and subsequent absorbance reading. Blank samples contained no substrate.
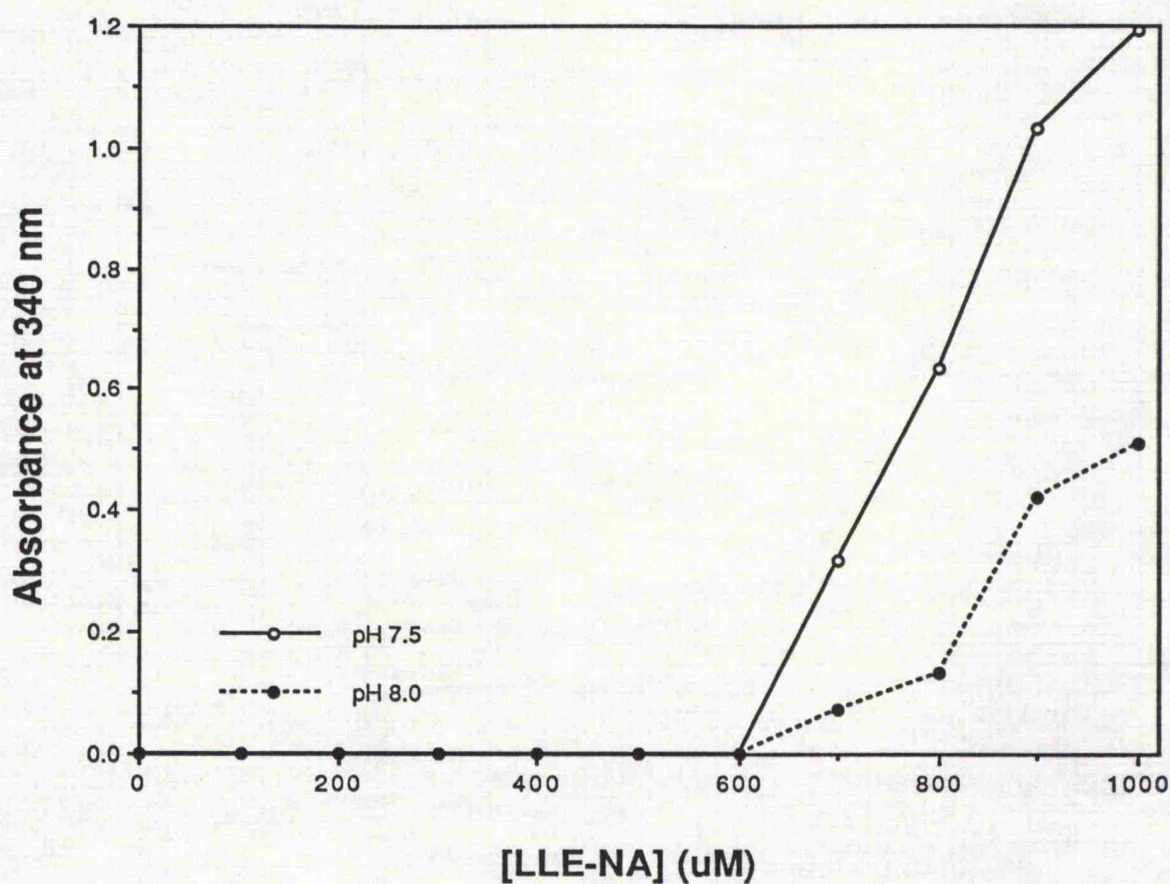
**Figure 3.9: Dependence of the solubility of LLE-NA on pH.**

The absorbance at 340 nm was measured in a double beam spectrophotometer with a thermostated cell holder set at 37°C. Samples were set out under assay conditions in 0.2 ml of 50 mM Hepes/KOH buffer, pH 7.5 or 8.0 containing 6% DMSO and appropriate LLE-NA concentration as indicated. Test tubes were first equilibrated aty 37°C in a water bath before addition of LLE-NA, vortexing, and subsequent absorbance reading. Blank samples contained no substrate.

Figure 3.10: MCP activity with varying LLE-NA concentrations.

Hydrolysis rates were measured in 50 mM Hepes/KOH buffer, pH 7.5, containing 6% DMSO and 0.01 mg/ml proteinase as described under Section 2.4. The error bars represent standard deviation from at least seven separate experiments carried out in duplicate. Standard deviations less than 5% are not shown.
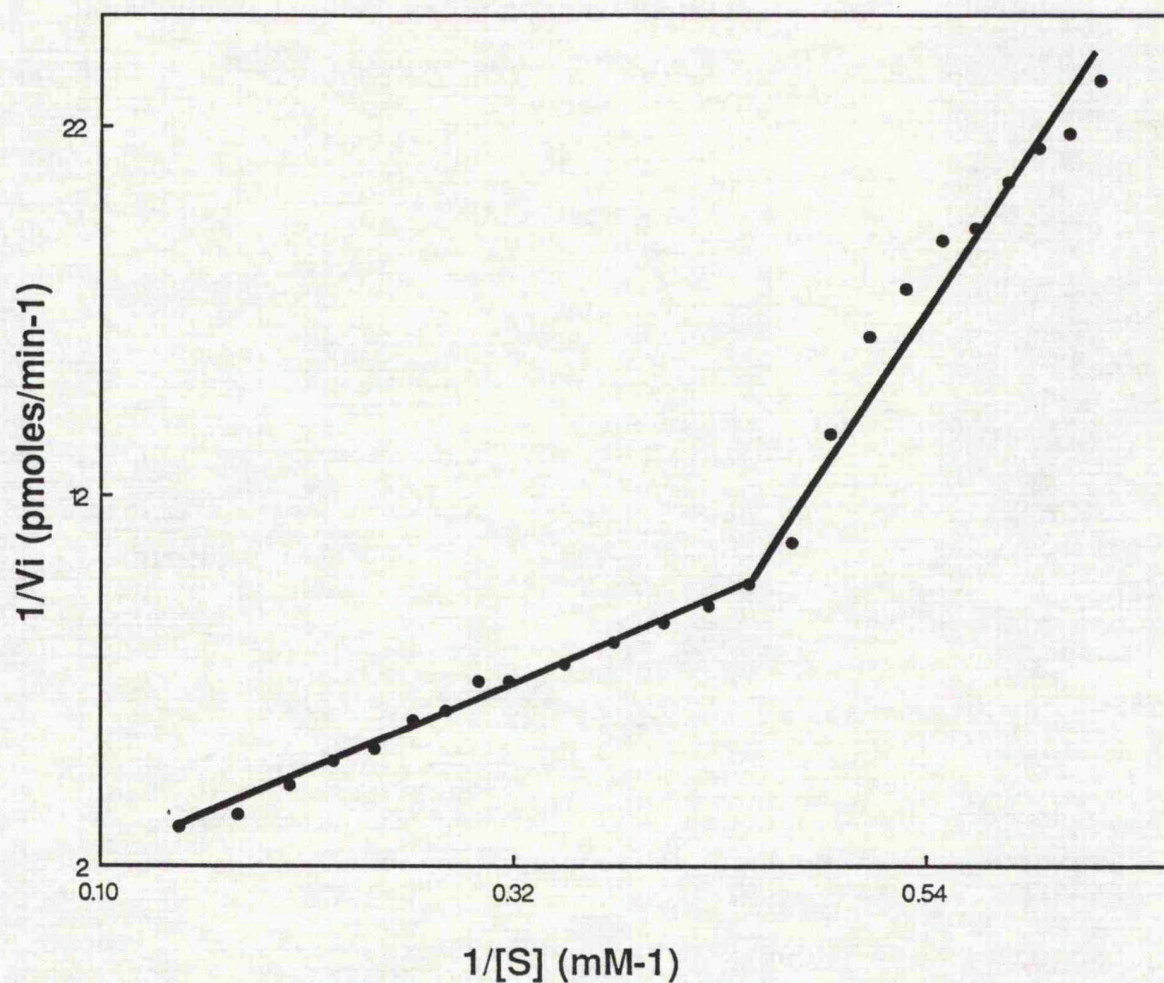
Activity (pmoles/min)

[LLE-NA] (μM)
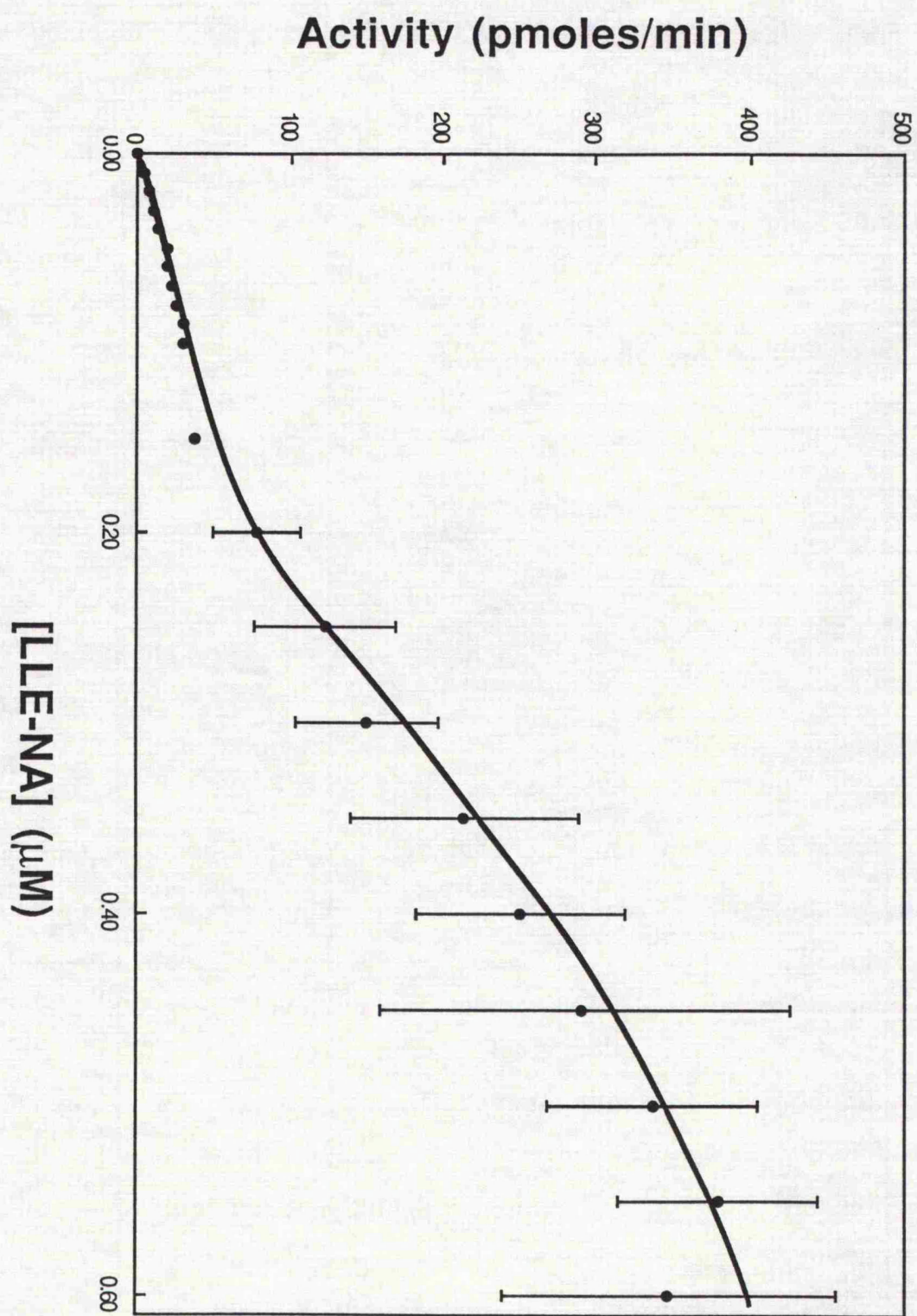
Figure 3.11: Double reciprocal plot of MCP activity with varying substrate concentrations.

The plot was performed using the method described by Lineweaver and Burk (1934). The data used in the plot is from Figure 3.12. For simplicity all standard deviations are not shown. Vi = Activity at indicated LLE-NA concentration. [S] = LLE-NA concentration.
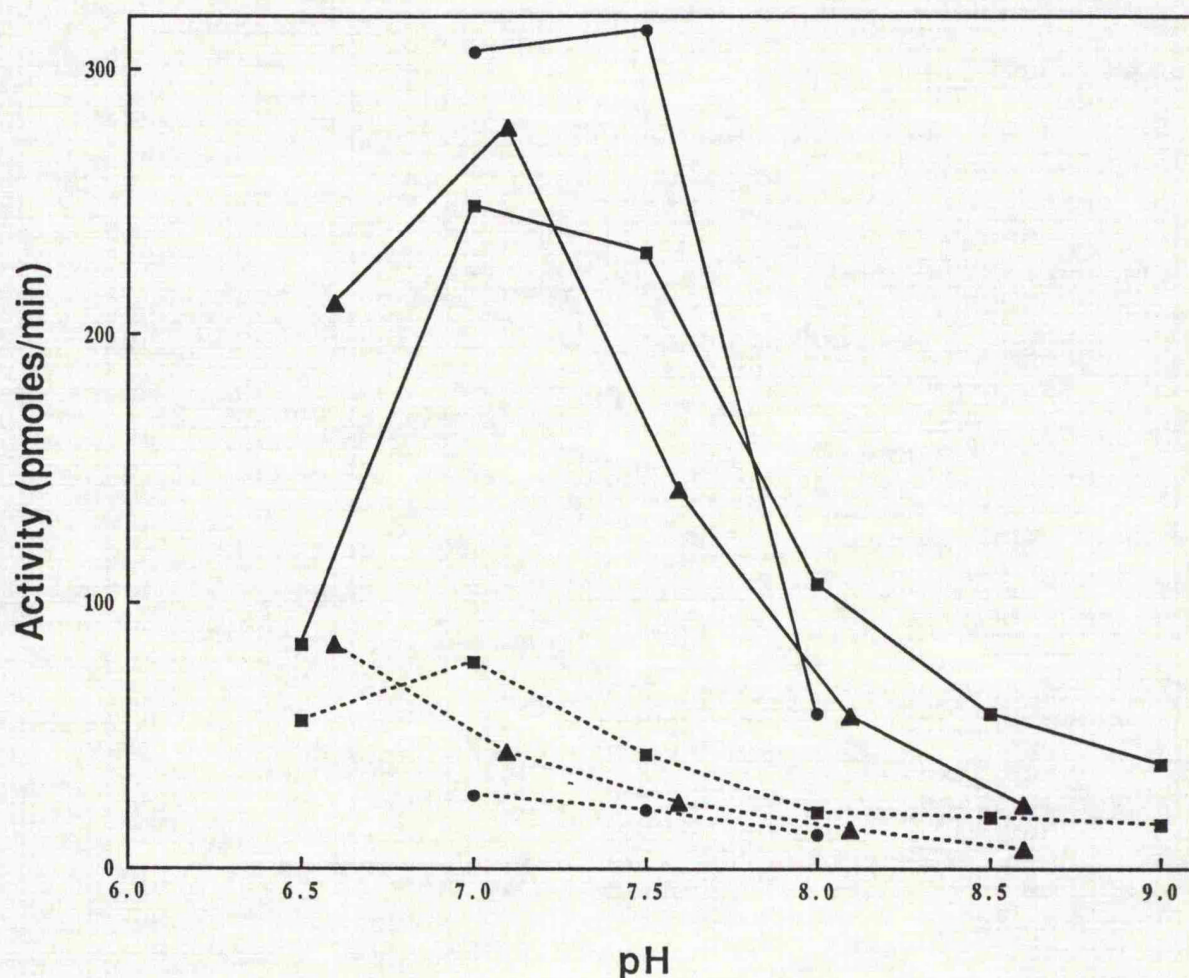
Figure 3.12: pH profile of the peptidylglutamyl-peptide hydrolase activity.

Hydrolysis rates of 0.1 mM (---) and 0.4 mM (——) LLE-NA were measured in 50 mM Hepes/KOH buffer (●), 50 mM Tris/HCl buffer (■), or 50 mM Bis-Tris-propane buffer (▲) as described under Section 2. The data is average of at least four separate experiments performed in duplicates, and the standard deviations are not shown for clarity of the graph.

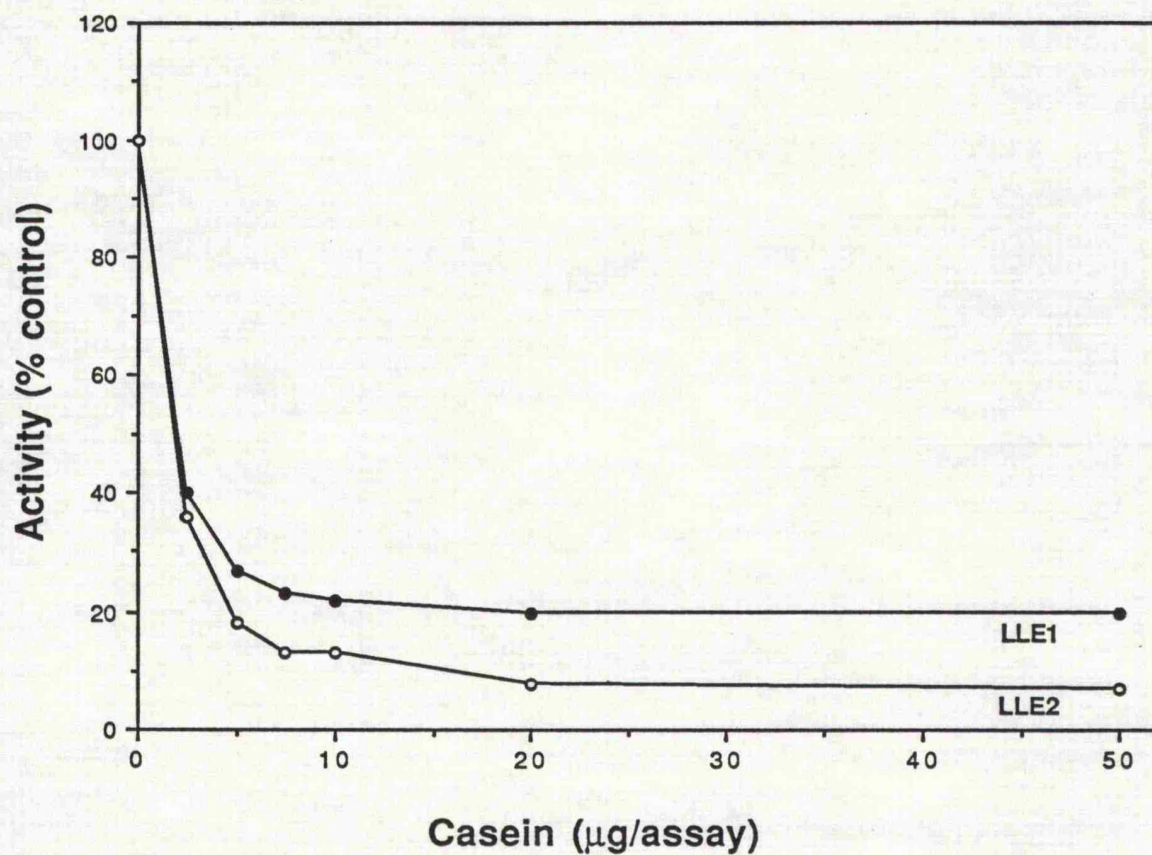Figure 3.13: Effect of casein on the hydrolysis of LLE-NA by the proteinase complex.

Hydrolysis rates were measured at 37°C in 50 mM Hepes/KOH buffer, pH 7.5, containing varying amounts of casein, 0.01 mg/ml proteinase, and either 0.1 mM LLE-NA (LLE1) or 0.4 mM LLE-NA (LLE2) as substrate as described under Section 2.4. Data is average of at least three separate experiments performed in duplicate.

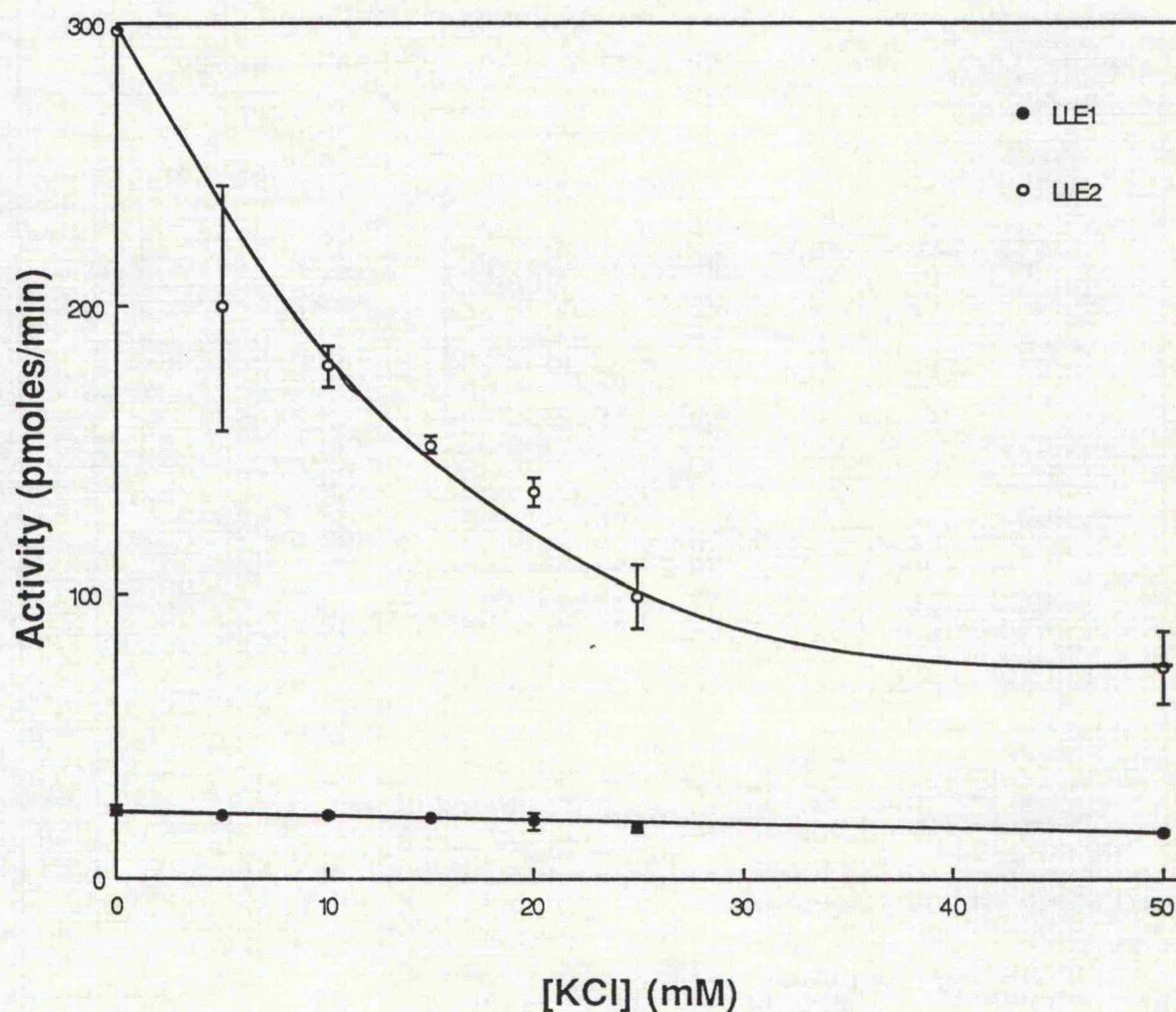**Figure 3.14:** Effect of potassium chloride on the peptidyl-glutamyl-peptide hydrolase activity.

Hydrolysis rates were measured in 50 mM Hepes/KOH chelex-treated buffer, pH 7.5 including appropriate KCl concentrations with either 0.1 mM LLE-NA (LLE1) or 0.4 mM LLE-NA (LLE2) as substrate. The error bars represent standard deviations from at least three separate experiments performed in duplicate.

Figure 3.15: Hydrolysis of LLE-NA by the proteinase complex in the presence of KCl as a function of substrate concentration.

Hydrolysis rates were measured in 50 mM Hepes/KOH chelex-treated buffer, pH 7.5, containing 50 mM KCl, 6% DMSO, and 0.01 mg/ml proteinase as described under Section2. The error bars represent standard deviations from at least four separate experiments performed in duplicate. Standard deviations less than 5% are not shown for simplicity.
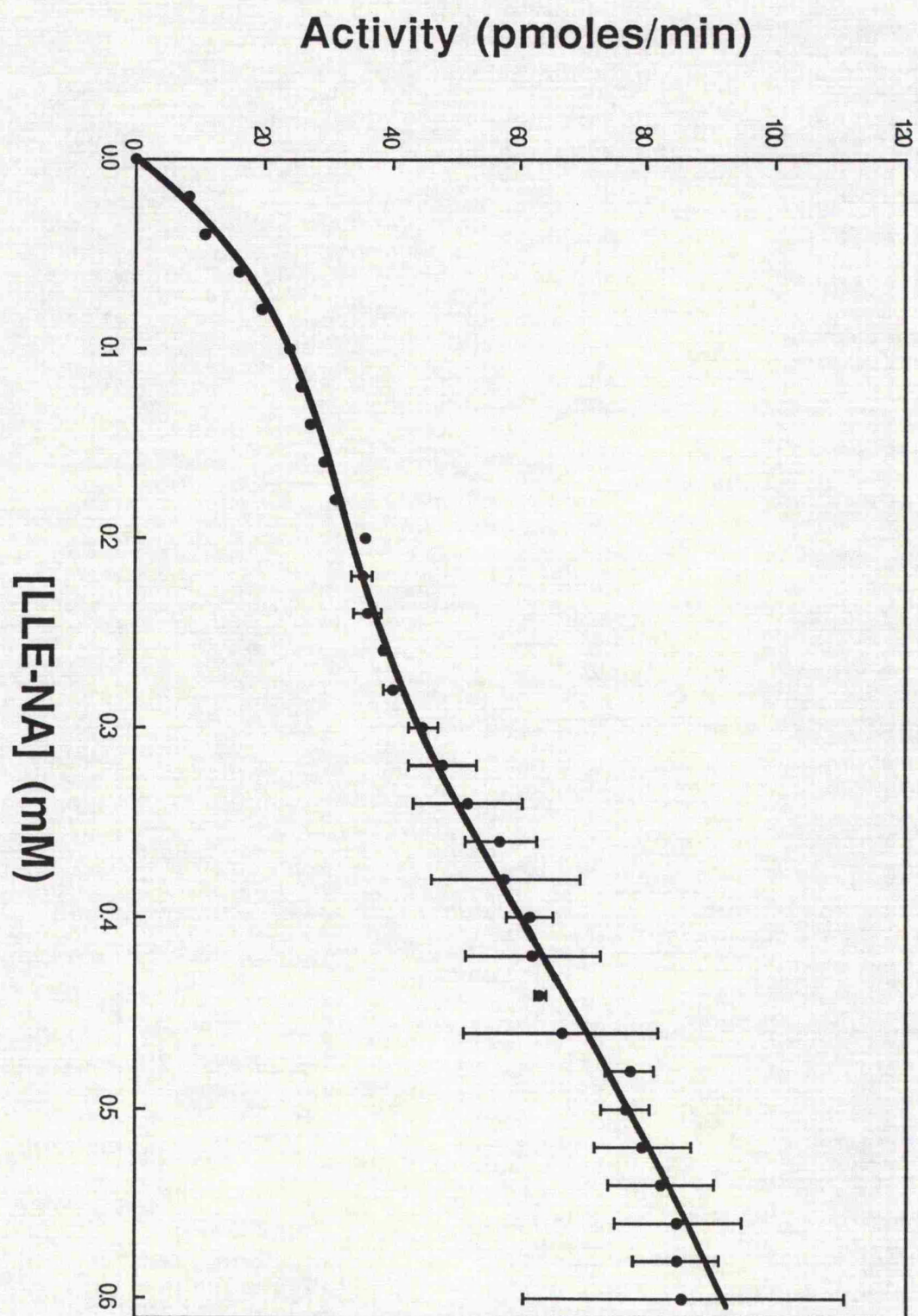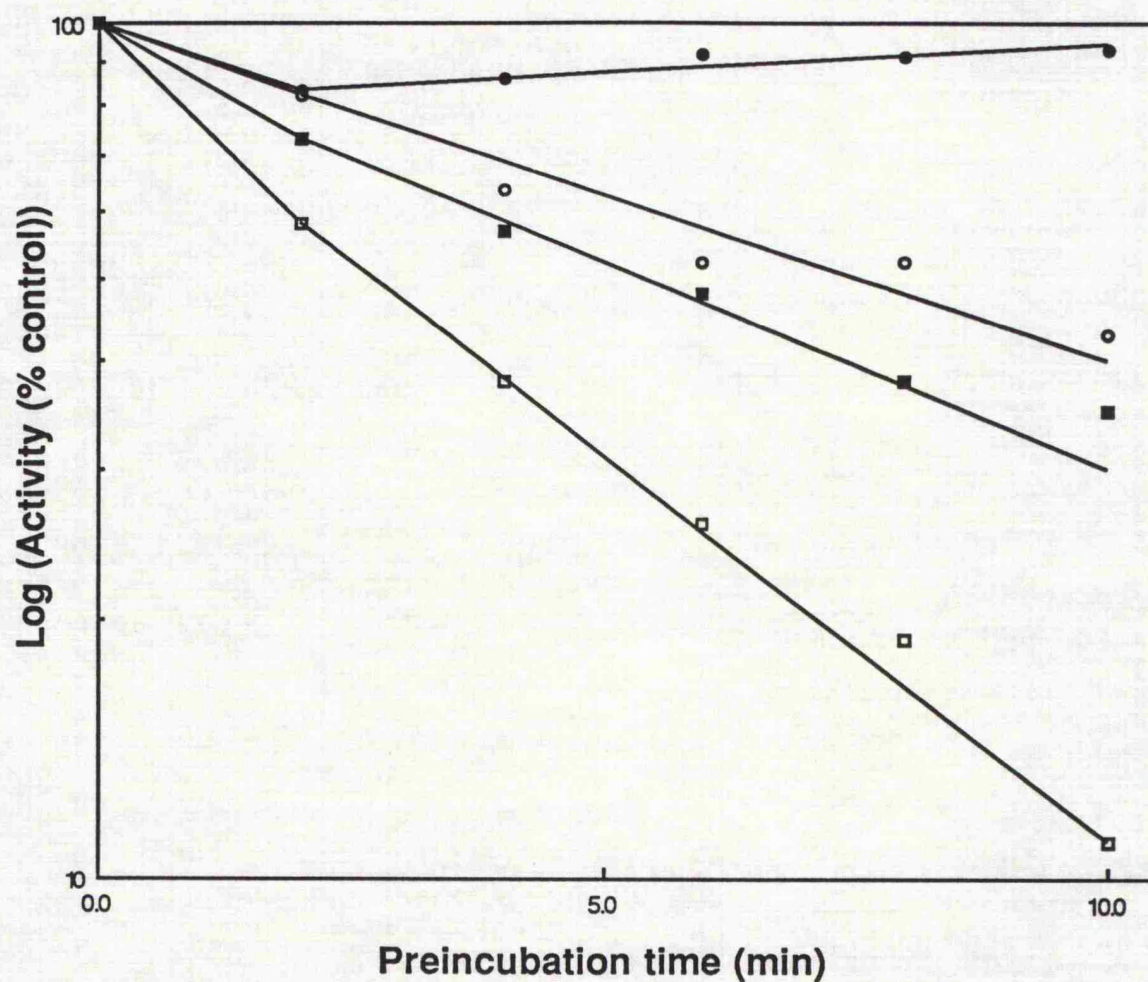
Figure 3.16: Thermal stability of petidylglutamyl-peptide hydrolase activities.

Hydrolysis of 0.1 mM (closed symbols) and 0.4 mM (open symbol) LLE-NA was assayed, following preincubation of MCP (0.2 mg/ml) at 55 °C (●, ○) or 60 °C (■ , □), as described under Section 2. Data are the average of three separate experiments performed in duplicate.
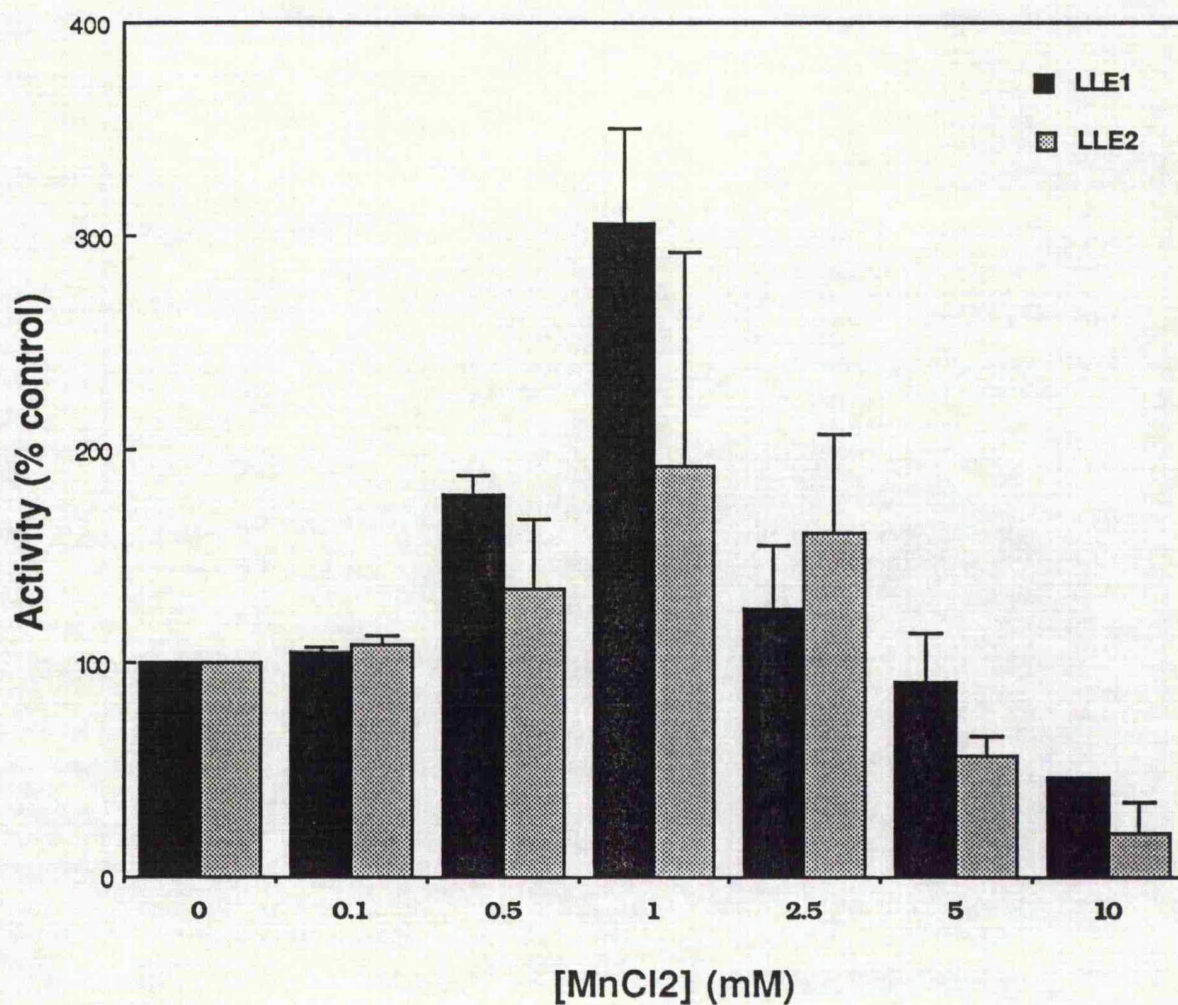
Figure 3.17: **Manganese dependence of the peptidylglutamyl-peptide hydrolase activity.**

Hydrolysis rates, expressed as percentage control, were determined in 50 mM Hepes/KOH chelex-treated buffer, pH 7.5, including appropriate $MnCl_2$ concentration, and 0.1 mM or 0.4 mM LLE-NA as described under Section 2.4. The error bars represent standard deviations from at least three separate experiments performed in duplicate.

Figure 3.18: Hydrolysis of LLE-NA by the proteinase in the presence of MnCl$_2$ as a function of substrate concentration.

Hydrolysis rates were measured in 50 mM Hepes/KOH chelex-treated buffer, pH 7.5, containing 1 mM MnCl$_2$, 6% DMSO, and 0.01 mg/ml proteinase as described under Section2. The error bars represent standard deviations from at least six separate experiments performed in duplicates. Standard deviations less than 5% are not shown.
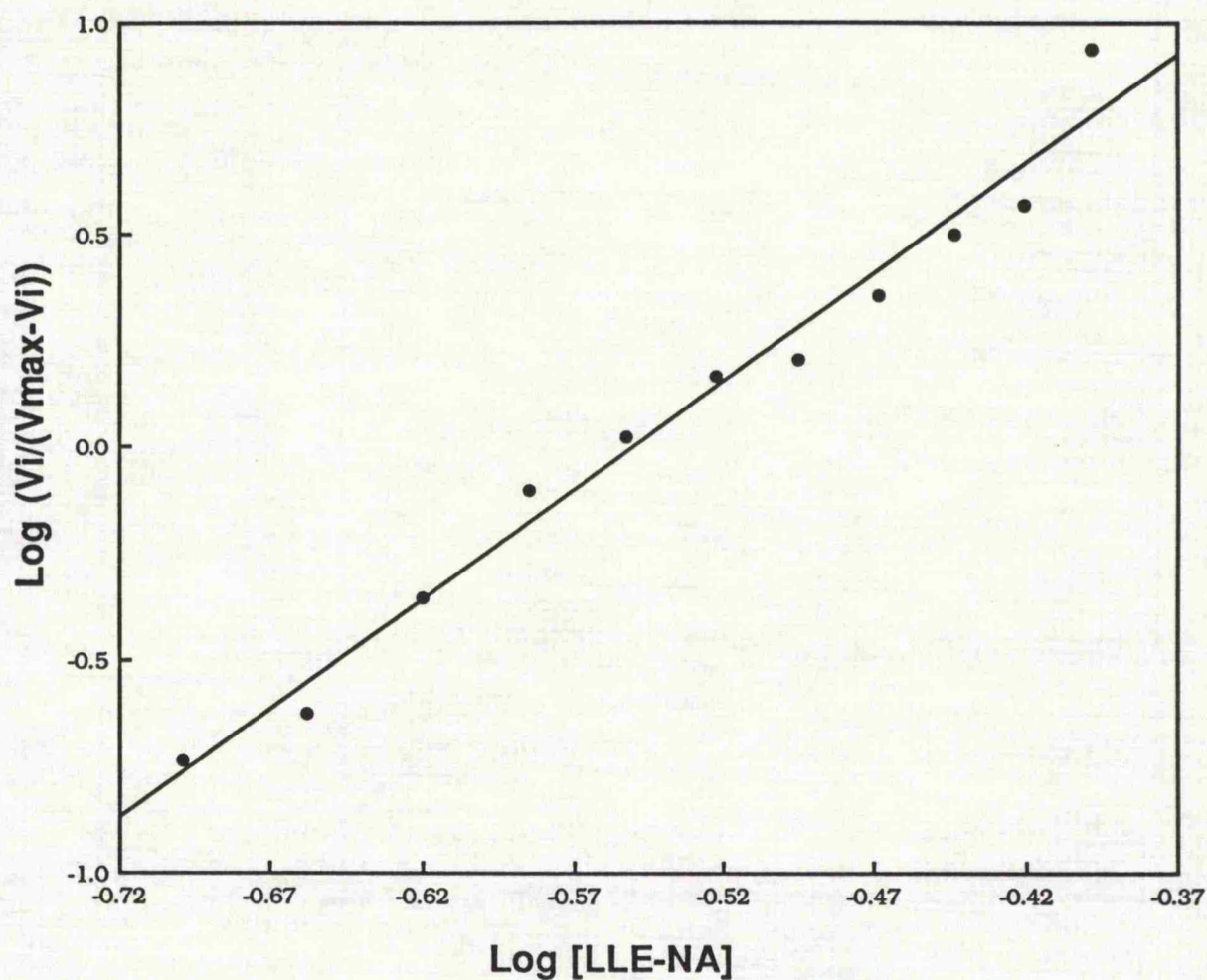
Figure 3.19:   Hill plot of the data from Figure 3.18.

The plot was performed by the method described by Hill (1925). V_{max} was estimated from Figure 3.19 and log $(V_i/(V_{max} - V_i))$ values were calculated for each of the data points within the appropriate substrate concentration range. The Hill coefficient calculated from the slope is 5.1.
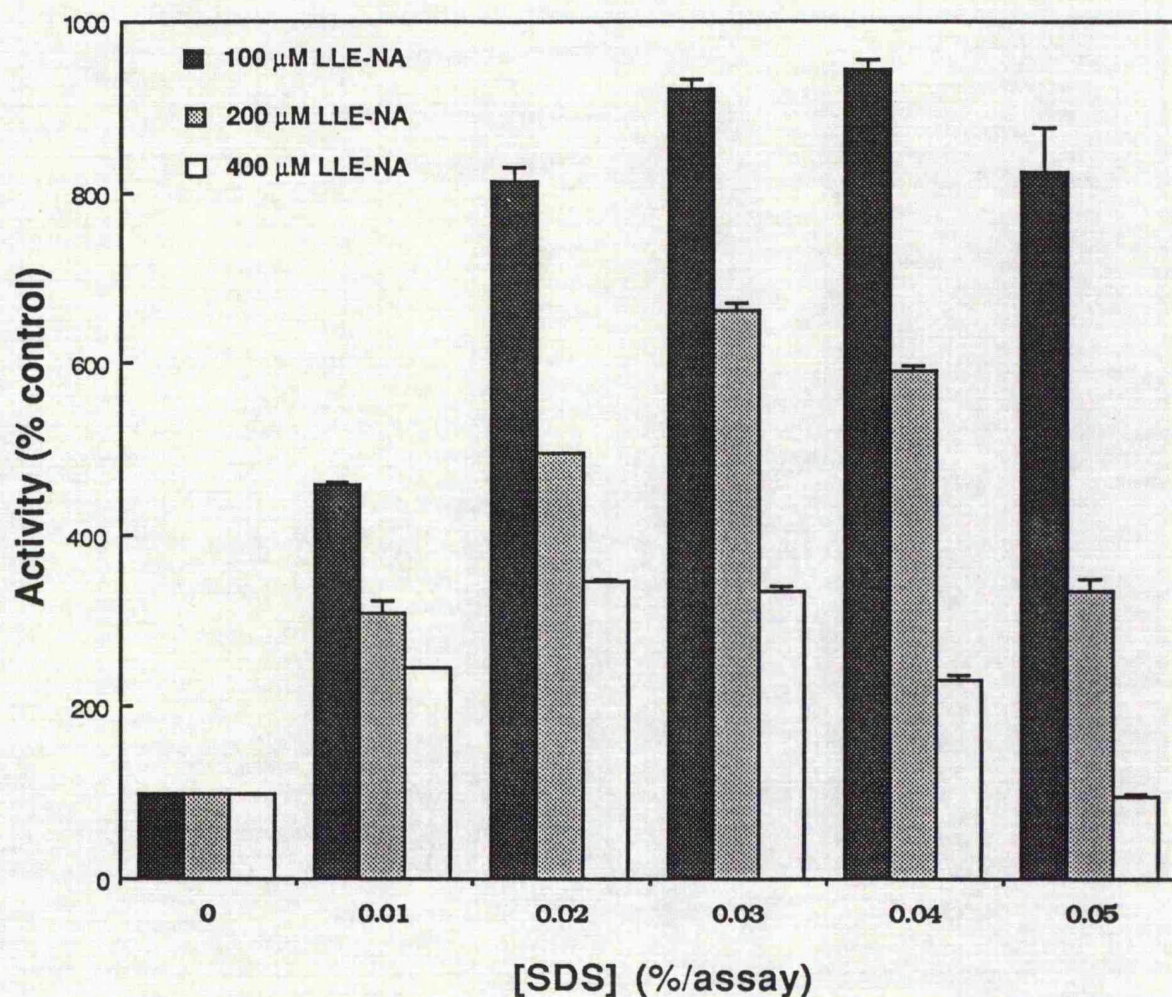
Figure 3.20: Effects of SDS on the peptidylglutamyl-peptide hydrolase activity.
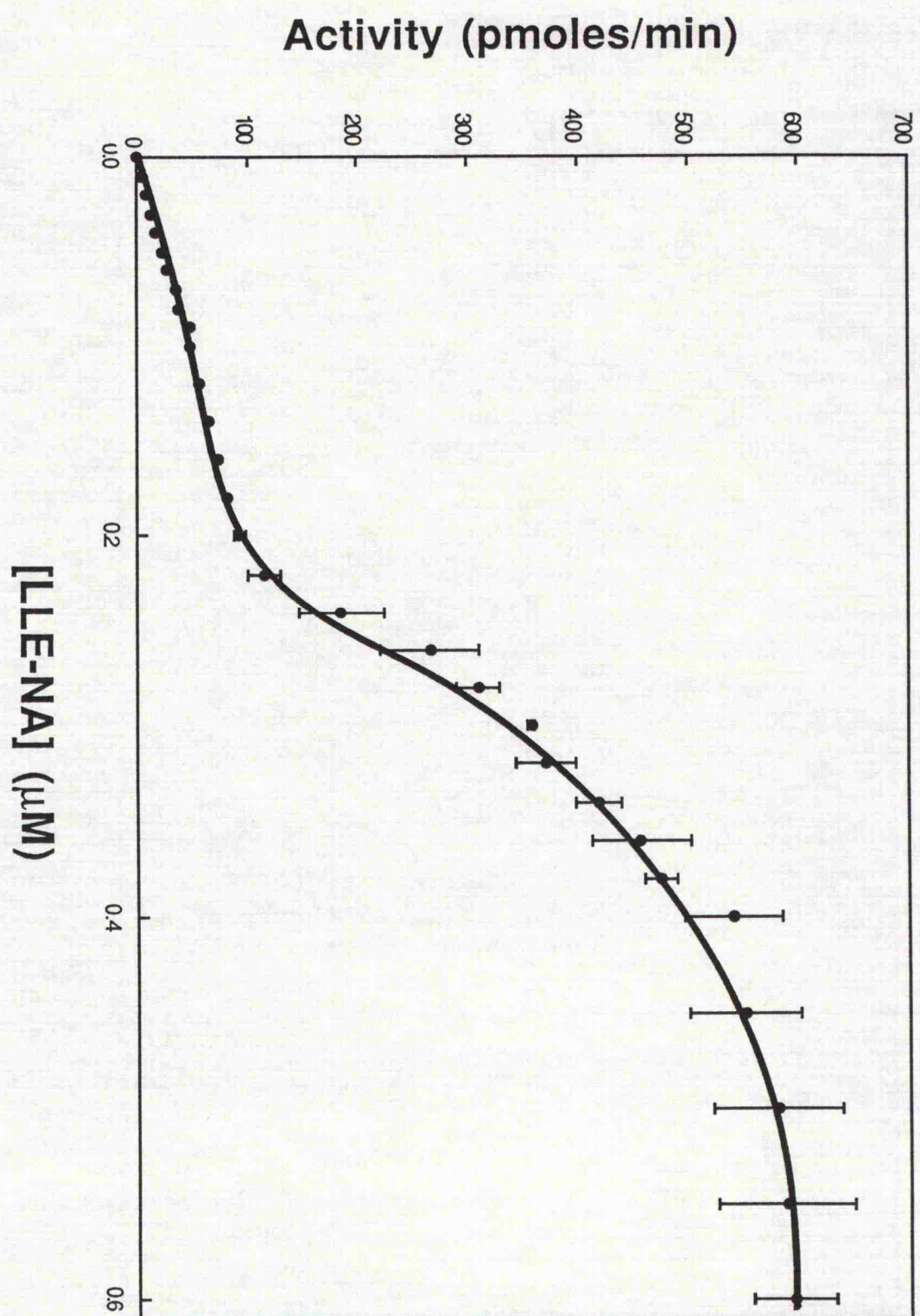
Hydrolysis rates, expressed as percentage control, were determined in 50 mM Hepes/KOH buffer, pH 7.5, including appropriate SDS concentration, and 0.1 mM, 0.2 mM, or 0.4 mM LLE-NA as indicated, as described under Section 2.4. The error bars represent standard deviations from at least three separate experiments performed in duplicate.
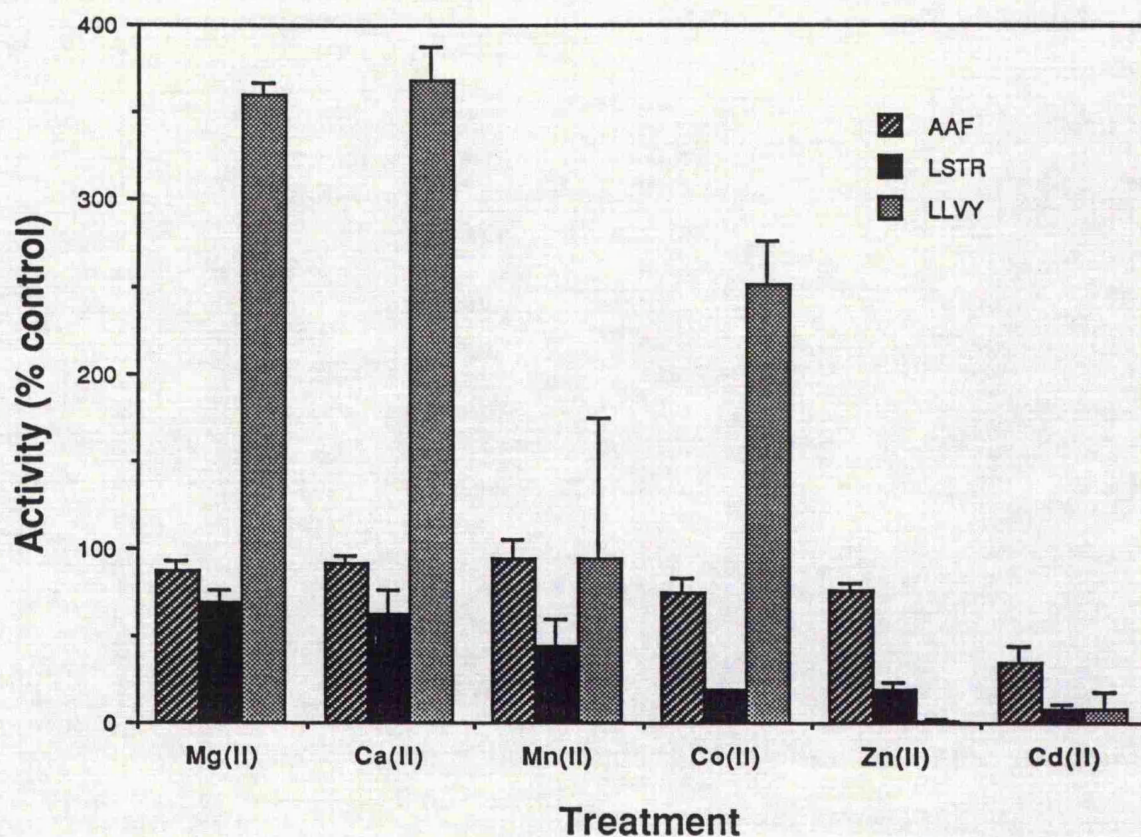
Figure 3.21: Effect of divalent metal ions on the different proteolytic activities of the proteinase complex.

Prior to activity determination, 50 mM Hepes/KOH buffer was pretreated with chelex-100. Activities were determined as described under Section 2.4 with either 50 mM AAF-AMC, or LSTR-AMC. The error bars represent standard deviations from six separate experiments performed in duplicate.

CHAPTER 4

Inhibitor Studies of the different proteolytic activities of the multicatalytic proteinase complex.

"The study of the effects of inhibitors on enzyme systems can fairly claim to have yielded as much, or more, information about the properties and structure of enzymes, and in particular of their active sites, than has been obtained from the study with substrates. This is especially true of enzymes which are so highly specific for one particular substrate that it has not been possible to study the influence of changes in the structure of the substrate on the reaction catalysed by the enzyme."

Gutfreund (1965)

4.1 Introduction.

It is not well established yet to which mechanistic class of protease the different activities of the multicatalytic proteinase complex belong. In some studies, the enzyme was classified as a cysteine protease because of its sensitivity to thiol reagents, mercury chloride, and some cysteine protease inhibitors (Ismail and Gevers, 1983; Rivett, 1985; McGuire and DeMartino, 1986; Mykles, 1989; Shaw, 1990).

More recently, the proteinase complex has also been described as an atypical serine protease because of its inactivation by: 1) The mechanism based serine protease inhibitor 3,4 dichloroisocoumarin (Orlowski and Michaud, 1989; Rivett et al., 1990; Mason, 1990), 2) Some isocoumarin derivatives (Orlowski and Michaud, 1989), 3) The serine protease inhibitor diisopropylfluorophosphate (Wagner et al., 1985; Mykles, 1989; Orlowski and Michaud, 1989; Sato and Shiratsuchi, 1990), and 4) The serine protease inhibitor phenylmethanesulphonyl fluoride (Tanaka et al., 1986a; Mykles, 1989).

The proteinase was found to be very unreactive towards most inhibitors. In most studies, the inhibitor concentration had to be used in large excess over enzyme concentration in order to observe any inhibitory effects ie [I] >> [E]. Under these conditions, the pool of inhibitor concentration could be assumed constant if the inhibitor is very stable in solution. Therefore, the reaction between inhibitor and enzyme becomes a pseudo-first-order process. The rate constant (k_{obs}) of the reaction is obtained from the slope of the plot of Log (residual activity) vs preincubation time.

Another useful quantity is the half-time for the reaction. This is the time taken for enzyme activity to fall to half its original value, and is inversely proportional to k_{obs} as follow:

$$t_{1/2} = 0.693/k_{obs} \hspace{3cm} (4.1)$$

This Chapter describes several studies undertaken to clarify the classification of the proteinase complex, to investigate the distinct proteolytic sites within the complex, and to identify any potent active site directed inhibitor(s) which could subsequently be used for labelling the respective active site(s).

4.2 Inhibition by 3,4 dichloroisocoumarin.

3,4 Dichloroisocoumarin (DCI) is a mechanism-based inhibitor of serine type proteases discovered by Harper et al. (1985). Recent studies by Powers and coworkers showed that inhibition by different substituted chloroisocoumarins could be reversed by hydroxylamine after solvolysis, if the covalent bond between the inhibitor and the enzyme was through the active site serine (Harper and Powers, 1985; Kam et al., 1988; Powers et al., 1990).

However, from the crystal structure of the complex of porcine pancreatic elastase with 7-amino-3-(2-bromoethoxy)-4-chloroiso-coumarin, it was clear that the inhibitor formed two covalent attachments with the enzyme: one with the active site serine, and the other with the active site histidine. In this case, the inhibition was found to be irreversible, as it was when the covalent attachment was found to be through the active site histidine only (Vijayakshmi et al.,

1991). The acyl enzyme formed by solvolysis contains a more stable histidine adduct, in contrast to the serine adduct which could be reactivable by hydroxylamine (Vijayakshmi et al., 1991). The proposed mechanism for the reaction of serine proteases with DCI is illustrated in Figure 4.1.

Prior to inactivation studies, the enzyme solution was dialysed overnight to remove the reducing agent 2-mercaptoethanol, as the latter was found to inactivate the inhibitor as illustrated in Figure 4.2. DCI has an estimated half life of 26 min in 50 mM Hepes/KOH buffer, pH 7.5, containing 2% DMSO. Under similar conditions and in the presence of 1 mM dithiothreitol, a half life of less than 1 min was observed for the inhibitor. A comparable half life of 18 min in 0.1 M Hepes/KOH buffer, pH 7.5, containing 0.5 M NaCl and 10% DMSO has been reported by Harper et al. (1985). The inactivation of the inhibitor by reducing agents and by cysteine was also reported previously (Harper et al., 1985; Mason, 1990).

The AAF and LLE2 activities were inactivated by DCI concentrations as low as 4 μM, whereas no inhibitory effects but stimulatory ones were observed for the LSTR activity (Table 4.1). The LLE1 activity, on the other hand, was activated by DCI at concentrations up to 20 μM, and inhibited at higher ones. At inhibitor concentrations as high as 200 μM, all activities were inhibited except the LSTR activity, which was not stimulated by the inhibitor as it was at lower DCI concentrations (Table 4.1). Caution must be taken when interpreting the effects of DCI at such high concentrations (> 100 μM), as Rusbridge and Beynon (1990) have shown that the serine protease inhibitor could also act as a general alkylating agent.

Preincubation of the proteinase with 20 μM inhibitor led to a rapid inactivation of the AAF activity, with an estimated $k_{obs}/[I]$ value of 120 M^{-1} s^{-1} (Figure 4.3). The LLE2 activity was also inactivated by DCI, with an estimated $k_{obs}/[I]$ value of 48 M^{-1} s^{-1}. There was no further inhibition of the above activities after 60 min preincubation (data not shown). The LLE1 activity was activated by DCI in a time-dependent fashion, with up to two-fold activation being observed after 30 min preincubation (Figure 4.3). The DCI treatment, on the other hand, had a spontaneous stimulatory effect on the LSTR activity, with up to four-fold activation being observed after 10 min preincubation (Figure 4.3). It is difficult to estimate accurate values for $k_{obs}/[I]$ because of the instability of the inhibitor under the chosen assay conditions.

Figure 4.4 shows similar time courses as in Figure 4.3 but in the presence of 2 mM dithiothreitol to inactivate the inhibitor. It was found that the re-inclusion of the reducing agent abolishes any inhibitory effects. There was no stimulatory nor inhibitory effect on the LLE1 activity. However, the LSTR activity was activated under these conditions but not to the same fold activation as in the absence of the reducing agent (compare Figures 4.3 and 4.4).

An attempt to reactivate the DCI-treated MCP using hydroxylamine (Vijayakshmi et al., 1991) was performed, bearing in mind that it was found to inhibit the LLE activities (Figure 4.5) as well as the AAF and LSTR activities (Savory and Rivett, unpublished observations). Treatment of the DCI-treated enzyme with hydroxylamine (Figure 4.6) failed to reactivate the inhibited activities as was expected; so did similar treatment in the presence of dithiothreitol (Figure 4.7).

The interesting result from the above attempt was that hydroxylamine reduced the activation of the LSTR activity (Figure 4.5), which is suggestive that the activation was a result of some kind of reaction of the enzyme with DCI or its breakdown products, which was probably reversed by the action of hydroxylamine as reflected by the two-fold reduction in the activation (Figure 4.6).

There was no observed recovery of activity, when the DCI-treated enzyme was left standing at room temperature for periods up to four hours (Table 4.2). Dialysis of the DCI-treated enzyme for a period of 24 hours did not lead to recovery of the inhibited activities, but led to a reduction in the observed activation of the LSTR activity to approximately control level (Table 4.2). The results again suggest that the activation by DCI.of the LSTR activity was a result of somekind of interaction of DCI or its breakdown products with the enzyme, which could be reversed.

Having observed the inhibition of the LLE2 activity by DCI, an attempt to investigate the substrate dependence of the peptidyl-glutamyl-peptide hydrolase activity was performed using the DCI-treated enzyme. Thus, looking at the high affinity site (non-cooperative component) of the activity in the absence of the low affinity sites (cooperative component). Activity with varying substrate concentration was found to obey Michaelis-Menten kinetics where V_{max} was reached (Figure 4.8), giving a K_m value of 70 µM and a V_{max} of 79 nmol/min/mg. This data provides the best evidence, so far, for the existence of the non-cooperative component of the peptidyl-glutamyl-peptide hydrolase activity.

4.3 Inhibition by 4-(2-Aminoethyl)-benzenesulphonyl fluoride and related compounds.

4-(2-Aminoethyl)-benzenesulphonyl fluoride (Pefabloc) is a newly designed serine protease inhibitor, based on the early observations of Gold (1965) that sulphonyl fluorides can sulphonylate the active site serine with the formation of an O-sulphonylserine, as has been shown in the cases of phenylmethylsulphonyl fluoride (PMSF) (Gold, 1965), and 4-amidinophenylmethanesulphonyl fluoride (APMSF) (Laura, 1980). The mechanism of reaction of serine proteases with sulphonyl containing compounds is shown in Figure 4.9. The structures of Pefabloc, APMSF, and PMSF are also shown in Figure 4.10 for illustration.

It was found that the LSTR activity was selectively inactivated by Pefabloc (Table 4.3), with 11% residual activity remaining after 60 min preincubation with 0.5 mM inhibitor. Complete inactivation of the activity was achieved at higher Pefabloc concentrations, with no observed inhibitory effects on the other activities (Table 4.3).

The addition of dithiothreitol had no effect on the extent of inhibition (Table 4.3), thus eliminating the possible involvement of sulfhydryl groups at the catalytic site of the activity. In comparison, PMSF and APMSF at concentration of 1 mM had little effect on any of the proteinase activities (Table 4.3).

Time courses of inhibition of the LSTR activity were investigated at Pefabloc concentrations of 0.5 and 1.0 mM, and are shown in Figure 4.11. The inhibition profiles were linear over the one hour period,

from which $k_{obs}/[I]$ of 1.21 M^{-1} s^{-1} ([I] = 0.5 mM) and 0.89 M^{-1} s^{-1} ([I] = 1.0 mM) were obtained.

4.4 Inhibition by 2-nitro-4-carboxylphenyl,N,N'-diphenyl-carbamate.

2-nitro-4-carboxylphenyl,N,N'-diphenylcarbamate (NCDC) is a chromogenic serine protease inhibitor, based on the earlier work of Erlanger and coworkers on the inhibitor diphenylcarbamyl chloride, which has been shown to inactivate proteases with serine residues at the active site (Erlanger and Edel, 1964; Erlanger et al., 1966; Walenga et al., 1980). The mechanism of which is shown in Figure 4.12.

The effects of NCDC on the different proteolytic activities of the complex were investigated. The LSTR, LLVY, LLE1, and LLE2 activities were partially inactivated at concentrations of 1.0 and 5.0 mM inhibitor (Table 4.4). In contrast, the AAF activity was unaffected at 1.0 mM NCDC but slightly activated at 5.0 mM NCDC. The difference in response of the AAF and LLVY activities is suggestive of them being hydrolysed at distinct sites.

4.5 Inhibition by diisopropylfluorophosphate.

The mechanism of reaction of serine proteases with DFP is shown in Figure 4.13. The LLVY and LLE1 activities were inhibited by 5.0 mM DFP, the AAF and LSTR activities were slightly affected, whereas the LLE2 activity was activated by the treatment (Table 4.4).

Time courses of inhibition of the LLVY and LLE1 activities are illustrated in Figure 4.14, from which $k_{obs}/[I]$ of 0.017 and 0.024 M^{-1}

9 2

s^{-1} were obtained, respectively. The inhibition of the LLE1 activity by DFP provides yet again another evidence for it being distinct from the LLE2 activity, and for it being of a serine protease type. Similarly, the inactivation of the LLVY activity supports the above suggestion for it being distinct from the AAF activity.

4.6 Inhibition by peptide aldehydes.

The peptide aldehydes chymostatin, leupeptin, antipain, and elastatinal were tested as potential inhibitors of the LLE activities, the effects of which are summarized in Table 4.5. Chymostatin did not inhibit at low concentrations, but some inhibition was observed when it was used at a concentration of 1.0 mg/ml with 72% and 59% residual activity remaining of the LLE1 and LLE2 activities, respectively (Table 4.5).

Leupeptin, however, inhibited the LLE1 activity at a lower concentration of 0.01 mg/ml with 66% residual activity remaining. No further inhibition was observed with concentrations up to 1.0 mg/ml. At a leupeptin concentration of 1.0 mg/ml, the LLE2 activity was inhibited with 65% residual activity remaining (Table 4.5). Leupeptin appears to discriminate between the two activities at lower but not at higher concentrations.

Antipain and elastatinal had less inhibitory effects on the activities, except the inhibition of the LLE2 activity in the presence of 1.0 mg/ml antipain (Table 4.5).

Several analogues of chymostatin were also tested as potential inhibitors of the LLE activities (Table 4.6). They were found to be not

very effective inhibitors, except the analogue Z-Val-Phe-CHO (0.01 mg/ml) which inhibited the LLE2 activity with 52% residual activity remaining (Table 4.6), again providing another evidence for the LLE1 and LLE2 activities as being distinct.

4.7 Inhibition by peptidylchloromethylketones and peptidyldiazomethanes.

The effects of the following peptidylchloromethylketones Z-Gly-Gly-Phe-CH_2Cl, Ala-Ala-Phe-CH_2Cl, Tyr-Glu-Arg-CH_2Cl, and Tyr-Pro-CH_2Cl on the peptidylglutamyl-peptide hydrolase activity were investigated. At a concentration of 0.1 mM of each, there was no observed inhibitory effect on either activity (Table 4.7).

The peptidylchloromethylketone Z-Tyr-Ala-Glu-CH_2Cl was synthesized as a potential affinity label for the LLE sites. It was found that the affinity label, at a concentration of 0.1 mM, failed to inactivate the LLE activities, but rather inactivated the AAF and LLVY activities with no effects on the LSTR activity as illustrated in Table 4.8. When the affinity label was used at a concentration of 0.2 mM, there was no further increase in the inhibitory effects registered with 0.1 mM inhibitor, with 68% and 52% of residual activity remaining (Table 4.8).

Time courses of inhibition by 0.1 mM inhibitor were investigated for all activities for a period of 90 min, and are shown in Figure 4.15. It is interesting to note activation of the LLE activities after longer preincubation period with the affinity label. After 30 min preincubation, there was no further inhibitory effects on the AAF and

94

LLVY activities, even when an extra 0.1 mM inhibitor was added to the preincubation mix (data not shown).

The effects of several peptidyldiazomethanes on the LLE activities were investigated and are summarized in Table 4.9. The inhibitors Z-Ala-Ala-Leu-CHN$_2$ and Z-Leu-Trp-CHN$_2$, at a concentration of 0.1 mM, inactivated the LLE2 activity preferentially to the LLE1 activity. The inhibitor Val-Lys-Gly-Lys-CHN$_2$ inhibited both LLE activities, whereas the other inhibitors tested had a slight inhibitory effect (Table 4.9). It should be noted here that peptidyldiazomethanes have been also found to react with serine proteases (Shaw, 1990).

4.8 Inhibition by thiol-reactive reagents.

The effects of the thiol-reactive reagents N-ethylmaleimide (NEM), methylmethanethiosulphonate (MMTS), and iodoacetic acid (IAA) on the peptidylglutamyl-peptide hydrolase activity were investigated. Partial inactivation of both the LLE1 and LLE2 activities was only observed at higher inhibitor concentrations eg 5.0 mM (Table 4.10). However, at lower concentration, there was little inhibitory effect on either activity (Table 4.10), supporting the above suggestions that the activities are of the serine type. In view of the high inhibitor concentrations used to inactivate both activities, non specific interactions could have been the reason for the above observations.

4.9 Inhibition by protein protease inhibitors.

Aprotinin (Ap), lima bean trypsin inhibitor (LBTI), soya bean trypsin inhibitor (SBTI), antichymotrypsin (ACT), and a mutant of

antichymotrypsin (ACT*) (where the P1 leucine residue was changed to an arginine residue) were investigated as potential inactivators of the proteinase activities. Ap, LBTI, and SBTI did not have any inhibitory effects on the different activities. However, a slight activation of the AAF and LSTR activities was observed (Table 4.11). ACT and ACT* did not activate nor inhibit the AAF and LSTR activities, but inactivated the LLVY, LLE1 and LLE2 activities (Table 4.11).

Furthermore the possibility of cleavage of both ACT and ACT* by the proteinase complex also was investigated. The results showed that on SDS-PAGE gels (Figures 4.16 and 4.17), there was an appearance of a protein band below the inhibitor band, suggestive of the inhibitor being cleaved by the proteinase. Due to the mobility of the cleaved ACT and ACT* bands, it is most probable that the cleavage site, irrespective of the inhibitor, was at its N-terminal region rather than at its reactive loop.

Further investigation of the cleavage concentrated mainly on ACT, where attempts were made in order to observe whether complete conversion of ACT to the cleaved form would be possible. It was found that as the enzyme to inhibitor ratio increased, there appeared to be more of the cleaved form as assessed by SDS PAGE (Figure 4.18). The cleaved form was electroblotted and subjected to protein sequencing. Sequencing, after six cycles, revealed the following sequence:

Sequence: Glu-Glu-Asn-Leu-Thr.

Thus, making the cleavage site at the Asp_7-Glu_8 peptide bond (numbering of residues based on the sequence obtained from the

Data Base). In view of the cleavage being after an aspartic acid residue, similar experiment was repeated using DCI-treated MCP (Section 4.2). The results, as judged by SDS PAGE (Figure 4.18, Lane h), appear to be similar ie generation of the cleaved form occurred even though the AAF, LLVY, and LLE2 activities were blocked, which in turn suggests the possible involvement of the LLE1 activity in the cleavage

4.10 Introducing LLE1.MCP.

LLE1.MCP is defined as a modified MCP with only the LLE1 activity being active. As described above, DCI was found to inhibit the AAF, LLVY, and LLE2 activities (Section 4.2). Pebabloc was also found to selectively inactivate the LSTR activity (Section 4.3). In this study, an attempt to make an enzyme with only the LLE1 activity was performed, and the results are shown in Table 4.12. It was found that inhibition by Pefabloc followed by inhibition by DCI led to inactivation of the AAF, LSTR, and LLVY activities with less than 5% residual activity remaining after treatment.

However, if the order of inhibitors is changed so that DCI was used first then Pefabloc, it was found that the inactivation of the LSTR activity was not complete ie about 30% residual activity remaining (data not shown).

An attempt to study the LLE-NA dependence of LLE1.MCP was performed, in order to investigate whether having the LSTR active site blocked would disrupt interaction, if any, between the LLE2 active site and the LSTR active site, in respect to the early study where DCI-treated MCP with an activated LSTR activity was used (Section 4.2).

97

It was found that the LLE1 activity behaved in Michaelis-Menten fashion where V_{max} was reached, giving a K_m value of 64 μM and an estimated V_{max} of 82 nmol/min/mg (Figure 4.19). The results are suggestive of very little interaction between the LLE1 and LSTR active sites, where the kinetic parameters obtained here are of similar magnitude to the one obtained with the DCI-treated enzyme (Table 4.16).

The inactivation of LLE1.MCP by DFP was investigated. Time course of inhibition is shown in Figure 4.20, from which a $k_{obs}/[I]$ of 0.014 M^{-1} s^{-1} was obtained. The inhibition by DFP was re-investigated in the presence of 1 mM $MnCl_2$, as the latter was found to be an activator of the LLE1 activity (Section 3.11). Time course of inhibition is shown in Figure 4.20, from which a $k_{obs}/[I]$ of 0.013 M^{-1} s^{-1} was obtained, which was of similar magnitude to the one obtained in the absence of metal. The results support the view of possible structural effects of $MnCl_2$ on the activity rather than catalytic ones.

4.11 Labelling the active site of the non cooperative component of the peptidylglutamyl-peptide hydrolase activity.

An attempt to label the active site of the non-cooperative component of the peptidylglutamyl-peptide hydrolase activity was performed using [^{3}H]-DFP. LLE1.MCP was used in the labelling experiment, the results of which are illustrated in Figure 4.21. Fluorography, after SDS PAGE, of the labelled LLE1.MCP showed one radioactive band, the mobility of which corresponded with a protein band with an approximate molecular mass of 25 kDa (Figure 4.21).

Using the methodology devised in this laboratory for the separation of MCP subunits (Savory, 1992), an attempt to identify and purify the polypeptide, with which the tritium activity is associated, was performed. Figure 4.22 illustrates the separation profile obtained for the labelled LLE1.MCP.

Radioactivity counts over area of individual protein peaks were calculated and are shown in Table 4.13. It was found that very little radioactivity was associated with the separated subunits, when about 20,064 cpm were used as the starting material for the HLPC separation (Table 4.13), which is suggestive of tritium activity loss during the various stages of the procedure, as reflected by only 609 cpm total counts in the collected protein peaks, therefore a 3% recovery of total starting counts. Moreover, it could be argued that the counts obtained in Table 4.13 are due to background labelling by [^{3}H]-DFP even at 20 μM concentration as described by Ogata et al. (1992).

4.12 Effects of phenylglyoxal and N-acetyl imidazole on the different activities of the proteinase complex.

It is widely accepted now that arginyl residues can serve as positively charged recognition sites for negatively charged substrates and anionic cofactors in enzyme active sites (Riordan et al., 1977). Riordan (1973) has shown that arginyl residues participate in binding the carboxyl group of substrates to the enzyme carboxypeptidase A. Phenylglyoxal (PGO) was developed by Takahashi as a reagent for the selective chemical modification of arginine residues in proteins, the mechanism of which is shown in Figure 4.23 (Takahashi, 1977).

PGO was used, in this study, as a potential inhibitor of the LLE activities. As illustrated in Table 4.14, the LLE1 and LLE2 activities were inactivated but at PGO concentrations as high as 10 mM, which cut short the aim of potentially using [^{14}C]-PGO as a label to identify the catalytic subunits responsible for the hydrolysis of LLE-NA. At higher PGO concentrations, non selective modifications have been shown to occur, thus modifying not only the arginyl residues of interest but also other exposed arginyl residues as well as lysine and cysteine residues (Day and Shaw, 1992). The AAF and LSTR activities were inaffected by the PGO treatment (Table 4.14).

N-Acetyl imidazole is a mild and selective protein acetylating reagent (Wilk et al., 1970). The mechanism of which is shown in Figure 4.24. It preferentially acetylates exposed tyrosine residues but can also react with thiol groups (to the same extent as the reagent acetic anhydride), and with ε-amino groups of lysine residues. Exposed tyrosine residues are involved in hydrophobic interactions between subunits of oligomeric proteins, where N-acetyl imidazole was shown to disrupt the interactions (Wilk et al., 1970).

The effects of N-acetyl imidazole on the different activities of the complex are summarized in Table 4.15. The LLE1 and LLE2 activities were partially inactivated, with 60% and 70% residual activity remaining after 30 min preincubation with no further inhibitory effects at higher concentrations ie 10 mM (Table 4.15). In contrast, the AAF and LSTR activities were not affected by the above treatment (Table 4.15).

4.13 Discussion.

DCI is an effective inhibitor of the rat liver enzyme, where the AAF and LLE2 activities were inactivated, and the LSTR and LLE1 activities were stimulated. The inhibition of the chymotrypsin-like and the peptidylglutamyl-peptide hydrolase activities is in agreement with the reported inhibition for the bovine pituitary enzyme (Orlowski and Michaud, 1989).

Recently, Mason (1990) has also reported similar inactivation for the chymotrypsin-like activity of the human liver enzyme, but with a much higher $k_{obs}/[I]$ value (250 compared to 120 M^{-1} s^{-1}). The chymotrysin-like activity of the rat liver enzyme assayed with the substrate LLVY-AMC was also inactivated by DCI and with similar $k_{obs}/[I]$, as for the AAF activity (Djaballah et al., 1992).

With regards to the proposed composition of the peptidyl-glutamyl-peptide hydrolase activity (Chapter 3; Djaballah and Rivett, 1992), the DCI studies provided the best evidence for the proposal, as the LLE1 activity can be studied in the absence of the LLE2 activity. Inhibition of the AAF and LLE2 activities is not readily reversible. Stimulation of the LSTR activity may be an allosteric effect but cannot easily be explained by the inhibition observed at other catalytic sites as suggested for the bovine pituitary enzyme (Orlowski and Michaud, 1989) because DCI in the presence of dithiothreitol (which inactivates the inhibitor) also stimulated the LSTR activity.

The LSTR activity can be rapidly and selectively inhibited by Pefabloc, which is a benzenesulphonylfluoride derivative, while the related phenylmethanesulphonylfluorides (Figure 4.10) have little

effect. The above observations provide the best evidence so far for the LSTR activity as being a serine type protease, in contrast to its early classification as a cysteine type protease by several groups.

The inhibition of hydrolysis of LLE-NA at high substrate concentration by DCI, allowed activity at the high affinity site of the Glu-X activity (Chapter 3) to be studied in the absence of the non cooperative component of the LLE2 activity. The results are suggestive of some negative interaction between the cooperative and the non cooperative components as reflected by an increase in k_{cat} from 0.357 to 0.856 s^{-1}, and a decrease in Km from 114 to 70 µM, thus a 4-fold increase in catalytic efficiency (Table 4.16). Kinetic parameters of similar magnitude were obtained for the LLE1.MCP, suggesting that there is little interaction between the LSTR active site and the LLE1 active site (Table 4.16).

Proteinase protein inhibitors are important tools of nature for regulating the proteolytic activity of their target proteinases. The ACT is a member of the serpin superfamily denoted serpins-serine protease inhibitors (Rubin, 1992). The ACT used in this study is a recombinant one, hence the low molecular mass of 46 kDa, which was shown to have identical biochemical properties to that of the native form (Rubin et al., 1990; Rubin, 1992).

The cleavage of antichymotrypsin by MCP has probably no physiological relevance, and it could have been due to some kind of hydrophobic interaction with the protease, which lead to the observed cleavage, as Potempa et al. (1991) have reported that other proteases, such as human trypsin, porcine trypsin, and clostripain, have been

shown to cleave ACT at its N-terminus with no effect on its inhibitory activity.

It is interesting to note that the same activities that were inhibited by ACT were also inhibited by casein (Sections 3.8 and 3.14), suggesting some close proximity arrangement of these activities, namely the LLVY, LLE1, and LLE2 activities, which appears to promote a hydrophobic cluster/region on the proteinase complex.

So far, there have been several reports in the literature with regards to endogenous protein inhibitors of the proteinase complex. Murakami and Etlinger (1986) have isolated a 250 kDa protein inhibitor from human erythrocytes (subunit molecular mass 40 kDa). Driscoll et al. (1992) have reported a protein inhibitor similar to that described by Murakami and Etlinger (1986). Li et al. (1991) have also isolated a 200 kDa protein inhibitor from human erythrocytes (subunit molecular mass 50 kDa), which was distinct from the one described by Murakami and Etlinger (1986). Chu-Ping et al. (1992a) have characterized a 60 kDa protein inhibitor from bovine blood cells (subunit molecular mass 31 kDa).

In view of the source of the above inhibitors, it would be of great importance to compare protein sequences of the reported inhibitors among themselves as well as with known serpin sequences But as yet no sequence information has been published for the above inhibitors. However, it seems unlikely that they will fall in the serpin category because of their described mode of action, and of the results obtained in this study with some of serpins (Section 4.9).

Although the inhibition by PGO did not satisfy the requirement of it to be used as a tool to label the LLE active sites, the results obtained do provide further evidence for the LLE activities being distinct from the others, as does the partial inactivation of LLE activities by N-acetyl imidazole. The effects of N-acetyl imidazole on the rat liver MCP differ from the reported rapid inactivation of the trypsin-like (assayed with Cbz-Ala-Leu-Arg-β-naphthylamide) and peptidylglutamyl-peptide hydrolase activities, with slow inactivation of the chymotrypsin-like activity (assayed with Cbz-Gly-Gly-Leu-p-nitroanilide (pNA)) of the bovine pituitary enzyme (Yu et al., 1991).

Based on the subsite specificity of the P1 position of the peptidylglutamyl-peptide hydrolase activity, the designed affinity label Z-Tyr-Ala-Glu-CH$_2$Cl selectively inactivated the AAF and LLVY activities. The differential effect of inhibitors on the different activities (Djaballah et al., 1992) together with the above observations are suggestive of the partial involvement of the P1 position in determining the specificity of any of the proteolytic activities, with possible involvement and/or contribution from other subsites.

Therefore, Wilk and Orlowski's (1983) definitions of "trypsin-like" and "chymotrypsin-like" activities are misleading, and defining the activities with respect to the substrate used appears to be a better way, for the time being, to name the different activities of the complex.

The different effects of the serine protease inhibitors, DCI, Pefabloc, NCDC, and DFP, on different activities of the proteinase suggest that most sites have the same serine type protease mechanism but may reflect considerable differences in the geometry of catalytic

104

residues at the different catalytic centres of the complex. MCP does not belong to any of the known families of serine proteinases (Tanaka et al., 1992; Rivett, 1993) and is generally not very reactive with serine proteinase inhibitors as evidenced by the low $k_{obs}/[I]$ values (Table 4.17). The partial inhibition by thiol blocking reagents and cysteine protease inhibitors, especially of the LSTR activity (Rivett, 1989b) could reflect an indirect involvement of thiol groups as has been shown in the case of proteinase K (Betzel et al., 1988).

The study has led to the identification of DFP, an active site directed inhibitor of serine proteases, for labelling the LLE1 active site using LLE1.MCP. Fluorography, after SDS-PAGE, of the [3H]-DFP-treated LLE1.MCP revealed a single band of radioactivity, with a molecular mass of approximately 25 kDa. Sato and Shiratsuchi (1990), working on the chicken liver enzyme, have also shown a single radioactive band on their fluorograph with a molecular mass of 22 kDa.

Tanaka et al. (1986a), working on the rat liver enzyme, have reported five radioactive bands obtained the fluorograph of the DFP labelled proteinase, with the strongest radioactive distribution being on the band with an approximate molecular mass of 25 kDa.

Unfortunately, attempts to identify and purify the labelled polypeptide were not as yet successful. One reason could have been the methodology employed, in which there seemed to be precipitation of the subunit of interest during the preparation of the sample for HPLC separation and/or precipitation during loading onto the column as reflected by the loss of the tritium activity. Savory and Rivett (unpublished observations) have also encountered similar problems during their labelling experiments.

Future methodology to identify the labelled subunit would be: 1) run a preparative SDS-PAGE gel of the labelled LLE1.MCP, 2) identify the labelled protein band by fluorography of the labelled LLE1.MCP run in a separate lane, and finally 3) cut the labelled band out and perform an in-gel digestion of the polypeptide for internal sequence analysis as described by Rosenfeld et al. (1992).

The studies presented here have shown that the different substrates used were hydrolysed predominantly at distinct active sites within the complex, which involve a serine-type mechanism. Three affinity labels have been identified for subsequent use in the characterization of catalytic subunits responsible for cleavage of respective substrates: 1) DFP, in a labelled form, for the labelling of the LLE1 active site using the modified MCP complex (LLE1.MCP) as discussed above, 2) Pefabloc, in a labelled form, to label the subunit responsible for LSTR-AMC hydrolysis, and 3) DCI, in a labelled form (Cardozo et al., 1992), to label subunits responsible for the LLE2 and AAF activities.

Table 4.1: Effects of 3,4 dichloroisocoumarin on the different activities of the proteinase complex.

Treatment	concentration (mM)	Activity (% control)			
		AAF	LSTR	LLE1	LLE2
3,4 dichloroisocoumarin	0.004	61	214	114	97
	0.020	20	309	130	38
	0.1	13	154	83	31
	0.2	12	112	49	31

Prior to treatment, 2-mercaptoethanol was removed by dialysis. MCP (0.1 mg/ml) was preincubated with appropriate inhibitor concentration for 30 min at 20°C in 50 mM Hepes/KOH buffer, pH 7.5. Aliquots were removed and diluted 20-fold for measurement of remaining activity with 40 µM AAF-AMC, LSTR-AMC, 0.1 mM LLE-NA or 0.4 mM LLE-NA as described under section 2.4. Controls contained no inhibior. Data are the average values from six separate experiments performed in duplicate.

Table 4.2: Reactivation attempts of the DCI-treated proteinase complex.

Treatment		Activity (% control)								
		AAF (40 µM AAF-AMC)				LLE2 (0.4 mM LLE-NA)			LSTR (40 µM LSTR-AMC)	
DCI-treated enzyme left standing at room temperature			t_0	t_{2hr}	t_{4hr}		t_0	t_{2hr}	t_{4hr}		t_0	t_{2hr}	t_{4hr}
	C	100	92	80	C	100	75	68	C	100	136	94
	T	20	20	11	T	38	20	20	T	309	289	212
Dialysis			t_0	t_{24hr}			t_0	t_{24hr}		t_0	t_{24hr}
	C	100	97	C	100	90	C	100	101
	T	20	10	T	38	12	T	309	158

Prior to treatment, 2-mercaptoethanol was removed by dialysis. MCP (0.1 mg/ml) was preincubated with 20 µM DCI for 30 min at 20°C. One treatment consisted of leaving the treated enzyme at room temperature for up to 4 h, and the other of dialysis against 50 mM Hepes/KOH buffer, pH 7.5 cont. 10% glycerol. Aliquots, from each treatment, were removed as indicated and diluted 20-fold for measurement of remaining activity as described under section 2.4. Controls contained no inhibitor. Data are the average values of three separate experiments.

Table 4.3:   Effects of sulphonylfluorides on the different activities of the proteinase complex.

Inhibitor	concentration (mM)	Activity (% control)				
		AAF	LSTR	LLVY	LLE1	LLE2
Pefabloc[a]	0.5	94	11	99	100	94
	1.0	91	3	107	95	110
	5.0	115	0	149	148	123
Pefabloc + DTT[a]	0.5 + 1.0	-	13	-	-	-
PMSF[b]	1.0	82	92	85	98	85
APMSF[b]	1.0	95	97	100	87	97

MCP (0.2mg/ml) was preincubated with inhibitor for 30[a] or 60[b] min at 25°C in 50 mM Hepes/KOH buffer, pH 7.5. Aliquots were removed and diluted 20-fold for measurement of remaining activity with 40 μM AAF-AMC, LSTR-AMC, LLVY-AMC, 0.1 mM LLE-NA or 0.4 mM LLE-NA as described under Section 2.4. Controls contained no inhibitor. Data are the average values from three separate experiments performed in duplicate. Pefabloc: 4-(-2-Aminoethyl)benzene-sulphonylfluoride. PMSF: phenylmethanesulphonylfluoride. APMSF: (p-Amidinophenyl)-methanesulphonyl-fluoride. DTT: dithiothreitol.

Table 4.4: Effects of NCDC and DFP on the different activities of the proteinase complex.

Inhibitor	Concentration (mM)	Activity (% control)				
		AAF	LSTR	LLVY	LLE1	LLE2
DFP[a]	5.0	87	81	64	66	122
NCDC[b]	1.0	92	76	83	73	83
	5.0	127	73	67	67	67

MCP (0.2 mg/ml) was preincubated for 60[a] or 120[b] min at 25°C in 50 mM Hepes/KOH buffer, pH 7.5. Aliquots were removed and diluted 20-fold for measurement of remaining activity with 40 μM AAF-AMC, LSTR-AMC, LLVY-AMC, 0.1 mM LLE-NA or 0.4 mM LLE-NA as described under Section 2.4. Controls contained no inhibitor. Data are the average values from four separate experiments performed in duplicate.

Table 4.5: Effects of peptide aldehydes on the peptidyl-glutamyl-peptide hydrolase activity of the complex.

Inhibitor	Concentration (mg/ml)	Activity (% control)	
		LLE1	LLE2
Chymostatin	0.01	86 ± 5	101 ± 3
	0.10	88 ± 4	83 ± 6
	1.00	72 ± 14	59 ± 7
Leupeptin	0.01	66 ± 4	98 ± 1
	0.10	67 ± 8	83 ± 3
	1.00	62 ± 5	65 ± 6
Antipain	0.01	71 ± 10	102 ± 2
	0.10	82 ± 13	80 ± 14
	1.00	97 ± 6	51 ± 16
Elastatinal	0.01	78 ± 3	89 ± 10
	0.10	91 ± 20	124 ± 24
	1.00	83 ± 9	103 ± 18

MCP (0.1 mg/ml) was preincubated with inhibitor for 30 min at 25°C in 50 mM Hepes/KOH buffer, pH 7.5. Controls contained no inhibitor. Assays were carried out as described under Section 2.4. Values are given as the mean ± SD for four separate experiments performed in duplicate.

Table 4.6:   Effects of chymostatin analogues on the peptidylglutamyl-peptide hydrolase activity.

Inhibitor	Activity (% control)	
	LLE1	LLE2
Z-Arg-Ile-Phe-CHO	81 ± 3	98 ± 8
Z-Arg-IlePhe-Semicarbazone	84 ± 3	81 ± 5
Z-Arg-Leu-Phe-CHO	82 ± 0	56 ± 5
Z-Val-Phe-CHO	90 ± 0	78 ± 12
Z-Val-Phe-Semicarbazone	85 ± 2	73 ± 2

MCP (0.1 mg/ml) was preincubated with 0.01 mg/ml inhibitor for 30 min at 25°C in 50 mM Hepes/KOH buffer, pH 7.5. Controls contained no inhibitor. Assays were carried out as described under Section 2.4. Values are given as the mean ± SD for three separate experiments performed in duplicate.

Table 4.7: Effects of peptidyl-chloromethylketones on the LLE activities.

Inhibitor	Activity (% control)	
	LLE1	LLE2
Z-Gly-Gly-Phe-CH$_2$Cl	98 ± 1	104 ± 13
Ala-Ala-Phe-CH$_2$Cl	89 ± 4	96 ± 12
Tyr-Gly-Arg-CH$_2$Cl	93 ± 4	96 ± 6
Tyr-Pro-CH$_2$Cl	82 ± 2	91 ± 11

Prior to preincubation, 2-mercaptoethanol was removed by dialysis. MCP (0.1 mg/ml) was preincubated with 0.1 mM inhibitor, at 25°C, in 50 mM Hepes/KOH buffer, pH 7.0 for 60 min. Aliquots were removed and diluted 20-fold for measurement of remaining activity with 0.1 mM or 0.4 mM LLE-NA as described under Section 2.4. Controls contained no inhibitor. Values are given as the mean ± SD for three separate experiments performed in duplicate.

Table 4.8: Effects of Z-YAE-CH$_2$Cl on the different activities of the proteinase complex.

Concentration			Activity (% control)		
	AAF	LSTR	LLVY	LLE1	LLE2
0.1 mM	64 ± 2	102 ± 0	48 ± 4	96 ± 7	106 ± 6
0.2 mM	68 ± 1	-	52 ± 2*	-	-

Prior to preincubation, 2-mercaptoethanol was removed by dialysis. MCP (0.2 mg/ml) was preincubated with inhibitor at 25°C in 50 mM Hepes/KOH buffer, pH 7.0 for 30 min. Aliquots were removed and diluted 20-fold for measurement of remaining activity with 40 μM AAF-AMC, LSTR-AMC, LLVY-AMC, 0.1 mM or 0.4 mM LLE-NA as described under Section 2.4. Controls contained no inhibitor. Values are given as the mean ± SD for four separate experiments performed in duplicate. Z-YAE-CH$_2$Cl: Z-Tyr-Ala-Glu-CH$_2$Cl.

Table 4.9: **Effects of peptidyldiazomethanes on the LLE activities.**

| Inhibitor	Activity (% control)	
	LLE1	LLE2
Z-Ala-Phe-CHN$_2$	92 ± 1	97 ± 8
Z-Phe-Ala-CHN$_2$	92 ± 2	96 ± 5
Z-Phe-CHN$_2$	85 ± 2	84 ± 12
Z-Phe-Gly-Tyr-CHN$_2$	94 ± 4	84 ± 1
Z-Ala-Ala-Val-CHN$_2$	84 ± 1	84 ± 11
Z-Ala-Ala-Leu-CHN$_2$	82 ± 2	68 ± 3
Z-Leu-Trp-CHN$_2$	89 ± 2	46 ± 11
Val-Lys-Gly-Lys-CHN$_2$	72 ± 1	70 ± 14

Prior to preincubation, 2-mercaptoethanol was removed by dialysis. MCP (0.1 mg/ml) was preincubated with 0.1 mM inhibitor, at 25°C, in 50 mM Hepes/KOH buffer, pH 7.0 for 60 min. Aliquots were removed and diluted 20-fold for measurement of remaining activity with 0.1 mM or 0.4 mM LLE-NA as described under Section 2.4. Controls contained no inhibitor. Values are given as the mean ± SD for three separate experiments performed in duplicate.

Table 4.10:   Effect of thiol reactive reagents on the LLE
activities.

Treatment	concentration (mM)	Activity (% control)	
		LLE1	LLE2
N-ethylmaleimide	0.1	98 ± 2	108 ± 4
	1.0	84 ± 8	97 ± 3
	5.0	46 ± 0	42 ± 4
Methylmethane-thiosulphonate	0.1	95 ± 3	100 ± 3
	1.0	92 ± 4	88 ± 6
	5.0	93 ± 1	68 ± 3
Iodoacetic acid	0.1	98 ± 0	99 ± 2
	1.0	92 ± 1	93 ± 4
	5.0	70 ± 1	78 ± 3

Prior to preincubation, 2-mercaptoethanol was removed by dialysis.
MCP (0.1 mg/ml) was preincubated with inhibitor for 30 min, at 25°C,
in 50 mM Hepes/KOH buffer, pH 7.5. Aliquots were removed and
diluted 20-fold for measurement of remaining activity with 0.1 or 0.4
mM LLE-NA as described under Section 2.4. Controls contained no
inhibitor. Values are given as the mean ± SD for three separate
experiments performed in duplicate.

Table 4.11: Effects of protein protease inhibitors on the different activities of the proteinase complex.

Treatment	Activity (% control)				
	AAF	LSTR	LLVY	LLE1	LLE2
Aprotinin	135 ± 2	139 ± 3	131 ± 0	110 ± 4	80 ± 7
Lima bean trypsin inhibitor	138 ± 1	157 ± 4	117 ± 1	109 ± 1	89 ± 1
Soya bean trypsin inhibitor	123 ± 2	135 ± 2	108 ± 1	103 ± 8	98 ± 2
Antichymotrypsin	103 ± 0	95 ± 4	74 ± 5	58 ± 3	59 ± 5
Antichymotrypsin mutant*	95 ± 2	92 ± 3	66 ± 1	61 ± 8	53 ± 0

MCP (0.2 mg/ml) was preincubated with 0.1 mg/ml inhibitor for 30 min at 25°C in 50 mM Hepes/KOH buffer, pH 7.5. Aliquots were removed and diluted 20-fold for measurement of remaining activity with 40 μM AAF-AMC, LSTR-AMC, LLVY-AMC, 0.1 mM LLE-NA or 0.4 mM LLE-NA as described under section 2.4. Controls contained no inhibitor. Values are given as the mean ± SD for three separate experiments performed in duplicate. *mutation of the P1 Leucine to an Arginine.

Table 4.12: The making of LLE1.MCP.
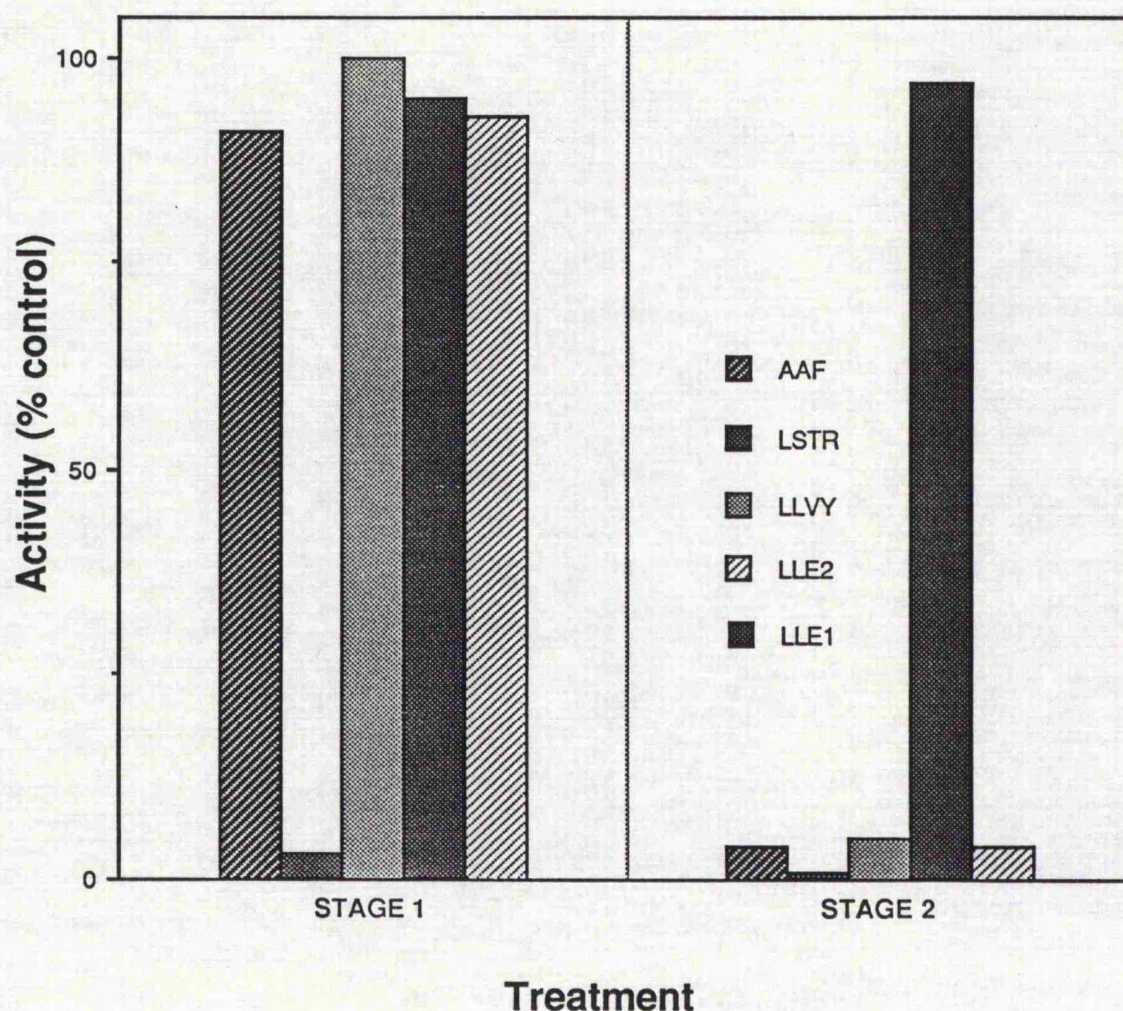
Prior to treatment, 2-mercaptoethanol was removed by dialysis. MCP (0.2 mg/ml) was first preincubated with 1.0 mM Pefabloc (stage 1), at 25°C, in 50 mM Hepes/KOH buffer, pH 7.5 for 60 min. Then 20 μM DCI (stage 2) was added to the reaction mix, and the mixture was preincubated for a further 30 min. Aliquots from each stage were removed and diluted 20-fold for measurement of remaining activity with 40 μM AAF-AMC, LSTR-AMC, LLVY-AMC, 0.1 mM LLE-NA or 0.4 mM LLE-NA as described under Section 2.4. Controls contained no inhibitor. Data are the average values for four separate experiments performed in duplicate.

Table 4.13: Measured tritium activity versus the
integrated area of protein fraction peak.

Protein peak fraction	Counts (cpm)	Integrated area	Ratio (x 10)
1	0.0	1136	0.00
2	15.0	4506	3.33
3	10.4	1754	5.93
4	38.2	8708	4.38
5	70.8	5666	12.49
6	20.2	496	40.72
7	56.8	3180	17.86
8	40.0	2240	17.86
9	85.6	8846	9.68
10	43.0	3155	13.63
11	46.6	2774	16.79
12	100.4	8849	11.35
13	81.6	2501	32.63

The separation of the proteinase's components and the measurement of their tritium activity was performed as described under Section 2.7. The area under the protein peaks was integrated using the microprocessor-integrator of the Chem station of the HP1090 liquid chromatograph.

Table 4.14: Effects of phenylglyoxal on the different activities of the proteinase complex.

Treatment	concentration (mM)	Activity (% control)			
		AAF	LSTR	LLE1	LLE2
Phenylglyoxal	1.0	100 ± 12	88 ± 4	43 ± 8	74 ± 3
	5.0	104 ± 12	95 ± 5	22 ± 4	49 ± 2
	10.0	100 ± 15	103 ± 11	17 ± 5	29 ± 4

MCP (0.2 mg/ml) was preincubated with appropriate inhibitor concentration in the dark at 25°C in 50 mM Hepes/KOH buffer, pH 7.5 for 3 h. Aliquots were removed and diluted 20-fold for measurement of remaining activity with 40 µM AAF-AMC, LSTR-AMC, 0.1 mM LLE-NA or 0.4 mM LLE-NA as described under section 2.4. Controls contained no inhibitor. Values are given as the mean ± SD for three separate expreiments performed in duplicate.

Table 4.15: Effects of N-acetyl imidazole on the different activities of the proteinase complex.

Treatment	concentration (mM)	Activity (% control)			
		AAF	LSTR	LLE1	LLE2
N-acetyl imidazole	1.0	103 ± 2	91 ± 11	59 ± 2	69 ± 15
	5.0	104 ± 1	103 ± 1	60 ± 0	67 ± 0
	10.0	104 ± 1	83 ± 17	58 ± 15	65 ± 7

MCP (0.2 mg/ml) was preincubated with appropriate inhibitor concentration at 25°C in 50 mM Hepes/KOH buffer, pH 7.5 for 30 min. Aliquots were removed and diluted 20-fold for measurement of remaining activity with 40 µM AAF-AMC, LSTR-AMC, 0.1 mM LLE-NA or 0.4 mM LLE-NA as described under section 2.4. Controls contained no inhibitor. Values are given as the mean ± SD for three separate expreiments performed in duplicate.

Table 4.16: Kinetic parameters of the non-cooperative component of the peptidylglutamyl-peptide hydrolase activity.

Treatment	Km (mM)	V max (nmol/min/mg)	Kcat (s^{-1})	Kcat/Km ($M^{-1} s^{-1}$)
normal assay conditions*	114	33.00	0.357	3130
in the presence of 1 mM MnCl2*	67	27.32	0.296	4420
using DCI-treated enzyme	70	79.00	0.856	12230
using LLE1.MCP	64	82.00	0.887	13917

Kinetic constants were determined using the method of Eisenthal and Cornish-Bowden (1974).

*Data from Chapter 3.

Table 4.17: Rates of inactivation of MCP activities by serine protease inhibitors.

Inhibitor	Activity	Concentration (mM)	$t_{1/2}$ (min)	$k_{obs}/[I]$ (M^{-1} s^{-1})
3,4 dichloroisocoumarin[a]	AAF	0.02	4.8	120
	LLF2	0.02	12.0	48
Diisopropylfluorophosphate[a]	LLVY	5.0	200	0.017
	LLE1	5.0	140	0.024
4-(2-Aminoethyl)-benzene-sulphonyl fluoride[a]	LSTR	0.5	20	1.21
	LSTR	1.0	12	0.89
Diisopropylfluorophosphate[b]	LLE1	5.0	239	0.014
Diisopropylfluorophosphate[c]	LLE1	5.0	246	0.013

[a]Using normal MCP. [b]Using LLE1.MCP. [c]Using LLE1.MCP and 1 mM $MnCl_2$.

3,4-Dichloroisocoumarin
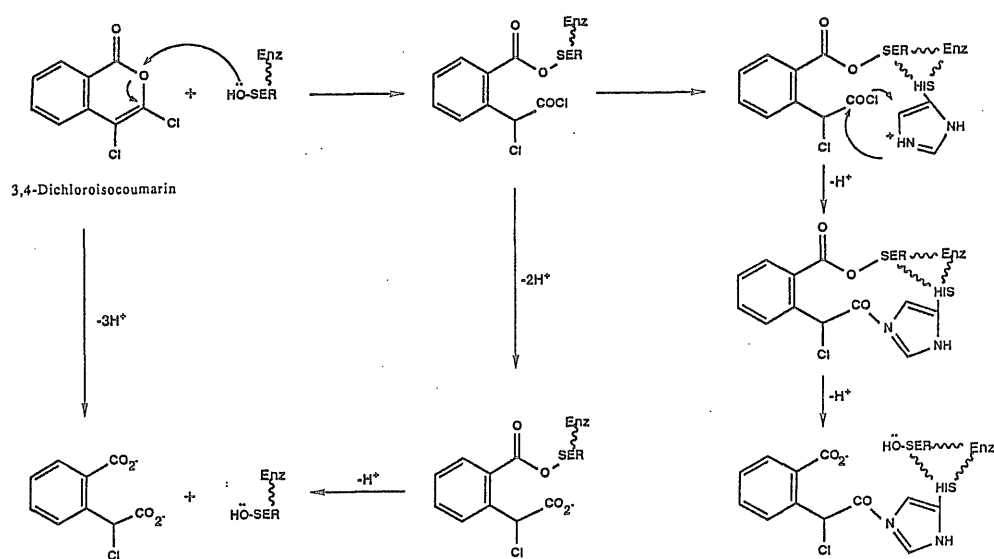
Figure 4.1: The proposed scheme for the reaction of serine proteases with 3,4 dichloroisocoumarin, after Powers et al. (1990).
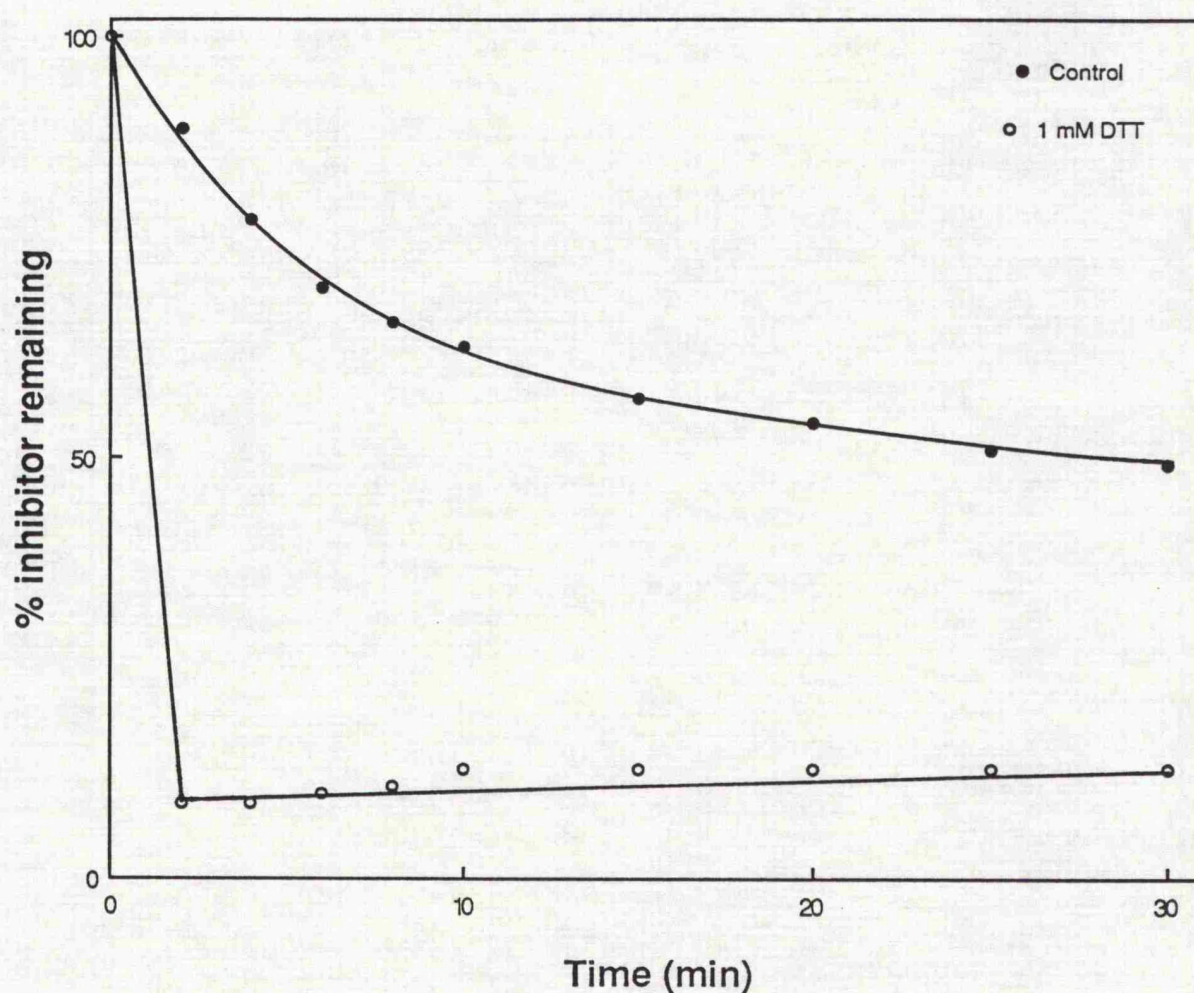
Figure 4.2: The effect of dithiothreitol on the stability of DCI.

The stability was measured as a decrease in absorbance caused by ring opening at 325 nm, and expressed as percentage remaining inhibitor by taking the t_0 absorbance as 100%. The absorbance was measured in a double beam spectrophotometer with a thermostated cell holder set at 37°C. Samples were set out under assay conditions in 50 mM Hepes/KOH buffer, pH 7.5 and 20 μM DCI. Blank samples contained no DCI.
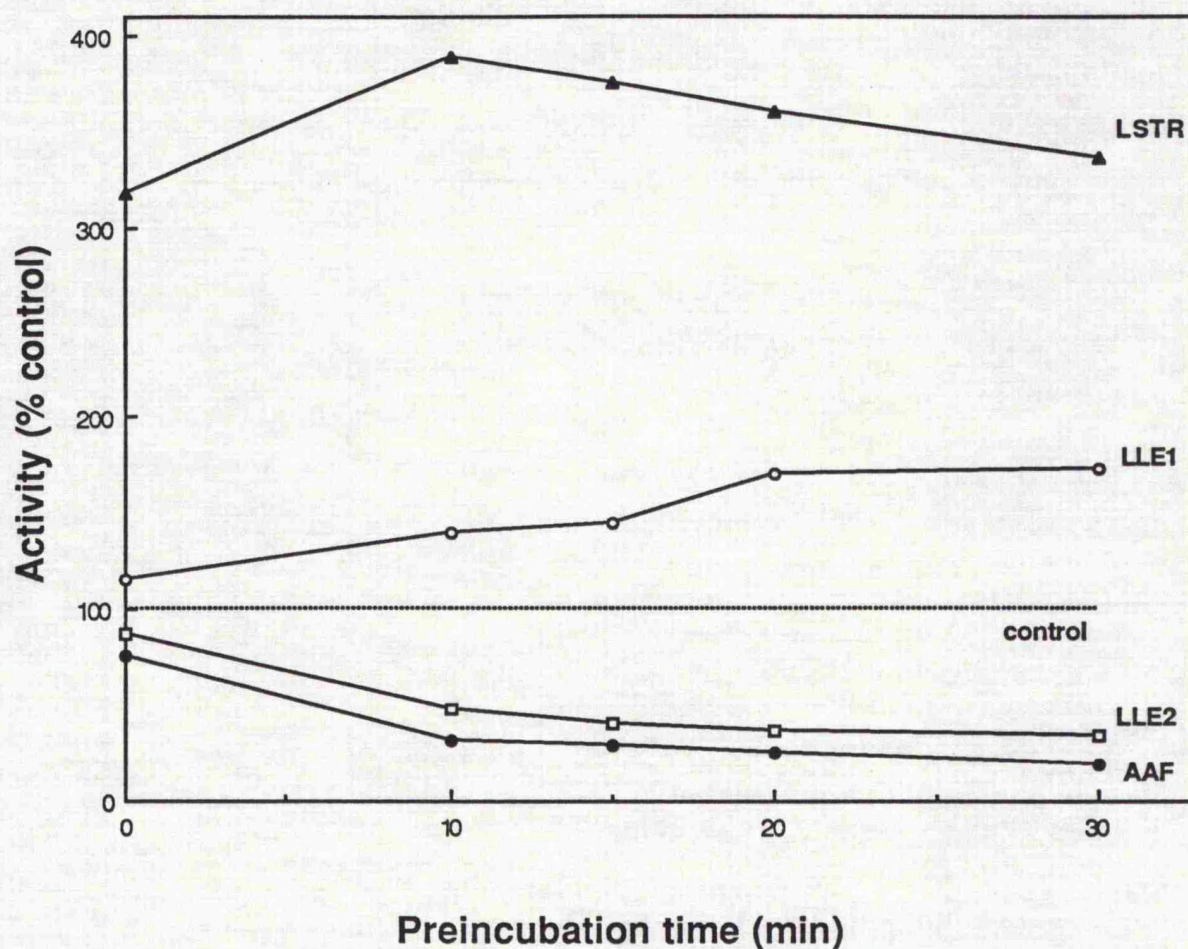
Figure 4.3: **Inhibition of MCP activities by DCI.**

Prior to preincubation, 2-mercaptoethanol was removed by dialysis. MCP (0.1 mg/ml) was preincubated at 20°C with 20 μM DCI in 50 mM Hepes/KOH buffer, pH 7.5, and aliquots were removed at various times for assays of residual activity with 40 μM AAF-AMC (AAF), LSTR-AMC (LSTR), 0.1 mM LLE-NA (LLE1) or 0.4 mM LLE-NA (LLE2) as described under Section 2.4. Control incubations contained no inhibitor. Data are the average values for six separate experiments performed in duplicate.
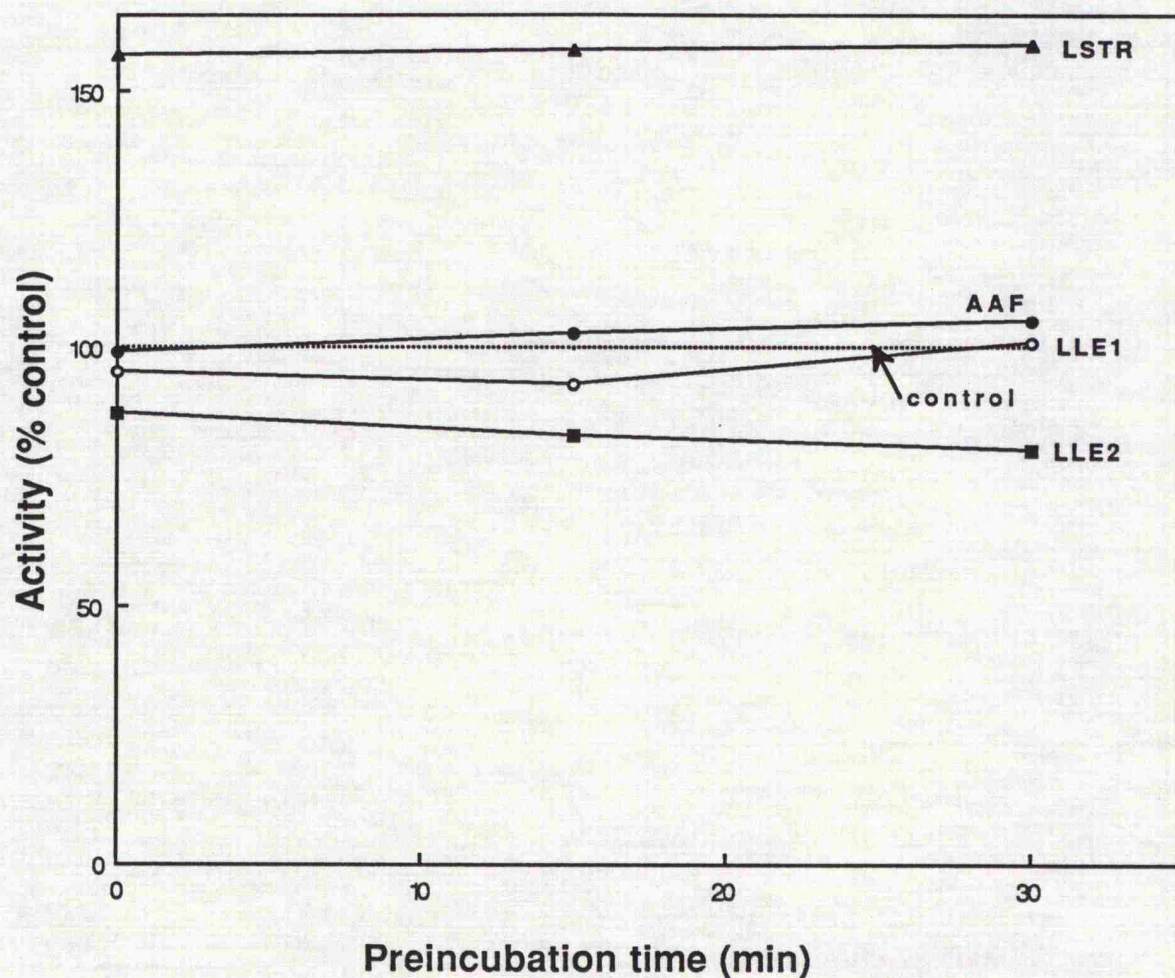
Figure 4.4: Stimulation of MCP activities by inactivated DCI.

As in Figure 4.3 except that preincubation mixtures with inhibitor (20 µM) contained 2 mM dithiothreitol to inactivate the inhibitor. Assays were carried out with 40 µM AAF-AMC (AAF), LSTR-AMC (LSTR), 0.1 mM LLE-NA (LLE1) or 0.4 mM LLE-NA (LLE2) as described under Section 2.4. Control incubations contained no inhibitor. Data are the average values for three separate experiments performed in duplicate.
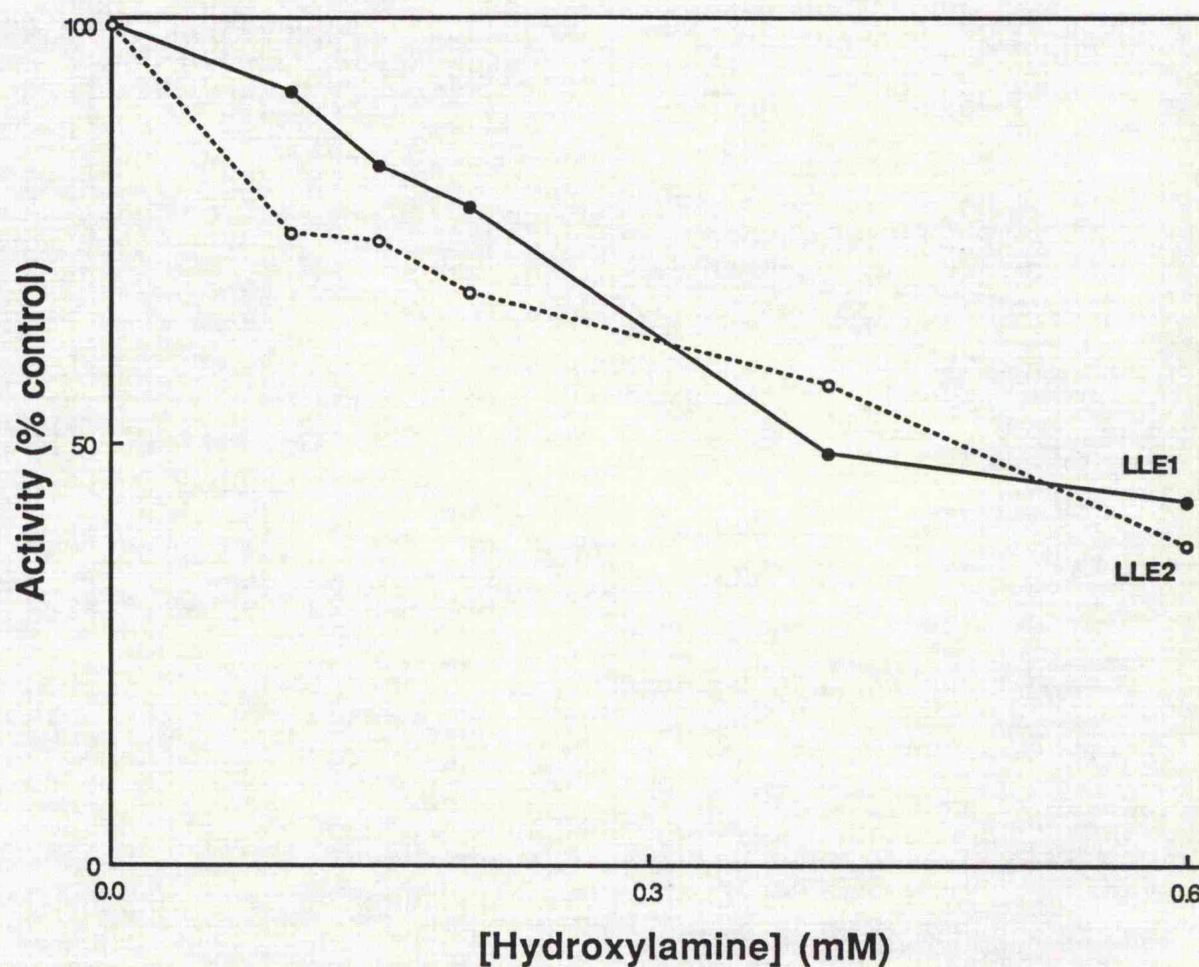
Figure 4.5:   Effect of hydroxylamine on the LLE activities.

Hydrolysis rates were measured in 50 mM Hepes/KOH buffer, pH 7.5 including appropriate hydroxylamine concentration, and 0.1 mM (LLE1) or 0.4 mM LLE-NA (LLE2) as described under Section 2.4. The hydroxylamine solution was freshly made and neutralised with KOH. Controls contained no hydroxylamine. Data are the average values for three separate experiments performed in duplicate.
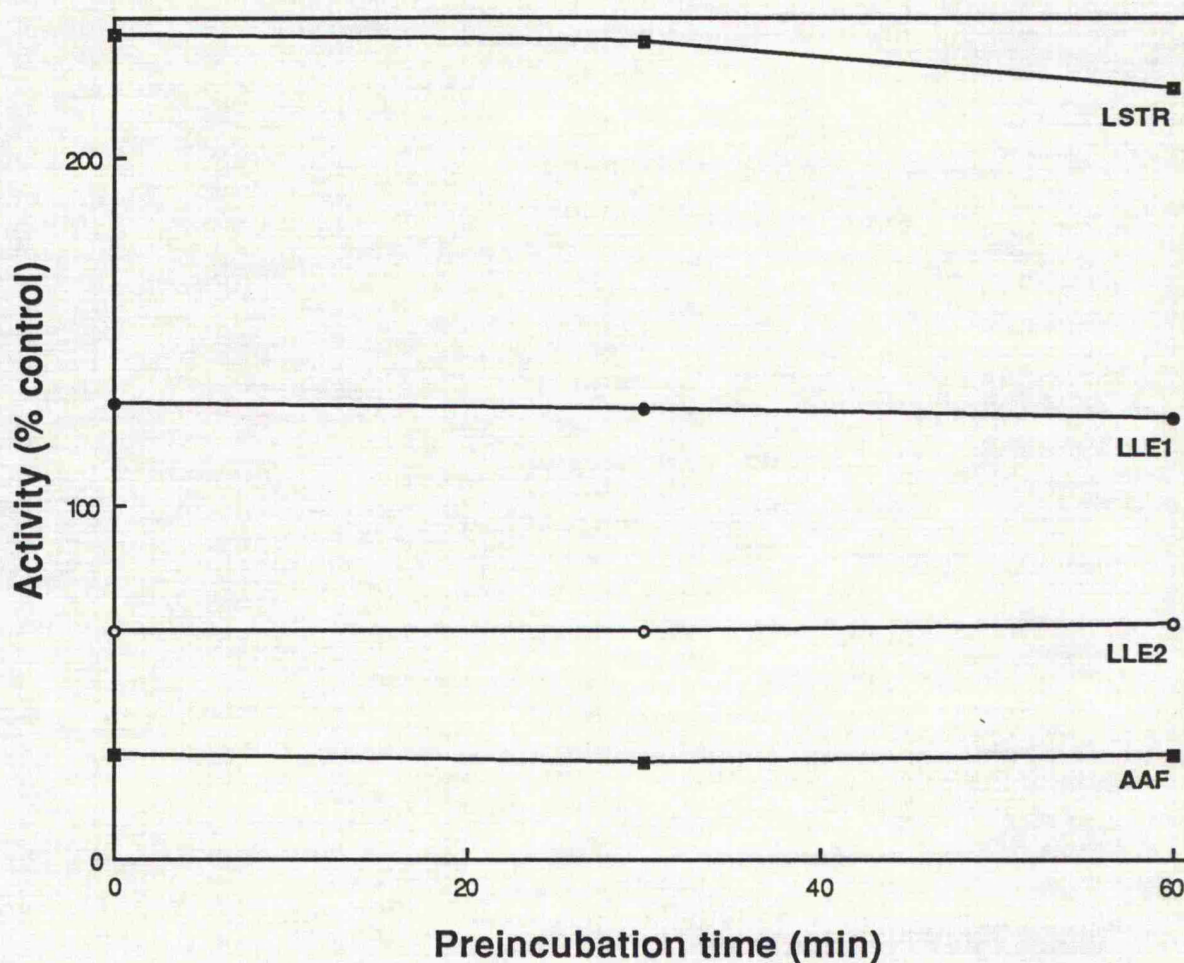
Figure 4.6:   Effect of hydroxylamine on the DCI-treated proteinase complex.

Prior to inhibition by DCI, 2-mercaptoethanol was removed by dialysis. MCP (0.1 mg/ml) was preincubated with 20 μM DCI for 30 min at 20°C, before addition of 0.1 M hydroxylamine, pH 7.0 and subsequent preincubation at 20°C in 50 mM Hepes/KOH buffer, pH 7.5. Aliquots were removed at various times and diluted 20-fold for assays of residual activity with 40 μM AAF-AMC (AAF), LSTR-AMC (LSTR), 0.1 mM LLE-NA (LLE1) or 0.4 mM LLE-NA (LLE2) as described under Section 2.4. Controls contained no inhibitor. Data are the average values for three separate experiments performed in duplicate.
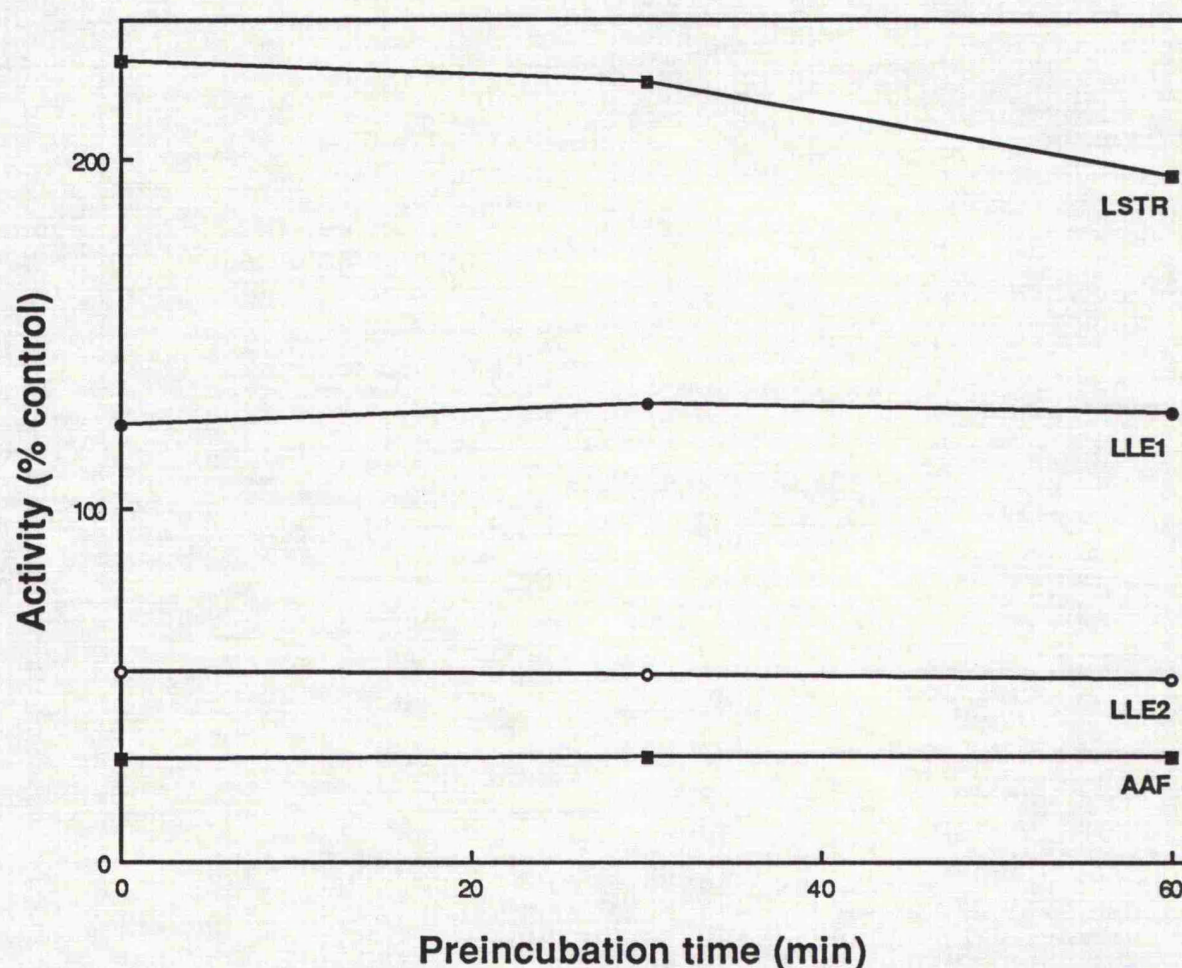
Figure 4.7:   Effect of dithiothreitol on the DCI-treated
proteinase complex.

Prior to inhibition by DCI, 2-mercaptoethanol was removed by dialysis. MCP (0.1 mg/ml) was preincubated with 20 µM DCI for 30 min at 20°C, before addition of 2 mM dithiothreitol and subsequent preincubation at 20°C in 50 mM Hepes/KOH buffer, pH 7.5. Aliquots were removed at various times and diluted 20-fold for assays of residual activity with 40 µM AAF-AMC (AAF), LSTR-AMC (LSTR), 0.1 mM LLE-NA (LLE1) or 0.4 mM LLE-NA (LLE2) as described under Section 2.4. Controls contained no inhibitor. Data are the average values for three separate experiments performed in duplicate.
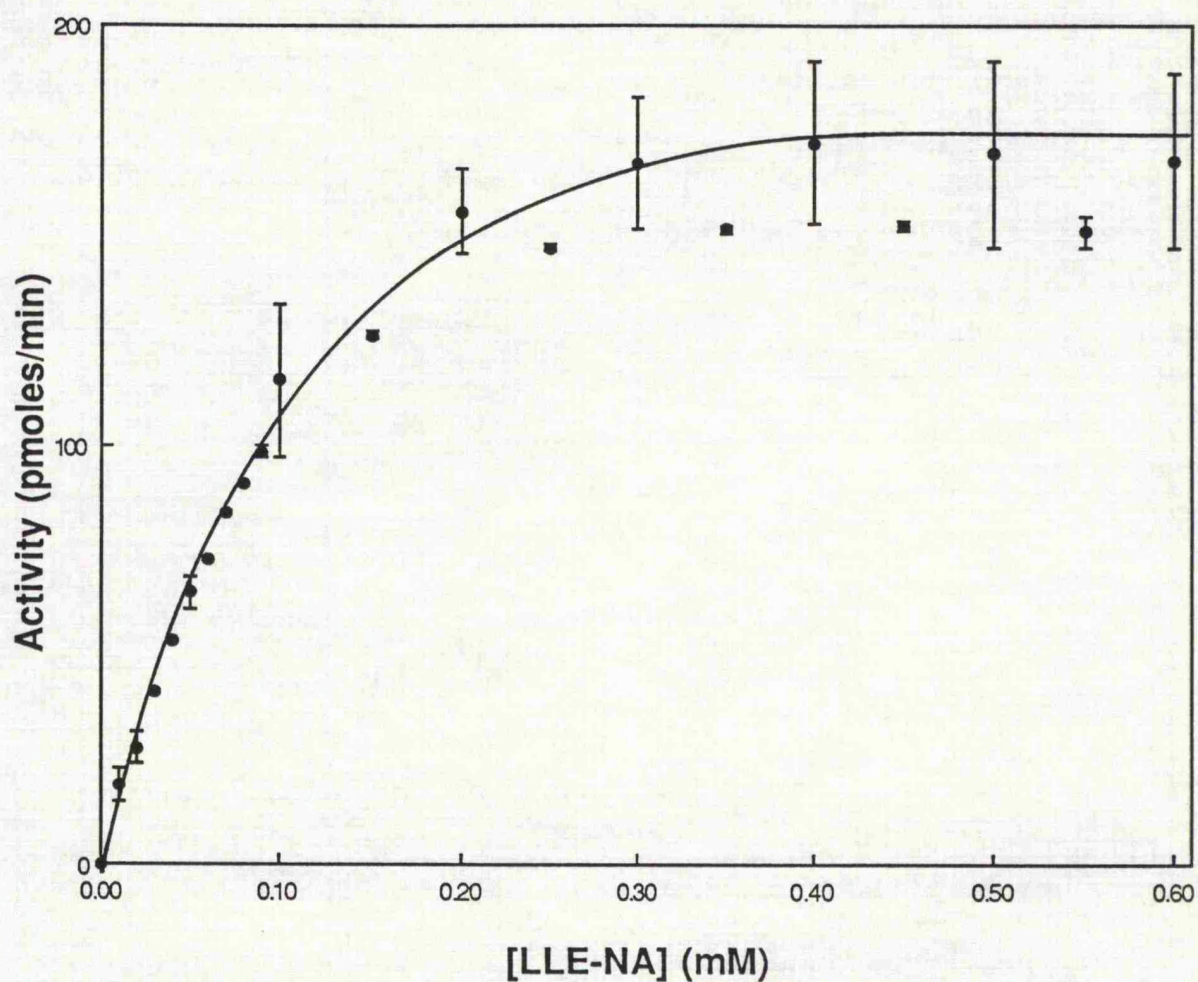
Figure 4.8: Effect of 3,4-dichloroisocoumarin on the rate of hydrolysis of LLE-NA as a function of substrate concentration.

The inactivation reaction was initiated by addition of 20 µM inhibitor to dialysed enzyme solution, and the residual activity measured as described under Section 2.4. The final concentration of DMSO was 6%. The error bars represent atandard deviation of at least three separate experiments.
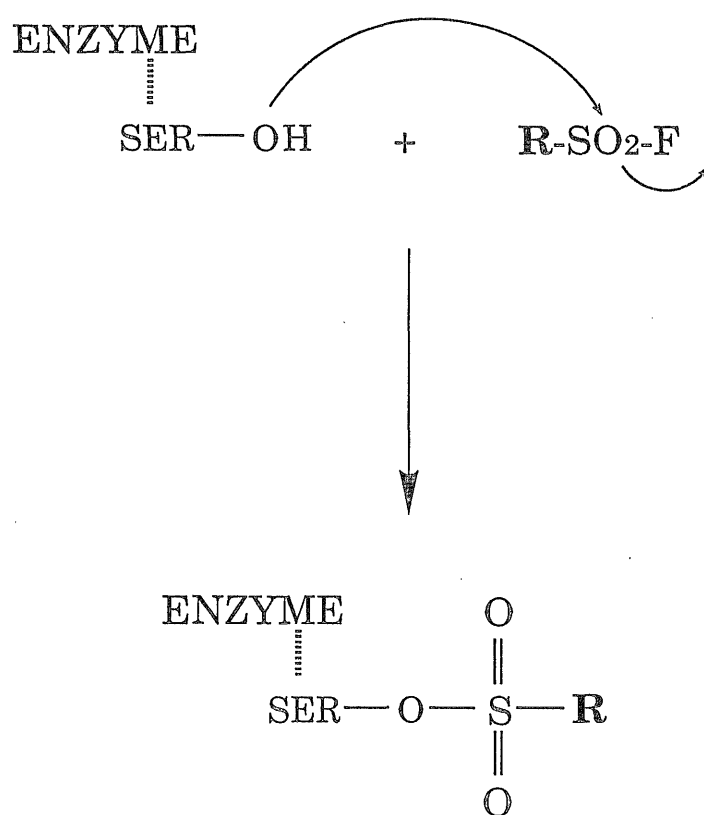
ENZYME
⋮
SER—OH   +   R-SO₂-F

↓

ENZYME   O
⋮   ‖
SER—O—S—R
              ‖
              O

Figure 4.9:   The proposed scheme for the reaction of serine
proteases with sulphonyl containing compounds,
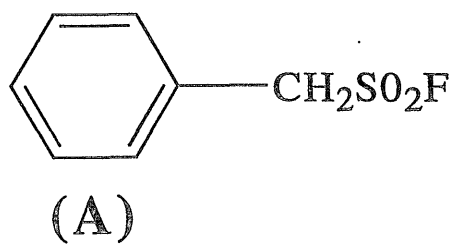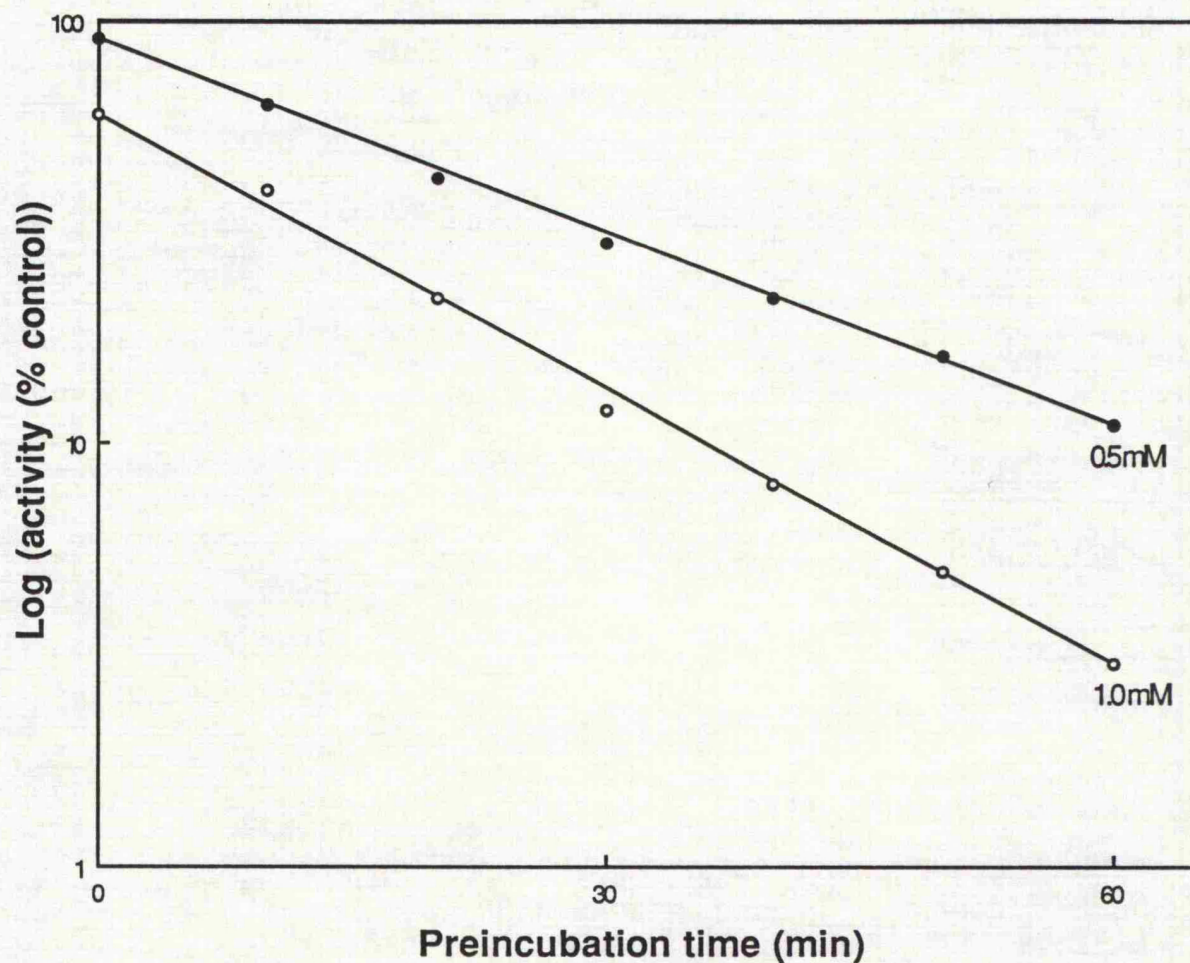after Gold (1965).
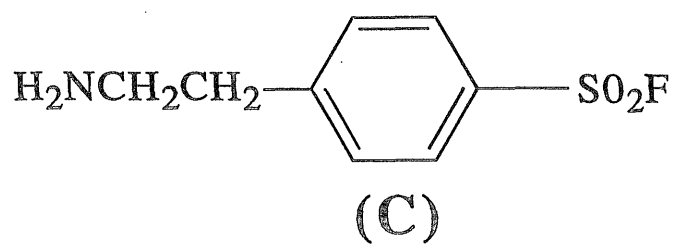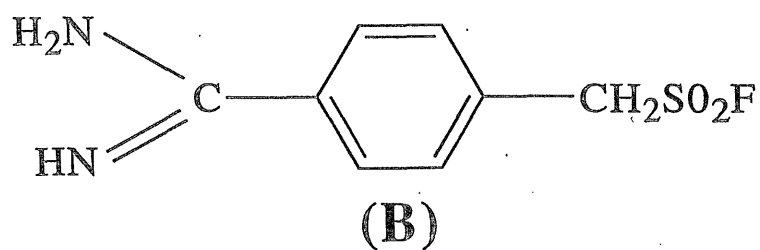
Figure 4.10: Structure of PMSF (A), APMSF (B), and Pefabloc (C).

Figure 4.11: Inactivation of the LSTR activity by Pefabloc.

MCP (0.2 mg/ml) was preincubated with either 0.5 mM or 1.0 mM Pefabloc in 50 mM Hepes/KOH buffer, pH 7.5 at 25°C. Aliquots were removed at various times and diluted 20-fold for assays of residual activity with 40 µM LSTR-AMC as describe under Section 2.4. Control incubations contained no inhibitor. Data are the average values for four separate experiments performed in duplicate.
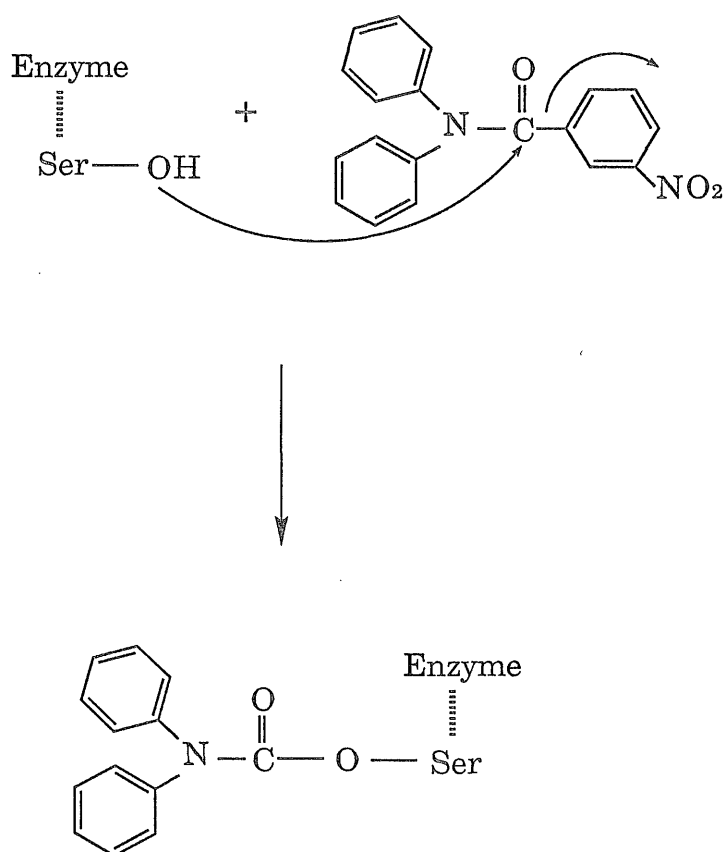
Figure 4.12 : The proposed scheme for the reaction of serine proteases with NCDC, after Erlanger et al. (1966).
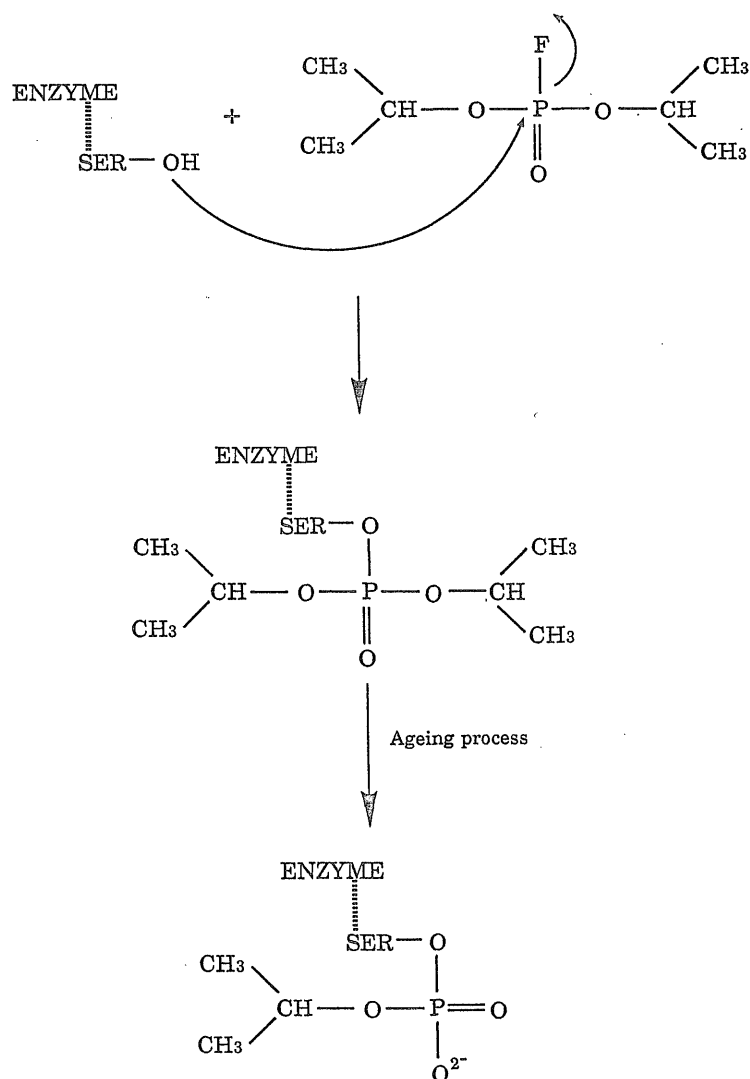
Figure 4.13 : The proposed scheme for the reaction of serine
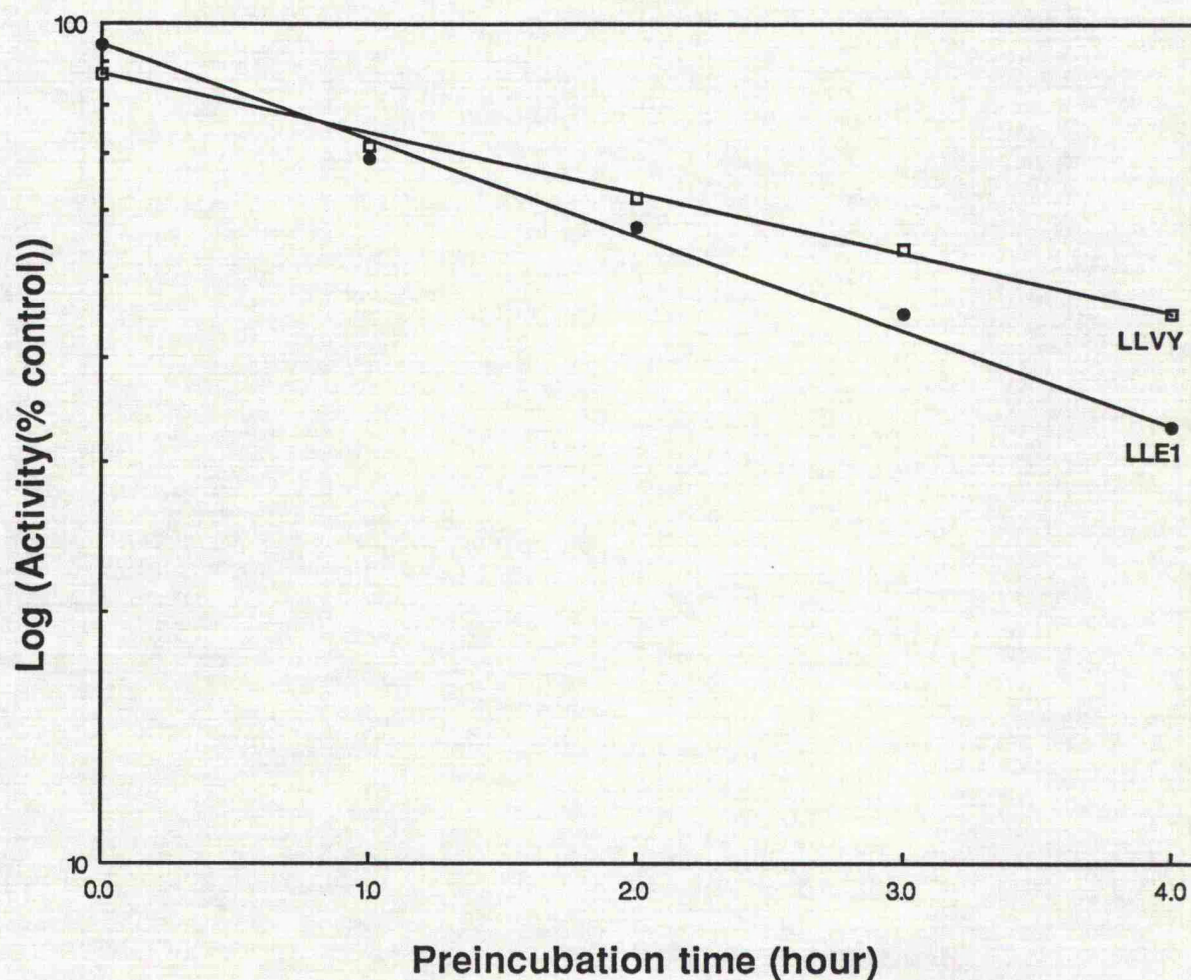proteases with DFP, after Stroud et al. (1974).

**Figure 4.14: Inactivation of the LLVY and LLE1 activities by DFP**.

MCP (0.2 mg/ml) was preincubated with 5 mM DFP in 50 mM Hepes/KOH buffer, pH 7.5 at 25°C. Aliquots were removed at various times and diluted 20-fold for measurement of residual activity with 40 µM LLVY-AMC (LLVY) or 0.1 mM LLE-NA (LLE1) as described under Section 2.4. Control incubations contained no inhibitor. Data are the average values for three separate experiments performed in duplicate.
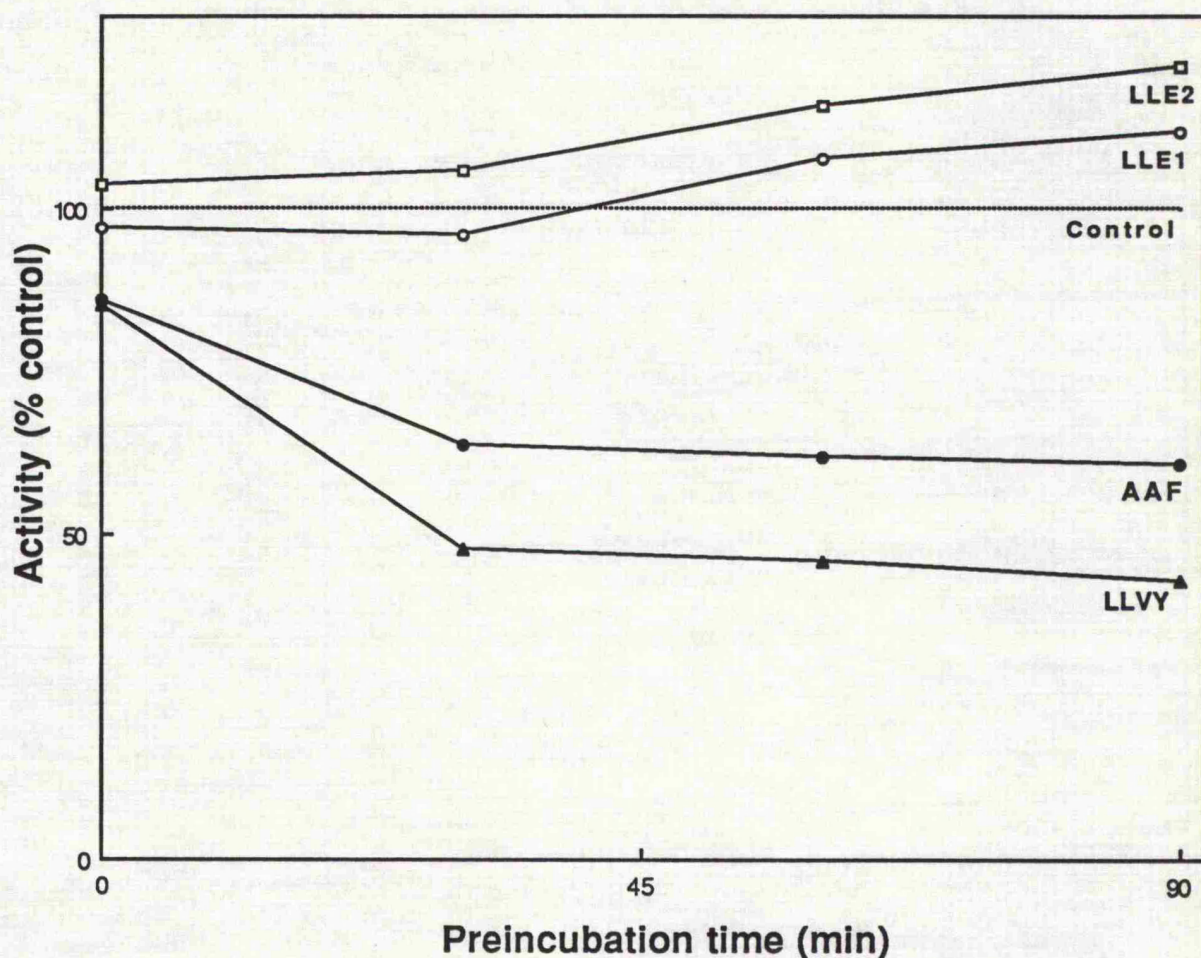
Figure 4.15: Effect of the affinity label Z-Tyr-Ala-Glu-CH$_2$Cl on MCP activities.

Prior to treatment, 2-mercaptoethanol was removed by dialysis. MCP (0.2 mg/ml) was preincubated with 0.1 mM inhibitor in 50 mM Hepes/KOH buffer, pH 7.0 at 25°C. Aliquots were removed at various times and diluted 20-fold for measurement of remaining activity with 40 µM AAF-AMC (AAF), LSTR-AMC (LSTR), LLVY-AMC (LLVY), 0.1 mM LLE-NA (LLE1), or 0.4 mM LLE-NA (LLE2) as described under Section 2.4. Control incubations contained no inhibitor. Data are the average values for four separate experiments performed in duplicate.
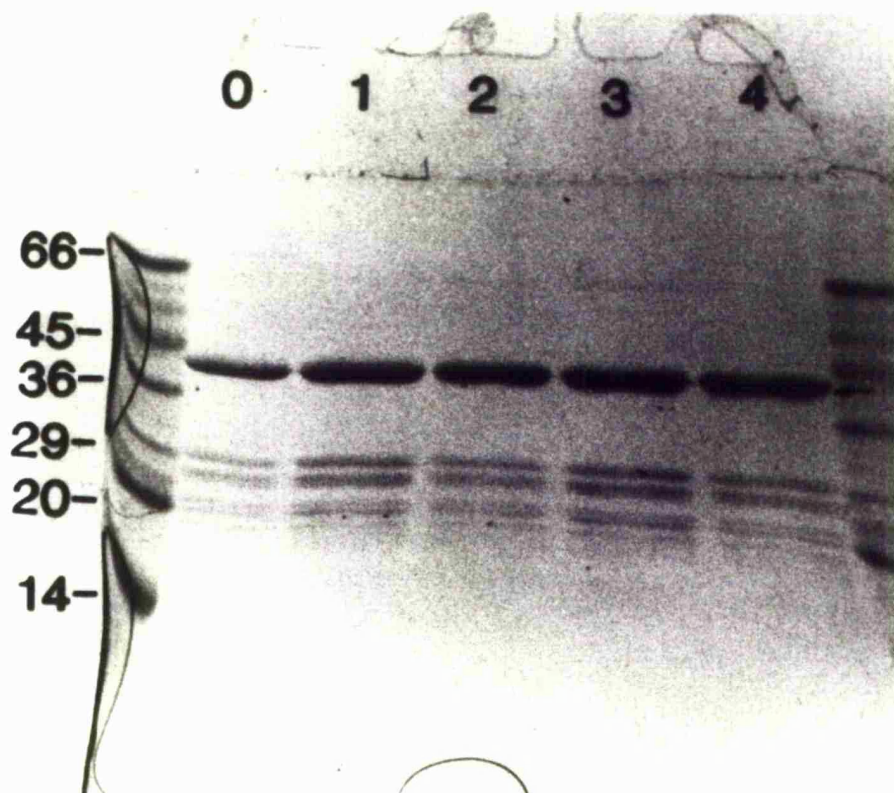
Figure 4.16: Time course of cleavage of antichymotrypsin by the proteinase complex as ascertained by SDS gel electrophoresis.

Antichymotrypsin (ACT) (0.1 mg/ml) was incubated with MCP (0.05 mg/ml) in 50 mM Hepes/KOH buffer, pH 7.5 at 37°C. Aliquots (5 μg ACT and 2.5 μg MCP) were removed at various times, and the reaction was stopped by addition of 300 μl ethanol. The precipitated protein was then prepared for gel electrophoresis as described under Section 2.7. The top legend of the gel is the incubation time in hours, and the left side legend is the standard molecular mass in kDa.
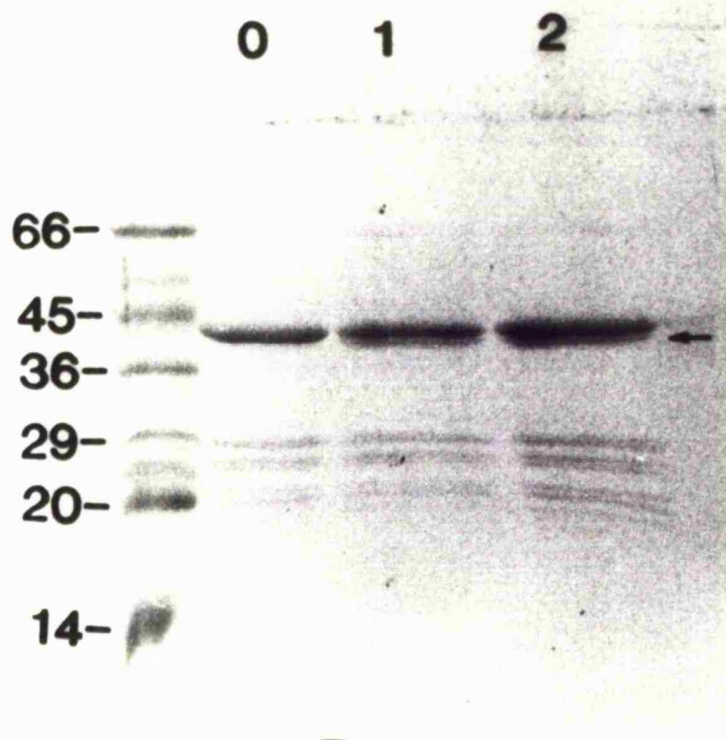
Figure 4.17: Time course of cleavage of antichymotrypsin* by the proteinase complex as ascertained by SDS gel electrophoresis.

Antichymotrypsin* (ACT*) (0.1 mg/ml) was incubated with MCP (0.05 mg/ml) in 50 mM Hepes/KOH buffer, pH 7.5 at 37°C. Aliquots (5 µg ACT and 2.5 µg MCP) were removed at various times, and the reaction was stopped by addition of 300 µl ethanol. The precipitated protein was then prepared for gel electrophoresis as described under Section 2.7. The top legend of the gel is the incubation time in hours, and the left side legend is the standard molecular mass in kDa.*Mutant antichymotrypsin.

Figure 4.18: Cleavage of antichymotrypsin by MCP as ascertained by SDS gel electrophoresis.

ACT (0.1 mg/ml) was incubated with various amounts of MCP to give the following enzyme to inhibitor (E:I) ratios 1:28 (lane c), 1:14 (lane d), 1:7 (lane e), 1:3.5 (lane f), and 1:1.53 (lane g), in 50 mM Hepes/KOH buffer, pH 7.5 at 37°C for a period of 90 min. Samples were then lyophilized and run on SDS PAGE as described under Section 2.10. Lanes b and i contain ACT alone. Lane h has similar E:I ratio as lane g, but the MCP used here was preincubated with 20 μM DCI for 30 min at 25°C before being used. Lane a contains standard molecular mass in kDa.
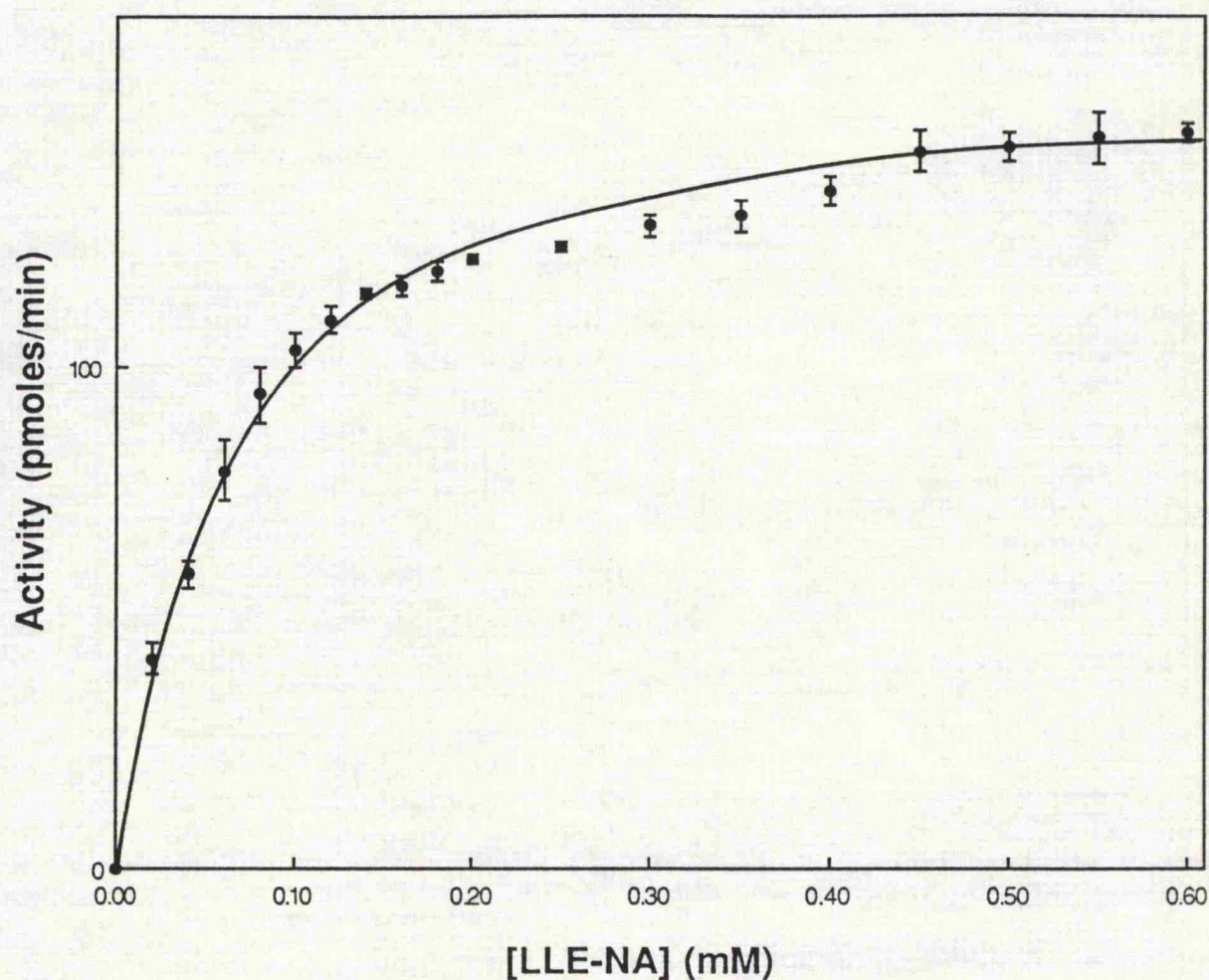
Figure 4.19: Effect of LLE1.MCP on the rate of hydrolysis of LLE·NA as a function of substrate concentration.

The inactivation reaction was initiated by addition of 1 mM Pefabloc to dialysed enzyme solution for a period of one hour, followed by the addition of 20 µM DCI for a further 30 min, and the residual activity measured as described under Section 2.4. The final DMSO concentration was 6%. The error bars represent standard deviation of at least three separate experiments performed in duplicate.
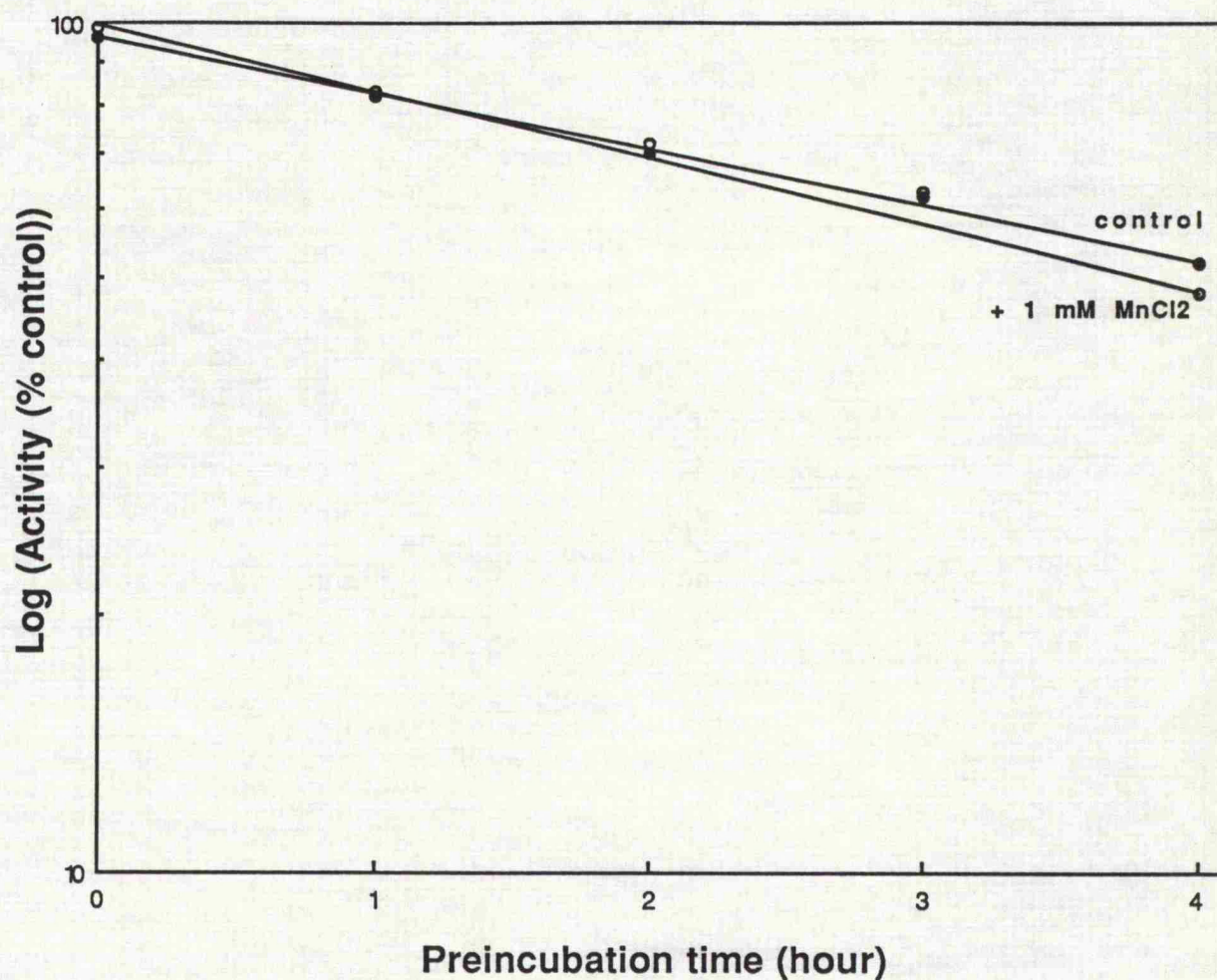
Figure 4.20: Inactivation of the LLE1 activity of LLE1.MCP by DFP.

The dialysed LLE1.MCP (0.2 mg/ml) was preincubated with 5 mM DFP in 50 mM Hepes/KOH chelex treated buffer with or without 1 mM $MnCl_2$, pH 7.5 at 25°C. Aliquots were removed at various times and diluted 20-fold for measurement of residual activity with 0.1 mM LLE-NA as described under Section 2.4. Control incubations contained no inhibitor. Data are the average values for three separate experiments performed in duplicate.
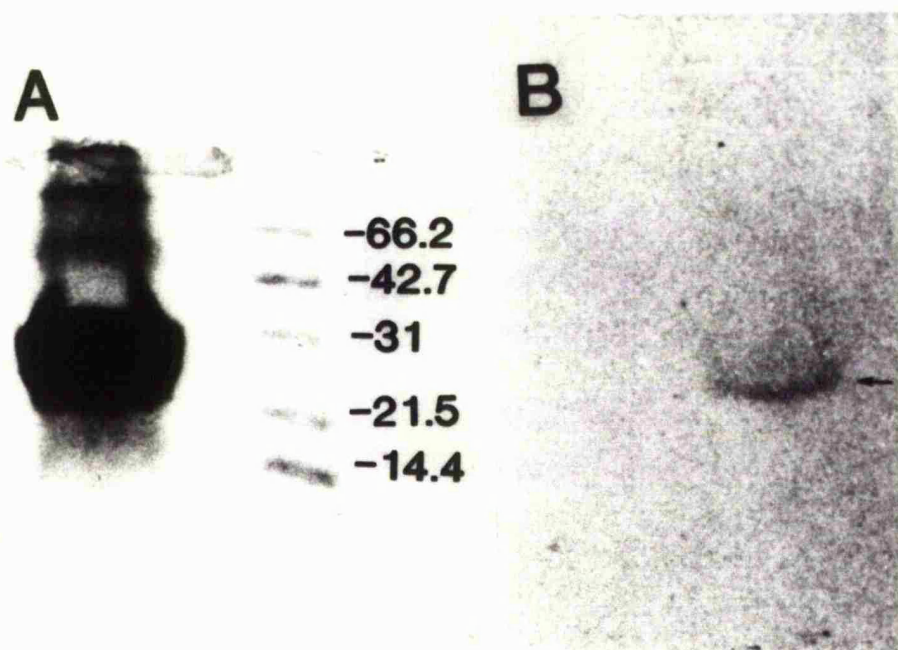
Figure 4.21: SDS polyacrylamide gel electrophoresis of [^{3}H]-DFP labelled LLE1.MCP.

LLE1.MCP was treated with [^{3}H]-DFP as described under Section 2.7. 60 µg labelled LLE1.MCP (1,650 cpm) was analysed on SDS polyacrylamide gel elctrophoresis (Section 2.10). The labelled protein band was visualised by fluorography (B) using a Kodak X-Omat AR film, which was exposed at -70°C for four weeks (Section 2.7).

Figure 4.22:   Separation profile of the components of the
                multicatalytic   proteinase   complex.

The separation of the different components was performed by reverse
phase chromatography using HPLC as described under Section 2.9. The
profile was monitored at 215 nm (1) or at 280 nm (2).
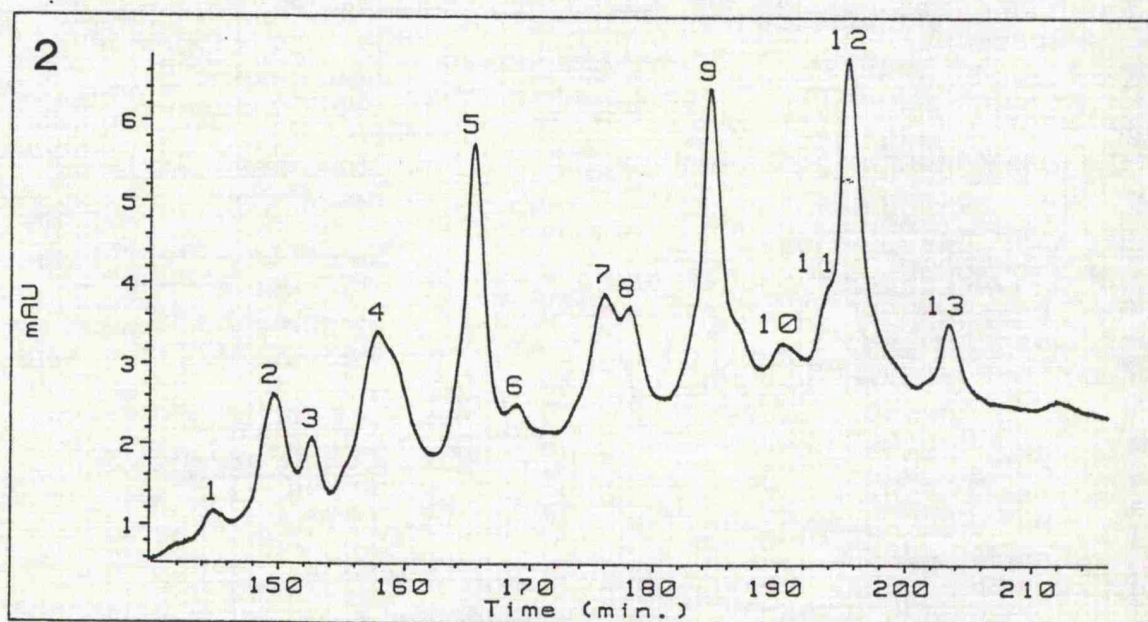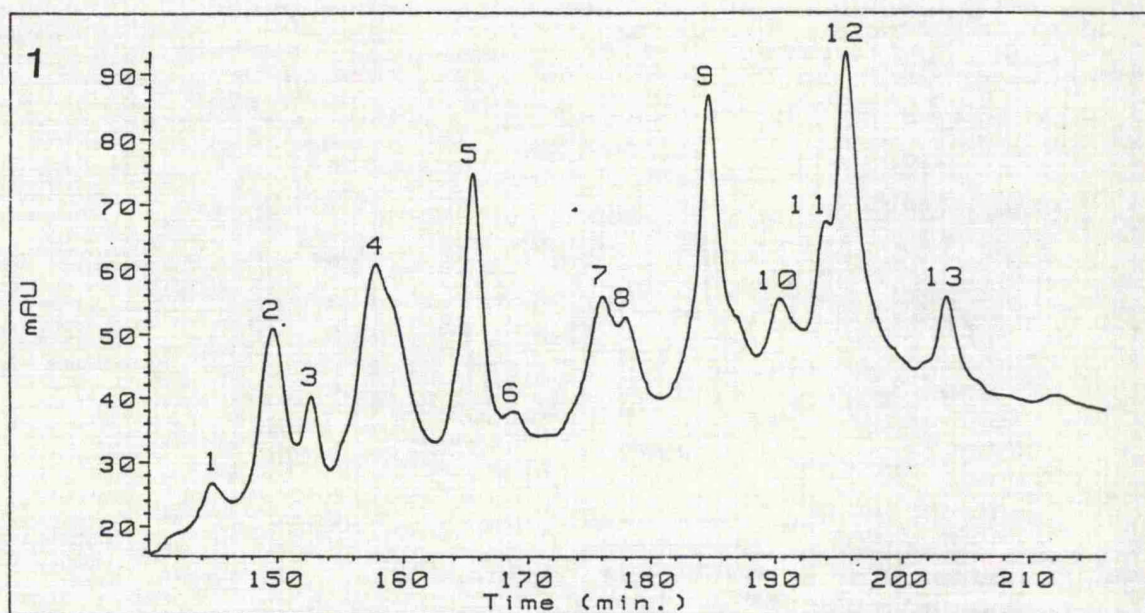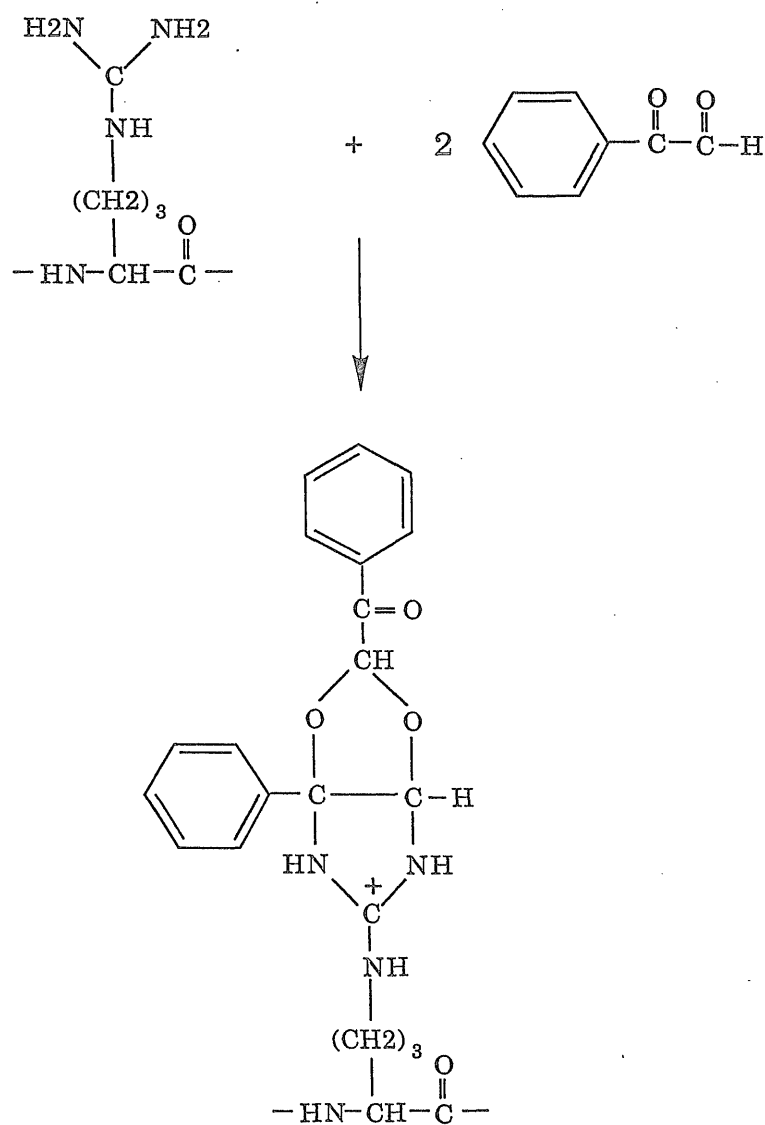
Figure 4.23: The proposed scheme for the reaction of phenylglyoxal with arginine, after Takahashi (1968).

OH

+ N—C—CH₃

N -Acetyl imidazole

CH₂
—HN—CH—C—

CH₃
C=O
O

CH₂
—HN—CH—C—

Figure 4.24: The proposed scheme for the reaction of tyrosyl residues with N-acetyl imidazole, after Riordan et al. (1965).

CHAPTER 5

Probing the specificities of the different proteolytic activities of the multicatalytic proteinase complex.

"The organising potentialities inherent in highly specific catalysis have not, I believe, been adequately appraised in chemical thought. The conc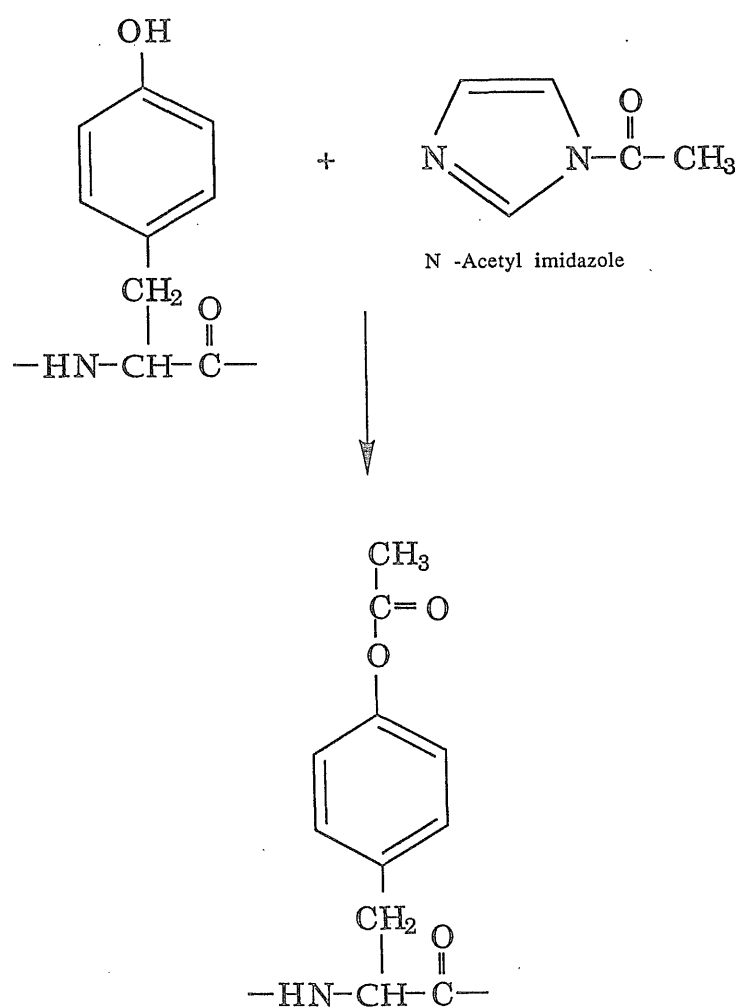entration of a catalyst or, alternatively, the extent of its active surface will determine the velocity of changes due to its influence, but highly specific catalysts determine in addition just what particular materials, rather than any others, shall undergo change. In this respect they are like the living cell itself, for they select from their environment. Finally the specific catalyst, in virtue of its own intimate structure, determines which among possible paths the course of change shall follow. It has directive powers. It is at any rate, sure that the inter-related activity of highly specific catalysts represents a notable device of Nature which has supported during the course of evolution those dynamic manifestations which characterize living things."

Hopkins, F. G. (1932)

5.1 Introduction.

The different proteolytic activities of the multicatalytic proteinase complex have been measured via a sensitive fluorometric monitoring assay, which makes use of fluorescent groups as fluorophores. Among such substrates, it is worth mentioning the naphthylamide and coumarin derivatives of peptides, which have been used to assay the different proteolytic activities of the proteinase complex (Chapters 3 and 4).

In this method, however, the fluorophore is linked directly to the bond undergoing enzymatic cleavage. Most of the fluorophores used are bulky aromatic groups, different in nature from the naturally occurring amino acids in substrates, where the bond of the synthetic derivative differs from that joining the amino acid residues of the corresponding substrates. The method allows only the study of the influence of the substrate positions P_1, P_2, . . ., P_n and not of the positions P'_1, P'_2, . . ., P'_n, which are as important in determining subsite specificities of the different proteolytic activities of the complex.

In view of the above drawbacks and of the scarce information with regards to subsite specificity of the different proteolytic activities, an alternative way for assaying the different activities has been considered for investigation. It is based on intramolecular quenching described by Yaron et al. (1979), where it allows the preparation of derivatives with an uninterrupted oligopeptide. A fluorescent group is attached to one end of the molecule and another group, normally, a chromophore that can quench the fluorescence, is

108

linked to the other end. Cleavage of the peptide chain at any point between the interacting groups results in separation between them, causing an increase in fluorescence (Yaron et al., 1979).

There have been several reports in the literature describing the use of intramolecularly quenched fluorogenic substrates for assaying proteolytic activity, and were found to be very sensitive for assaying rates of the order of nmoles/min (Yaron et al., 1979; Barrett et al., 1989; Tisljar et al., 1990; Dauch et al., 1991; Meldal and Breddam, 1991; Breddam and Meldal, 1992).

This chapter describes the use of peptides for studying their cleavage patterns generated after digestion by the proteinase complex. The aim was to generate as much information about the cleavage sites as possible, and with the use of the modified MCPs (namely the proteinase treated with the pefabloc inhibitor which selectively inhibits the LSTR activity (Chapter 4, enzyme will be referred to as LSTR-MCP in the text) and the enzyme treated with the pefabloc inhibitor followed by the 3,4 dichloroisocoumarin inhibitor which inhibit the AAF, LSTR, LLVY, and LLE2 activities (Chapter 4, enzyme will be referred to as LLE1.MCP in the text)), to be able to relate back any cleavage site to the proteolytic activity responsible for it. Thus, possible identification of unique sequence specificities can be achieved, for some of the proteolytic activities of the complex, within an oligopeptide which could be used for the design of specific intramolecular quenched fluorogenic substrates.

Finally, this chapter also describes the use of the Carlsberg peptides as models of the intramolecularly quenched fluorogenic

substrates to assay the different proteolytic activities of the complex, with emphasis on the peptidylglutamyl-peptide hydrolase activity as the substrates were designed for Glu/Asp-specific proteases (Breddam and Meldal, 1992).

5.2 The commercial peptides.

The commercial peptides, neurotensin, neurotensin fragment 1-8, bradykinin, splenopentin fragment 1-5, and luteinizing hormone releasing hormone (LH-RH), were investigated as potential substrates for the proteinase complex. Results summarized in Table 5.1 show that neurotensin, bradykinin, neurotensin fragment 1-8, and LH-RH were not cleaved by the purified rat liver proteinase complex (Table 5.1)

Splenopentin fragment 1-5 (SP5), on the other hand, was cleaved by the purified proteinase complex as illustrated in Figure 5.1, and the site of cleavage was determined to be at the peptide bond Lys_2-Glu_3 (Table 5.1). The determined cleavage site is suggestive of the possible involvement of the trypsin-like activity.

5.3 The Oxford peptides.

The Oxford peptides, which range in size for 9mer to 15mer, were investigated as possible substrates for the proteinase complex. Four out of the seventeen peptides tested were not cleaved by the proteinase complex, namely the Ox 1, Ox 3, Ox 4, and Ox 9 peptides (Tables 5.2 and 5.3).

110

The Ox 2 peptide was cleaved three times by MCP (Figure 5.2), and the sites of peptide cleavage were determined to be at the Thr_1-Tyr_2, Thr_5-Arg_6, and Arg_6-Ala_7 peptide bonds (Table 5.2). The results suggest the possible involvement of the trypsin-like activity in the cleavage at the Arg_6-Ala_7 peptide bond. However, it is not clear from these results which proteolytic activity is involved in the Thr_1-Tyr_2 and Thr_5-Arg_6 cleavages.

It is interesting to note that the Arg_{10}-Thr_{11} peptide bond was not cleaved, which reflects the importance of subsite specificity where valine and glycine happen to be in the P2 and P2' positions in the case of the Arg_{10}-Thr_{11} peptide bond, respectively. Whereas in the case of the Arg_4-Thr_5 and Arg_6-Ala_7 cleavages, glutamine and threonine are in the P2 positions, respectively, and arginine and leucine are in the P2' positions, respectively. One might, therefore, conclude that charged and hydrophobic residues are preferred in those positions.

The Ox 5 peptide was cleaved twice (Figure 5.3), and the sites of peptide cleavage were determined to be at the Tyr_3-Val_4 and Tyr_5-Gln_6 peptide bonds (Table 5.2). The results are suggestive of the possible involvement of the chymotrypsin-like activity in the observed cleavages. The Tyr_3-Val_4 cleavage has a glycine in the P2 and a tyrosine in the P2' positions, whereas the Tyr_5-Gln_6 cleavage has a valine in the P2 and a glycine in the P2' positions. Both cleavages, however, have either hydrophobic or charged residues in the P3 and P3' positions.

The Ox 6 peptide was cleaved once (Figure 5.4), and the site of peptide cleavage was determined to be at the Lys_7-Trp_8 peptide bond

(Table 5.2). Cleavage after a lysine residue is suggestive, once more, of the possible involvement of the trypsin-like activity.

In comparison to this result, the Ox 7 peptide (Figure 5.5), which differ from the Ox 6 peptide by an asparagine substitution in position 6, was also cleaved at similar site by the proteinase (Table 5.2).

Examination of the subsites of both cleavages revealed that the substitution in the P2 position from a negatively charged aspartic acid residue (in the Ox 6 peptide) to an uncharged asparagine residue (in the Ox 7 peptide) did not alter the cleavage pattern, suggesting that in this case, the P2 position prefers both uncharged and charged residues. Here again, we observe that the residues in the P3 and P2' positions are charged and hydrophobic, whereas in the P2 and P1' positions the residues are neutral or hydrophobic, respectively.

The Ox 8 peptide was cleaved twice (Figure 5.6), and the sites of peptide cleavage were determined to be at the Glu_4-Asn_5.and Asp_7-Ala_8 peptide bonds (Table 5.3). The results are suggestive of possible involvement of the peptidylglutamyl-peptide hydrolase activity. It is interesting to not that the Glu_{10}-Ser_{11} peptide bond was note cleaved by MCP.

The non-cleaved Ox 9 peptide (Table 5.3) has similar sequence to the Ox 8 peptide (Table 5.3) but in the opposite direction, that is the N-terminus of the Ox 8 peptide is the C-terminus of the Ox 9 peptide. It is interesting to note that 180° rotation of the peptide does not make it a substrate. In the Asp_7-Ala_8 cleavage, methionine and

112

asparagine are in the P2 and P3 positions, respectively. A 180° rotation around the aspartic acid residue brings alanine and methionine in those positions, respectively. Having an alanine residue in the P2 position might explain the lack of cleavage by the respective activity. In the Glu_4-Asn_5 cleavage, asparagine and serine are in the P2 and P3 positions, respectively.

A 180° rotation around the glutamic acid residue brings an asparagine and a methionine in those positions, which might explain the lack of cleavage, or the presence of the serine residue in the P2' position might be the cause, as was found for the non-cleaved Glu_{10}-Ser_{11} peptide bond.

The Ox 10 peptide was cleaved three times by MCP (Figure 5.7), and the sites of peptide cleavage were determined to be at the Cys_4-Thr_5, Leu_9-Ser_{10}, and Asp_{11}-Tyr_{12} peptide bonds (Table 5.3). The results suggest that the cleavage after a leucine residue could involve the chymotrypsin-like activity, and the one after the aspartic acid could involve the peptidylglutamyl-peptide hydrolase activity, whereas the activity which caused the cleavage after the cysteine residue is not yet defined.

The Ox 11 peptide was cleaved three times by MCP (Figure 5.8), and the sites of peptide cleavage were determined to be at the Met_7-Glu_8, Glu_8-Thr_9, and Ser_{12}-Ser_{13} peptide bonds (Table 5.4). The results suggest that the Glu_8-Thr_9 cleavage might involve the peptidylglutamyl-peptide hydrolase activity, whereas the activity or activities involved in the other observed cleavages are not as yet defined.

It is interesting to note that the non-cleaved Ox 3 peptide (Table 5.2) has a sequence similar to the Ox 11 peptide, except for an extra leucine residue at position 15 (Table 5.3). The data suggests that this extra residue appears to make a difference to whether the peptide is going to be cleaved by MCP or not: its absence makes the Ox 3 peptide a good substrate (cf. the Ox 11 peptide), and its presence does not. The leucine residue somehow prevents binding and subsequent degradation of the Ox 3 peptide.

The Ox 12 peptide was cleaved once by MCP (Figure 5.9), and the site of peptide cleavage was determined to be at the Met_6-Asp_7 peptide bond (Table 5.3). Again the activity responsible for such a cleavage is not as yet identified nor defined.

The Ox 13 peptide was cleaved twice by MCP (Figure 5.10), and the sites of peptide cleavage were determined to be at the Arg_4-Thr_5 and Arg_6-Ala_7 peptide bonds (Table 5.3). The results are suggestive of the possible involvement of the trypsin-like activity.

It is interesting to note that the Ox 2 peptide (Figures 5.2 and Table 5.2) has similar sequence to the Ox 13 peptide, except for the extra arginine residue at position 10 (Table 5.3). This difference appears to have induced different cleavage patterns, with the Arg_6-Ala_7 peptide bond cleavage being common to the two peptides (see Tables 5.2 and 5.3, and compare Figures 5.2 and 5.10).

The Ox 14 peptide was cleaved three times by MCP (Figure 5.11), and the sites of peptide cleavage were determined to be at the Lys_1-

Thr_2, Arg_9-Val_{10}, and Lys_{13}-Trp_{14} peptide bonds (Table 5.4). The results are suggestive of possible involvement of the trypsin-like activity in the observed cleavages.

The Ox 15 peptide was cleaved three times by MCP (Figure 5.12), and the sites of peptide cleavage were determined to be at the Lys_1-Thr_2, Arg_9-Val_{10}, and Lys_{13}-Trp_{14} peptide bonds (Table 5.4). The results are also suggestive of possible involvement of the trypsin-like activity in the observed cleavages.

The Ox 16 peptide was cleaved five times by MCP (Figure 5.13), and the site of peptide cleavages were determined to be at the Lys_1-Thr_2, Tyr_7-Arg_8, Arg_8-Val_9, Val_9-Asp_{10}, and Lys_{12}-Trp_{13} peptide bonds (Table 5.4). The results again suggest the possible involvement of the trypsin-like activity in the Lys_1-Thr_2, Arg_8-Val_9, and Lys_{12}-Trp_{13} cleavages, and the chymotrypsin-like activity in the Tyr_7-Arg_8 cleavage. However, it is not clear yet which proteolytic activity was responsible for the Val_9-Asp_{10} cleavage.

The Ox 17 peptide was cleaved five times by MCP (Figure 5.14), and the site of peptide cleavages were determined to be at the Tyr_7-Arg_8, Arg_8-Val_9, Val_9-Asp_{10}, and Asn_{12}-Trp_{13} peptide bonds (Table 5.4). The results again suggest the possible involvement of the trypsin-like activity in the Arg_8-Val_9 cleavage, and the chymotrypsin-like activity in the Tyr_7-Arg_8 cleavage. However, it is not clear yet which proteolytic activity or activities was responsible for the Val_9-Asp_{10} and Asn_{12}-Trp_{13} cleavage.

5.4 Peptide digestion using LSTR-MCP or LLE1.MCP.

Repeat of the above study, but this time using modified proteinase complexes described in Section 5.1, was carried out using selected peptides.

The Ox 2 peptide was not cleaved by LSTR-MCP, which suggests that the LSTR activity was responsible for the Thr_1-Tyr_2, Thr_5-Arg_6, and Arg_6-Ala_7 cleavages observed when MCP was used (Table 5.6). When LLE1.MCP was used, similar results were obtained (Table 5.7).

The Ox 5 peptide was not cleaved by LSTR-MCP (Table 5.6), which again suggests that the LSTR activity was responsible for the Tyr_3-Val_4 and Tyr_5-Gln_6 cleavages observed when MCP was used (Table 5.3). The data also suggest that the trypsin-like activity can cleave after hydrophobic residues in the P1 position. The Ox 5 peptide was not cleaved by LLE1.MCP (Table 5.7).

The Ox 7 peptide was not cleaved by LSTR-MCP (Table 5.6), which is suggestive of the involvement of the LSTR activity in the Lys_7-Trp_8 cleavage. The Ox 7 peptide was not cleaved by LLE1.MCP (Table 5.7).

The Ox 8 peptide was cleaved by LSTR-MCP at the same positions as when MCP was used for the digestion (Tables 5.4 and 5.6), suggesting that the LSTR activity was not involved in the Glu_4-Asn_5.or the Asp_7-Ala_8 cleavage. Furthermore, the use of LLE1.MCP gave similar results to the above (Table 5.7), which again is suggestive of the non-involvement of the LSTR, AAF, LLVY, and LLE2 activities in the

116

degradation of the Ox 8 peptide, leaving the possible involvement of the LLE1 activity in the observed cleavages.

The Ox 10 peptide was cleaved by LSTR-MCP at the same sites as when MCP was used ie the the Cys_4-Thr_5, Leu_9-Ser_{10}, and Asp_{11}-Tyr_{12} cleavages (Tables 5.4 and 5.6). In addition, the use of the LLE1.MCP gave similar results, which opens to question whether the LLE1 activity was responsible for the three observed cleavages or there is (are) other, as yet not identified, proteolytic sites which are involved in the cleavage of at least the Cys_4-Thr_5 and/or the Leu_9-Ser_{10} peptide bonds (Table 5.7).

The Ox 11 peptide was cleaved by LSTR-MCP at four different sites along the sequence (Table 5.6). three of the cleavages were found to be similar to the ones obtained when MCP was used, namely the Met_7-Glu_8, Glu_8-Thr_9, and Ser_{12}-Ser_{13} cleavages (Tables 5.3 and 5.5). The fourth cleavage, which was determined at the Asn_4-Glu_5 peptide bond, was found to be a novel one ie only observed when the LSTR-MCP was used to digest the peptide (Table 5.5), and because it was not observed when the LLE1.MCP was used (Table 5.6), suggesting that either of the following activities could have been involved in the observed cleavage: the AAF, LLVY, or the LLE2 activities.

Using the LLE1.MCP, similar results were obtained with the Ox 11 peptide as to when MCP was used (Table 5.7). The results are also suggestive of possible involvement of other sites in the observed cleavages, as the Glu_8-Thr_9 cleavage could be attributed to the LLE1 activity, which in turn could well have been involved in the other cleavages.

The Ox 12 peptide was cleaved by LSTR-MCP at the same site as when MCP was used ie the Met_6-Asp_7 cleavage (Tables 5.4 and 5.6). When the LLE1.MCP was used, similar results were obtained (Table 5.7), which suggests once again that either the LLE1 activity or other proteolytic sites, as yet not identified, were involved in the observed cleavage.

5.5 The Carlsberg peptides.

The Carlsberg peptides are based on anthranilamide (the fluorophore) and nitrotyrosine (the quencher) as a donor-acceptor pair in a fluorescence quenching process (Meldal and Breddam, 1991). The peptides were synthesized and used in the study of substrate preferences of the Glu/Asp-specific proteases from *Staphylococcus aureus* (V8), *Bacillus licheniformis* and *Streptomyces griseus* (Breddam and Meldal, 1992).

The Carlsberg peptides were investigated as possible substrates for the proteinase complex. The results summarized in Table 5.8 are of the substrates that were not hydrolysed by the proteinase complex.

Substrates in Tables 5.9 and 5.10, on the other hand, were hydrolysed by the proteinase complex, but at a relatively low specific activities ie values ranging from 0.5 to 4.0 nmoles/min/mg (Tables 5.9 and 5.10). Due to the very low concentration of substrate used (ie 0.25 μM), it was not possible to purify enough product for HPLC separation and subsequent amino acid analysis, thus determining cleavage site(s) on the peptide substrates.

5.6 The multicatalytic proteinase complex and antigen processing.

The generation of proteolytic fragments of viral proteins within the cell is poorly understood. Peptides of nine to eleven amino acids with the appropriate antigenic sequence have been shown to be by far the most efficient at promoting assembly of the class I MHC molecules, in the endoplasmic reticulum, for presentation at the cell surface (DeMars and Spies, 1992). These are the predominant lengths of class I-associated peptides found in mouse and human cells (DeMars and Spies, 1992).

A number of epitopes from the nucleoprotein (NP) of the influenza virus A/NT/60/68 (Huddleston and Brownlee, 1982) have been identified, and shown to be presented in association of MHC class I molecules at the cell surface (Townsend and Bodmer, 1989; Cerundolo et al., 1991).

The class I MHC molecules and bound peptide antigens serve, thus, as specific recognition elements for the detection and destruction of the diseased cells by cytotoxic T cells (Madden et al., 1992). The peptide synthesis of some of the Oxford peptides was based on the NP protein sequence, where the sequence of the identified peptide antigen was included together with flanking peptide regions on either the N- or C- terminus of the Oxford peptide.

The implication of MCP in antigen processing has been seen more of a hypothetical one (Chapter 1; Driscoll and Finley, 1992; van Bleek and Nathenson, 1992), where two MCP subunit genes (RING10

and RING 12; LMP2 and LMP7) (Section 1.5) were found to be localized in the MHC gene, which has been suggested to be a eukaryotic operon encoding a complete kit for the processing and presentation of antigens (Robertson, 1991).

In collaboration with Townsend and coworkers (Molecular Immunology Group, Institute of Molecular Medecine, John Radcliffe Hospital, Oxford), we have questioned the involvement of MCP in antigen processing by looking at the degradation products of some of the Oxford peptides *in vitro*, generated after cleavage by the rat liver MCP. Such experiments would allow us to investigate whether MCP can generate the exact peptide sequence of the respective epitope or not, as the sequence of the *in vivo* cleavages are known.

The results from such investigations are summarised in Tables 5.2, 5.3, and 5.4. The cleavage sites were found to be non specific with regards to their *in vivo* ones (Tables 5.2 and 5.3), except in the case of peptide Ox 11, where the exact cleavage on the C-terminus side of the epitope was observed (Table 5.3).

It was also observed that as the length of the peptide was extended on the C-terminus side of the epitope, the exact cleavage site was obtained on the C-terminus side ie see peptides Ox 14, Ox 15, Ox 16, and Ox 17 in Table 5.4. The Arg-Val peptide bond, which cleavage gives rise to the correct epitope, in each of those peptides (Table 5.4) was cleaved despite amino acid substitution or amino acid removal from the peptide sequence, suggesting somekind of recognition of the cleavage site by MCP. It should be added that the peptides Ox 14, Ox 15, Ox 16, and Ox 17 are longer versions of either peptides Ox 6 or

Ox 7, and were synthesized after results with the other peptides were obtained.

5.7 Discussion.

The rat liver MCP did not cleave the commercial peptides (Table 5.1). In contrast, Wilk and Orlowski (1980) and Cardozo et al. (1992) have reported cleavage of some of the peptides, namely neurotensin, bradykinin, and LH-RH, by their purified pituitary MCP. A possible explanation for the observed differences could be due the source of the enzyme and/or to the purification procedure.

The data obtained with the peptide substrates show the multicatalytic proteinase complex as a selective protease, where selectively appears to be determined by the sequence of the peptide to be cleaved. Several interesting observations came out of this investigation: 1) not every peptide presented was cleaved which reinforce the argument for selectivity, 2) an addition of an extra amino acid in any peptide sequence appears to change the outcome of the enzyme-substrate interaction, where the latter will or will not be cleaved, as was shown in the case of the Ox 3 and Ox 11 peptides, the Ox 16 and Ox 17 peptides, and also in the case of the Ox 2 and the Ox 13, where novel cleavage sites were observed in the Ox 13 peptide after addition of an arginine residue in position 10 (cf. the Ox 2 peptide), and finally, single substitution in any peptide sequence appears to also change the course of peptide cleavage in some cases (cf. the Ox 15 and Ox 16 peptides and the Ox 16 and Ox 17 peptides), and had no effect on the course in others (cf. the Ox 6 and Ox 7 peptides).

The chemically modified MCPs (cf. LSTR-MCP and LLE1.MCP) have proved to be useful in distinguishing between the different activities that were responsible for some of the observed cleavages. One striking result was that the two cleavage sites in the Ox 5 peptide (cf. the Tyr_3-Val_4 and Tyr_5-Gln_6 cleavages) were not generated by the pefabloc treated MCP (LSTR-MCP), an inhibitor found to selectively inactivate the trypsin-like activity (Chapter 4). This observation reinforces the argument put forward in Chapter 4 against Wilk and Orlowski's (1983) definitions for the three proteolytic activities of the complex, which were based merely on the cleavage of synthetic substrates with an emphasis on the P1 position only.

Another interesting aspect of the investigation, was the detection of some cleavage sites that were resistant to inhibition by pefabloc (ie LSTR-MCP) or by pefabloc and 3,4 dichloroisocoumarin (ie LLE1.MCP). In some instances, the resistant cleavages may be attributed to the LLE1 activity, which itself is resistant to inhibition by either pefabloc or 3,4 dichloroisocoumarin (Chapter 4), and such is probably the case for the Glu_4-Asn_5 and the Asp_7-Ala_8 cleavages in the Ox 8 peptide, the Glu_8-Thr_9 cleavage in the Ox 11 peptide, and possibly the Asp_{11}-Tyr_{12} cleavage in the Ox 10 peptide.

However, the other resistant sites, which include the Cys_4-Thr_5 and Leu_9-Ser_{10} cleavages in the Ox 10 peptide, the Met_7-Glu_8, and Ser_{12}-Ser_{13} cleavages in the Ox 11 peptides, and the Met_6-Asp_7 cleavage in the Ox 12 peptide, may probably be attributed to the LLE1 activity or to newly detected proteolytic sites within the complex. Because of the lack of potent inhibitors against the LLE1 activity

(Chapter 4), its possible involvement in the above cleavages cannot be ruled out completely.

There have been several reports in the literature describing use of peptides as substrates for MCP (Wilk and Orlowski, 1980; Rivett, 1985; Dick et al., 1991; Cardozo et al., 1992). The outcome of those studies, however, was the identification of cleavage sites, some of which could be related to the respective proteolytic activity responsible for the cleavage, such is the case of the Gln_4-His_5 cleavage in the oxidized insulin B chain which was inhibited by leupeptin, a specific inhibitor of the trypsin-like activity (Dick et al., 1991), but other cleavages are still as yet unclear of which proteolytic activity was responsible for them, such are the cases of the Glu_4-Asn_5, Asn_5-Lys_6, and Ile_{12}-Leu_{13} cleavages in neurotensin (Cardozo et al., 1992).

In view of what has been described so far, it seems likely that the multicatalytic proteinase complex has more than the five proteolytic sites (Djaballah et al., 1992), and further study is needed to fully characterize those novel site(s) in anticipation of a better understanding of the mechanistic action of MCP, bearing in mind the suggestion put forward by Dick et al. (1991) of channelling of peptide substrates between the different catalytic sites within MCP, and the finding, in this study, that novel cleavage sites can be detected if one or more activities of the complex are inhibited cf. the Asn_4-Glu_5 cleavage by LSTR-MCP in the Ox 11 peptide.

With regards to the design of intramolecularly quenched fluorescent substrates, the Ox 8 peptide (sequence: Ala-Ser-Asn-Glu-

Asn-Met-Asp-Ala-Met-Glu-Ser-Ser-Thr-Leu) appears to be a good candidate. The Glu_4-Asn_5 and the Asp_7-Ala_8 cleavages appear to be caused by at least the LLE1 activity, and the following products were collected: Ala-Ser-Asn-Glu and Ala-Ser-Asn-Glu-Asn-Met-Asp. Thus, one would expect the peptide Ala-Ser-Asn-Glu-Asn-Met-Asp to be cleaved once at the Glu_4-Asn_5 peptide bond, and similarly peptide Asn-Met-Asp-Ala-Met-Glu-Ser-Ser-Thr-Leu to be cleaved once at the Asp_7-Ala_8 peptide bond. If that is so, then the effects of the added chromophores on the enzyme-substrate interaction can be investigated, in the hope of generating a specific substrate for the LLE1 activity.

The results presented here concerning MCP and antigen processing do not suggest nor confirm in any way the involvement of the proteinase complex in such a process. However, they do tell us one important aspect regarding the peptide to be cleaved, where its size appears to determine, in the case of the present study, the correct cleavage of the epitope on the C-terminus side of the peptides tested (Table 5.4). Further investigation will require the use of longer peptides or even of the nucleoprotein itself.

The observation that the Arg-Val bond in peptides Ox 14 to Ox 17 was an interesting one and has led to further investigating such *in vitro* results. Based on the sequence of peptides Ox 14 to Ox 17, construction of recombinant vaccinia viruses expressing DNA fragment coding for either of the peptides is under way (Cerundolo and Townsend, personal communication). The constructs will then be used to infect a lymphoblastoid cell line capable of processing and

presentation at the cell surface, and has been shown to present antigens when infected by such constructs (Cerundolo et al., 1991).

The investigation will concentrate mainly on determining whether the four peptides will be processed thus leading to cell lysis or not. If processed and presented, it would be interesting to determine the efficiency of presentation or even to attempt to elute the presented antigens from the MHC class I complexes in each case, and determine their sequences. Such investigations are currently under way in Oxford.

In summary, the results presented here have given us a new insight into the specificities of the different activities, and have led to the identification of novel proteolytic site(s) that are awaiting full characterisation. In addition, the Carlsberg peptides have proved to be hydrolysed by MCP but with low specific activities, and will make the future design of intramolecularly quenched fluorescent substrates for the LLE1 activity in particular a worthwhile task.

Table 5.1: Cleavage of biologically active peptides by MCP.

Peptides (0.1 mg/ml) were incubated with 0.05 mg/ml purified MCP in 50 mM Hepes/KOH buffer, pH 7.5 as described under Section 2.4. *Sites of peptide bond cleavage were identified by HPLC separation and amino acid analysis of peptide products as described under Section 2.8. LH-RH = luteinizing hormone releasing hormone, SP5 = splenopentin fragment 1-5, and N.C. = not cleaved. ↓Cleavage site.

Substrate	Sequence	Products*
Neurotensin	pE-L-Y-E-K-P-R-P-Y-I-L.	N.C.
Neurotensin 1-8	pE-L-Y-E-N-K-P-R.	N.C.
Bradikynin	R-P-G-F-S-P-F-R.	N.C.
LH-RH	pE-H-W-S-Y-G-L-R-P-G.	N.C.
SP5	R-K↓E-V-Y.	EVY.

Table 5.2: Cleavage of the Oxford peptides by MCP: Part I.

Peptides (0.1 mg/ml) were incubated at 37°C, for 120 min, with 0.05 mg/ml purified MCP in 50 mM Hepes/KOH buffer, pH 7.5 as described under Section 2.4. *Sites of peptide bond cleavage were identified by HPLC separation and amino acid analysis of peptide products as described under Section 2.8. N.C. = not cleaved. ↓Cleavage site. Bolded and underlined sequence indicate epitope sequence or part of its sequence.

Peptide	Products*
Ox 1: S-D-Y-E-G-R-L-I-O-N-S-L-T-I.	N.C.
Ox 2: T-↓Y-O-R-T↓R-↓A-L-V-R-T-G.	YQRT, TYQRTR, & RALVRTG.
Ox 3: I-A-S-N-E-N-M-E-T-M-E-S-S-T-L-E.	N.C.
Ox 4: Y-S-N-E-N-M-E-T-M.	N.C.
Ox 5: R-G-Y↓V-Y↓Q-G-L.	RGY, VYQGL & QGL.
Ox 6: Y-KR-V-N-D-G-K↓W-M.	YKRVNDGK.
Ox 7: Y-K-R-V-N-N-G-K↓W-M.	YKRVNNGK.

Table 5.3: Cleavage of the Oxford peptides by MCP: Part II.

Peptides (0.1 mg/ml) were incubated at 37°C with 0.05 mg/ml purified MCP in 50 mM Hepes/KOH buffer, pH 7.5, for 120 min as described under Section 2.4. *Sites of peptide bond cleavage were identified by HPLC separation and amino acid analysis of peptide products as described under Section 2.8. Subs = substrate and N.C. = not cleaved. ↓Cleavage site. Bolded and underlined sequence indicate epitope sequence or part of its sequence.

Peptide	Products*
Ox 8: A-S-N-E↓N-M-D↓A-M-E-S-S-T-L.	ASNE & ASNENMD.
Ox 9: L-T-S-S-E-M-A-D-M-N-E-N-S-A.	N.C.
Ox 10: I-Q-M-C↓T-E-L-K-L↓S-D↓Y-E-G-R.	YEGR, SDYEGR, & TELKLSDYEGR.
Ox 11: I-A-S-N-E-N-M↓E↓T-M-E-S↓S-T-E.	ETMES, TMESSTE, IASNENME, & IASNENMETMES.
Ox 12: Y-S-N-E-N-M↓D-A-M.	YSNENM.
Ox 13: T-Y-Q-R↓T-R↓A-L-V-T-G.	TYQR, TYQRTR, & ALVTG.

Table 5.4: Cleavage of the Oxford peptides by MCP: Part III.

Peptides (0.1 mg/ml) were incubated at 37ºC with 0.05 mg/ml purified MCP in 50 mM Hepes/KOH buffer, pH 7.5, for 120 min as described under Section 2.4. *Sites of peptide bond cleavage were identified by HPLC separation and amino acid analysis of peptide products as described under Section 2.8. ↓Cleavage site. Bolded and underlined sequence indicate epitope sequence or part of its sequence.

Peptide	Products*
Ox 14: K↓T-G-G-P-I-Y-K-R↓V-D-G-K↓W-M.	TGGPIYKR, KTGGPIYKR, KTGGPIYKRVDGK, TGGPIYKRVDGKWM, & TGGPIYKRVDGKWM.
Ox 15: K↓T-G-G-P-I-Y-K-R↓V-N-G-K↓W-M.	TGGPIYKRVNGK, KTGGPIYKRVNGK, TGGPIYKRVNGKWM, & KTGGPIYKR.
Ox 16: K↓T-G-G-P-I-Y↓R↓V↓D-G-K↓W-M.	RVDGK, DGKWM, KTGGPIYR, KTGGPIYRV, TGGPIYRVDGK, & KTGGPIYRVDGK.
Ox 17: K-T-G-G-P-I-Y↓R↓V↓D-G-N↓W-M.	DGNWM, KTGGPIY, KTGGPIYR, KTGGPIYRV, & KTGGPIYRVDGN.

Table 5.5: Cleavage of selected Oxford peptides by LSTR-MCP.

Peptides (0.1 mg/ml) were incubated at 37°C with 0.05 mg/ml LSTR-MCP in 50 mM Hepes/KOH buffer, pH 7.5, for 120 min as described under Section 2.4. *Sites of peptide bond cleavage were identified by HPLC separation and amino acid analysis of peptide products as described under Section 2.8. N.C. = not cleaved. ↓Cleavage site.

Peptide	Products*
Ox 2: T-Y-Q-R-T-R-A-L-V-R-T-G.	N.C.
Ox 5: R-G-Y-V-Y-Q-G-L.	N.C.
Ox 7: Y-K-R-V-N-N-G-K-W-M.	N.C.
Ox 8: A-S-N-E↓N-M-D↓A-M-E-S-S-T-L.	ASNE & ASNENMD.
Ox 10: I-Q-M-C↓T-E-I-K-L↓S-D↓Y-E-G-R.	YEGR, SDYEGR, & TELKLSDYEGR.
Ox 11: I-A-S-N-E-N↓M↓E↓T-M-E-S↓S-T-E.	IASNEN, ETMES, TMESSTE, IASNENME, & IASNENMETMES.
Ox 12: Y-S-N-E-N-M↓D-A-M.	YSNENM.

Table 5.6: Cleavage of the Oxford peptides by LLE1.MCP.

Peptides (0.1 mg/ml) were incubated at 37°C with 0.05 mg/ml LLE1.MCP in 50 mM Hepes/KOH buffer, pH 7.5, for 120 min as described under Section 2.4. *Sites of peptide bond cleavage were identified by HPLC separation and amino acid analysis of peptide products as described under Section 2.8. N.C. = not cleaved. ↓Cleavage site.

Peptide	Products*
Ox 2: T-Y-Q-R-T-R-A-L-V-R-T-G.	N.C.
Ox 5: R-G-Y-V-Y-Q-G-L.	N.C.
Ox 7: Y-K-R-V-N-G-K-W-M.	N.C.
Ox 8: A-S-N-E↓N-M-D↓A-M-E-S-S-T-L.	ASNE, AMESSTL, & ASNENMD.
Ox 10: I-Q-M-C↓T-E-L-K-I↓S-D↓Y-E-G-R.	YEGR, SDYEGR, & TELKLSDYEGR.
Ox 11: I-A-S-N-E-N-M↓E↓T-M-E-S↓S-T-E.	ETMES, TMESSTE, IASNENME, & IASNENMETMES.
Ox 12: Y-S-N-E-N-M↓D-A-M.	YSNENM.

Table 5.7: Summary of cleavage sites generated by MCP, LSTR-MCP, and LLE1MCP: Part II.

Sites of peptide bond cleavage were identified by HPLC separation and amino acid analysis of peptide products as described under Section 2.4. Data obtained from Tables 5.2, 5.3,5.5, and 5.6. N.C. = not cleaved.

Peptide	MCP	Observed cleavage sites LSTR-MCP	LLE1MCP
Ox 2: T-Y-Q-R-T-R-A-L-V-R-T-G	Thr1-Tyr2 Thr5-Arg6 Arg6-Ala7	N.C. N.C. N.C.	N.C. N.C. N.C.
Ox 5: R-G-Y-V-Y-Q-G-L	Tyr3-Val4 Tyr5-Gln6	N.C. N.C.	N.C. N.C.
Ox 7: Y-K-R-V-N-N-G-K-W-M	Lys6-Trp7	N.C.	N.C.
Ox 8: A-S-N-E-N-M-D-A-M-E-S-S-T-L	Glu4-Asn5 Asp7-Ala8	Glu4-Asn5 Asp7-Ala8	Glu4-Asn5 Asp7-Ala8

Table 5.8: Summary of cleavage sites generated by MCP, LSTR-MCP, and LLE1.MCP: Part II.

Sites of peptide bond cleavage were identified by HPLC separation and amino acid analysis of peptide products as described under Section 2.4. Data obtained from Tables 5.2, 5.3,5.5, and 5.6. N.C. = not cleaved. *Novel cleavage site.

Peptide	Observed cleavage sites		
	MCP	LSTR-MCP	LLE1MCP
Ox 10: I-Q-M-C-T-E-L-K-L-S-D-Y-E-G-R	Cys4-Thr5	Cys4-Thr5	Cys4-Thr5
	Leu9-Ser10	Leu9-Ser10	Leu9-Ser10
	Asp11-Tyr12	Asp11-Tyr12	Asp11-Tyr12
Ox 11: I-A-S-N-E-N-M-E-T-M-E-S-S-T-E	Met7-Glu8	Met7-Glu8	Met7-Glu8
	Glu8-Thr9	Glu8-Thr9	Glu8-Thr9
	Met10-Glu11	Met10-Glu11	Met10-Glu11
	Ser12-Ser13	Ser12-Ser13	Ser12-Ser13
	N.C.	Asn4-Glu5*	N.C.
Ox 12: Y-S-N-E-N-M-D-A-M	Met6-ASP7	Met6-ASP7	Met6-ASP7

Table 5.9: Intramolecularly quenched fluorogenic compounds which were not substrates (Carlsber peptides) for MCP.

Hydrolysis rates were measured in 50 mM Hepes/KOH buffer, pH 7.5, containing appropriate substrate at a concentration of 0.25 μM with 0.01 mg/ml purified MCP as described under Section 2.4. ABz = o-aminobenzoyl. *Substrate nomenclature from Breddam and Meldal (1992).

Substrate	Sequence
AH12*	ABz-Ala-Ala-Glu-Ala-Phe-TyrNO₂-Asp-OH
AE12	ABz-Ala-Ala-Glu-Ala-Ser-TyrNO₂-Asp-OH
FH12	ABz-Ala-Ala-Glu-Ala-Pro-TyrNO₂-Asp-OH
AB11	ABz-Ala-Ala-Glu-Ala-Ala-TyrNO₂-Asp-OH
AA11	ABz-Ala-Ala-Glu-Ala-Val-TyrNO₂-Asp-OH
AA10	ABz-Ala-Ala-Glu-Val-TyrNO₂-Asp-OH
DD8	ABz-Ala-Phe-Ala-Ser-Glu-Val-Phe-TyrNO₂-Asp-OH
EG4	ABz-Ala-Ser-Ala-Glu-Val-Phe-TyrNO₂-Asp-OH
ED4	ABz-Ala-Asp-Ala-Ala-Glu-Val-Phe-TyrNO₂-Asp-OH
DE8	ABz-Ala-Phe-Ala-Val-Glu-Val-Phe-TyrNO₂-Asp-OH
DC8	ABz-Ala-Phe-Asp-Ala-Glu-Val-Phe-TyrNO₂-Asp-OH
FE2	ABz-Ala-Pro-Ala-Ala-Glu-Val-Phe-TyrNO₂-Asp-OH

Table 5.10: Intramolecularly quenched fluorogenic substrates (Carlsberg peptides) for MCP.

Hydrolysis rates were measured in 50 mM Hepes/KOH buffer, pH 7.5, containing appropriate substrate at a concentration of 0.25 µM with 0.01 mg/ml purified MCP as described under Section 2.4. *Data is the average calculated from two separate experiments performed in duplicate. ABz = o-aminobenzoyl. *Substrate nomenclature from Breddam and Meldal (1992).

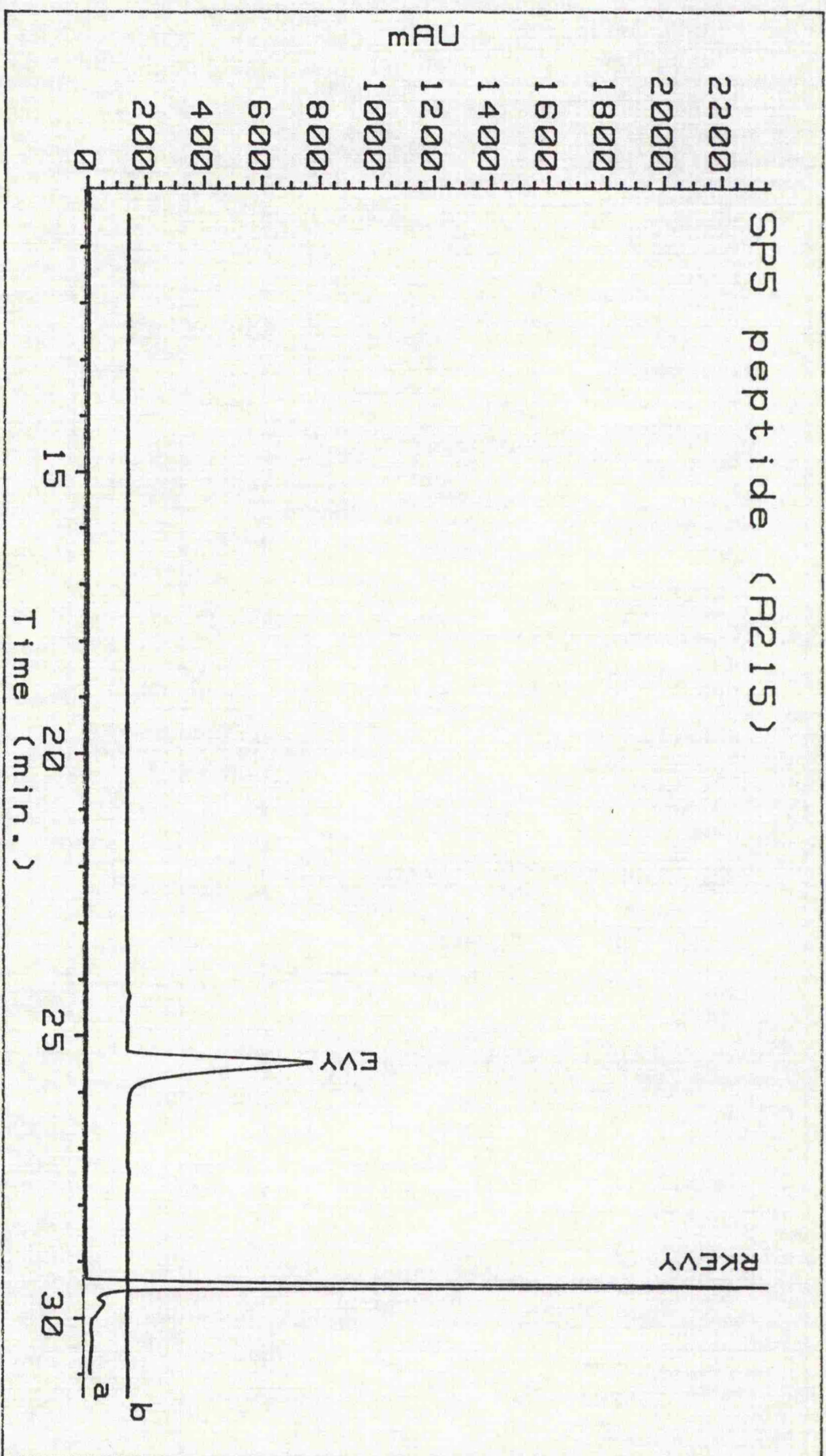| Substrate	Sequence	Rate of Hydrolysis* (nmoles/min/mg)
DB8*	ABz-Ala-Phe-Ala-Phe-Ala-Glu-Val-TyrNO$_2$-Asp-OH	4.0 ± 0.1
AD11	ABz-Ala-Ala-Glu-Ser-TyrNO$_2$-Asp-OH	2.0 ± 0.1
EB3	ABz-Ala-Phe-Ser-Ala-Glu-Val-TyrNO$_2$-Asp-OH	2.0 ± 0.0
FG2	ABz-Ala-Ala-Glu-Pro-TyrNO$_2$-Asp-OH	2.0 ± 0.1
AF11	ABz-Ala-Ala-Glu-Arg-TyrNO$_2$-Asp-OH	2.0 ± 0.0
AG12	ABz-Ala-Ala-Glu-Ala-Arg-TyrNO$_2$-Asp-OH	1.0 ± 0.1
AE11	ABz-Ala-Ala-Glu-Ala-Arg-TyrNO$_2$-Asp-OH	1.0 ± 0.0
EC4	ABz-Ala-Ala-Glu-Asp-TyrNO$_2$-Asp-OH	1.0 ± 0.1
AH11	ABz-Ala-Ala-Glu-Phe-TyrNO$_2$-Asp-OH	1.0 ± 0.0
EC3	ABz-Ala-Phe-Arg-Ala-Glu-Val-TyrNO$_2$-Asp-OH	1.0 ± 0.0
EB4	ABz-Ala-Ala-Glu-Ala-Asp-TyrNO$_2$-Asp-OH	1.0 ± 0.0

Table 5.11: Intramolecularly quenched fluorogenic substrates (Carlsberg peptides) for MCP.

Hydrolysis rates were measured in 50 mM Hepes/KOH buffer, pH 7.5, containing appropriate substrate at a concentration of 0.25 μM with 0.01 mg/ml purified MCP as described under Section 2.4. *Data is the average calculated from two separate experiments performed in duplicate. ABz = o-aminobenzoyl. *Substrate nomenclature from Breddam and Meldal (1992).

Substrate	Sequence	Rate of Hydrolysis* (nmoles/min/mg)
DA7*	ABz-Ala-Phe-Ala-Phe-Ala-Val-Phe-TyrNO₂-Asp-OH	3.0 ± 0.0
FE1	ABz-Ala-Phe-Ala-Glu-Val-Phe-TyrNO₂-Asp-OH	3.0 ± 0.0
DG8	ABz-Ala-Phe-Ala-Phe-Glu-Val-Phe-TyrNO₂-Asp-OH	2.0 ± 0.1
DF8	ABz-Ala-Phe-Ala-Phe-Asp-Val-Phe-TyrNO₂-Asp-OH	2.0 ± 0.1
DA5	ABz-Ala-Phe-Pro-Ala-Glu-Val-Phe-TyrNO₂-Asp-OH	2.0 ± 0.0
EE4	ABz-Ala-Val-Ala-Ala-Glu-Val-Phe-TyrNO₂-Asp-OH	1.0 ± 0.1
FG1	ABz-Ala-Phe-Ala-Asp-Glu-Val-Phe-TyrNO₂-Asp-OH	1.0 ± 0.0
DH8	ABz-Ala-Phe-Ala-Phe-Val-Phe-TyrNO₂-Asp-OH	1.0 ± 0.1
FF2	ABz-Ala-Phe-Val-Ala-Glu-Val-Phe-TyrNO₂-Asp-OH	1.0 ± 0.0
FF1	ABz-Ala-Phe-Ala-Arg-Glu-Val-Phe-TyrNO₂-Asp-OH	1.0 ± 0.0
EF4	ABz-Ala-Ala-Ala-Glu-Val-Phe-TyrNO₂-Asp-OH	1.0 ± 0.0
DB5	ABz-Ala-Phe-Ala-Ala-Glu-Val-Phe-TyrNO₂-Asp-OH	0.5 ± 0.0

Figure 5.1: HPLC profile of SP5 cleavage by MCP.

SP5 (0.2 mg/ml) was incubated with 0.05 mg/ml purified MCP in 50
mM Hepes/KOH buffer, pH 7.5 at 37°C as described under Section 2.4.
The reaction was stopped by addition of TFA (25 μl of 1% TFA solution).
HPLC separation of the reaction mixture was performed as described
under Section 2.8, using a C_{18} Vydac reverse phase column. The traces
were monitored at 215 nm. **a** = control and **b** = 120 min.

SP5 peptide (A215)

mAU

2200
2000
1800
1600
1400
1200
1000
800
600
400
200
0

EVY

RKEVY

a
b

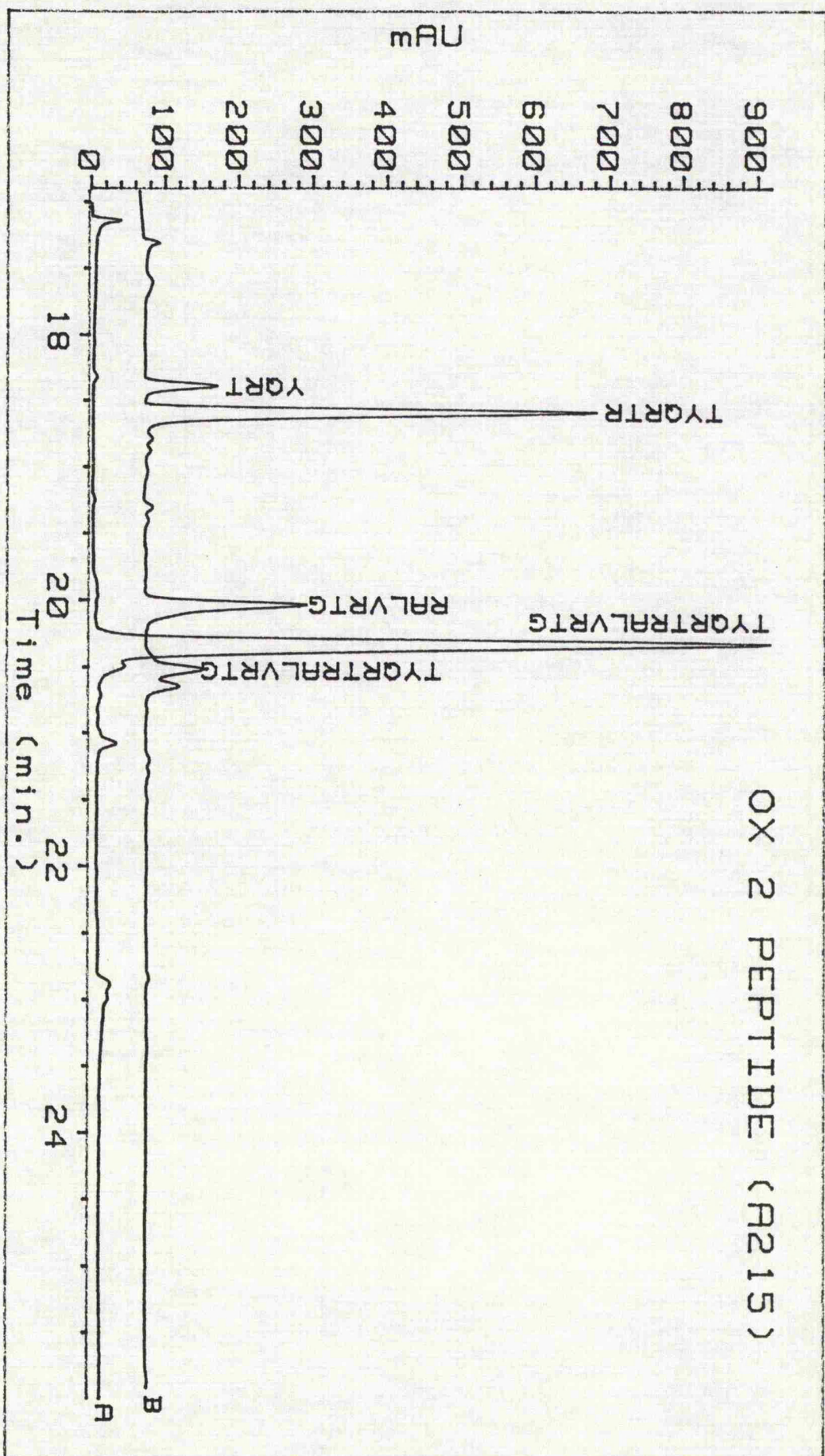15   20   25   30

Time (min.)

Figure 5.3: HPLC profile of the Ox 5 peptide cleavage by MCP.

Ox 5 peptide (0.1 mg/ml) was incubated with 0.05 mg/ml purified MCP in 50 mM Hepes/KOH buffer, pH 7.5 at 37°C as described under Section 2.4. The reaction was stopped by addition of TFA (25 µl of 1% TFA solution). HPLC separation of the reaction mixture was performed as described under Section 2.8, using a C_{18} Vydac reverse phase column. The traces were monitored at 215 nm. **a** = control and **b** = 120 min.
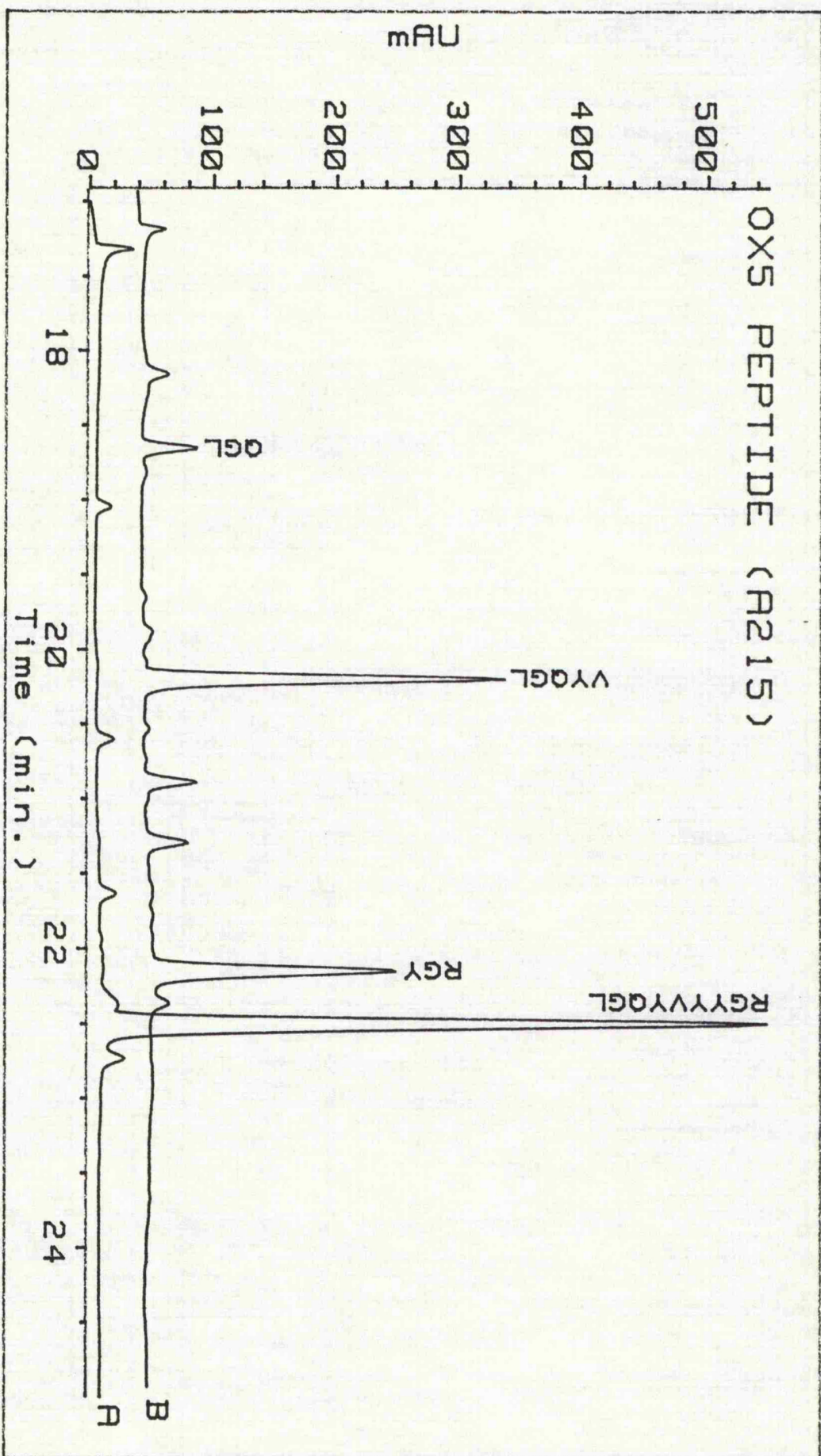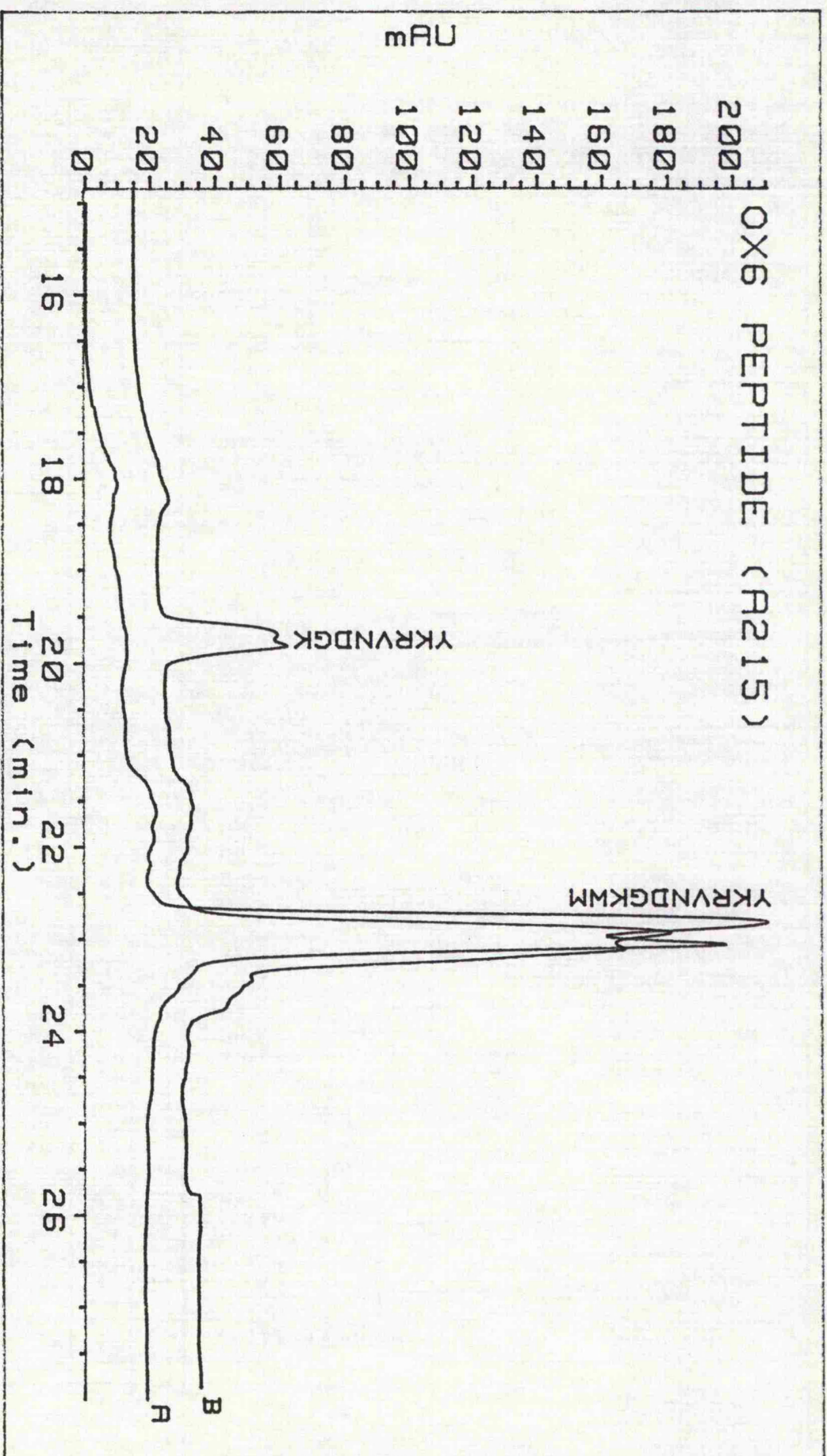
OX 2 PEPTIDE (A215)

Figure 5.3: HPLC profile of the Ox 5 peptide cleavage by MCP.

Ox 5 peptide (0.1 mg/ml) was incubated with 0.05 mg/ml purified MCP
in 50 mM Hepes/KOH buffer, pH 7.5 at 37°C as described under Section
2.4. The reaction was stopped by addition of TFA (25 µl of 1% TFA
solution). HPLC separation of the reaction mixture was performed as
described under Section 2.8, using a C_{18} Vydac reverse phase column.
The traces were monitored at 215 nm. **a** = control and **b** = 120 min.

OX5 PEPTIDE (A215)

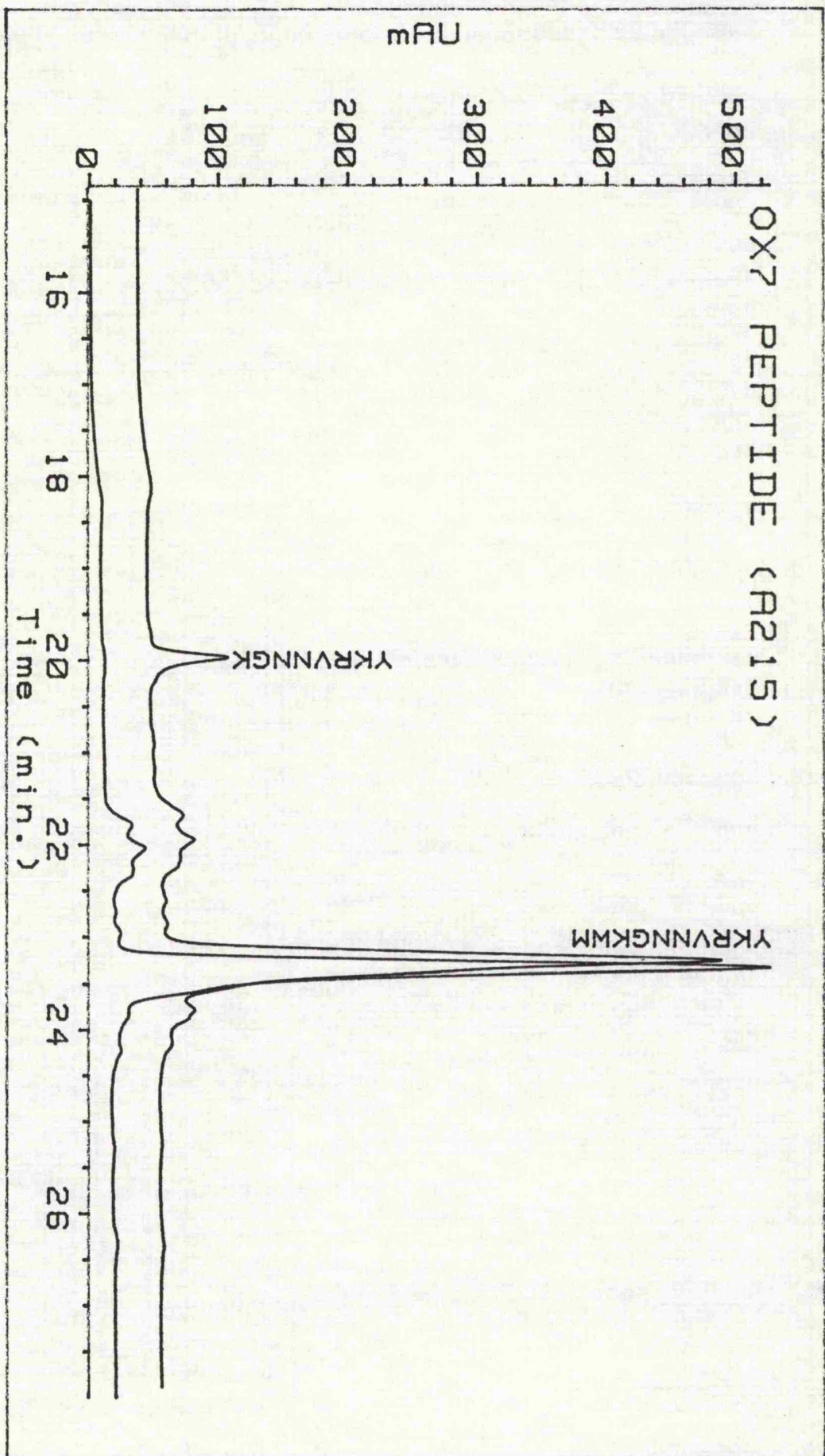Figure 5.4: HPLC profile of the Ox 6 peptide cleavage by MCP.

Ox 6 peptide (0.1 mg/ml) was incubated with 0.05 mg/ml purified MCP
in 50 mM Hepes/KOH buffer, pH 7.5 at 37°C as described under Section
2.4. The reaction was stopped by addition of TFA (25 µl of 1% TFA
solution). HPLC separation of the reaction mixture was performed as
described under Section 2.8, using a C_{18} Vydac reverse phase column.
The traces were monitored at 215 nm. **a** = control and **b** = 120 min.

OX6 PEPTIDE (A215)

Figure 5.5: HPLC profile of the Ox 7 peptide cleavage by MCP.

Ox 7 peptide (0.1 mg/ml) was incubated with 0.05 mg/ml purified MCP

in 50 mM Hepes/KOH buffer, pH 7.5 at 37°C as described under Section

2.4. The reaction was stopped by addition of TFA (25 μl of 1% TFA

solution). HPLC separation of the reaction mixture was performed as

described under Section 2.8, using a C_{18} Vydac reverse phase column.

The traces were monitored at 215 nm. a = control and b = 120 min.
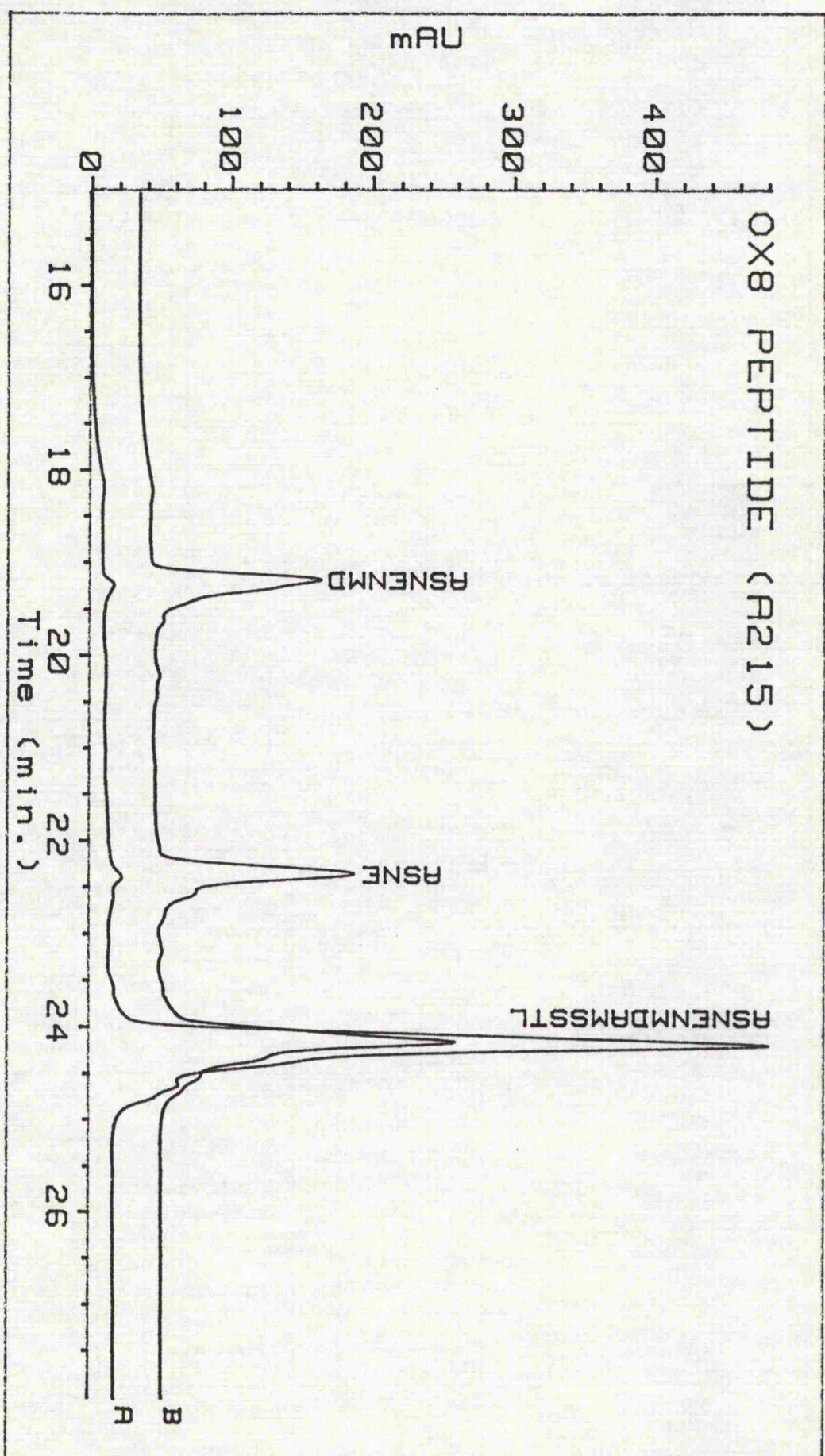
OX7 PEPTIDE (A215)

Figure 5.6: HPLC profile of the Ox 8 peptide cleavage by MCP.

Ox 8 peptide (0.1 mg/ml) was incubated with 0.05 mg/ml purified MCP

in 50 mM Hepes/KOH buffer, pH 7.5 at 37°C as described under Section

2.4. The reaction was stopped by addition of TFA (25 μl of 1% TFA

solution). HPLC separation of the reaction mixture was performed as

described under Section 2.8, using a C_{18} Vydac reverse phase column.

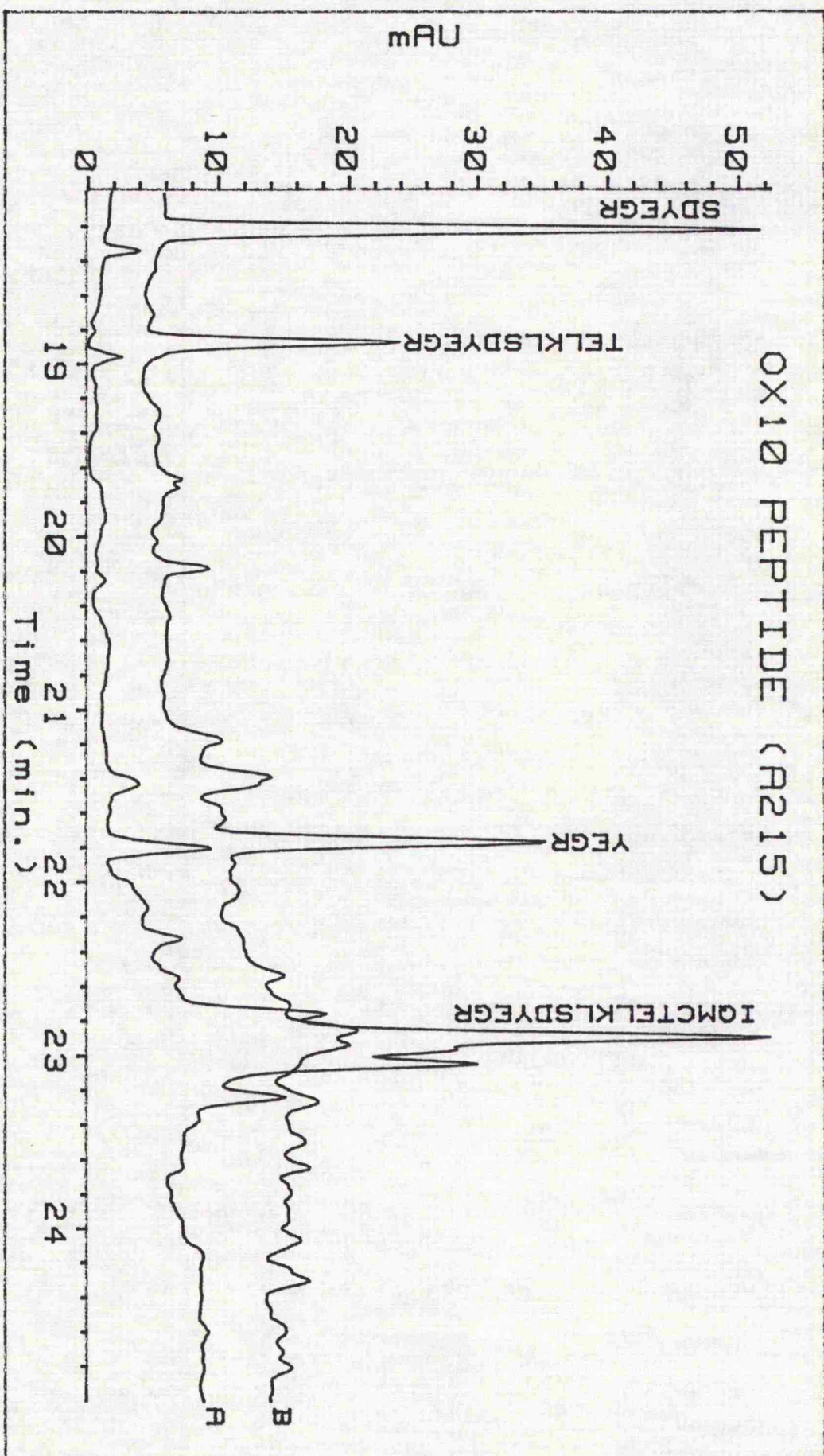The traces were monitored at 215 nm. **a** = control and **b** = 120 min.

OX8 PEPTIDE (A215)

Figure 5.7: HPLC profile of the Ox 10 peptide cleavage by MCP.

Ox 10 peptide (0.1 mg/ml) was incubated with 0.05 mg/ml purified MCP in 50 mM Hepes/KOH buffer, pH 7.5 at 37°C as described under Section 2.4. The reaction was stopped by addition of TFA (25 µl of 1% TFA solution). HPLC separation of the reaction mixture was performed as described under Section 2.8, using a C_{18} Vydac reverse phase column. The traces were monitored at 215 nm. **a** = control and **b** = 120 min.

OX10 PEPTIDE (A215)

Figure 5.8: HPLC profile of the Ox 11 peptide cleavage by MCP.

Ox 11 peptide (0.1 mg/ml) was incubated with 0.05 mg/ml purified MCP in 50 mM Hepes/KOH buffer, pH 7.5 at 37°C as described under Section 2.4. The reaction was stopped by addition of TFA (25 µl of 1% TFA solution). HPLC separation of the reaction mixture was performed as described under Section 2.8, using a C_{18} Vydac reverse phase column. The traces were monitored at 215 nm. **a** = control and **b** = 120 min.
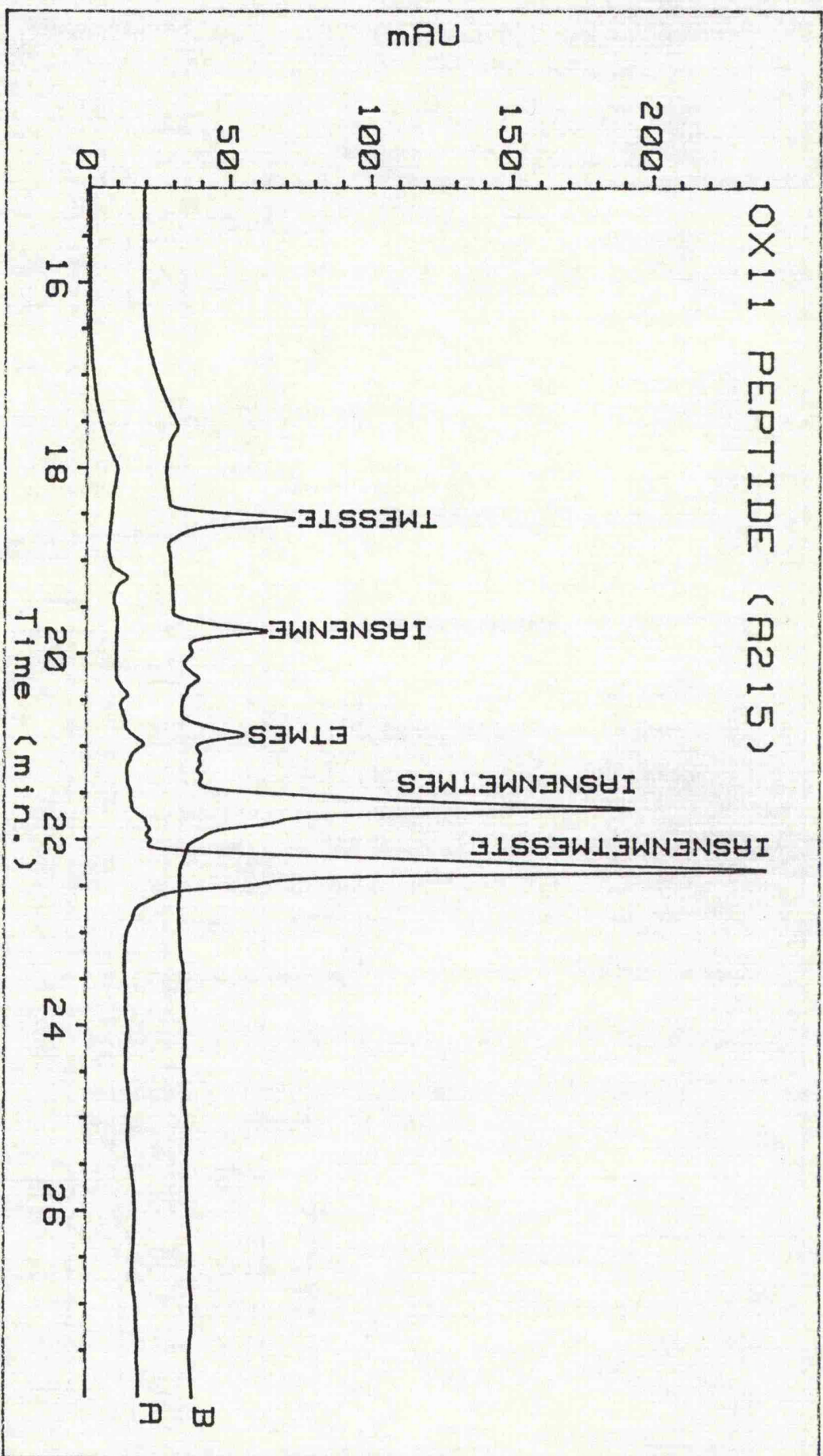
OX11 PEPTIDE (A215)

Figure 5.9: HPLC profile of the Ox 12 peptide cleavage by
         MCP.

Ox 12 peptide (0.1 mg/ml) was incubated with 0.05 mg/ml purified
MCP in 50 mM Hepes/KOH buffer, pH 7.5 at 37°C as described under
Section 2.4. The reaction was stopped by addition of TFA (25 µl of 1%
TFA solution). HPLC separation of the reaction mixture was performed
as described under Section 2.8, using a C_{18} Vydac reverse phase column.
The traces were monitored at 215 nm. **a** = control and **b** = 120 min.
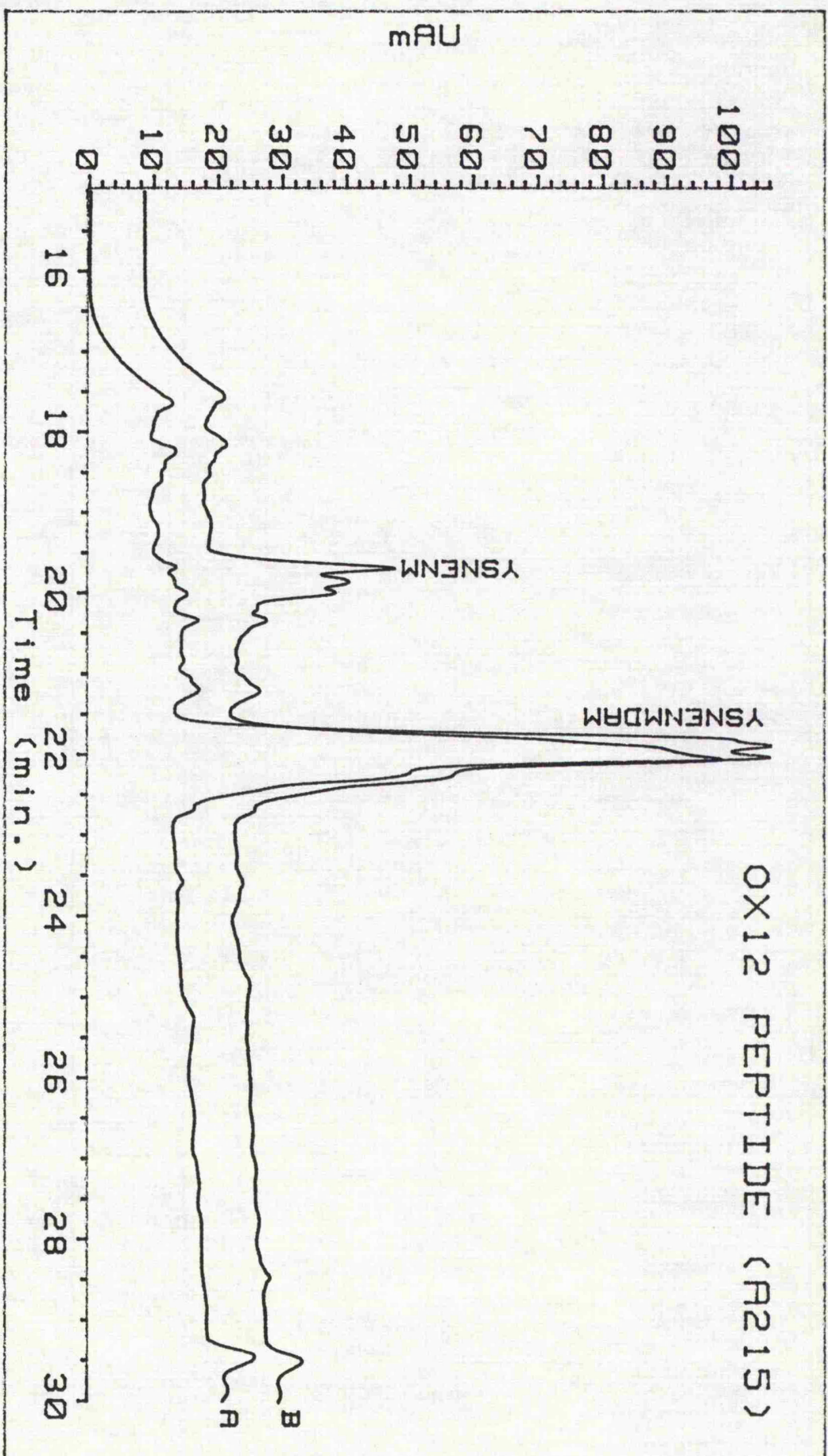
OX12 PEPTIDE (A215)

Figure 5.10: HPLC profile of the Ox 13 peptide cleavage by
MCP.

Ox 13 peptide (0.1 mg/ml) was incubated with 0.05 mg/ml purified

MCP in 50 mM Hepes/KOH buffer, pH 7.5 at 37°C as described under

Section 2.4. The reaction was stopped by addition of TFA (25 μl of 1%

TFA solution). HPLC separation of the reaction mixture was performed

as described under Section 2.8, using a C_{18} Vydac reverse phase column.

The traces were monitored at 215 nm. **a** = control and **b** = 120 min.
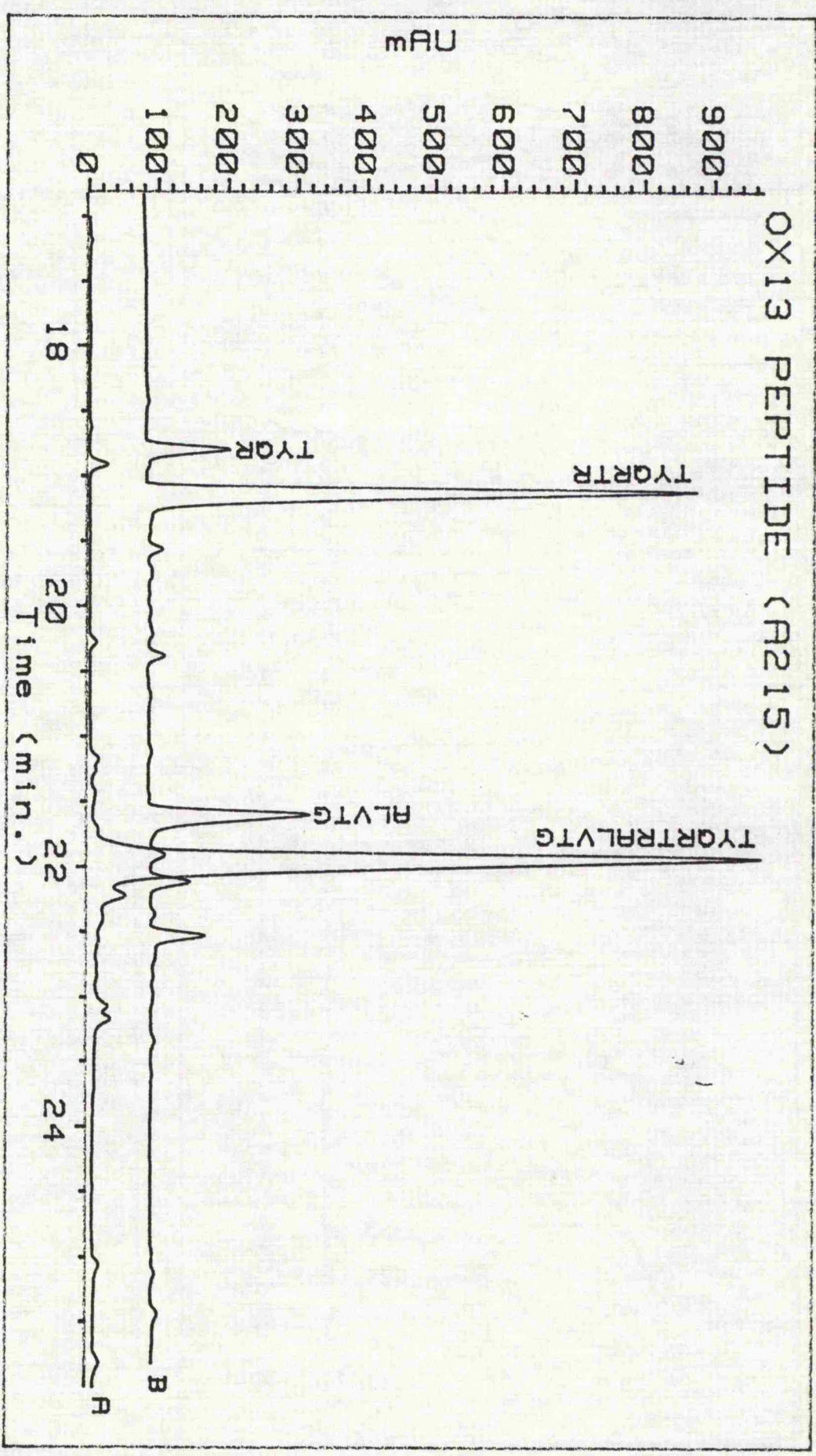
OX13 PEPTIDE (A215)

Figure 5.11: HPLC profile of the Ox 14 peptide cleavage by MCP.

Ox 14 peptide (0.1 mg/ml) was incubated with 0.05 mg/ml purified MCP in 50 mM Hepes/KOH buffer, pH 7.5 at 37°C as described under Section 2.4. The reaction was stopped by addition of TFA (25 µl of 1% TFA solution). HPLC separation of the reaction mixture was performed as described under Section 2.8, using a C_{18} Vydac reverse phase column. The traces were monitored at 215 nm. **a** = control and **b** = 120 min.
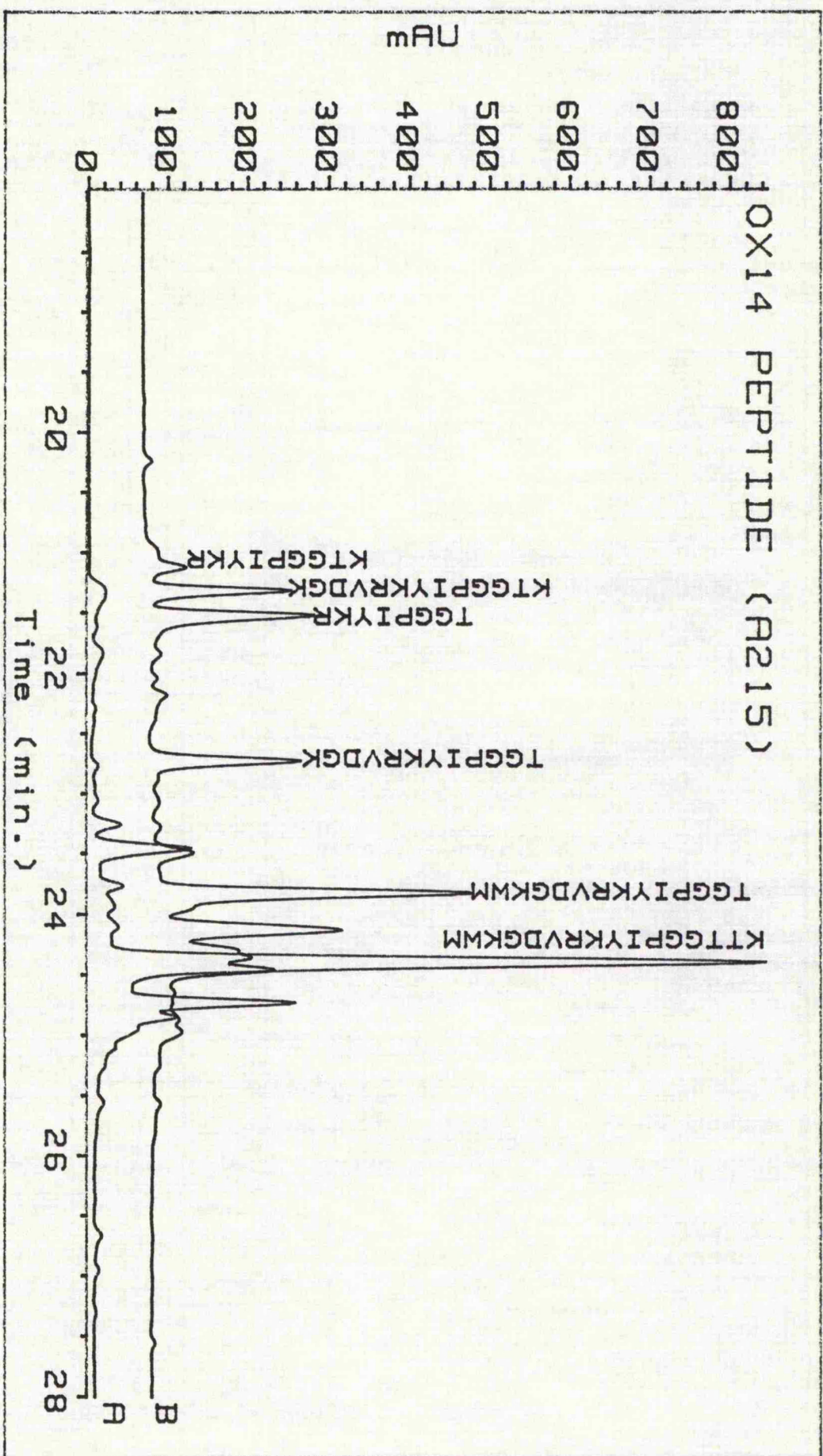
OX14 PEPTIDE (A215)

Figure 5.12: HPLC profile of the Ox 15 peptide cleavage by MCP.

Ox 15 peptide (0.1 mg/ml) was incubated with 0.05 mg/ml purified MCP in 50 mM Hepes/KOH buffer, pH 7.5 at 37°C as described under Section 2.4. The reaction was stopped by addition of TFA (25 µl of 1% TFA solution). HPLC separation of the reaction mixture was performed as described under Section 2.8, using a C_{18} Vydac reverse phase column. The traces were monitored at 215 nm. **a** = control and **b** = 120 min.
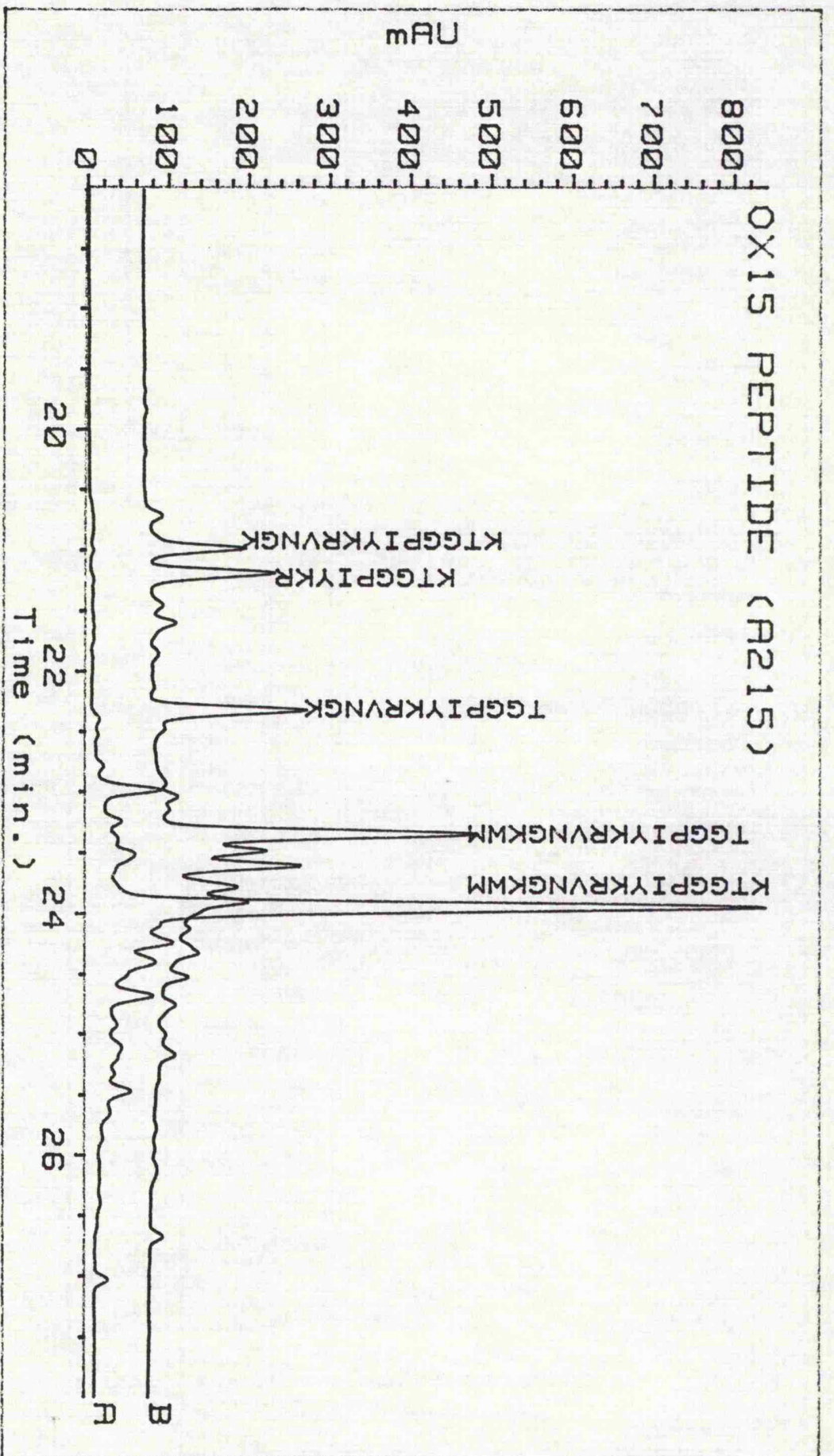
OX15 PEPTIDE (A215)

Figure 5.13: HPLC profile of the Ox 16 peptide cleavage by MCP.

Ox 16 peptide (0.1 mg/ml) was incubated with 0.05 mg/ml purified MCP in 50 mM Hepes/KOH buffer, pH 7.5 at 37°C as described under Section 2.4. The reaction was stopped by addition of TFA (25 µl of 1% TFA solution). HPLC separation of the reaction mixture was performed as described under Section 2.8, using a C_{18} Vydac reverse phase column. The traces were monitored at 215 nm. **a** = control and **b** = 120 min.
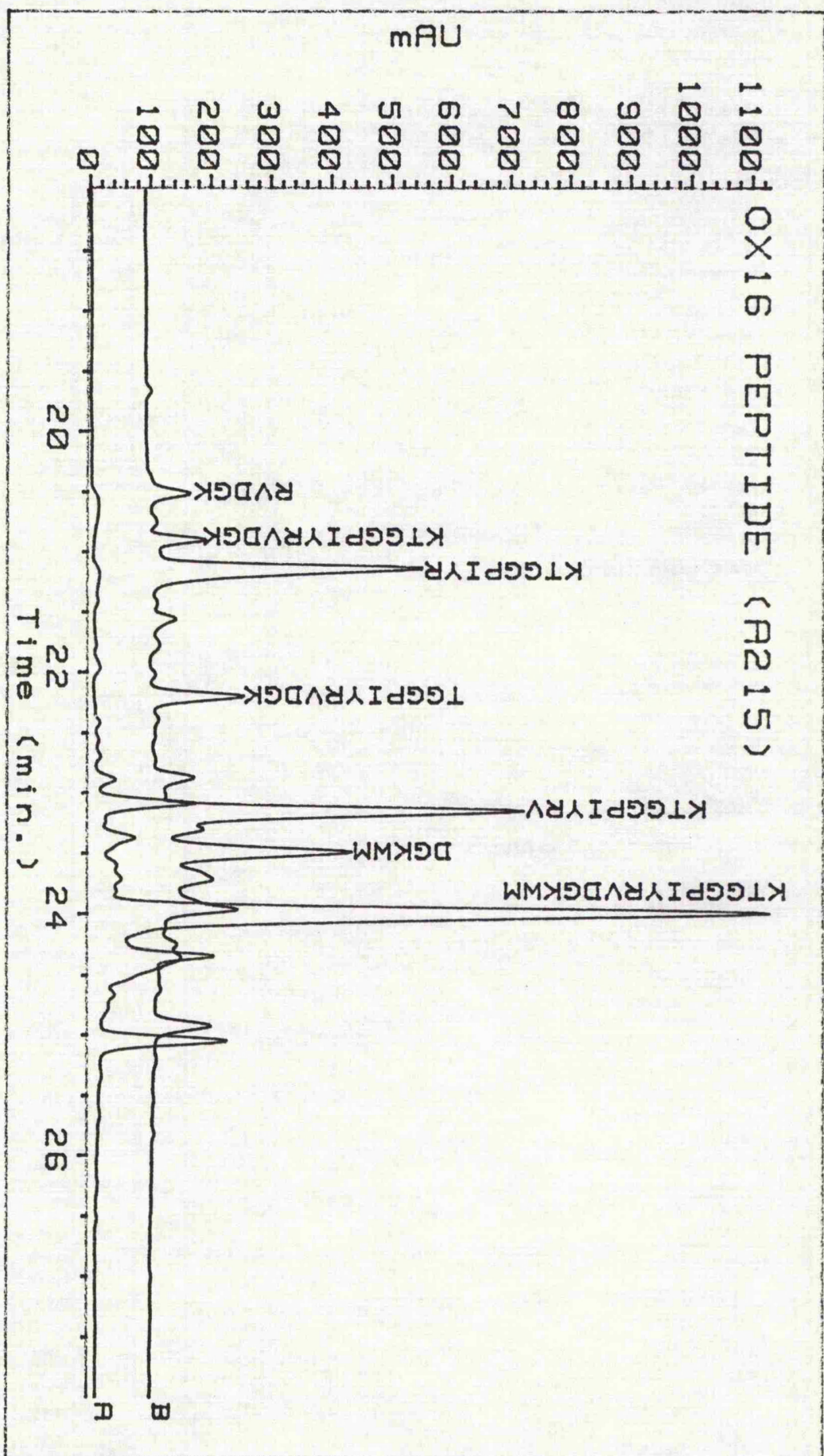
OX16 PEPTIDE (A215)

Figure 5.14: HPLC profile of the Ox 17 peptide cleavage by MCP.

Ox 17 peptide (0.1 mg/ml) was incubated with 0.05 mg/ml purified MCP in 50 mM Hepes/KOH buffer, pH 7.5 at 37°C as described under Section 2.4. The reaction was stopped by addition of TFA (25 µl of 1% TFA solution). HPLC separation of the reaction mixture was performed as described under Section 2.8, using a C_{18} Vydac reverse phase column. The traces were monitored at 215 nm. a = control and b = 120 min.
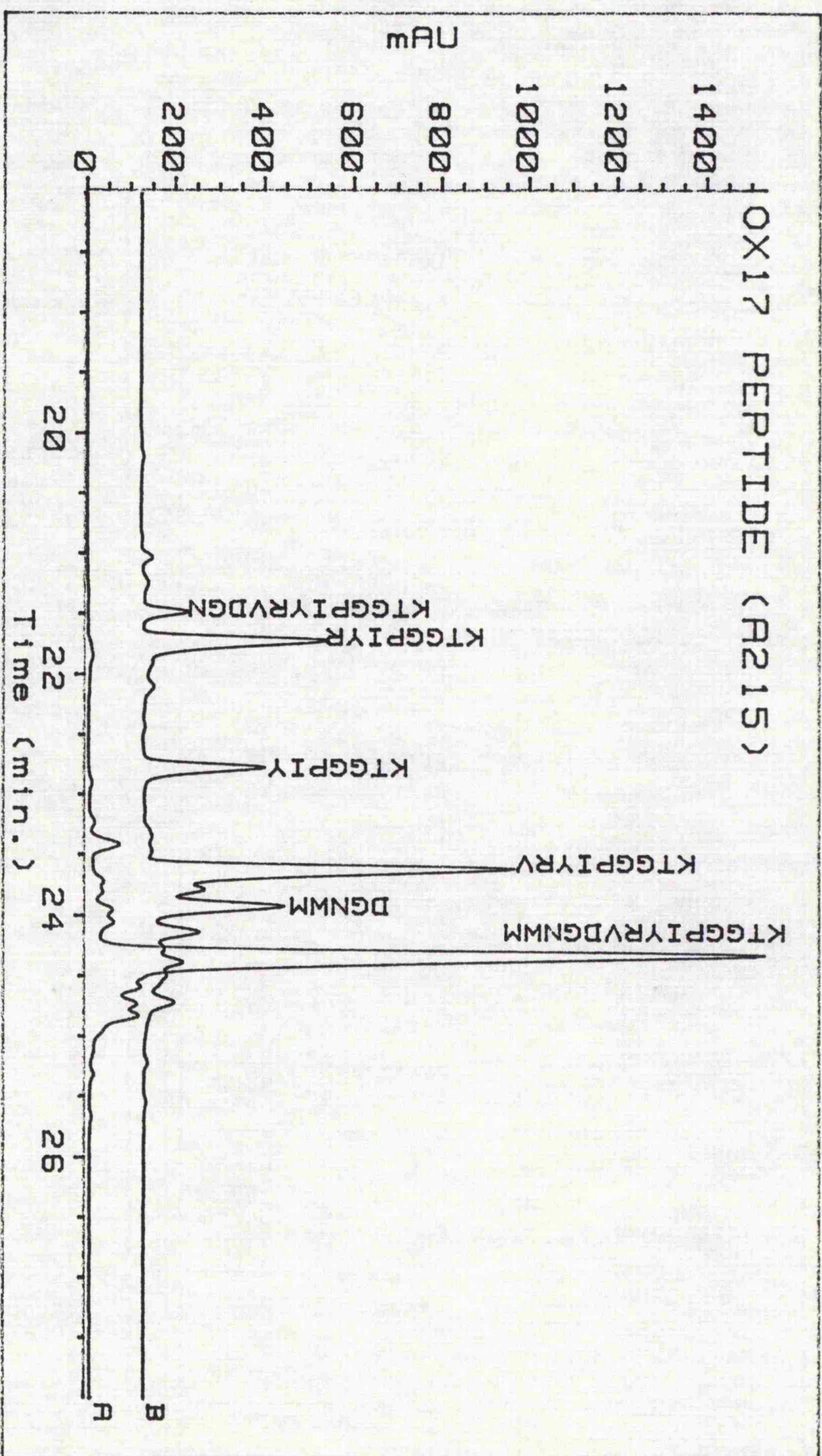
OX17 PEPTIDE (A215)

CHAPTER 6

Structural studies of the multicatalytic proteinase complex.

"One often encounters evidence of conformational changes in the study of macromolecules. These structural changes are frequently documented by spectroscopic techniques. Although, methods such as fluorescence, UV absorbance, and circular dichroism are highly sensitive spectroscopic techniques, the information yielded may reflect only localized structural perturbations. While these local conformational changes are certainly important, they do not necessarily reflect the overall changes that may be occuring in the macromolecule. In order to define accurately the conformational change in question, and to differentiate between local and global structural change, the overall picture of the macromolecule must be examined."

Oberfelder et al. (1985)

6.1 Introduction.

In view of the complex subunit composition of the rat liver multicatalytic proteinase complex (Rivett and Sweeney, 1991), electron microscopy reveals a very ordered oligomeric structure for the enzyme (Rivett et al., 1991). The ordered structure and the size of the proteinase complex make it a suitable candidate for studying its structural behaviour by hydrodynamic and electron microscopy methods.

Conventional sedimentation studies yield information about the size and shape of proteins according to the following equation:

$$s_{20,w} = M(1-\upsilon\rho)/f. \tag{6.1}$$

Where the sedimentation coefficient ($s_{20,w}$) depends on: (a) the molecular properties of the sedimenting particles, such as: molecular mass (M), partial specific volume (υ), and frictional coefficient (f). And (b) on the properties of the solution, such as: density (ρ) and viscosity (η) (f depends on the viscosity of the solvent). Thus, perturbation in the properties of particles or of the solvent would lead to changes in the sedimentation coefficient.

According to the theory of dynamic laser light scattering of macromolecules in solution (Berne and Pecora, 1976), the translational diffusion coefficient (D_T), can be determined very accurately from the exponentially decaying autocorrelation function. D_T is, thus, a measure for the shape of the particles as they move

under "Brownian" motion, and can be used to assess how disperse and heterogenous the particles in solution are.

According to the Stokes-Einstein equation, the hydrodynamic radius (r_H) of a protein can be calculated, once D_T is known, as follows:

$$r_H = kT/6\pi\eta D_T. \tag{6.2}$$

Where k = Boltzmann's constant, T = absolute temperature, and η = viscosity of the solvent.

For ideal solutions the translational diffusion coefficient (D_T) is inversely proportional to the frictional coefficient (f) according to the following equation:

$$D_T = RT/f. \tag{6.3}$$

Where R = gas constant and T = absolute temperature.

Thus, the molecular mass of a protein can be expressed in terms of its sedimentation ($s_{20,w}$) and diffusion (D_T) coefficients according to the Svedberg equation:

$$M = RTs_{20,w}/D_T(1-\upsilon\rho). \tag{6.4}$$

This Chapter describes the use of sedimentation velocity and dynamic light scattering as an approach for looking at the hydrodynamic properties of the proteinase complex upon action of

different effectors. Negative staining electron microscopy has also been employed to detect any gross changes in the macromolecule shape upon action of manganese ions.

Information obtained from the different methods would help to interpret the kinetic observations in Chapter 3, where conformational changes were the prime candidates for the observed activation by manganese ions, positive cooperativity with respect to LLE-NA concentration, inhibition of the LLE2 activity by 50 mM KCl, and SDS activation of the LLE activities.

6.2 Negative staining electron microscopy analysis.

The purpose of this study was to investigate whether gross conformational changes in the proteinase complex could be revealed via production of images of sufficient magnification (eg 183,000X), and of such quality and resolution. Electron microscopy of the enzyme preparations using uranyl acetate as a negative contrast medium showed two types of image: a rectangular outline with four bands transverse to the longer axis, and approximately circular ring-shaped outline, with a hollow centre (Figure 6.1a).

The images also revealed some evidence of the complex's architecture, where six or seven is the most probable number of subunits forming the ring and four is the number of these rings stacked on top of each other as illustrated in Figure 6.2. Breaks in the ring domain were not infrequently seen but it is unclear as to whether these correspond to a real feature (Figure 6.2).

The outer diameter of the ring was measured as 12.42 $\pm$ 0.14 S.E. nm, which corresponds closely to the width of the rectangular images which was measured as 11.68 $\pm$ 0.22 S.E. nm. The length of the rectangular images was measured as 19.61 $\pm$ 0.20 S.E. nm.

At a manganese concentration of 1 mM, there appear to the eye to be more particles adhering to the grid (compare Figures 6.1a and 6.1b). Moreover, the hollow centre of most of the particles disappeared with an adoption of a raspberry-like shape as illustrated in Figure 6.3. Some particles, however, still had what looked like a hollow centre viewed end-on (Figures 6.3g,h,i).

An end-to-end aggregation of some particles was also observed (Figure 6.1b). The particles viewed side-on had less defined structure to the eye, where the four stacks could hardly be distinguished from each other as illustrated in Figures 6.3j,k,l. The changes were also reflected by the increase in the size of particles from an outer diameter of 12.42 $\pm$ 0.14 S.E. nm to 14.83 $\pm$ 0.13 S.E. nm, and from a length of 19.61 $\pm$ 0.20 S.E. nm to 20.65 $\pm$ 0.93 S.E. nm, respectively.

At a manganese concentration of 10 mM, destruction of particles was noted from the observed remaining debris (Figures 6.1c, 6.1d). Aggregated material was also observed, together with some features of an end-to-end arrangement of some particles (Figure 6.1c). Some intact particles with control-like structure were observed, in which the hollow centre was clear to the eye (Figure 6.4 d,e,f). Also some particles with the raspberry-like shape, but of smaller size to those shown in Figure 6.3 a,b,c, were observed (Figure 6.4 a,b,c). Damaged particles viewed end-on are illustrated in Figure 6.4 g,h,i.

Some particles viewed side-on are also illustrated in Figure 6.4 j,k,l. An outer diameter of 13.1 $\pm$ 0.34 S.E. nm was measured for the remaining intact particles, which is slightly higher than the measured outer diameter in the absence of metal ions (12.42 $\pm$ 0.14 S.E. nm) and less than the measured outer diameter in the presence of 1 mM $MnCl_2$ (14.83 $\pm$ 0.13 S.E. nm).

6.3 Sedimentation velocity analysis.

The effects of effectors of the LLE activities on the conformational state of the proteinase complex were investigated, by means of measuring the sedimentation coefficient ($s_{20,w}$) of the complex under various conditions (Table 6.2). The proteinase was found to sediment with an $s_{20,w}$ value of 17.7. A typical trace recorded using the Centriscan 75 is shown in Figure 6.5a. The inclusion of 1 mM $MnCl_2$, an activator of the LLE1 and LLE2 activities (Section 3.11), reduced the $s_{20,w}$ from 17.7 to 13.9.

The reduction is also visible to the eye from the recorded trace (Figure 6.5b), where the protein boundary was travelling much slower in the presence than in the absence of $MnCl_2$. $CaCl_2$ and $MgCl_2$ both at a concentration of 1 mM, both activators of the LLE activities (Section 3.11), induced similar reduction in the $s_{20,w}$ from 17.7 to 15.5 and 16.7, respectively.

In contrast to the above, the inclusion of 1.0 mM $ZnCl_2$, an inhibitor of the complex (Section 3.11), caused complete precipitation of the proteinase complex as revealed by the trace

recorded using the Centriscan 75 (Figure 6.6b), where the precipitated proteinase probably sedimented while the centrifuge was taken up to speed (ie 25,000 rpm). At a lower concentration of $ZnCl_2$ (0.3 mM), precipitation of the complex was also detected (data not shown). Moreover, $CdCl_2$, also an inhibitor of the complex (Section 3.11), gave similar results to the $ZnCl_2$ treatment.

The observed inhibition of the different proteolytic activities of the complex by either $ZnCl_2$ or $CdCl_2$ (Table 3.3 and Figure 3.21) could have been probably caused by the precipitation of the enzyme during the assay, in which the enzyme was used at a concentration of 0.01 mg/ml, rather than by dissociation of the complex as has been suggested for the duck erythroblast enzyme, where 1 mM $ZnCl_2$ was found to cause complete dissociation of the complex (Coux et al.,1992; Northwang et al., 1992).

The inclusion of 50 mM KCl, an inhibitor of the LLE2 activity (Section 3.9), reduced the $s_{20,w}$ value from 17.7 to 13.9. Although the shift is of similar magnitude and in the same direction as the one caused by 1 mM $MnCl_2$ ($s_{20,w}$ = 13.9), the consequences on the kinetics of the complex were quite different: The AAF and LSTR activities were not affected by 50 mM KCl (data not shown), whereas the LLE1 activity was slightly inhibited and the cooperative component of the LLE2 activity was inhibited (Section 3.9; Table 3.9). The results are suggestive of a process in which kinetic activity appears to be dependent on the conformational state of the enzyme.

SDS is an activator of the LLE activities (Section 3.13). The presence of a low concentration of SDS (0.01%) increased the $s_{20,w}$

value from 17.7 to 21.2. Moreover, the inclusion of 0.02% SDS also induced a shift but in the opposite direction ie a decrease in the $s_{20,w}$ value from 17.7 to 15.5, with evidence for dissociation of the complex as reflected by the appearance of slower travelling material in the protein boundary (data not shown).

The results, yet again, are suggestive of a similar process as the one described above. The presence of 0.01% SDS seems to tighten the structure of the enzyme and in the process of doing so, it induces an active conformation. On the other hand, 0.02% SDS seems to loosen the structure of the complex, and in the process of doing so it also induces an active conformation.

Although the measured $s_{20,w}$ values in the presence of either 0.01 % or 0.02 % SDS are of different magnitude and in the opposite directions, the kinetic consequences on complex were similar, because of the length of time the kinetic assays were carried at (order of 20-30 min) in comparison to the length of time the sedimentation velocity experiments were carried out at (order of 50-60 min).

Exposing the proteinase complex at 65°C for a period of 5 min reduced the $s_{20,w}$ value from 17.7 to 16.7, suggesting a loosening of the structure. The AAF, LSTR, LLE1, and LLE2 activities were completely inhibited under similar treatment (data not shown). Yet again the conformation of the complex appears to dictate the kinetic consequences of the different activities. Here the change in the $s_{20,w}$ value was in the same direction as for the one caused by $MnCl_2$ ($s_{20,w}$ =13.9), but the effects were inhibitory rather than stimulatory.

The inclusion of LLE-NA at a concentration of 0.1 mM (LLE1 activity) gave an $s_{20,w}$ value of 17.3, whereas a concentration of 0.4 mM (LLE2 activity) increased the $s_{20,w}$ value from 17.7 to 19.7, respectively. The presence of 0.4 mM LLE-NA, which accounts for a major contribution from the cooperative component and a minor one from the LLE1 activity, tightened the structure of the complex with a resulting activation of the LLE activity (Figure 3.10). On the other hand, the presence of 0.1 mM LLE-NA caused only a slight change in the $s_{20,w}$.

6.4 Effects of MnCl$_2$ activation on the structure of MCP.

The multicatalytic proteinase complex has a maximum absorbance at a wavelength of 231 nm, which is up to seven-fold higher than the absorbance at a wavelength of 280 nm (Figure 6.7), which made possible some of the sedimentation velocity work by using lower amounts of the proteinase complex.

An attempt to correlate the activation by manganese ions with the hydrodynamic behaviour of the proteinase was performed. The $s_{20,w}$ value of the proteinase complex was investigated as a function of MnCl$_2$ concentration. The $s_{20,w}$ dependence on MnCl$_2$ was found to be very complicated as illustrated in Figure 6.8. As MnCl$_2$ concentration was increased up to 1 mM, $s_{20,w}$ was found to decrease from a value of 17.9 to a value of 14 in a more or less linear fashion. Under similar increase in the concentration of the metal ion, the non-cooperative component of the peptidylglutamyl-peptide hydrolase activity (LLE1 activity) was activated by up to three-fold at 1 mM MnCl$_2$ (Figure 6.8), as was the cooperative component of the activity

134

(LLE2 activity) by up to two-fold at the same $MnCl_2$ concentration (Figure 6.9)

At a $MnCl_2$ concentration of 2.5 mM, there was an increase in the $s_{20,w}$ from 14 to 16.1. The LLE1 activity was neither stimulated nor inhibited (Figure 6.8), whereas the LLE2 activity was slightly stimulated (Figure 6.9). Above 2.5 mM $MnCl_2$, the $s_{20,w}$ increased in a linear fashion from a value of 16.1 to a value of 17.6 at 10 mM $MnCl_2$. Under these conditions, $MnCl_2$ treatment was found to be inhibitory to both activities (Figures 6.8 and 6.9).

6.5 The multicatalytic proteinase complex as a dimer?

Dialysis treatment, against 50 mM Hepes/KOH buffer, pH 7.5, of the proteinase complex for a period of two days led to an increase in the $s_{20,w}$ from 17.7 to 25.5. The calculated $s_{20,w}$ value of 25.5 is suggestive of a dimerisation process, that could have taken place during the extended dialysis period, of the proteinase complex. Calculated molecular mass for the treated enzyme, using an $s_{20,w}$ value of 25.5 and a D_T of 1.94×10^{-7} cm^2/s, was found to be twice that of the proteinase (Table 6.3).

The $s_{20,w}$ dependence on $MnCl_2$ was also investigated for this preparation. The increase in $MnCl_2$ concentration, up to a concentration of 1.0 mM, induced a decrease in the $s_{20,w}$ from 25.5 to 17.7 (Figure 6.10). The decrease in the $s_{20,w}$ value could reflect a displacement of the dimer form towards the monomer form. At a $MnCl_2$ concentration of 2.5 mM, the $s_{20,w}$ value was similar to the one at 1 mM $MnCl_2$ at 17.5. Above 2.5 mM $MnCl_2$, the effects on the

structure of the proteinase became very complex to interpret. Although there was a measurable protein boundary from which $s_{20,w}$ values could be obtained, aggregated protein as well as lighter protein boundaries that could be due to MCP subunits were also observed as illustrated in Figure 6.11.

6.6 Dynamic light scattering analysis.

A translational diffusion coefficient (D_T) of 2.78×10^{-7} cm^2/s was obtained for the proteinase complex from the logarithm of an autocorrelation function obtained at an angle of 90°, indicating a defined size of the proteinase molecule.

In the presence of 1 mM MnCl$_2$, there was about 1% change in the D_T of the proteinase complex, as reflected by the D_T value of 2.76 $\times 10^{-7}$ cm^2/s when compared to a D_T value of 2.78×10^{-7} cm^2/s in the metal's absence.

However, the presence of 10 mM MnCl$_2$ induced a 50% reduction in the D_T value (Table 6.3). When the two days dialysed proteinase preparation was investigated, a D_T of 1.94×10^{-7} cm^2/s was obtained (Table 6.3).

According to the Stokes-Einstein equation (6.2), a hydrodynamic radius (r_H) of 9.01 nm was calculated for the complex, compared to an r_H of 8.95 nm in the presence of 1 mM MnCl$_2$. An r_H of 13.4 nm was also calculated for the two days dialysed proteinase preparation (Table 6.3).

6.7 Discussion.

Electron microscopy of negatively stained MCP preparations confirmed that the rat liver enzyme has an overall hollow cylindrical structure as has been suggested for the enzyme purified from duck erythroblasts (Coux et al., 1992), higher plants (Schliephacke et al., 1991), and archaebacteria (Dahlmann et al., 1989; Hegerl et al., 1991; Puhler et al., 1992). However, optical transform of individual molecules suggests a pseudo-helical arrangement of the four stacked rings (A. J. Rowe, personal communication). The pseudo-helical arrangement could, however, explain the lack of true symmetry (six or seven-fold) of molecules viewed end-on as well as the discontinuities observed in the rings of the rat liver enzyme.

This structure for mammalian MCP resembles that of the simpler archaebacterial MCP which is reported to be a barrel-shaped molecule possessing clear seven-fold symmetry, and the arrangement of the outer rings being rotated 25° with respect to the inner ones (Dahlmann et al., 1989; Puhler et al., 1992). The structure reported by Kopp et al. (1986) for the muscle MCP reveals a six-fold symmetry with a simple stacked array of the four rings, is quite similar to the one described above.

A different structural model for the rat liver enzyme has been reported by Tanaka and coworkers (1988). The overall shape of the complex examined by small angle X-ray scattering was described as a prolate ellipsoidal structure with an ellipsoid cavity in the centre. As pointed out by Puhler et al. (1992), the difference in the proposed

137

model could be due to a mis-interpretation of the data. Table 6.4 summarizes the four different models for the proteinase complex.

The dimensions of the molecule (Table 6.3) were significantly greater than the dimension ranges of 10 to 16 nm in diameter and up to 16 nm in length reported by several groups (Kopp et al., 1986; Baumeister et al., 1988; Falkenburg et al., 1988; Tanaka et al., 1988; Dahlmann et al., 1989; Hegerl et al., 1991; Schliephacke et al., 1991; Coux et al., 1992; Puhler et al., 1992). However, particular care was taken with calibration of the electron microscopic magnification in this study. In order to cross-check with a predicted solution size, a hydrodynamic radius (r_H) of 8.7 nm for the equivalent sphere was calculated for the complex. This is in good agreement with an r_H of 8.00 nm obtained from the electron microscopic analysis (Table 6.3), bearing in mind that negative staining will normally slightly under-estimate dimensions because of stain penetration.

Electron microscopic observations indicate a transition from a compact to an extended conformation of the complex in the presence of manganese ions (1 mM), as reflected by the increase in the size of the molecules, and providing evidence for conformational changes occuring upon action of $MnCl_2$.

Although 50 mM KCl was found to be an inhibitor of the LLE2 activity (Section 3.9), its effects on the conformational state of the proteinase were similar to that of 1 mM $MnCl_2$, which is an activator of the LLE activities (Table 3.3). The differential response of the LLE

activities to MnCl$_2$, MgCl$_2$, and CaCl$_2$ (Table 3.3) was due to their respective effects on the structure of the enzyme (Table 6.2).

The observed conformational changes in the proteinase caused by 0.01% or 0.02% confirms early suggestions by Saitoh et al. (1989), working on MCP purified from eggs of the ascidian *Halocynthia roretzi*, that activation of the complex was due to a rapid conformational change in the enzyme upon action of SDS, followed by a decrease in activation because of the activated conformation being labile as assessed by fluorescence spectroscopy.

Tanaka et al. (1989), working on MCP purified from rat liver, have shown that activation by SDS was reversible only in the presence of substrate and removal of the substrate caused irreversible inactivation of the complex because the substrate helps to stabilize the activated conformation of the complex.

Mykles and Haire (1991), working on MCP purified from lobster muscle, have reported that SDS (0.03%) induced an active form of the complex, which could be reversed to the basal form by SDS precipitation. Reversing the activation, however, to basal level only restored the trypsin-like activity, which was inhibited by SDS treatment, and inhibited the activated peptidylglutamyl-peptide bond hydrolase activity.

In view of the difference in time frame required to perform kinetic experiments and to determine $s_{20,w}$ values, sedimentation velocity analysis appears to be a more adequate technique in detecting any dissociating material from the complex, which could

explain the irreversible inactivation of the enzyme after longer exposure to SDS (0.02%-0.08%), and in the case of Mykles and Haire's observations (1991) the restored trypsin-like activity could be associated with a partially dissociated molecules or even with individual subunits.

Based merely on kinetic evidence, the peptidylglutamyl-peptide hydrolase activity was described as being composed of two components: a non-cooperative component and a cooperative one (Chapters 3 and 4). Here, a structural evidence was obtained for the existence of two states of conformation in the enzyme: a normal state in the presence of 0.1 mM LLE-NA, and a tight state in the presence of 0.4 mM LLE-NA. Thus, confirming and backing the above kinetic evidence.

The $MnCl_2$ dependence of $s_{20,w}$ provided an insight into the action of the former on the structure of the proteinase. As the concentration of $MnCl_2$ increased to 1 mM, a loosening in the structure of the complex was observed. The latter structure appears to have adopted a novel structure with similar $s_{20,w}$ value as control, as $MnCl_2$ concentration increased to 10 mM. Kinetic changes (Figure 3.17) correlated well with conformational changes (Figures 6.9 and 6.10). A concentration of 1 mM $MnCl_2$ was optimal for activation of the peptidylglutamyl-peptide hydrolase activity, and also gave the maximum change in conformation.

The dimeric form of the complex was confirmed by the calculated molecular mass (Table 6.3). The dependence of the $s_{20,w}$ on $MnCl_2$ was found to promote dissociation of the dimer form, which

could have been caused by the loosening of the structure. In view of the estimated r_Hs for both the monomer and dimer forms, a side by side dimerisation process is more likely to occur than an end-to-end one, because the former would give an r_H value of 15.38 nm for the equivalent sphere which is in good agreement with the estimated value of 12.98 nm (Table 6.3). Electron microscopy would be the method to be used next, in order to cross-check the proposed scheme.

A proteinase complex with an $s_{20,w}$ value of 26 has been reported (Orlowski, 1990). Ikai et al. (1991) and Peters et al. (1991), however, have reported a dumbell structure (presumably MCP) with two terminal domains (presumably the other components) as the closest form to the intact 26S complex viewed under the electron microscope, which probably differs from the expected dimer form of MCP.

Dynamic light scattering analysis provided a measure for the translational diffusion coefficient for the proteinase complex, and confirmed that the observed electron microscopic and hydrodynamic changes in the complex, upon action of 1 mM $MnCl_2$, are of the conformational type within the molecule (Table 6.3). Tanaka et al. (1986) have reported a $D_{20,w}$ value of 2.50×10^{-7} cm^2/s and an $s_{20,w}$ value of 19.8 for the rat liver enzyme, thus giving a calculated molecular mass of 722 kDa and an r_H value of 8.5 nm (see Table 6.5). Although, the r_H value is similar to the one described in Table 6.5, their other measures are different to the ones obtained in my study, and two possible explanation to that would be either the adopted methodology for purifying the enzyme or data interpretation.

Kopp et al. (1986) have reported a $D_{20,w}$ value of 3.90×10^{-7} cm^2/s and an r_H value of 5.05 nm for the rat skeletal muscle enzyme (Table 6.5). Their results are suggestive of much smaller MCP molecules than the one described above. They have estimated a molecular mass of 650 kDa from gel filtration (Table 6.5). Although their molecular mass estimate is of similar magnitude to the measure in Table 6.5, their $D_{20,w}$ and r_H values are quiet different to the one obtained in my study, suggesting either a possible difference between the enzyme from rat liver and the one from the rat skeletal muscle, or again the differences in purification of the enzyme complex. It should be also added that data interpretation could well be an important factor in the obtained result discrepancies.

The above conformational changes could be categorized into productive and non-productive change, depending on the resulting kinetic effect, which involve subunit-subunit interactions as a possible way of regulating the different proteolytic activities of the complex as has been suggested by Tanaka et al. (1989) and by Mykles and Haire (1991).

The studies undertaken have provided evidence for conformational changes in the proteinase complex upon the action of different effectors, in particular manganese chloride. The effects of $MnCl_2$ assessed by three independent methods of analysis confirmed the early suggestions of conformational changes made from kinetic observations. Crystallization attempts, for the rat liver enzyme, have, as yet, been unsuccessful in generating crystals big enough for use in diffraction studies (A. J. Rivett, personal communication).

Investigation of the complex's structure at higher atomic resolution is not yet possible.

CHAPTER 7

Discussion

"We have now reached a situation in which on the one hand we have many articles giving the impression that the problem is all but solved, and on the other hand assessments like the opinion of W. H. Thorpe in 1974 that 'I think it is fair to say that all the facile speculations and discussion published during the last 10-15 years explaining the mode of the origin of life have been shown to be far too simple-minded and to bear very little weight. The problem in fact seems as far from solution as it ever was.'"

7.1 Proteolytic activities of the proteinase complex.

Since its first description as a multicatalytic proteinase (Wilk and Orlowski, 1980; 1983) and up to the past four years, only three different proteolytic activities have been described for MCP in the literature.

However, from the present work (Chapters 3, 4, and 5), there appears to be at least seven different proteolytic activities associated with the complex: (a) One component catalysing the trypsin-like activity (LSTR), (b) Two components hydrolysing the peptidylglutamyl-peptide hydrolase activity, with one being noncooperative (LLE1) whereas the other component being a cooperative one (LLE2), (c) Three components catalysing the chymotrypsin-like activity (AAF, LLVY, and the Leu_9-Ser_{10} cleavage in the Ox 10 peptide), and finally (d) At least one component appearing to catalyse a variety of cleavages with the following residues in the P1 position: cysteine, leucine, methionine, and serine, and cleavages after such residues were found to be resistant to inhibition by DCI or pefabloc, so did the Leu_9-Ser_{10} cleavage in the Ox 10 peptide (Section 5.4).

Studies carried out by other groups have also made similar observations regarding the increasing number of proteolytic activities. Arribas and Castano (1991), working on the rat liver MCP, have reported two components for the peptidylglutamyl-peptide hydrolase activity with one being cooperative at lower LLE-NA concentrations, and the other one being noncooperative at higher concentrations, thus making at least four different proteolytic activities.

Similarly, Orlowski et al. (1991), working on the pituitary MCP, have reported that the peptidylglutamyl-peptide hydrolase activity is composed of two components, although their conclusions were drawn from the fact that the observed sigmoidal curve allowed a calculation of a Hill coefficient of 2. Their observations bring the number of the different proteolytic activities to at least four.

More recently, studies from the same lab. have shown a novel proteolytic activity that was found to be resistant to inhibition by DCI, and which appears to be of the chymotrypsin-like type (Cardozo et al., 1992), thus making the number of different proteolytic sites for the pituitary enzyme as at least five.

Pereira et al. (1991) have reported a fourth proteolytic site(s) activated by treating the pituitary MCP with DCI, and shown to be involved in casein degradation. Similarly, Mykles and Haire (1989) have also described a fourth proteolytic activity that degrades myofibrillar proteins in the case of the Lobster muscle MCP, and have shown its stimulation by heat. The concept of a separate protein degradation site, which is often referred to as caseinolytic activity (Orlowski, 1990), is highly unlikely to occur because:

(1) In the two described studies (Mykles and Haire, 1989; Pereira et al., 1991), there was some kind of treatment of the enzyme before observing full caseinolytic activities, which could have induced conformational changes in the complex thus exposing, on the way, novel active sites, as some effectors, including heat treatment, were found to induce conformational changes in the complex (Chapter 5),

and the DCI treatment was found, in my studies, to activate the LSTR and LLE1 activities, which could well account for the observed stimulation in the case of the pituitary enzyme.

And (2) The study on the degradation of oxidized insulin B chain has revealed an unexpectedly new concept for protein degradation by MCP, where sequential peptide hydrolysis and channelling of peptide intermediates are thought to occur, thus more than one proteolytic site would be involved, therefore eliminating the possibility of a single proteolytic site involvement (Dick et al., 1991).

7.2 MCP as an atypical serine protease.

The inhibition of the AAF, LLVY, and LLE2 activities by DCI, of the LSTR activity by pefabloc, and partial inactivation of the LLE1 activity by DFP (Djaballah et al., 1992), and the reported inhibition of the chymotrypsin-like, trypsin-like, and peptidylglutamyl-peptide hydrolase activities by mechansim based serine protease inhibitors ie the isocoumarin derivatives (Orlowski and Michaud, 1989; Cardozo et al., 1992) have led to the accepted view now of classifying MCP as an atypical serine protease.

The earlier classification of MCP as a cysteine protease was because of the sensitivity of the trypsin-like activity, in particular, to thiol reagents (Rivett, 1985). Cases where serine proteases are found to be sensitive to thiol reagents are not unusual. Betzel et al. (1988) reported that although proteinase K is a serine protease belonging to the subtilisin superfamily, it was found to be very sensitive to thiol reagents. And recently, Dick et al. (1992), working on MCP purified

from bovine erythrocytes, bovine heart, and human erythrocytes, have identified the cysteinyl residue that is essential in the trypsin-like activity, which was localized in a subunit with an average molecular mass of 27.2 kDa (Dick et al., 1992).

An unusual feature about MCP is its unreactivity towards most of the inhibitors tested, especially the mechanism based ones (Chapter 4; Orlowski and Michaud, 1989; Djaballah et al., 1992; Cardozo et al., 1992), which in turn suggests novel geometries at the catalytic sites, which could in turn reflect a novel arrangement of the catalytic residues at these sites.

In view of the wide specificity of MCP in degrading peptide and protein substrates (Orlowski, 1990; Rivett, 1993), such novel geometries could well have evolved in this manner to probably be involved in an interactive process between the different catalytic sites for the expression of a conceived unique catalytic properties of the multicatalytic complex, as has been described in the case of the evolution of multicomplex enzymes by Gaertner (1978) and Welch (1977).

Such an expression was reported by Dick et al. (1991), who, while studying the degradation of oxidized insulin B chain by MCP, showed that MCP can catalyse sequential peptide bond hydrolysis involving channelling of peptide intermediates. Their results are exciting and encourage further studies in the degradation of larger protein substrates in order to determine a mechanism of action for the protease.

7.3 Identifying catalytic subunits and residues.

One way in establishing the identity of these proteolytic activities, to whether they reside within individual subunits or whether they are located at interfaces of at least two or more subunits, would be to label them selectively, and to sequence them for information with regards to the catalytic residues as well as any novel consensus sequences around the catalytic residues.

The labelling experiment of the LLE1 active site using [^{3}H]-DFP revealed one labelled polypeptide on one dimensional SDS PAGE, with a molecular mass of 25 kDa. This observation is interesting and important because DFP forms covalent bond with the catalytic serines, so do PMSF, APMSF, and pefabloc. In contrast to identifying the catalytic serines, the peptidylchloromethylketones, the peptidyldiazomethanes, or isocoumarin derivatives form covalent bonds with catalytic histidine residues (Shaw, 1990; Powers et al., 1990), which will be heplful in identifying the catalytic subunits, it would not, however, identify the essential serine residues in those subunits.

In view of limited availability of good inhibitors of the proteinase activities, few studies describing identification of catalytic subunits have been reported in the literature. A 22 kDa subunit of the chicken MCP was identified by [3H]-DFP labelling (Sato and Shiratsuchi, 1990), whereas up to five subunits were labelled using the same label in the case of rat liver MCP (Tanaka, et al., 1986a). Recently, Orlowski and coworkers have also reported labelling of 7 different subunits of the pituitary enzyme using [^{14}C]-DCI (Cardozo et

al., 1992). Unfortunately, none of the described studies have sequenced the identified catalytic subunits.

The suggestion by Glynne et al. (1991) that the cDNA sequence of RING10 has sequence homology to the conserved regions around catalytic residues in subtilisin-like proteases, thus making it a catalytic one, is a very hypothetical one and highly biased until catalytic residues of such conserved regions will be labelled, identified, and their chemical or other modification shown to cause inactivation of the respective proteolytic activity. Aki et al. (1992) have shown that the rat RC1 subunit is a homolog of the RING10 subunit, with the putative catalytic histidine being replaced by an asparagine residue.

The primary structures of MCP subunits,which have been cloned and sequenced, so far (Tanaka et al., 1992), have been found to have no sequence homology with other proteins and with other proteases in particular (Tanaka et al., 1992; Rivett, 1993). These and some of the above observations have led to the suggestion that MCPs are a novel family of proteolytic enzymes, and have been described by Rawlings and Barrett (1992) as "Multicatalytic endopeptidase complexes; EC. 3.4.99.46", and are awaiting full classification which will depend eventually on the identification of catalytic residues of the different proteolytic activities.

7.4 Structure of the proteinase complex.

It is still debatable whether six or seven is the number of subunits making the ring domains of the proteinase complex. By

simple analogy to the archaebacterial MCP which has seven subunits in the ring (Puhler et. al, 1992), one would favour the rat MCP to also have seven subunits, and to the GroEL proteins which have a seven-fold symmetry, thought to be important in binding unfolded proteins (Zwickl et al., 1990), one also would favour a seven-fold symmetry as MCP at some stage during protein degradation would probably unfold it and would wrap it around itself.

Activation by manganese ions was first suggested by kinetic methods to be structural (Chapter 3), and later confirmed to be so by biophysical methods (Chapter 6). The activation was found to be mediated via an overall changes in the conformation of the molecule, where a transition from a more compact one to an extended one was measured using three independent biophysical methods (Chapter 6). Other effectors, including SDS, KCl, $CaCl_2$, and $MgCl_2$, have also been found to mediate their effects via conformational changes in the complex as measured by sedimentation velocity analysis.

The general conclusion from these and other observations is that upon activation or inhibition by an effector, changes in conformation are observed. However, it is not possible to predict the direction of the change nor its magnitude depending on whether the effector is activating or inhibiting the complex. The measurable conformational changes in the complex reflects the tight subunit-subunit interactions, which could play an *in vivo* regulatory role of proteolytic activity.

7.5 MCP and antigen processing.

The implication of MCP in antigen processing has been so far a hypothetical one, and to my best knowledge there have not been any published reports implicating the proteinase complex in the processing of proteins in the cytoplasm, to generate the correct antigens to be presented at the cell surface within the MHC class I complexes.

The preliminary study described in Section 5.6 does not conclusively show that MCP is responsible for the proteolytic generation of antigens *in vivo*; however, it is one step towards understanding the interaction of the proteinase complex with peptide substrates, which in turn has proven useful in pointing out the importance of the size of the peptide to be degraded, in view of generating the correct antigen.

It is, however, poorly understood how antigens are generated *in vivo*. Are they generated from the protein itself after limited proteolysis or from secondary proteolytic products? This question is currently under investigation by infecting cell lines with a recombinant vaccinia virus construct encoding fragment peptides of the nucleoprotein, in order to observe whether the *in vivo* expression of such peptides is sufficient for processing and presentation or not (Cerundolo and Townsend, personal communication).

In view of the different proteolytic activities associated with MCP, of the MCP localization near the endoplasmic reticulum (Rivett et al., 1992), and of the MCP's high concentration in cells (Hendil,

1988), one would expect the proteinase complex to have at least some action in the processing of at least the viral proteins.

7.6 Future lines of investigation.

The past three years have seen a good progress in elucidating the kinetic properties of MCP. Although there could well be more proteolytic sites to be identified, attention has to focus, now, on labelling the ones that we know about. Thus, future work should concentrate on the following:

1) As a first priority, the identification of the LLE1 active site using DFP (Chapter 4) and sequencing the labelled subunit to obtain sequence information around the catalytic serine, and also to obtain some internal sequence information, that could subsequently be used for cloning the LLE1 catalytic subunit.

2) Search for specific inhibitors of the different proteolytic activities will concentrate on testing some potential phosphorous containing inhibitors, which will be kindly provided by Dr M. Johnson (MRC Toxicology Unit, London). It would be extremely valuable if any of them will inhibit the LLE2 activity selectively, which will lead to its labelling, identification of the catalytic serine, and subsequently cloning the respective site(s).

3) The identification of some of the activities having the described inhibition resistant cleavages (Chapter 5), could be further characterized using peptide substrates, especially the Ox 12 peptide (sequence: Tyr-Ser-Asn-Glu-Asn-Met-Asp-Ala-Met) which is cleaved at

the Met_6-Asp_7 peptide bond, and will make the study much easier than having multiple cleavage sites.

4) In view of the non conclusive results obtained with the Oxford peptides regarding antigen processing, future lines of investigation will concentrate on the use of longer versions of peptides, and possibly to use the whole nucleoprotein to investigate the involvement of MCP in such a process. Also attempts will be made to purify MCP from human cell line sources, and to use it in future digestion studies. In parallel to that, the *in vivo* studies will be carried out in Oxford by Townsend and coworkers.

5) Recently, Zwickl et al. (1992) have reported the exciting result of successfully expressing functional archaebacterial MCP in *Escherichia* coli. Such observation is the basis of a long term study, where making a multi-complex version of the simpler archaebacterial MCP, which has only the chymotrypsin-like activity, would be attempted. Once the catalytic subunits of the known activities of the rat liver MCP are known and cloned, expression systems containing such clones could be constructed under similar strategy to Zwickl et al. (1992).

Then different ratios of either the A type or the B type subunits plus some of the catalytic ones, which could be used under different combinations, it would be possible to express them in *Escherichia* coli, hoping to generate functional multi-activity archaebacterial MCP. Assays for expression, correct folding, and functionality will include kinetic assays and electron microscopy. The results of such studies will open up new lines of investigation, especially into MCP sub-

populations.

Concluding remarks.

Our current understanding of intracellular protein degradation in general and the proteinases involved in particular has been progressing at a speed as fast as a tortoise gallop! The field has experienced, however, some memorable periods, starting with the discovery of the lysosomal pathway of protein degradation in the earlier seventies, and in the late seventies with the discovery of the ubiquitin-dependent pathway. The field is experiencing, now, a very exciting era around the subject of the multicatalytic proteinase complex, which was co-discovered by Wilk and Orlowski in the earlier eighties.

Though some considerable progress has been made on the biochemistry, molecular biology, and genetics of the multicatalytic proteinase complex as judged by the ever increasing number of publications, it must be said that we are just starting to understand the complexities involved, and to value Nature for what it can make and conserve, as MCPs are found across a wide spectrum from simple archaebacteria to a more complicated eukaryotes, and the encoding genes appear to form a class of their own, conserved through evolution and referred to as the proteasome gene family.

Many questions have been asked about the nature of the subject, its complex structure, its proteolytic activities, its intracellular localization, its genetics, its involvement in antigen processing, and most importantly its involvement in nonlysosomal

155

protein degradation in general, and in the ubiquitin pathway in particular. Some answers to the questions are only just beginning to emerge, in view of the complexity of the subject, and major research efforts should be encouraged in order to provide the answers.

With optimistic views in mind, research is going to further our little knowledge of the subject, and in doing so, will bring with it a new insight into the field of intracellular protein degradation.

Table 6.1: Dimensions of the multicatalytic proteinase complex obtained by electron microscopy.

Values given are mean ± S.E. for n molecules evaluated. Methylamine tungstate and uranyl acetate are negative contrast media used for staining the proteinase preparations. *A. J. Rowe (personal communication).

Treatment	Diameter (nm)	Width (nm)	Length (nm)	n
Control (methylamine tungstate)*	10.91 ± 0.10	-	16.81 ± 0.10	114
Control (uranyl acetate)	12.42 ± 0.14	11.68 ± 0.22	19.61 ± 0.20	94
1 mM MnCl2 (uranyl acetate)	14.83 ± 0.13	-	20.65 ± 0.93	273
10 mM MnCl2 (uranyl acetate)	13.10 ± 0.34	-	-	70

Table 6.2: Sedimentation velocity of the multicatalytic
proteinase complex.

Determinations of $s_{20,w}$ values were carried out using a Centriscan 75 as described under Section 2.13. Values are given as mean $\pm$ S.E. for at least three separate determinations.

Treatment	Concentration	$s_{20,w}$
Control	-	17.7 $\pm$ 0.2
MnCl$_2$	(1 mM)	13.9 $\pm$ 0.2
CaCl$_2$	(1 mM)	15.5 $\pm$ 0.1
MgCl$_2$	(1 mM)	16.7 $\pm$ 0.1
KCl	(50 mM)	13.9 $\pm$ 0.2
SDS	(0.01%)	21.2 $\pm$ 0.2
SDS	(0.02%)	15.5 $\pm$ 0.6
LLE-NA	(0.1 mM)	17.3 $\pm$ 0.5
LLE-NA	(0.4 mM)	19.7 $\pm$ 0.7
Five minute exposure at 65°C	-	16.7 $\pm$ 0.5

Table 6.3: Physicochemical properties of the multicatalytic proteinase complex.

A = the proteinase complex alone, B = in the presence of 1 mM MnCl₂, C = in the presence of 10 mM MnCl₂, and D = the two days dialysed proteinase preparation. *A. J. Rowe (personal communication).

Property	Method of analysis	Value			
		A	B	C	D
Mr (kDa)	Sedimentation equiliiberium	650*	-	-	-
	Sedimentation velocity and diffusion	575	-	-	1160
s₂₀,w	Sedimentation velocity	17.7S	13.9S	17.6S	25.5S
D_T (x10⁻⁷ cm²/s)	Dynamic light scattering	2.78	2.76	1.35	1.94
Partial specific volume	From amino acid composition	0.73 ml/g*	-	-	-
r_H (nm)	From Mr and s₂₀,w	8.70*	-	-	-
	From D_T	8.59	8.53	-	12.98
	From electron microscopy	8.00	8.87	-	-

Table 6.4: The proposed architecture for the multicatalytic proteinase complex.

Model one: Proposed by Kopp et al. (1986) and Baumeister et al. (1988) as a disc-Shaped Structure with an inner cavity, and has a diameter of 11 nm and a length of 16 nm. It is composed of four stacked rings, each consisting of six centres of mass, the position of which deviates from a true six-fold symmetry.

Model two: Proposed by Tanaka et al. (1988c) as a prolate ellipsoidal structure with an ellipsoid cavity in the centre. It has a diameter of 16 nm and a length of 11 nm. The structure shows an eight- fold symmetry (Arrigo et al., 1988).

Model three: Proposed by Puhler et al. (1992) for the archaebacterial MCP as a barrel-shaped structure with an inner cavity, and has a diameter of 11.4 nm and a length of 17.8 nm. It is composed of four stacked rings, each consisting of seven subunits. The structure shows a seven-fold symmetry, but the subunits making the outer and inner rings are not in register along the axis of the barrel; rather the outer rings are rotated with respect to the inner rings by approximately 25°.

Model four: (Current study) as a cylindrical structure with an inner cavity, and has a diameter of 12.4 nm and a length of 19.6 nm. It is composed of four stacked rings in a pseudo-helical arrangement (A. J. Rowe, personal communication), each consisting of six or seven subunits. The structure shows a lack of symmetry (A. J. Rowe, personal communication).

Table 6.5: Comparison of the physicochemical properties of MCP with published values.

A = the proteinase complex alone, B = Data from Tanaka et al. (1988c), and C = Data from Kopp et al. (1986). *From rat liver. @From rat skeletal muscle.

Property	Method of analysis	A*	B*	C@
Mr (kDa)	Sedimentation equiliberium	650*	743	-
	Sedimentation velocity and diffusion	575	722	-
	Gel filtration	-	-	650
$s_{20,w}$	Sedimentation velocity	17.7S	19.8S	-
D_T (x10^{-7} cm^2/s)	Dynamic light scattering	2.78	2.50	3.90
r_H (nm)	From Mr and $s_{20,w}$	8.70*	-	-
	From D_T	8.59	8.50	5.05
	From electron microscopy	8.00	-	5.35

.

Figure 6.1: Electron microscopy of MCP particles negatively
stained in 2% uranyl acetate.

(a) Electron micrograph of MCP particles, control, (b) Electron micrograph of MCP particles, in the presence of 1 mM $MnCl_2$, and (c) Electron micrograph of MCP particles, in the presence of 10 mM $MnCl_2$. Magnification 183,000x. (d) Electron micrograph of MCP particles enlarged from (c), magnification 250,000x. Methodology described under Section 2.12.
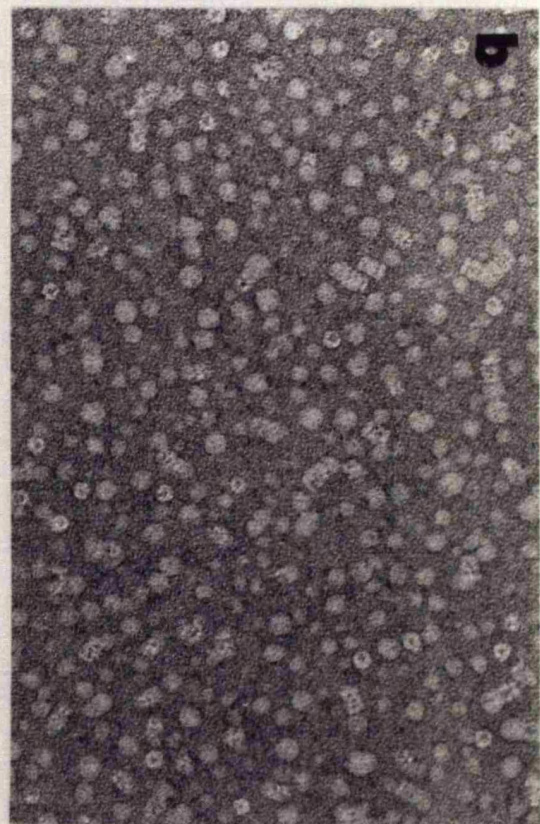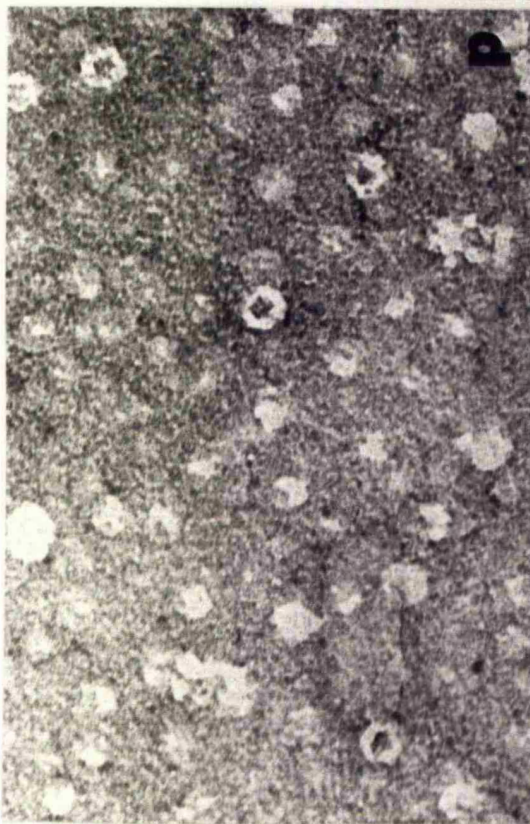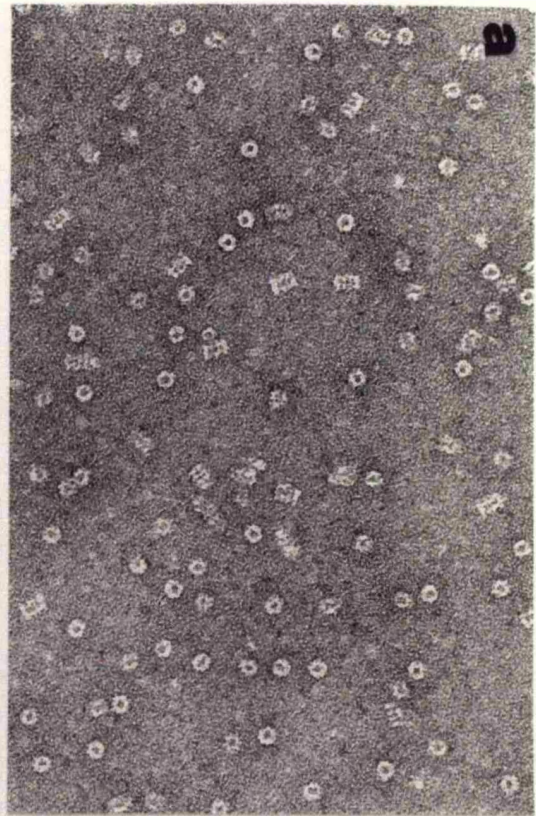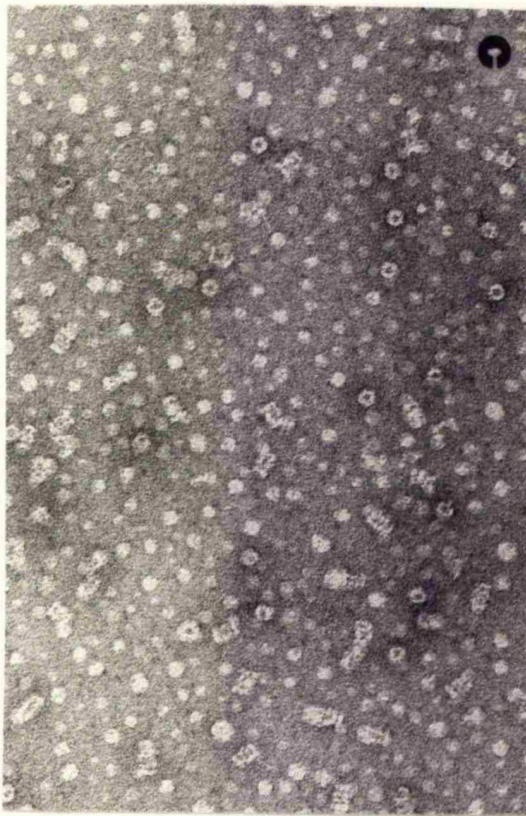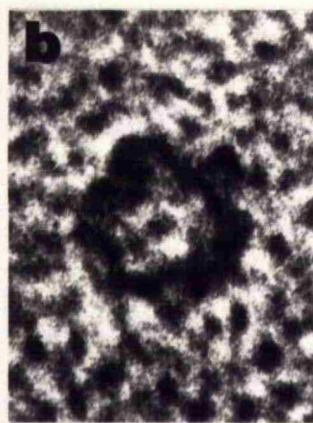
Figure 6.2: Electron micrographs of individual molecules from Figure 6.1a at higher magnification.

(a,b,c) show commonest "normal" type with a ring-like appearance, (d,e,f) show molecules in which the hole is deformed or displaced from the centre, or (g,h,i) in which there are gaps in the ring domain, and (j,k,l) show rectangular particles. Methodology described under Section 2.12.
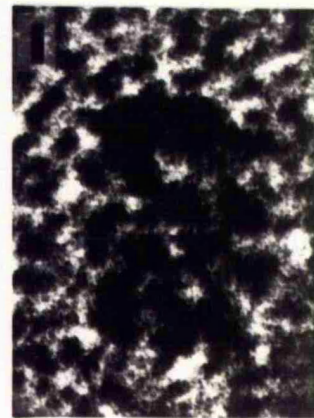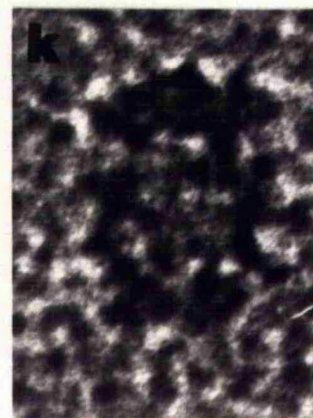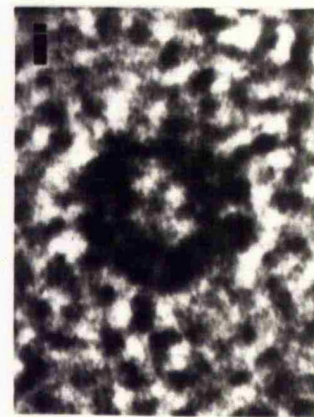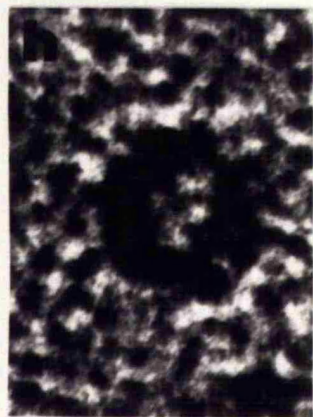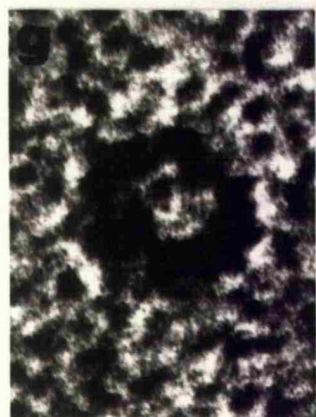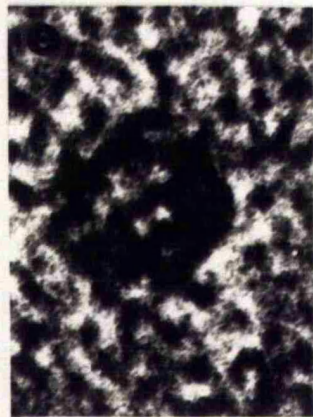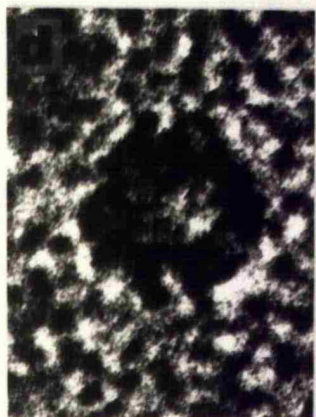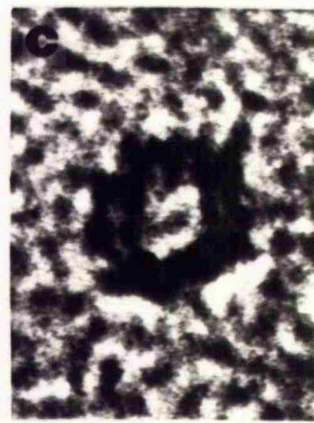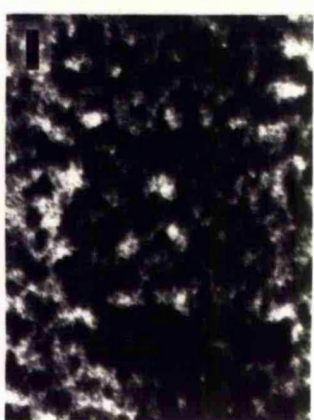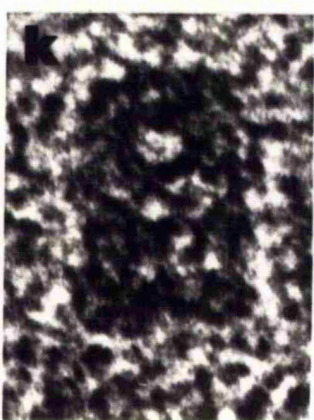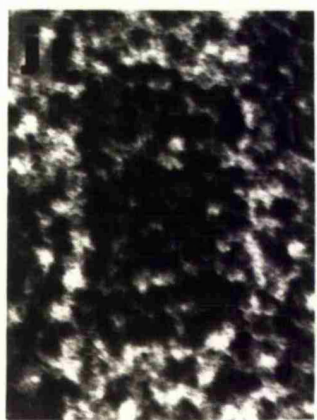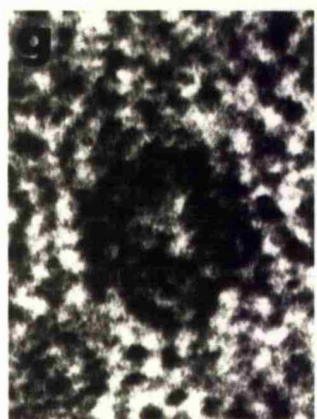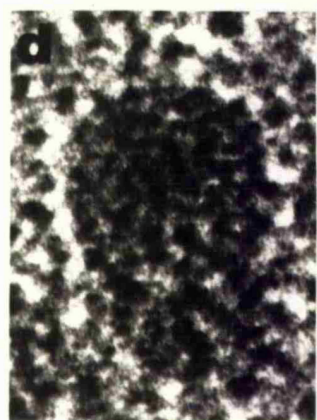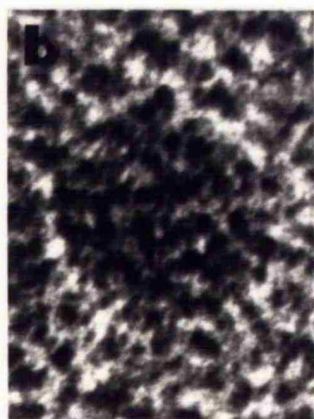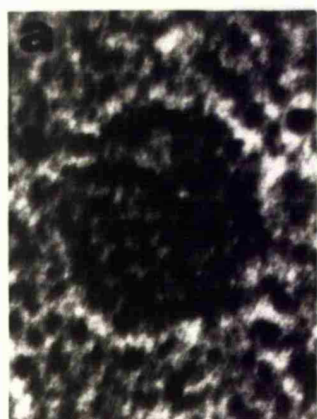
Figure 6.3: Electron micrographs of individual molecules
from Figure 6.1b at higher magnification.

(a,b,c,d,e,f) show commonest type with a raspberry-like
appearance, (g,h,i) show molecules in which the hole is deformed or
displaced from the centre, and (j,k,l) show rectangular particles.
Methodology described under Section 2.12.

Figure 6.4: Electron micrographs of individual molecules from Figure 6.1c at higher magnification.

(a,b,c) show a type with a raspberry-like appearance, (d,e,f) show molecules with normal ring-like appearance, (g,h,i) show destructed molecules with no defined phenotype, and (j,k,l) show rectangular particles. Methodology described under Section 2.12.
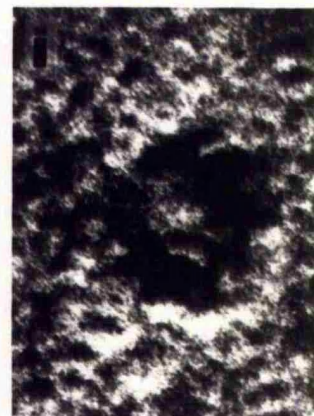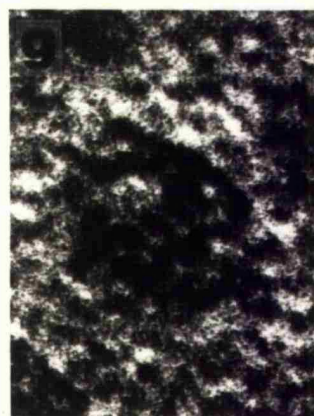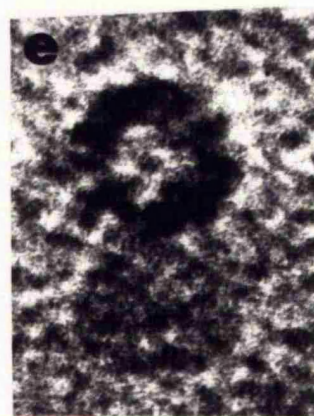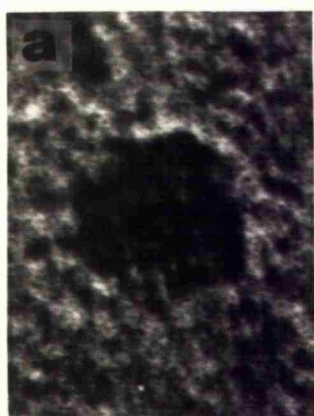
Figure 6.5: Sedimentation velocity profiles of the
multicatalytic proteinase complex.

Traces were recorded using a Centriscan 75 ultracentrifuge as
described under Section 2.13. (a) Traces of MCP alone monitored at
280 nm. (b) Traces of MCP + 1 mM $MnCl_2$ monitored at 280 nm.

Figure **6.6:** Sedimentation velocity profiles of the
multicatalytic proteinase complex.

Traces were recorded using a Centriscan 75 ultracentrifuge as
described under Section 2.13. (a) Traces of MCP alone monitored at
280 nm. (b) Traces of MCP + 1 mM $ZnCl_2$ monitored at 280 nm.

a)

b)

Cell 1   8-6-1992 10:48:17
MCP sample A   A:\39\----10_1.WOO
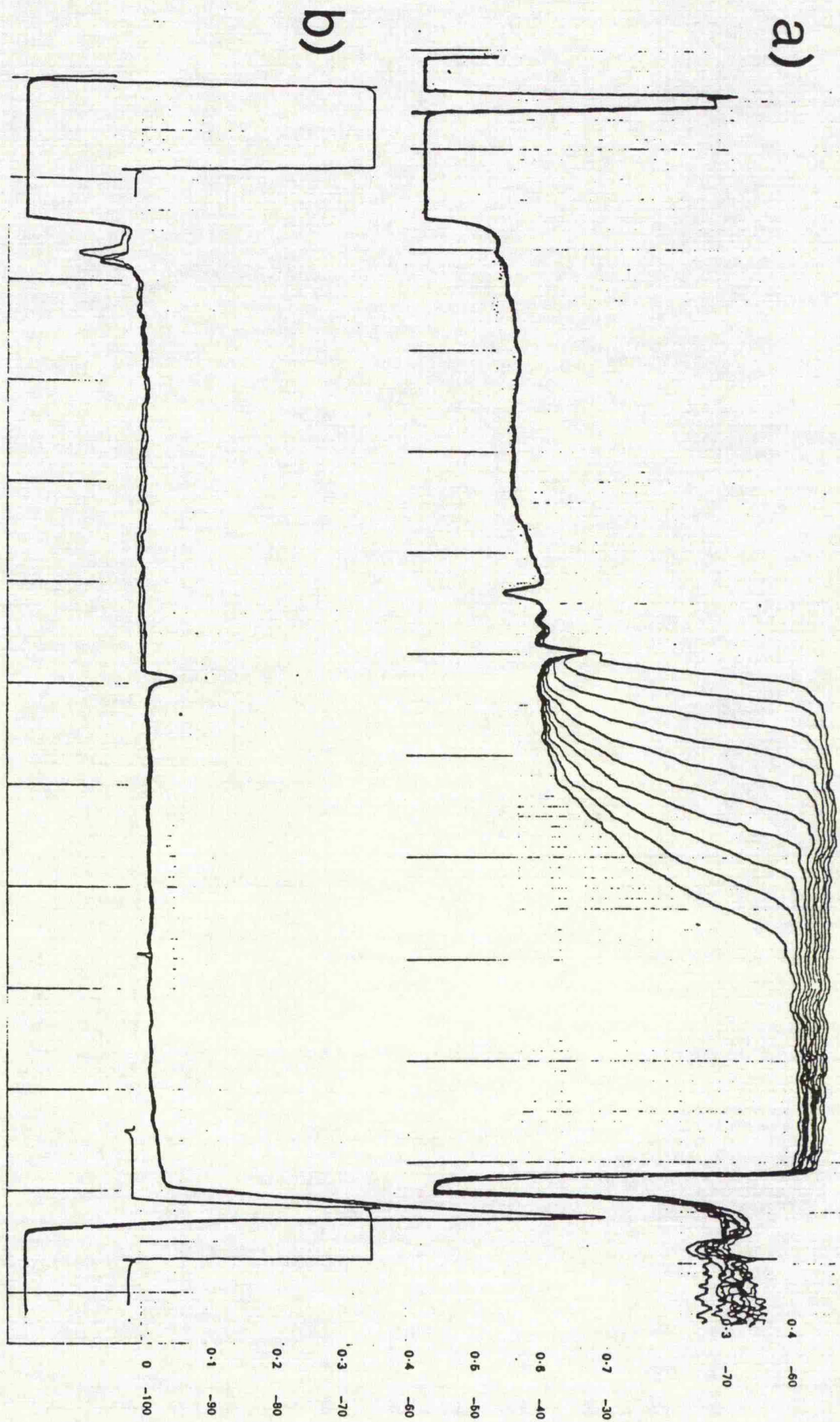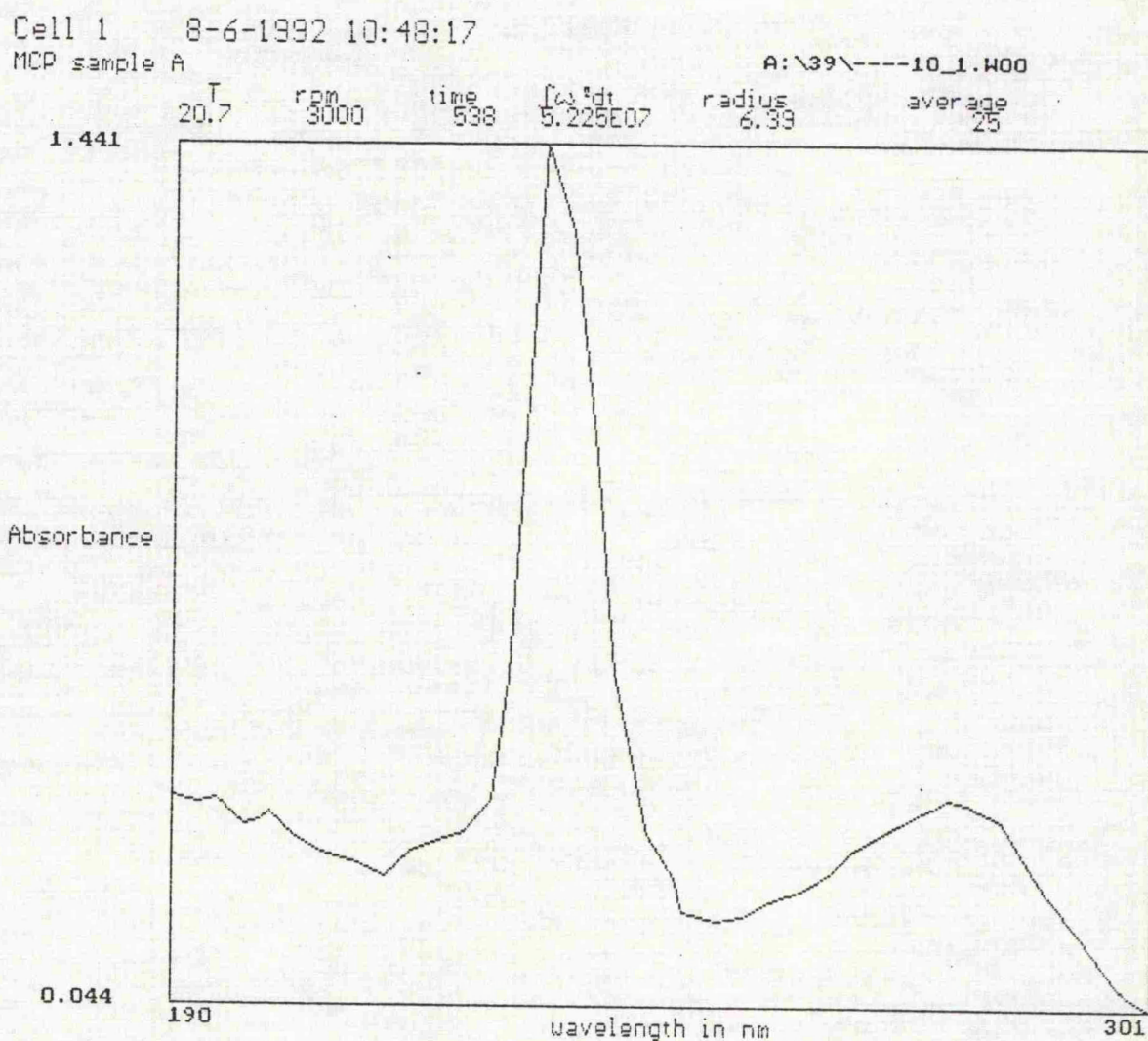
Figure 6.7: Absorption scanning of the multicatalytic proteinase complex.

MCP (0.4 mg/ml) was scanned on an Beckman XLA ultracentrifuge using its in vacuum UV optics detection system as described under Section 2.13.
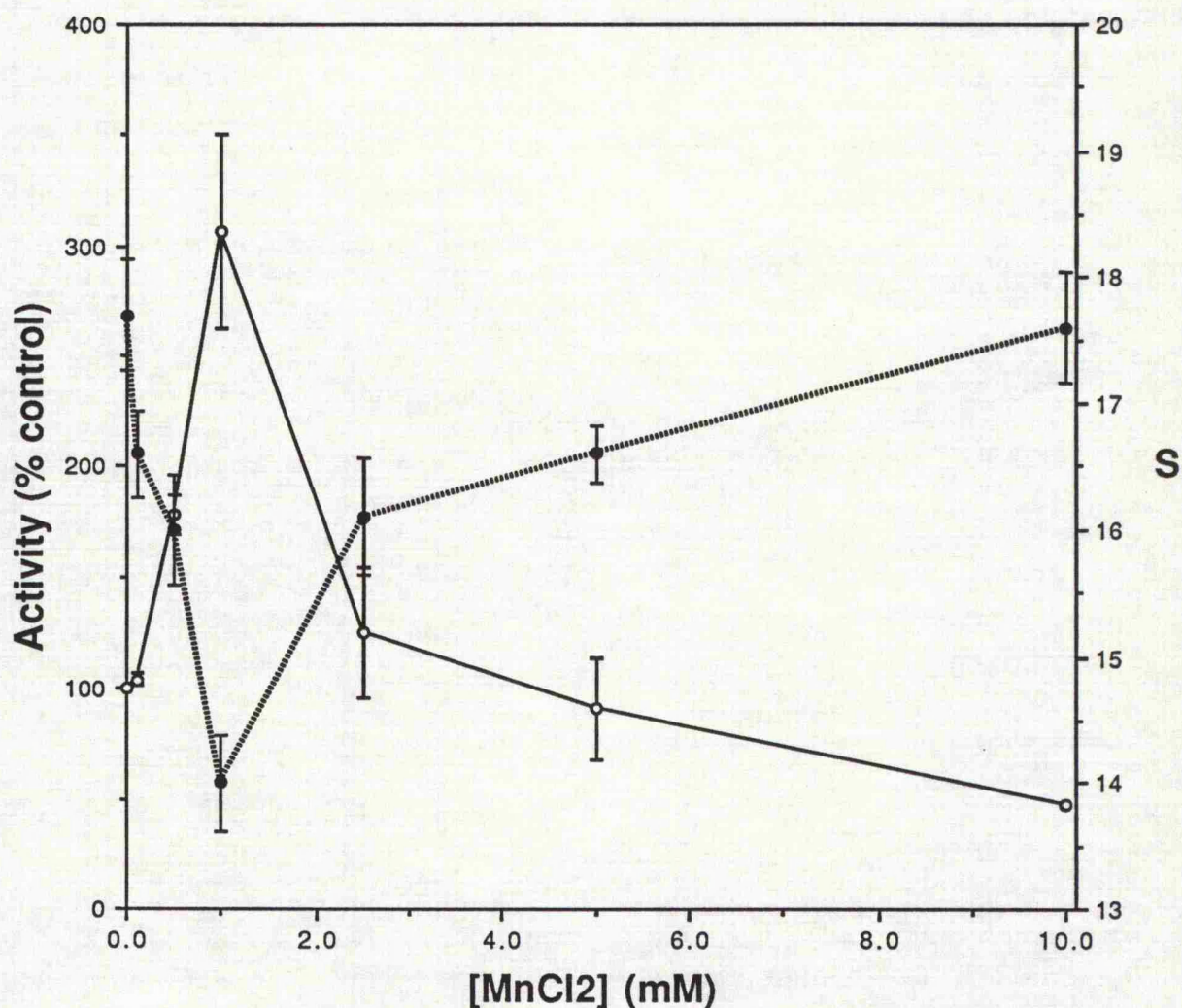
Figure 6.8: Dependence of the LLE1 activity and the $s_{20,w}$ on $MnCl_2$.

The kinetic data was obtained from Figure 3.17. Determination of the $s_{20,w}$ were carried out using the XLA ultracentrifuge as described under Section 2.13. S ($\cdot$) = $s_{20,w}$. Error bars represent mean $\pm$ S.D. for two separate determinations of the $s_{20,w}$ values.
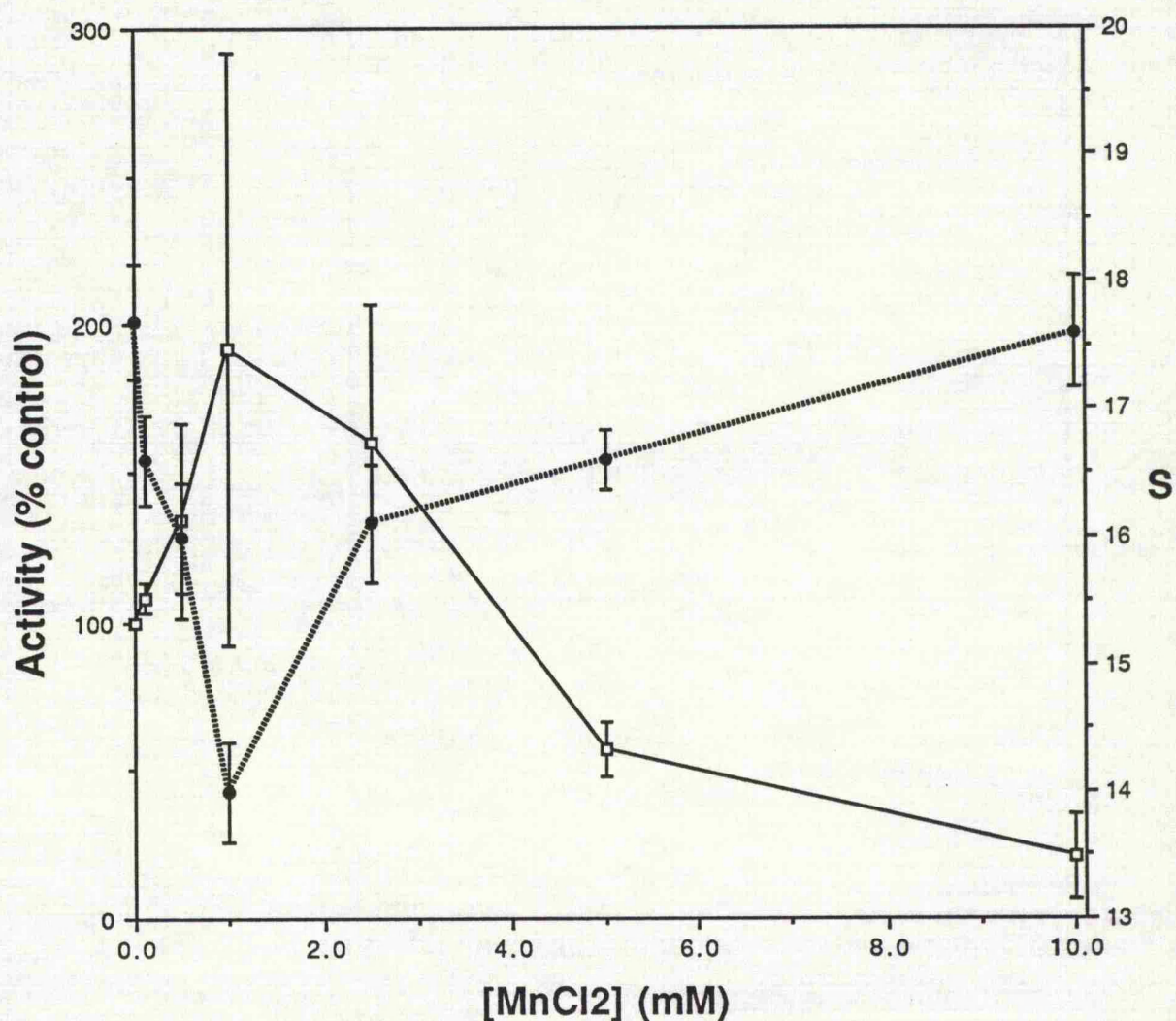
Figure 6.9: Dependence of the LLE2 activity and the $s_{20,w}$ on $MnCl_2$.

The kinetic data was obtained from Figure 3.17. determination of the $s_{20,w}$ were carried out using the XLA ultracentrifuge as described under Section 2.13. S ($\bullet$) = $s_{20,w}$. Error bars represent mean $\pm$ S.D. for two separate determinations of the $s_{20,w}$ values.
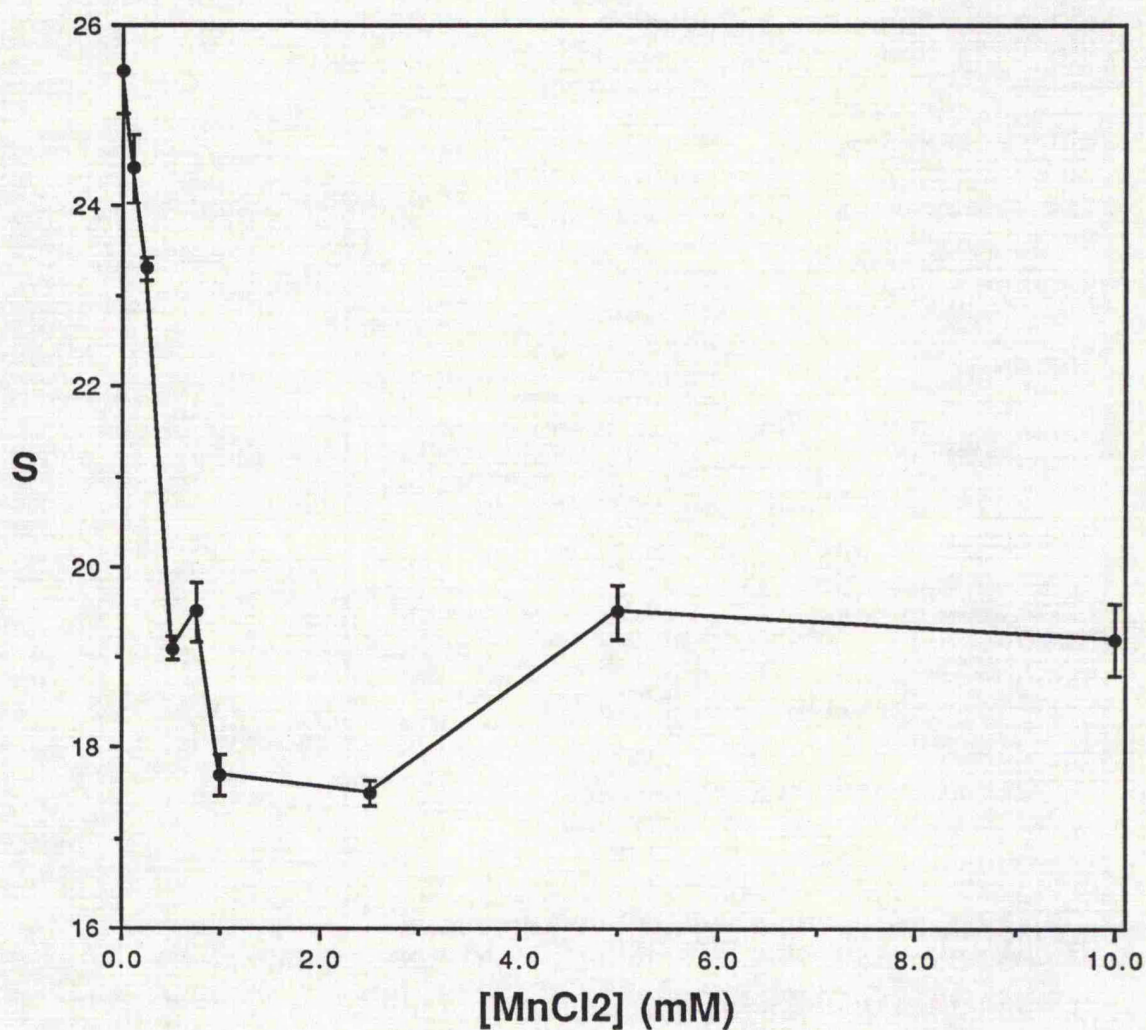
Figure 6.10: Dependence of the $s_{20,w}$ of the dimer form of MCP on $MnCl_2$.

Determination of the $s_{20,w}$ were carried out using the XLA ultracentrifuge as described under Section 2.13. $S = s_{20,w}$. Error bars represent mean $\pm$ S.D. for two separate determinations of the $s_{20,w}$ values.
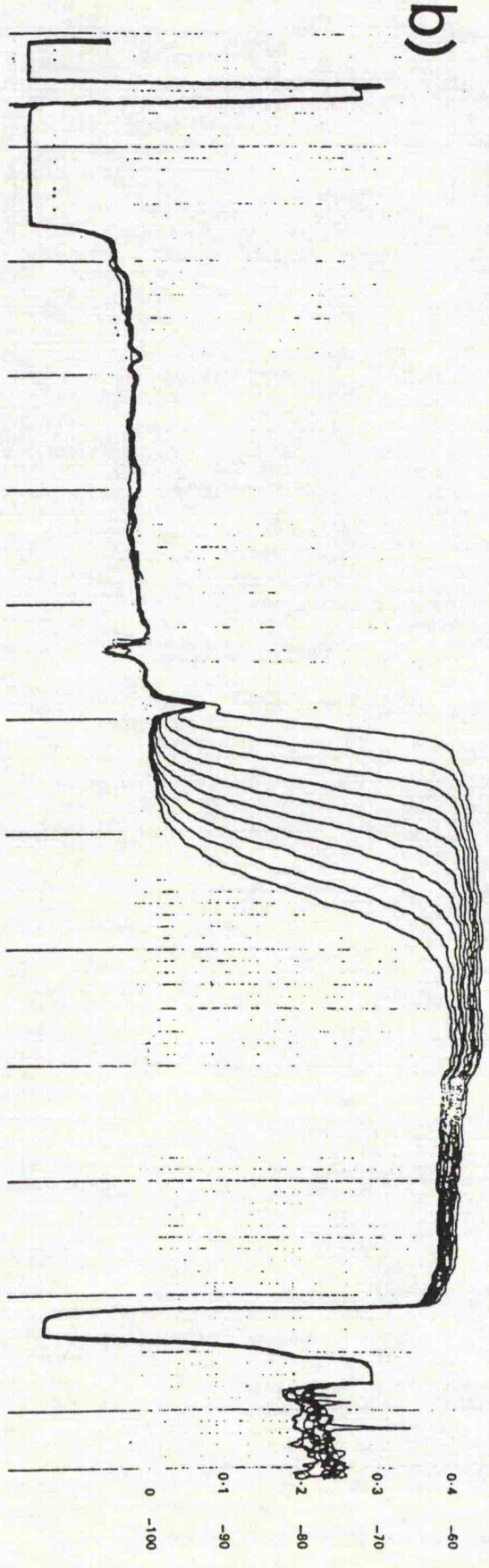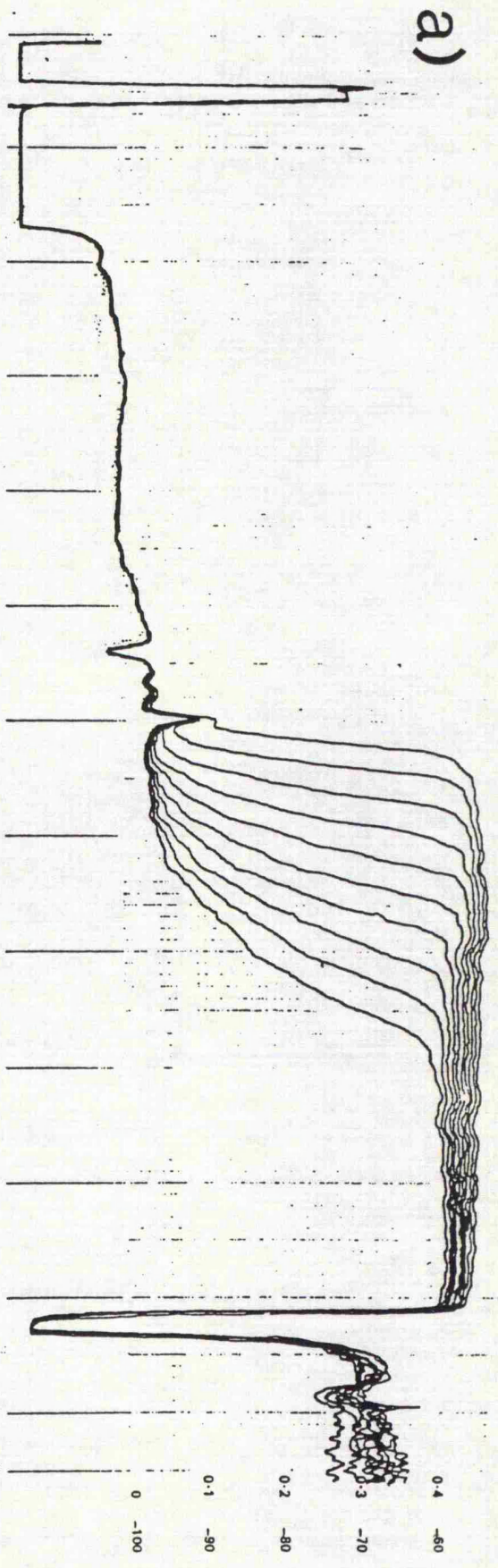
Figure 6.11: Sedimentation velocity profiles of the
multicatalytic proteinase complex.

Traces were recorded using an XLA ultracentrifuge as described under
Section 2.13. (A) Traces of MCP alone monitored at 280 nm. (B)
Traces of MCP + 10 mM MnCl₂ monitored at 231 nm.

CHAPTER 7

Discussion

"We have now reached a situation in which on the one hand we have many articles giving the impression that the problem is all but solved, and on the other hand assessments like the opinion of W. H. Thorpe in 1974 that 'I think it is fair to say that all the facile speculations and discussion published during the last 10-15 years explaining the mode of the origin of life have been shown to be far too simple-minded and to bear very little weight. The problem in fact seems as far from solution as it ever was.'"

7.1 Proteolytic activities of the proteinase complex.

Since its first description as a multicatalytic proteinase (Wilk and Orlowski, 1980; 1983) and up to the past four years, only three different proteolytic activities have been described for MCP in the literature.

However, from the present work (Chapters 3, 4, and 5), there appears to be at least seven different proteolytic activities associated with the complex: (a) One component catalysing the trypsin-like activity (LSTR), (b) Two components hydrolysing the peptidylglutamyl-peptide hydrolase activity, with one being noncooperative (LLE1) whereas the other component being a cooperative one (LLE2), (c) Three components catalysing the chymotrypsin-like activity (AAF, LLVY, and the Leu_9-Ser_{10} cleavage in the Ox 10 peptide), and finally (d) At least one component appearing to catalyse a variety of cleavages with the following residues in the P1 position: cysteine, leucine, methionine, and serine, and cleavages after such residues were found to be resistant to inhibition by DCI or pefabloc, so did the Leu_9-Ser_{10} cleavage in the Ox 10 peptide (Section 5.4).

Studies carried out by other groups have also made similar observations regarding the increasing number of proteolytic activities. Arribas and Castano (1991), working on the rat liver MCP, have reported two components for the peptidylglutamyl-peptide hydrolase activity with one being cooperative at lower LLE-NA concentrations, and the other one being noncooperative at higher concentrations, thus making at least four different proteolytic activities.

Similarly, Orlowski et al. (1991), working on the pituitary MCP, have reported that the peptidylglutamyl-peptide hydrolase activity is composed of two components, although their conclusions were drawn from the fact that the observed sigmoidal curve allowed a calculation of a Hill coefficient of 2. Their observations bring the number of the different proteolytic activities to at least four.

More recently, studies from the same lab. have shown a novel proteolytic activity that was found to be resistant to inhibition by DCI, and which appears to be of the chymotrypsin-like type (Cardozo et al., 1992), thus making the number of different proteolytic sites for the pituitary enzyme as at least five.

Pereira et al. (1991) have reported a fourth proteolytic site(s) activated by treating the pituitary MCP with DCI, and shown to be involved in casein degradation. Similarly, Mykles and Haire (1989) have also described a fourth proteolytic activity that degrades myofibrillar proteins in the case of the Lobster muscle MCP, and have shown its stimulation by heat. The concept of a separate protein degradation site, which is often referred to as caseinolytic activity (Orlowski, 1990), is highly unlikely to occur because:

(1) In the two described studies (Mykles and Haire, 1989; Pereira et al., 1991), there was some kind of treatment of the enzyme before observing full caseinolytic activities, which could have induced conformational changes in the complex thus exposing, on the way, novel active sites, as some effectors, including heat treatment, were found to induce conformational changes in the complex (Chapter 5),

and the DCI treatment was found, in my studies, to activate the LSTR and LLE1 activities, which could well account for the observed stimulation in the case of the pituitary enzyme.

And (2) The study on the degradation of oxidized insulin B chain has revealed an unexpectedly new concept for protein degradation by MCP, where sequential peptide hydrolysis and channelling of peptide intermediates are thought to occur, thus more than one proteolytic site would be involved, therefore eliminating the possibility of a single proteolytic site involvement (Dick et al., 1991).

7.2 MCP as an atypical serine protease.

The inhibition of the AAF, LLVY, and LLE2 activities by DCI, of the LSTR activity by pefabloc, and partial inactivation of the LLE1 activity by DFP (Djaballah et al., 1992), and the reported inhibition of the chymotrypsin-like, trypsin-like, and peptidylglutamyl-peptide hydrolase activities by mechansim based serine protease inhibitors ie the isocoumarin derivatives (Orlowski and Michaud, 1989; Cardozo et al., 1992) have led to the accepted view now of classifying MCP as an atypical serine protease.

The earlier classification of MCP as a cysteine protease was because of the sensitivity of the trypsin-like activity, in particular, to thiol reagents (Rivett, 1985). Cases where serine proteases are found to be sensitive to thiol reagents are not unusual. Betzel et al. (1988) reported that although proteinase K is a serine protease belonging to the subtilisin superfamily, it was found to be very sensitive to thiol reagents. And recently, Dick et al. (1992), working on MCP purified

147

from bovine erythrocytes, bovine heart, and human erythrocytes, have identified the cysteinyl residue that is essential in the trypsin-like activity, which was localized in a subunit with an average molecular mass of 27.2 kDa (Dick et al., 1992).

An unusual feature about MCP is its unreactivity towards most of the inhibitors tested, especially the mechanism based ones (Chapter 4; Orlowski and Michaud, 1989; Djaballah et al., 1992; Cardozo et al., 1992), which in turn suggests novel geometries at the catalytic sites, which could in turn reflect a novel arrangement of the catalytic residues at these sites.

In view of the wide specificity of MCP in degrading peptide and protein substrates (Orlowski, 1990; Rivett, 1993), such novel geometries could well have evolved in this manner to probably be involved in an interactive process between the different catalytic sites for the expression of a conceived unique catalytic properties of the multicatalytic complex, as has been described in the case of the evolution of multicomplex enzymes by Gaertner (1978) and Welch (1977).

Such an expression was reported by Dick et al. (1991), who, while studying the degradation of oxidized insulin B chain by MCP, showed that MCP can catalyse sequential peptide bond hydrolysis involving channelling of peptide intermediates. Their results are exciting and encourage further studies in the degradation of larger protein substrates in order to determine a mechanism of action for the protease.

7.3 Identifying catalytic subunits and residues.

One way in establishing the identity of these proteolytic activities, to whether they reside within individual subunits or whether they are located at interfaces of at least two or more subunits, would be to label them selectively, and to sequence them for information with regards to the catalytic residues as well as any novel consensus sequences around the catalytic residues.

The labelling experiment of the LLE1 active site using [^{3}H]-DFP revealed one labelled polypeptide on one dimensional SDS PAGE, with a molecular mass of 25 kDa. This observation is interesting and important because DFP forms covalent bond with the catalytic serines, so do PMSF, APMSF, and pefabloc. In contrast to identifying the catalytic serines, the peptidylchloromethylketones, the peptidyldiazomethanes, or isocoumarin derivatives form covalent bonds with catalytic histidine residues (Shaw, 1990; Powers et al., 1990), which will be heplful in identifying the catalytic subunits, it would not, however, identify the essential serine residues in those subunits.

In view of limited availability of good inhibitors of the proteinase activities, few studies describing identification of catalytic subunits have been reported in the literature. A 22 kDa subunit of the chicken MCP was identified by [3H]-DFP labelling (Sato and Shiratsuchi, 1990), whereas up to five subunits were labelled using the same label in the case of rat liver MCP (Tanaka, et al., 1986a). Recently, Orlowski and coworkers have also reported labelling of 7 different subunits of the pituitary enzyme using [^{14}C]-DCI (Cardozo et al., 1992).

Unfortunately, none of the described studies have sequenced the identified catalytic subunits.

The suggestion by Glynne et al. (1991) that the cDNA sequence of RING10 has sequence homology to the conserved regions around catalytic residues in subtilisin-like proteases, thus making it a catalytic one, is a very hypothetical one and highly biased until catalytic residues of such conserved regions will be labelled, identified, and their chemical or other modification shown to cause inactivation of the respective proteolytic activity. Aki et al. (1992) have shown that the rat RC1 subunit is a homolog of the RING10 subunit, with the putative catalytic histidine being replaced by an asparagine residue.

The primary structures of MCP subunits,which have been cloned and sequenced, so far (Tanaka et al., 1992), have been found to have no sequence homology with other proteins and with other proteases in particular (Tanaka et al., 1992; Rivett, 1993). These and some of the above observations have led to the suggestion that MCPs are a novel family of proteolytic enzymes, and have been described by Rawlings and Barrett (1992) as "Multicatalytic endopeptidase complexes; EC. 3.4.99.46", and are awaiting full classification which will depend eventually on the identification of catalytic residues of the different proteolytic activities.

7.4 Structure of the proteinase complex.

It is still debatable whether six or seven is the number of subunits making the ring domains of the proteinase complex. By simple analogy to the archaebacterial MCP which has seven subunits in

the ring (Puhler et. al, 1992), one would favour the rat MCP to also have seven subunits, and to the GroEL proteins which have a seven-fold symmetry, thought to be important in binding unfolded proteins (Zwickl et al., 1990), one also would favour a seven-fold symmetry as MCP at some stage during protein degradation would probably unfold it and would wrap it around itself.

Activation by manganese ions was first suggested by kinetic methods to be structural (Chapter 3), and later confirmed to be so by biophysical methods (Chapter 6). The activation was found to be mediated via an overall changes in the conformation of the molecule, where a transition from a more compact one to an extended one was measured using three independent biophysical methods (Chapter 6). Other effectors, including SDS, KCl, $CaCl_2$, and $MgCl_2$, have also been found to mediate their effects via conformational changes in the complex as measured by sedimentation velocity analysis.

The general conclusion from these and other observations is that upon activation or inhibition by an effector, changes in conformation are observed. However, it is not possible to predict the direction of the change nor its magnitude depending on whether the effector is activating or inhibiting the complex. The measurable conformational changes in the complex reflects the tight subunit-subunit interactions, which could play an *in vivo* regulatory role of proteolytic activity.

7.5 MCP and antigen processing.

151

The implication of MCP in antigen processing has been so far a hypothetical one, and to my best knowledge there have not been any published reports implicating the proteinase complex in the processing of proteins in the cytoplasm, to generate the correct antigens to be presented at the cell surface within the MHC class I complexes.

The preliminary study described in Section 5.6 does not conclusively show that MCP is responsible for the proteolytic generation of antigens *in vivo*; however, it is one step towards understanding the interaction of the proteinase complex with peptide substrates, which in turn has proven useful in pointing out the importance of the size of the peptide to be degraded, in view of generating the correct antigen.

It is, however, poorly understood how antigens are generated *in vivo*. Are they generated from the protein itself after limited proteolysis or from secondary proteolytic products? This question is currently under investigation by infecting cell lines with a recombinant vaccinia virus construct encoding fragment peptides of the nucleoprotein, in order to observe whether the *in vivo* expression of such peptides is sufficient for processing and presentation or not (Cerundolo and Townsend, personal communication).

In view of the different proteolytic activities associated with MCP, of the MCP localization near the endoplasmic reticulum (Rivett et al., 1992), and of the MCP's high concentration in cells (Hendil, 1988), one would expect the proteinase complex to have at least some action in the processing of at least the viral proteins.

7.6 Future lines of investigation.

The past three years have seen a good progress in elucidating the kinetic properties of MCP. Although there could well be more proteolytic sites to be identified, attention has to focus, now, on labelling the ones that we know about. Thus, future work should concentrate on the following:

1) As a first priority, the identification of the LLE1 active site using DFP (Chapter 4) and sequencing the labelled subunit to obtain sequence information around the catalytic serine, and also to obtain some internal sequence information, that could subsequently be used for cloning the LLE1 catalytic subunit.

2) Search for specific inhibitors of the different proteolytic activities will concentrate on testing some potential phosphorous containing inhibitors, which will be kindly provided by Dr M. Johnson (MRC Toxicology Unit, London). It would be extremely valuable if any of them will inhibit the LLE2 activity selectively, which will lead to its labelling, identification of the catalytic serine, and subsequently cloning the respective site(s).

3) The identification of some of the activities having the described inhibition resistant cleavages (Chapter 5), could be further characterized using peptide substrates, especially the Ox 12 peptide (sequence: Tyr-Ser-Asn-Glu-Asn-Met-Asp-Ala-Met) which is cleaved at the Met_6-Asp_7 peptide bond, and will make the study much easier than having multiple cleavage sites.

4) In view of the non conclusive results obtained with the Oxford peptides regarding antigen processing, future lines of investigation will concentrate on the use of longer versions of peptides, and possibly to use the whole nucleoprotein to investigate the involvement of MCP in such a process. Also attempts will be made to purify MCP from human cell line sources, and to use it in future digestion studies. In parallel to that, the *in vivo* studies will be carried out in Oxford by Townsend and coworkers.

5) Recently, Zwickl et al. (1992) have reported the exciting result of successfully expressing functional archaebacterial MCP in *Escherichia* coli. Such observation is the basis of a long term study, where making a multi-complex version of the simpler archaebacterial MCP, which has only the chymotrypsin-like activity, would be attempted. Once the catalytic subunits of the known activities of the rat liver MCP are known and cloned, expression systems containing such clones could be constructed under similar strategy to Zwickl et al. (1992).

Then different ratios of either the A type or the B type subunits plus some of the catalytic ones, which could be used under different combinations, it would be possible to express them in *Escherichia* coli, hoping to generate functional multi-activity archaebacterial MCP. Assays for expression, correct folding, and functionality will include kinetic assays and electron microscopy. The results of such studies will open up new lines of investigation, especially into MCP sub-populations.

Concluding remarks.

Our current understanding of intracellular protein degradation in general and the proteinases involved in particular has been progressing at a speed as fast as a tortoise gallop! The field has experienced, however, some memorable periods, starting with the discovery of the lysosomal pathway of protein degradation in the earlier seventies, and in the late seventies with the discovery of the ubiquitin-dependent pathway. The field is experiencing, now, a very exciting era around the subject of the multicatalytic proteinase complex, which was co-discovered by Wilk and Orlowski in the earlier eighties.

Though some considerable progress has been made on the biochemistry, molecular biology, and genetics of the multicatalytic proteinase complex as judged by the ever increasing number of publications, it must be said that we are just starting to understand the complexities involved, and to value Nature for what it can make and conserve, as MCPs are found across a wide spectrum from simple archaebacteria to a more complicated eukaryotes, and the encoding genes appear to form a class of their own, conserved through evolution and referred to as the proteasome gene family.

Many questions have been asked about the nature of the subject, its complex structure, its proteolytic activities, its intracellular localization, its genetics, its involvement in antigen processing, and most importantly its involvement in nonlysosomal protein degradation in general, and in the ubiquitin pathway in particular. Some answers to the questions are only just beginning to emerge, in view of the complexity of the subject, and major research efforts should be

encouraged in order to provide the answers.

With optimistic views in mind, research is going to further our little knowledge of the subject, and in doing so, will bring with it a new insight into the field of intracellular protein degradation.

Appendix: Publications.

1) Rivett, A. J., Savory, P. J. & Djaballah, H. "Characterisation of
   Proteolytic Activities of the Multicatalytic Proteinase Complex."
   (1990) *FASEB J.* 4, A2147.

2) Djaballah, H. & Rivett, A. J. " The Multicatalytic Proteinase
   Complex: Interaction Between Catalytic sites." (1991) *Biochem.
   Soc. Trans.* 19, 291S.

3) Djaballah, H. & Rivett, A. J. " Peptidylglutamyl-Peptide Hydrolase
   Activity of the Multicatalytic Proteinase Complex: Evidence for
   New High-Affinity Site, Analysis of Cooperative Kinetics, anf the
   Effect of Manganese Ions." (1992) *Biochemistry* 31, 4133-4141.

4) Djaballah, H., Harness, J. A., Savory, P. J. & Rivett, A. J. " Use of
   Serine Protease Inhibitors As Probes for the Different Proteolyti
   Activities of the Rat Liver Multicatalytic Proteinase Complex."
   (1992) *Eur. J. Biochem.* 209, 629-634.

5) Djaballah, H., Rowe, A. J., Harding, S. E. & Rivett, A. J.
   " Conformational Changes in the Multicatalytic Proteinase
   Complex (Proteasome) Associated with Positive Cooperativity
   and Stimulation of Peptidylglutamyl-Peptide Hydrolase
   Activities." (1993) *Biochem. J.* (in press).

6) Rivett, A. J., Mason, G. G. F., Djaballah, H., Savory, P. J., Palmer,
   A., & Knecht, E. "Structure, activities, and Subcellular
   Localization of the Rat Liver Multicatalytic Proteinase Complex
   (Proteasome) (1992) *Proc. 9th ICOP Conference on Proteolysis
   and Protein Turnover* (Virginia, USA) (submitted).

References

Ahn, J. Y., Hong, S. O., Kwak, K. B., Kang, s. S., Tanaka, K., Ichihara, A., Ha, D. B. & Chung, C. H. (1991) *J. Biol. Chem.* **266**, 15746-15749.

Aki, M., Tamura, T., Tokunaga, F., Iwanga, S., Kawamura, Y., Shimbara, N., Kagawa, S., Tanaka, K. & Ichihara, A. (1992) *FEBS Lett.* **301**, 65-68.

Alazard, R., Bechet, J-J., Dupaix, A. & Yon, J. (1973) *Biochim. Biophys. Acta* **309**, 379-396.

Aoyagi, T. & Umezawa, H. (1975) *"In Proteases and Biological Control."* Reich, E., Rifkin, D. B. & Shaw, E. Eds., Cold Spring Harbor, New York.

Arnold, D., Driscoll, J., Androlewicz, M., Hughes, E., Cresswell, P. & Spies, T. (1992) *Nature* **360**, 171-174.

Arribas, J. & Castano, J. G. (1990) *J. Biol. Chem.* **265**, 13969-13973.

Arrigo, A. P., Simon, M., Darlix, J-L. & Spahr, P. F. (1987) *J. Mol. Evol.* **25**, 141-150.

Arrigo, A. P., Tanaka, K., Goldberg, A. L. & Welch, W. J. (1988) *Nature* **331**, 192-194.

Baumeister, W., Dahlmann, B., Hergel, R., Kopp, L. & Pfeifer, G. (1988) *FEBS Lett.* **241**, 239-245.

Barrett, A. J. (1986) *"In Proteinase Inhibitors"*. Barrett, A. J. & Salvesen, G. Eds. Elseiver Science Publishers BV (Biomedical Division).

Barrett, A. J. (1987) *Trends Biochem. Sci* **12**, 193-196.

Barrett, A. J., Knight, C. G., Brown, M. A. & Tisljar, U. (1989) *Biochem. J.* **260**, 259-263.

Bechet, J-J., Dupaix, A., Roucous, C. & Bonamy, A. M. (1977) *Biochimie* **59**, 241-246.

Beltzel, C., Pal, G. P. & Saenger, W. (1988) *Eur. J. Biochem.* **178**, 155-171.

Benoist, P., Muller, A., Diem, H. G. & Schwencke, J. (1992) *J. Bacteriol.* **174**, 1495-1504.

Berne, B. J. & Pecora, R. (1976) *In Dynamic Light Scattering*. John Wiley & Sons, New York.

Bond, J. S. & Butler, P. E. (1987) *Ann. Rev. Biochem.* **56**, 333-364.

Bonifacino, J. S. & Lippincott-Schwartz, J. (1991) *Curr Opin. Cell Biol.* **3**, 592-600.

Bowen, T. J. & Rowe, A. J. (1970) *In An Introduction to Ultracentrifugation*. Wiley.

Bradford, M. M. (1976) *Anal. Biochem.* **72**, 248-254.

Breddam, K. & Meldal, M. (1992) *Eur. J. Biochem.* **206**, 103-107.

Brown, M. G., Driscoll, J. & Monaco, J. J. (1991) *Nature* **353**, 355-357.

Cardozo, C., Vinitsky, A., Hidalgo, M. C., Michaud, C. & Orlowski, M. (1992) *Biochemistry* **31**, 7373-7380.

Cerundolo, V., Tse, A. G. D., Salter, R. D., Parham, P. & Townsend, A. (1991) *Proc. R. Soc. Lond. B.* **244**, 169-177.

Chiang, H. L., Terlecky, S. R., Plant, C. P. & Dice J. F. (1989) *Science* **246**, 382-385.

Chu-Ping, M., Slaughter, C. A. & DeMartino, G. N. (1992a) *Biochim. Biophys. Acta* **1119**, 303-311.

Chu-Ping, M., Slaughter, C. A. & DeMartino, G. N. (1992b) *J. Biol. Chem.* **267**, 10515-10523.

Claes, P., Dunford, M., Kenney, A. & Vardy, P. (1992) *In Laser Light Scattering in Biochemistry*. Harding, S. E., Sattle, D. B. & Bloomfield, V. A. Eds. The Royal Society of Chemistry, Cambridge.

Coux, O., Northwang, H. G., Scherrer, K., Bergsma-Schutter, W., Arnberg, A. C., Timmins, T. A., Langowski, J. & Cohen-Addad, C. (1992) *FEBS Lett.* **300**, 49-55.

Dauch, P., Barelli, H., Vincent, J. P. & Checler, F. (1991) *Biochem. J.* **280**, 421-426.

Dahlmann, B., Kuehn, L., Rutschmann, M. & Reinauer, H. (1985) *Biochem. J.* **228**, 161-170.

Dahlmann, B., Kuehn, L., Ishiura, S., Tsukahara, T., Sugita, H., Tanaka, K., Rivett, J., Hough, R. F., Rechsteiner, M., Mykles, D. L., Fagan, J. M., Waxman, L., Ishil, S., Sasaki, M., Kloetzel, P. M., Harris, H., Ray, K., Behal, F. J., DeMartino, G. N. & McGuire, M. J. (1988) *Biochem. J.* **255**, 750-751.

Dahlmann, B., Kopp, F., Kuehn, L., Niedel, B., Pfeifer, G., Hergel, R. & Baumeister, W. (1989) *FEBS Lett.* **251**, 125-131.

Daniels, S. B., Cooney, E., Sofia, M. J., Chakravarty, P. K. & Katzenellenbogen, J. A. (1983) *J. Biol. Chem.* **258**, 15046-15053.

Day, P. & Shaw, W. V. (1992) *J. Biol. Chem.* **267**, 5122-5127.

Dean, R. T. & Barrett, A. J. (1976) *Essays Biochem.* **12**, 1-40.

DeMars, R. & Spies, T. (1992) *Trends Cell Biol.* **2**, 81-86.

Dice, J. F. (1987) *FASEB J.* **1**, 349-357.

Dice, J. F. (1990) *Trends Biochem. Sci.* **15**, 305-309.

Dick, L. R., Moomaw, C. R., DeMartino, G. N. & Slaughter, C. A. (1991) *Biochemistry* **30**, 2725-2734.

Dick, L. R., Moomaw, C. R., Pramanik, B. C., DeMartino, G. N. & Slaughter, C. A. (1992) *Biochemistry* **31**, 7347-7355.

Djaballah, H. & Rivett, A. J. (1992) *Biochemistry* **31**, 4133-4141.

Djaballah, H., Harness, J. A., Savory, P. J. & Rivett, A. J. (1992) *Eur. J. Biochem.* **209**, 629-634.

Drapeau, G. R. (1977) *Methods Enzymol.* **47**, 188-191.

Driscoll, J. & Goldberg, A. L. (1989) *Proc. Natl. Acad. Sci. USA* **86**, 787-791.

Driscoll, J. & Goldberg, A. L. (1990) *J. Biol. Chem.* **265**, 4789-4792.

Driscoll, J. & Finley, D. (1992) *Cell* **68**, 823-825.

Driscoll, J., Frydman, J. & Goldberg, A. L. (1992) *Proc. Natl. Acad. Sci. USA* **89**, 4986-4990.

Dubiel, W., Pratt, G., ferrell, K. & Rechsteiner, M. (1992) *J. Biol. Chem.* **267**, 22369-22377.

Eisenthal, R. & Cornish-Bowden, A. (1974) *Biochem. J.* 139, 715-720.

Emori, Y., Tsukahara, T., Kawasaki, H., Ishiura, S., Sugita, H. & Suzuki, K. (1991) *Mol. Cell. Biol.* 11, 344-353.

Enenkel, C., Hilt, W. & Wolf, D. H. (1990) *Yeast* 3, S341-06-3B.

Erlanger, B. F. & Edel, F. (1964) *Biochemistry* 3, 346-349.

Erlanger, B. F., Cooper, A. G. & Cohen W. (1966) *Biochemistry* 5, 190-196.

Eytan, E., Ganoth, D., Armon, T. & Hershko, A. (1989) *Proc. Natl. Acad. Sci. (USA)* 86, 7751-7755.

Fagan, J. M. & Waxman, L. (1989) *J. Biol. Chem.* 264, 17868-17872.

Falkenberg, P. E., Haass, C., Kloetzel, P. M., Niedel, B., Kopp, F., Kuehn, L. & Dahlmann, B. (1988) *Nature* 334, 190-192.

Fersht, A. R. (1985) *In Enzyme Structure and Mechanism* (Second edition), W. H. Freeman & CO., New York.

Finley, D. & Chau, V. (1991) *Ann. Rev. Cell Biol.* 7, 25-70.

Frentzel, S., troxell, M., Haass, C., Pesold-Hurt, B., Glatzer, K. H. & Kloetzel, P. M. (1992) *Eur. J. Biochem.* 205, 1043-1051.

Frieden, C. (1970) *J. Biol. Chem.* 245, 5788-5799.

Fritz, P. J., Vesell, E. S., White, E. L. & Pruitt, K. M. (1969) *Proc. Natl. Acad. Sci. (USA)* 62, 558.

Fujiwara, T., Tanaka, K., Orino, E., Yoshimura, T., Kumatori, A., Tamura, T., Chung. C., Nakai, T., Yamaguchi, K., Shin, S., Kakizuka, A., Nakanishi, S. & Ichihara, A. (1990) *J. Biol. Chem.* 265, 16604-16613.

Gaertner, F. H. (1978) *Trends Biochem. Sci* 3, 63-65.

Ganoth, D., Leshinsky, E., Eytan, E. & Hershko, A. (1988) *J. Biol. Chem.* 263, 12412-12419.

Georgatsou, E., georgakopoulos, T. & Thireos, G. (1992) *FEBS Letts.* 299, 39-43.

Glotzer, M., Murray, A. W. & Kirschner, M. W. (1991) *Nature* **349**, 132-138.

Glover, G. & Shaw, E. (1971) *J. Biol. Chem.* **246**, 4594-4601.

Glynne, R., Powis, S. H., Beck, S., Kelly, A., Kerr, L. A. & Trowsdale, J. (1991) *Nature* **353**, 357-360.

Gold, A. M. (1965) *Biochemistry* **4**, 897-902.

Goldberg, A. L. & St John, A. C. (1976) *Ann. Rev. Biochem.* **45**, 747-803.

Goldberg, A. L. (1992) *Eur. J. Biochem.* **203**, 9-23.

Goldberg, A. L. & Rock, K. L. (1992) *Nature* **357**, 375-379.

Gonen, H., Schwartz, A. L. & Ciechanover, A. (1991) *J. Biol. Chem.* **266**, 19221-19231.

Grossi de Sa, M. F., Martins de Sa, C., Harper, F., Coux, O., Akhayat, O., Pal, J. K., Florintin, Y. & Scherrer, K. (1988) *J. Cell Sci.* **89**, 151-165.

Grziwa, A., Baumeister, W., Dahlmann, B. & Kopp, F. (1991) *FEBS Lett.* **290**, 186-190.

Hadari, T., Warms, J. V. B., Rose, I. A. & Hershko, A. (1992) *J. Biol. Chem.* **267**, 719-727.

Harris, J. R. (1988) *Indian J. Biochem. Biophys.* **25**, 459-456.

Hartly, B. S. (1960) *Ann. Rev. Biochem.* **29**, 45-72.

Harper, J. W., Hemmi, K. & Powers, J. C. (1983) *J. Am. Chem. Soc.* **105**, 6518-6520.

Harper, J. W. & Powers, J. C. (1985) *Biochemistry* **24**, 7200-7213.

Harper, J. W., Hemmi, K. & Powers, J. C. (1985) *Biochemistry* **24**, 1831-1841.

Haass, C. & Kloetzel, P. M. (1989) *Exp. Cell Res.* **180**, 243-252.

Haass, C., Pesold-Hurt, B., Multhaup, G., Beyreuther, K. & Kloetzel, P. M. (1989) *EMBO J.* **8**, 2373-2379.

Heinmeyer, W., Kleinschmidt, J. A., Saidowsky, J., Escher, C. & Wolf, D. H. (1991) *EMBO J.* 10, 555-562.

Hemmi, K. J., Harper, J. W. & Powers, J. C. (1985) *Biochemistry* 24, 1841-1848.

Hendil, K. B. (1988) *Biochem. Intl.* 17, 471-477.

Hergel, R., Pfeifer, G., Puhler, G., Dahlmann, B. & Baumeister, W. (1991) *FEBS Lett.* 283, 117-121.

Hershko, A. & Ciechanover, A. (1982) *Ann. Rev. Biochem.* 51, 335-364.

Hershko, A. (1991) *Trends Biochem. Sci.* 16, 265-268.

Hershko, A., Ganoth, D., Pehrson, J., Palazzo, R. E. & Cohen, L. H. (1991) *J. Biol. Chem.* 266, 16376-16379.

Hershko, A. & Ciechanover, A. (1992) *Ann. Rev. Biochem.* 61, 761-807.

Hill, R. (1925) *Proc. R. Soc.* B100, 224.

Hingamp, P., Arnold, J. E., Mayer, R. J. & Dixon, L. K. (1992) *EMBO J.* 11, 361-366.

Huddleston, J. A. & Brownlee, G. G. (1982) *Nuc. Acids Res.* 10, 1029-1037.

Hough, R., Pratt, G., & Rechsteiner, M. (1987) *J. Biol. Chem.* 262, 8303-8313.

Ikai, A., Nishigai, M., Tanaka, K. & Ichihara, A. (1991) *FEBS Lett.* 292, 21-24.

Ismail, R. & Gevers, W. (1983) *Biochim. Biophys. Acta* 742, 399-408.

Jentsch, S. (1992) *Trends Cell Biol.* 2, 98-102.

Johnston, N. L. & Cohen, R. E. (1991) *Biochemistry* 30, 7514-7522.

Johnson, E. S., Bartel, B., Seufert, W. & Varshavsky, A. (1992) *EMBO J.* 11, 497-505.

Kam, C-M., Fujikawa, K. & Powers, J. C. (1988) *Biochemistry* 27, 2547-2557.

Kanayama, H., Tanaka, K., Aki, M., Kagawa, S., Miyaji, H., Satoh, M., Okada, F., Saeto, S., Shimbara, N. & Ichihara, A. (1991) *Cancer Res.* **51**, 6677-6685.

Kawahara, H. & Yokosawa, H. (1992) *Develop. Biol.* **151**, 27-33.

Kelly, A., Powis, S. H., Glynne, R., Radley, E., Beck, S. & Trowsdale, J. (1991) *Nature* **353**, 667-668.

Kettelhut, I. C., Ving, S. S. & Goldberg, A. L. (1988) *Diab. Met. Rev.* **4**, 751-772.

Kinoshita, M., Toyohara, H. & Shimizu, Y. (1990a) *Comp. Biochem. Physiol.* **97B**, 315-319.

Kinoshita, M., Toyohara, H. & Shimizu, Y. (1990b) *Comp. Biochem. Physiol.* **96B**, 565-569.

Klausner, R. D. & Sitia, R. (1990) *Cell* **62**, 611-614.

Klein, U., Gernold, M. & Kloetzel, P. M. (1990) *J. Cell Biol.* **111**, 2275-2282.

Kleinschmidt, J. A., Escher, C. & Wolf, D. H. (1988) *FEBS Letts.* **239**, 35-40.

Kong, S-K. & Chock, P. B. (1992) *J. Biol. Chem.* **267**, 14189-14192.

Kopp, F., Steiner, R., Dahlmann, B., Kuehn, L. & Reinauer, H. (1986) *Biochim. Biophys. Acta* **872**, 253-260

Kreutzer-Schmid, C. & Schmid, H. P. (1990) *FEBS Letts.* **267**, 142-146.

Krut, J. (1977) *Ann. Rev. Biochem.* **46**, 331-358.

Kuehn, L., Dahlmann, B. & Reinauer, H. (1992) *Arch. Biochem. Biophys.* **295**, 55-60.

Kumatori, A., Tanaka, K., Inamura, N., Sone, S., Ogura, T., Matsumoto, T., Tachikawa, T., Shin, S. & Ichihara, A. (1990) *Proc. Natl. Acad. Sci. (USA)* **87**, 7071-7078.

Kurganov, B. I. (1982) *In Allosteric Enzymes: Kinetic Behavior.* (Yakolvev, V. A., Ed.) Wiley, Chichester.

Laemmli, U. K. (1970) *Nature* **227**, 680-685.

Laura, R., Robinson, D. J. & Bing, D. H. (1980) *Biochemistry* **19**, 4859-4864.

Lee, L. L., Moomaw, C. R., Orth, K., McGuire, M. J., DeMartino, G. N. & Slaughter, C. A. (1990) *Biochim. Biophys. Acta* **1037**, 178-185.

Lee, D. H., Tanaka, K., Tamura, T., Chung, C. H. & Ichihara, A. (1992) *Biochim. Biophys. Res. Commun.* **182**, 452-460.

Li, X., Gu, M. & Etlinger, J. D. (1991) *Biochemistry* **30**, 9709-9715.

Lilley, K. S., Davison, M. D., & Rivett, A.J. (1990) *FEBS Letts.* **262**, 327-329.

Lineweaver, H. & Burk, J. (1934) *J. Am. Chem. Soc.* **56**, 658.

Lundblad, R. L. & Noyes, C. M. (1984) *In Chemical Reagents for Protein Modification* (Volume II). CRC Press Inc., Florida (USA).

Madden, D. R., Gorga, J. C., Strominger, J. L. & Wiley, D. C. (1992) *Cell* **70**, 1035-1048.

Martinez, C. K. & Monaco, J. J. (1991) Nature 353, 664-667

Martins de Sa, C., Grossi de Sa, M. F., Akhayat, O., Broders, F. & Scherrer, K. (1986) *J. Mol. Biol.* **187**, 479-493.

Mason, R. W. (1990) *Biochem. J.* **265**, 479-484.

Matthews, W., Tanaka, K., Driscoll, J., Ichihara, A. & goldberg, A. L. (1989) *Proc. Natl. Acad. Sci. (USA)* **86**, 2597-2601.

Matsudaira, P. T. (1987) *J. Biol. Chem.* **262**, 10035.

McGuire, M. J. & DeMartino, G. (1986) *Biochim. Biophys. Acta* **873**, 279-289.

McGuire, M. J., Croall, D. E. & DeMartino, G. (1988) *Arch. Biochem. Biophys.* **262**, 273-285.

McGuire, M. J., McCullough, M. L., Croall, D. E. & DeMartino, G. (1989) *Biochim. Biophys. Acta* **995**, 181-186.

McDermott, J. R., Gibson, A. M., Oakley, A. E. & Biggins, J. A. (1991) *J. Neurochem.* **56**, 1509-1517.

Meldal, M. & Breddam, K. (1991) *Anal. Biochem.* **195**, 141-147.

Mellgren, R. L. (1990) *Biochim. Biophys. Acta* **1040**, 28-34.

Momburg, F., Ortiz-Navarrete, V., Neefjes, J., Goulmy, E., van de Wal, Y., Spits, H., Powis, S. J., Butchers, G. W., Howard, J. C., Walden, P. & Hammerling, G. J. (1992) *Nature* **360**, 174-177.

Monaco, J. J. & McDevitt, H. O. (1982) *Proc. Natl. Acad. Sci. (USA)* **79**, 3001-3005.

Monaco, J. J. & McDevitt, H. O. (1986) *Hum. Immun.* **15**, 416-426.

Mortimore, G. E., Poso, A. R. & Lardeux, B. R. (1989) *Diab. Met. Rev.* **5**, 49-70.

Murakami, K. & Etlinger, J. D. (1986) *Proc. Natl. Acad. Sci. USA* **83**, 7588-5992.

Murakami, Y., Matsufuji, S., Kameji, T., Hayashi, S. I., Igarashi, K., Tamura, T., Tanaka, K. & Ichihara, A. (1992) *Nature* **360**, 597-599.

Murachi, T. (1983) *Trends Biochem. Sci.* **8**, 167-169.

Mykles, D. L. (1989) *Arch. Biochem. Biophys.* **274**, 216-228.

Mykles, D. L. & Haire, M. F. (1991) *Arch. Biochem. Biophys.* **288**, 543-551.

Northwang, H. G., Coux, O., Bey, F. & Scherrer, K. (1992) *Eur. J. Biochem.* **207**, 621-630.

Oberfelder, R. W., Consler, T. G., & Lee, J. C. (1985) *Methods Enzymol.* **117**, 27-40.

Odake, S., Kam, C-M., Narasimhan, L., Poe, M., Blake, J. T., Krahenbuhl, O., Tschopp, J. & Powers, J. C. (1991) *Biochemistry* **30**, 2217-2227.

Ogata, S., Misumi, Y., Tsuji, E., Takami, N., Oda, K. & Ikehara, Y. (1992) *Biochemistry* **31**, 2582-2587.

Okhuma, S. & Poole, B. (1978) *Proc. Natl. Acad. Sci. (USA)* **75**, 3327-3331.

Ortiz-Navarette, V., Seelig, A., Gernold, M., Frentzel, S., Kloetzel, P. M. & Hammeling, G. J. (1991) *Nature* **353**, 662-664.

Orlowski, M. & Michaud, C. (1989) *Biochemistry* **28**, 9270-9278.

Orlowski, M. (1990) *Biochemistry* **29**, 10289-10297.

Orlowski, M., Cardozo, C., Hidalgo, M. C. & Michaud, C. (1991) *Biochemistry* **30**, 5999-6005.

Olson, T. S. & Dice, J. F. (1989) *Curr. Opp. Cell Biol.* **1**, 1194-1200.

Parham, P. (1990) *Nature* **348**, 674-675.

Pereira, M. E., Yu, B. & Wilk, S. (1992) *Arch. Biochem. Biophys.* **294**, 1-8.

Peters, J-M., Harris, J. R. & Kleinschmidt, J. A. (1991) *Eur. J. Cell Biol.* **56**, 422-432.

Poe, M., Bennett, C. D., Biddison, W. E., Blake, J. T., Norton, G. P., Rodkey, J. A., Sigal, N. H., Turner, R. V., Wu, J. K. & Zweerink, H. J. (1988) *J. Biol. Chem.* **263**, 13215-13222.

Pontremoli, S. & Melloni, E. (1986) *Ann. Rev. Biochem.* **55**, 455-481.

Pontremoli, S., Melloni, E., Michetti, M., Salamino, F., Sparatore, B. & Horecker, B. L. (1988) *Proc. Natl. Acad. Sci. (USA)* **85**, 1740-1743.

Potempa, J., Fedak, D., Dubin, A., Mast, A. & Travis, J. (1991) *J. Biol. Chem.* **266**, 21482-21487.

Powers, J. C., Oleksyszyn, J., Narasimhan, L. & Kam, C-M. (1990) *Biochemistry* **29**, 3108-3118.

Puhler, G., Weinkauf, S., Bachmann, L., Muller, S., Hergel, R. & Baumeister, W. (1992) *EMBO J.* **11**, 1607-1616.

Rawlings, N. D. & Barrett, A. J. (1990) *Comput. Appl. Biosci.* **6**, 118-119.

Rawlings, N. D. & Barrett, A. J. (1992) *Biochem. J.* (in press).

Ray, K. & Harris, H. (1985) *Proc. Natl. Acad. Sci. USA* **82**, 7545-7549.

Ray, K. & Harris, H. (1986) *FEBS Letts.* **194**, 91-95.

Riordan, J. F., Wacker, W. E. C., & Vallee, B. L. (1965) *Biochemistry* **4**, 1785-1765.

Riordan, J. F. (1973) *Biochemistry* **12**, 3915.

Riordan, J. F., McElvany, K. D. & Borders, Jr., C. L. (1977) *Science* **195**, 884-886.

Ritcher-Ruoff, B., Heinmeyer, W. & Wolf, D. H. (1992) *FEBS Letts.* **302**, 192-196.

Rivett, A. J. (1985) *J. Biol. Chem.* **260**, 12600-12606.

Rivett, A. J. (1986) *Curr. Top. Cell Reg.* **28**, 291-337.

Rivett, A. J. (1989a) *Biochem. J.* **263**, 625-633.

Rivett, A. J. (1989b) *J. Biol. Chem.* **264**, 12215-12219.

Rivett, A. J. (1989c) *Arch. Biochem. Biophys.* **268**, 1-8.

Rivett, A. J. (1990a) *Essays Biochem.* **25**, 39-81.

Rivett, A. J. (1990b) *Curr. Op. Cell Biol.* **2**, 1143-1149.

Rivett, A. J., Savory, P. J. & Djaballah, H. (1990c) *FASEB J.* **4**, A2157.

Rivett, A. J. & Sweeny, S. T. (1991) *Biochem. J.* **278**, 171-177.

Rivett, A. J., Skilton, H. E., Rowe, A. J., Eperon, I. C. & Sweeney, S. T. (1991) *Biomed. Biochim. Acta* **50**, 447-450.

Rivett, A. J., Palmer, A. & Knecht, E. (1992) *J. Histochem. Cytochem.* **40**, 1165-1172.

Rivett, A. J. (1993) *Biochem. J.* (in press).

Roberston, M. (1991) *Nature* **353**, 300-301.

Rogers, S., Wells, R. & Rechsteiner, M. (1986) *Science* **234**, 364-368.

Rogers, S. W. & Rechsteiner, M. (1988) *J. Biol. Chem.* **263**, 19843-19849.

Rosenfeld, J., Capdeville, J., Guillemot, J. C. & Ferrara, P. (1992) *Anal. Biochem.* **203**, 173-179.

Rubin, H., Wang, Z., Nickbarg, E. B., McLarney, S., Naidoo, N., Schoenberger, O. L., Johnson, J. L. & Cooperman, B. S. (1990) *J. Biol. Chem.* **265**, 1199-1207.

Rubin, H. (1992) *Biol. Chem. Hoppe-Seyler* **373**, 497-502.

Rusbridge, N. M. & Beynon, R. J. (1990) *FEBS Letts.* 268, 133-136.

Sacchetta, P., Santarone, S., Battista, P. & Di Cola, D. (1990a) *Eur. J. Biochem.* 191, 275-280.

Sacchetta, P., Battista, P., Santarone, S. & Di Cola, D. (1990b) *Biochim. Biophys. Acta* 1037, 337-343.

Saitoh, Y., Yokosawa, H. & Ishii, S-I. (1989) *Biochem. Biophys. Res. Comm.* 162, 334-339.

Sato, S. & Shiratsuchi, A. (1990) *Biochim. Biophys. Acta* 1041, 269-272.

Schmidt, H. P., Akhayat, O., Martins de Sa, C., Puvion, F. & Scherrer, K. (1984) *EMBO J.* 3, 29-34.

Seelig, A., Kloetzel, P. M., Kuehn, L. & Dahlmann, B. (1991) *Biochem. J.* 280, 225-232.

Seglen, P. O. (1983) *Methods Enzymol.* 96, 737-764.

Seufert, W. & Jentsch, S. (1992) *EMBO J.* 11, 3077-3080.

Schliephacke, M., Kremp, A., Schmid, H. P., Kohler, K. & Kull, U. (1991) *Eur. J. Cell Biol.* 55, 114-121.

Schimke, R. T. (1973) *Adv. Enzymol.* 37, 135-187.

Shaw, E. (1990) *Adv. Enzymol.* 63, 271-347.

Shiba, E., Ariyoshi, H., Yano, Y., Kawasaki, T., Sakon, M., Kambayashi, J-I. & Mori, T. (1992) *Biochem. Biophys. Res. Comm.* 182, 461-465.

Shimbara, N., Orino, E., Sones, S., Ogura, T., Takashina, M., Shono, M., Tamura, T., Yasuda, H., Tanaka, K. & Ichihara, A. (1992) *J. Biol. Chem.* 267, 18100-18109.

Skilton, H. E., Eperon, I. C. & Rivett, A. J. (1989) *FEBS Letts.* 279, 351-355.

Stadtman, E. R. (1990) *Biochemistry* 29, 6323-6330.

Stroud, R. M., Kay, L. M. & Dickerson, R. E. (1974) *J. Mol. Biol.* 83, 185-208.

Suzuki, K., Imajoh, S., Emori, Y., kawasaki, H., Minami, Y. & Ohno, S. (1987) *FEBS Letts.* **220**, 271-277.

Takahashi, K. (1968) *J. Biol. Chem.* **23**, 6171-6179.

Takahashi, K. (1977) *J. Biochem.* **81**, 403-414.

Tamura, T. Lee, D. H., Osaka, F., Fujiwara, T., Shin, S., Chung, C. H., Tanaka, K. & Ichihara, A. (1991) *Biochim. Biophys. Acta* **1089**, 95-102.

Tamura, T., Shimbara, N., Aki, M., Ishida, N., Bey, F., Scherrer, K., Tanaka, K. & Ichihara, A. (1992) *J. Biochem.* **112**, 530-534.

Tanaka, K., Ii, K., Ichihara, A., Waxman, L. & Goldberg, A. L. (1986a) *J. Biol. Chem.* **261**, 15197-15203.

Tanaka, K., Yushimoura, T., Ichihara, A., Kameyama, K. & Takagi, T. (1986b) *J. Biol. Chem.* **261**, 15204-15207.

Tanaka, K. & Ichihara, A. (1988a) *FEBS Letts.* **236**, 159-162.

Tanaka, K., Yoshimura, T., Kumatori, A., Ichihara, A., Ikai, A., Nishigai, M., Kameyama, K. & Takagi, T. (1988b) *J. Biol. Chem.* **263**, 16209-16226.

Tanaka, K., Yoshimura, T., Kumatori, A., Ichihara, A., Ikai, A., Nishigai, M., Morimoto, Y., Sato, M., Tanaka, N., Katsube, Y., Kameyama, K. & Takagi, T. (1988c) *J. Mol. Biol.* **203**, 985-996.

Tanaka, K. & Ishihara, A. (1989) *Biochem. Biophys. Res. Commun.* **159**, 1309-1315.

Tanaka, K., Yoshimura, T. & Ichihara, A. (1989) *J. Biochem.* **106**, 495-500.

Tanaka, K., Tamura, T., Yoshimura, T. & Ichihara, A. (1992) *New Biol.* **4**, 173-187.

Tisljar, U., Knight, C. G. & Barrett, A. J. (1990) *Anal. Biochem.* **186**, 112-115.

Tomek, W., Adam, G. & Schmid, H. P. (1988) *FEBS Letts.* **239**, 155-158.

Tokunago, F., Aruga, R., Iwanaga, S., Tanaka, K. , Ichihara, A., Takao, T. & Shimonishi, Y. (1990) *FEBS Letts.* **262**, 373-375.

Townsend, A. & bodmer, H. (1989) *Ann. Rev. Immunol.* 7, 601-624.

Tsukahara, T., Ishiura, S. & Sugita, H. (1988) *Eur. J. Biochem.* 177, 261-266.

Vaithilingam, I. & Cook, R. A. (1989) *Biochem. Intl.* 19, 1297-1307.

Van Bleek, G. M. & Nathenson, S. G. (1992) *Trends Cell Biol.* 2, 202-207.

Van Holde, K. E. (1985) *In Physical Biochemistry.* Prentice Hall, Englewood Cliffs.

Varshavsky, A. (1992) *Cell* 69, 725-735.

Vijayalakshmi, J., Meyer Jr., E. F., Kam, C-M. & Powers, J. C. (1991) *Biochemistry* 30, 2175-2183.

Vilain, A-C., Okochi, V., Vergley, I., Reboud-Ravaux, M., Mazaleyrat, J-P. & Wakselman, M. (1991) *Biochim. Biophys. Acta* 1076, 401-405.

Wagner, B. J., Margolis, J. W., Abramovitz, A. S. & Fu, S-C. (1985) *Biochem. J.* 228, 517-519.

Walenga, R., Vanderhoek, J. Y. & Feinstein, M. B. (1980) *J. Biol. Chem.* 255, 6024-6027.

Wang, K. K. W., Villalobo. A., & Roufogalis, B. D. (1989) *Biochem. J.* 262, 693-706.

Westkaemper, R. B. & Abeles, R. H. (1983) *Biochemistry* 22, 3256-3264.

Weitman, D. & Etlinger, J. D. (1992) *J. Biol. Chem.* 267, 6977-6982.

Welch, G. R. (1977) *Prog. Biophys. Molec. Biol.* 32, 103-191.

White, E. H., Jelinski, L. W., Politzer, I. R., Branchini, B. R. & Roswell, D. F. (1981) *J. Am. Chem. Soc.* 103, 4231-4239.

Wibo, M. & Poole, B. (1974) *J. Cell Biol.* 63, 430-440.

Wilk, S., Meister, A. & Haschemeyer, R. H. (1970) *Biochemistry* 9, 2039-2043.

Wilk, S. & Orlowski, M. (1980) *J. Neurochem.* 35, 1172-1182.

Wilk, S. & Orlowski, M. (1983) *J. Neurochem.* **40**, 842-849.

Wilk, S., Pereira, M. & Yu, B. (1991) *Biomed. Biochim. Acta* **50**, 471-478.

Yaron, A., Carmel, A. C. & Katchalski-Katzir, E. (1979) *Anal. Biochem.* **95**, 228-235.

Yu, B., Pereira, M. & Wilk, S. (1991) *J. Biol. Chem.* **266**, 17396-17400.

Yukawa, M., Sakon, M., Kambayashi, J., Shiba, E., Kawasaki, T., Ariyosih, H. & Mori, T. (1991) *Biochem. Biophys. Res. Commun.* **178**, 256-262.

Zolfaghari, R., Baker, C. R. F., Amirgholami, A., Canizaro, P. C. & Behal, F. J. (1987) *Arch. Biochem. Biophys.* **258**, 42-50.

Zwickl, P., Pfeifer, G., Lottspeich, F., Kopp, F., Dahlmann, B. & Baumeister, W. (1990) *J. Struct. Biol.* **103**, 197-203.

Zwickl, P., Lottspeich, F. Dahlmann, B. & Baumeister, W. (1991) *FEBS Lett.* **278**, 217-221.

Zwickl, P., Lottspeich, F. & Baumeister, W. (1992) *FEBS Lett.* **312**, 157-160.